PACIFIC EARTHQUAKE ENGINEERING RESEARCH CENTER

Design and Instrumentation of the 2010 E-Defense Four-Story Reinforced Concrete and Post-Tensioned Concrete Buildings

Takuya Nagae, Kenichi Tahara, Taizo Matsumori,
Hitoshi Shiohara, Toshimi Kabeyasawa,
Susumu Kono, Minehiro Nishiyama
(Japanese Research Team)
and
John Wallace, Wassim Ghannoum, Jack Moehle, Richard Sause,
Wesley Keller, Zeynep Tuna
(U.S. Research Team)

PEER 2011/104
JUNE 2011

Design and Instrumentation of the 2010 E-Defense Four-Story Reinforced Concrete and Post-Tensioned Concrete Buildings

Takuya Nagae, Kenichi Tahara, Taizo Matsumori,
Hitoshi Shiohara, Toshimi Kabeyasawa, Susumu Kono, Minehiro Nishiyama

(Japanese Research Team)

and

John Wallace, Wassim Ghannoum, Jack Moehle, Richard Sause, Wesley Keller, Zeynep Tuna

(U.S. Research Team)

PEER Report 2011/104
Pacific Earthquake Engineering Research Center
College of Engineering
University of California, Berkeley

June 2011

ABSTRACT

This study reports on a collaborative research on the design, instrumentation, and preliminary analytical studies of two, full-scale, four-story buildings tested simultaneously on the NIED E-Defense shake table in December 2010. The two buildings are similar, with the same height and floor plan; one building utilized a conventional reinforced concrete (RC) structural system with shear walls and moment frames, whereas the other utilized the same systems constructed with post-tensioned (PT) members. The buildings were subjected to increasing intensity shaking using the JMA-Kobe record until a near-collapse state was reached. This report summarizes design issues and design documents, and provides detailed information on the type and location of sensors used. Initial analytical studies conducted both in the Japan and U.S. to support the design strategy and instrumentation of the buildings also are documented. The intent of this report is to provide a resource document for post-test research and high-impact education and outreach efforts.

ACKNOWLEDGMENTS

Funding for the test program and for Japanese researchers was provided by the Japanese Ministry of Education, Culture, Sports, Science, and Technology. Modest funding was provided by U.S. National Science Foundation under award number CMMI-1000268 in support of this collaboration between U.S. and Japanese researchers.

This report was motivated by the desire to document the importance of these tests and to disseminate the rationale behind this testing program to the broader earthquake engineering communities in Japan and the U.S., as well as other countries, and to highlight important objectives. The joint report also documents the extraordinary level of collaboration between Japanese and U.S. researchers studying the response and performance of reinforced concrete structures. This collaboration has been so incredibly fruitful that universally the authors desire to continue such joint efforts in the future for many years to come.

The authors' wish to acknowledge all the participants within the Reinforced Concrete Group of the various NEES–E-Defense workshops held in recent years in Japan and the U.S. These meetings and the relationships that have developed between the meeting participants have been key in laying the foundation for continued strong research collaboration in the present and the future.

Any opinions, findings, and conclusions or recommendations expressed in this material are those of the authors and do not necessarily reflect those of the Japanese Ministry of Education, Culture, Sports, Science, and Technology, the U.S. National Science Foundation, or other individuals mentioned or who have participated in the workshops and meetings.

CONTENTS

LIST OF FIGURES

LIST OF TABLES

1 Introduction

1.1 BACKGROUND

In the 1994 Northridge and 1995 Hyogo-ken Nanbu (Kobe) earthquakes, many older reinforced concrete (RC) buildings suffered severe damage, and some collapsed due to brittle failure of key structural elements. In general, buildings designed to newer standards—such as the 1981 amendments to Japanese Building Standard Law Enforcement Orders and the 1976 and later versions of the U.S. Uniform Building Code—performed well. Some newer U.S. buildings performed poorly due to substandard behavior of diaphragms, particularly in precast prestressed concrete parking structures and gravity systems. In both Japan and the U.S., although building response to strong ground shaking generally satisfied code requirements and performed adequately in providing life safety, high repair costs as a result of nonlinear behavior produced large member cracks and residual deformations.

As a result, new design approaches were developed that focused on defining deformation limits that can be used to assess both collapse safety and the impact of damage on repair costs and loss of building use (down time). In the U.S., these new approaches are documented in FEMA-356 report and by reports published by the Pacific Earthquake Engineering Research (PEER) Center and others. Damage observed from significant earthquakes often results in an evolution of design practice, as witnessed in the 1994 Northridge earthquake for structural steel buildings and in the 2010 Chile earthquake for reinforced concrete wall buildings. As well, there is continuous pressure to develop structural systems that allow for longer spans and more flexible floor plans using new materials or new systems, such as prestressed and post-tensioned (PT) concrete systems. These new systems often have attributes that are different from commonly used systems, where laboratory testing and experience in earthquakes of both components and systems have been used to assess expected performance and to verify design approaches. For example, PT systems typically have low hysteretic energy dissipation capacity relative to reinforced concrete (RC) systems; however, this same attribute tends to limit residual deformations. Therefore, it is important to continuously assess the expected performance of buildings constructed using new codes and new systems via testing of large-scale components and full-scale buildings models subjected to realistic loading histories expected in both frequent and rare earthquakes.

1.2 OBJECTIVES AND SCOPE

A series of shaking table tests were conducted on essentially full-scale RC and PT buildings designed using the latest code requirements and design recommendations available in both Japan and the U.S. To assess performance in both moderate-intensity frequent earthquakes (service-level) and large-intensity very rare earthquakes (collapse-level), the buildings were subjected to increasing intensity shaking using the JMA-Kobe and Takatori records until a near-collapse state was reached. The tests were designed to produce a wealth of data on stiffness, strength, and damping over a large range of deformations to assess current codes and recommendations, and will be used to develop new analysis tools and design recommendations, and determine if limit states and fragility relations used in current performance-based approaches to limit repair costs and assess collapse are consistent with measured responses and observed performance. The tests also will provide a wealth of data to assess and improve existing analytical tools used to model RC and PT components and systems, as well as help to identify future research needs.

1.3 ORGANIZATION

This report is divided into four chapters. The first chapter includes a brief introduction and background, followed by a short summary of the overall research objectives from both U.S. and Japan perspective. Chapter 2 provides an overview of the two test buildings, including a summary of design requirements, construction materials, structural drawings, and specimen construction. Chapter 3 includes a detailed description of the instrumentation used for each test building. Chapter 4 provides a brief summary and conclusions, as well as an overview of planned future studies.

1.4 BRIEF LITERATURE REVIEW AND OVERALL RESEARCH OBJECTIVES

The lengthy planning process and extensive collaboration between U.S. and Japan researchers leading up to the December 2010 tests produced test buildings that were designed to provide vital and important behavior and design information for both the U.S. and Japan. Because design objectives/requirements and performance expectations are somewhat different between the U.S. and Japan, a more detailed description of specific research objectives is provided in the following sections. In Chapter 2, the final building designs are reviewed using ASCE 7-05, ACI 318-08, and ACI ITG 5.1-07 to provide detailed information on U.S. code provisions and design recommendations that were met or not met.

1.4.2 Overall Objectives

When the Japanese Building Standard Law Enforcement Orders was substantially updated in 1981, the guiding principles of the new code were to prevent damage in minor and moderate earthquakes and to prevent collapse in severe earthquakes. These principles are essentially the same as those embodied in U.S. codes at the time (e.g., the Uniform Building Code). However, observations based on the 1994 Northridge earthquake and the 1995 Kobe earthquake, as well as other moderate to strong earthquakes that have occurred in recent years near major urban cities in Japan, have revealed that many buildings became nonfunctional and nonoperational due to damage to non-structural systems even if the structural damage was light to moderate. Based on these experiences, new design approaches have emerged in the 1990s and 2000s that address both structural and non-structural damage over a wider range of hazard levels. These approaches, which differ from prescriptive codes such as Uniform Building Code or the International Building Code, are commonly referred to as performance-based approaches, since the objective is to provide a more rigorous assessment of building performance.

Performance-based design approaches also provide a means to communicate expectations of building performance to the general public, building owners, and government agencies. This dialogue is essential, as there is a perception among the general public that buildings, both in Japan and the U.S., are “earthquake proof.” This perception is inconsistent with the stated code objectives of collapse avoidance. The economic losses and societal impacts associated with buildings designed with current prescriptive code requirements are likely to be very significant, potentially impacting the affected region for many years.

Novel approaches have emerged to provide improved performance, for example, approaches that utilize response modification such as base isolation or using dampers. Although these approaches may offer excellent performance, in general, initial costs are high and other challenges exist (for base isolation one significant hurdle is accommodating the relative movement between the superstructure and the surrounding foundation, including utilities). Consequently, only a limited number of buildings are constructed utilizing these approaches.

Therefore, it is essential to continue developing performance-based approaches in conjunction with innovative cost-effective building systems that are capable of better performance relative to conventional construction. The RC and PT Buildings that are described in Chapter 2 were designed and the test protocol developed to provide vital information to address both of these issues. In the following three subsections, more detailed descriptions of test objectives are provided.

1.4.2 Test Building Specific Objectives

1.4.2.1 Performance-Based Seismic Design and Evaluation

Application of performance-based seismic design (PBSD), or performance-based seismic evaluation (PBSE), e.g., based on the PEER framework, has become fairly common. At a minimum, two hazard levels are considered: one associated with fairly frequent earthquakes with a return period of 25 or 43 years (a service-level event), and one associated with very rare earthquakes with a return period of approximately 2500 years (the Maximum Considered Earthquake, or MCE). A comprehensive PBSE might consider many hazard levels, e.g., ATC-58 [ATC 2007] considers 11.

Although relatively complex nonlinear modeling approaches are used to model frame and wall buildings, there is a lack of field and laboratory data available to assess the reliability of these models. With respect to shake table testing, data are mostly available for simple systems with one or two bays and one or two stories, often for effectively two-dimensional, moderate-scale structures utilizing a single lateral-force-resisting system (references) and without gravity-load-resisting systems/members. The test buildings described Chapter 2 and 3 are essentially full-scale, three-dimensional buildings with different lateral-force resisting systems in the orthogonal directions. The availability of detailed measured response data along with observed damage will enable comprehensive system-level studies to assess the following issues: (i) the ability of both simple and complex nonlinear models to capture important global and local responses, including system interactions, both prior to and after loss of significant lateral strength; (ii) the capability of existing modeling approaches to capture loss of axial-load-carry-capacity (collapse); and (iii) the reliability of proposed PBSE approaches for new buildings (e.g., ATC-58) to predict the degree and distribution of damage and the related repair costs, as well as the margin against collapse for very rare events (e.g., MCE or higher level shaking).

1.4.2.1 High-Performance Building with Bonded RC Frame and Unbonded Post-tensioned Walls

One approach that improves a building's performance is self-centering structural systems that utilize unbonded prestressed tendons. Initial research, conducted as part of the U.S. National Science Foundation's (NSF) PREcast Seismic Structural Systems (PRESSS) program in the 1990s [Shiohara 2001; Zhao and Sritharan 2007; Priestley 1991] demonstrated that such systems sustained relatively low damage compared to conventional RC systems under similar loading. This system has been implemented in a 39-story building in California [Priestley 1996] and for bridges [Priestley et al. 1999]. The self-centering framing system tested by the PRESSS program involved relatively complex beam-column connection details. Subsequent research has been conducted to develop alternative systems/details [Englekirk 2002] and to extend the concept to steel structures [Pampanin et al. 2006] and timber structures [Pampanin 2005].

Primary research on self-centering systems in Japan began in 2000, with tests on hybrid column-beam joints with unbonded prestressing tendons and mild steel inside members by Sugata and Nakatsuka [2004], which was similar to the U.S. hybrid column-beam joint system. Sugata and Nakatsuka also proposed a numerical model [2005] to simulate flag shape hysteresis behavior exhibited by these connections, and Niwa et al. [2005] studied unbonded PT precast column-beam joint with external damping devices under the beam. Ichioka et al.

[2009] tested PT precast concrete portal frames with a corrugated steel shear panel placed between the beam and the foundation beam.

As shown in Figure 1.1, shake table testing has been conducted on reduced-scale (25%), three-story PT frames with bonded and unbonded beams [Maruta and Hamada 2010]. Test results demonstrated that PT precast concrete frames were very ductile, yet only minor damage was observed for velocities less than 50 kine. However, due to the self-centering capability, the system displayed low energy dissipation capacity (no damping devices were used). Self-centering systems have been developed and tested for structural steel systems [Ikenaga et al. 2007; Ichioka et al. 2009]; these systems have not yet been used in practice because design procedures have not been established to satisfy the Japanese Building Standard. In addition, the initial cost for the self-centering system is higher than conventional RC systems, and the potential long-term benefits of the system have not been sufficiently studied to assess if the higher initial cost is justified.

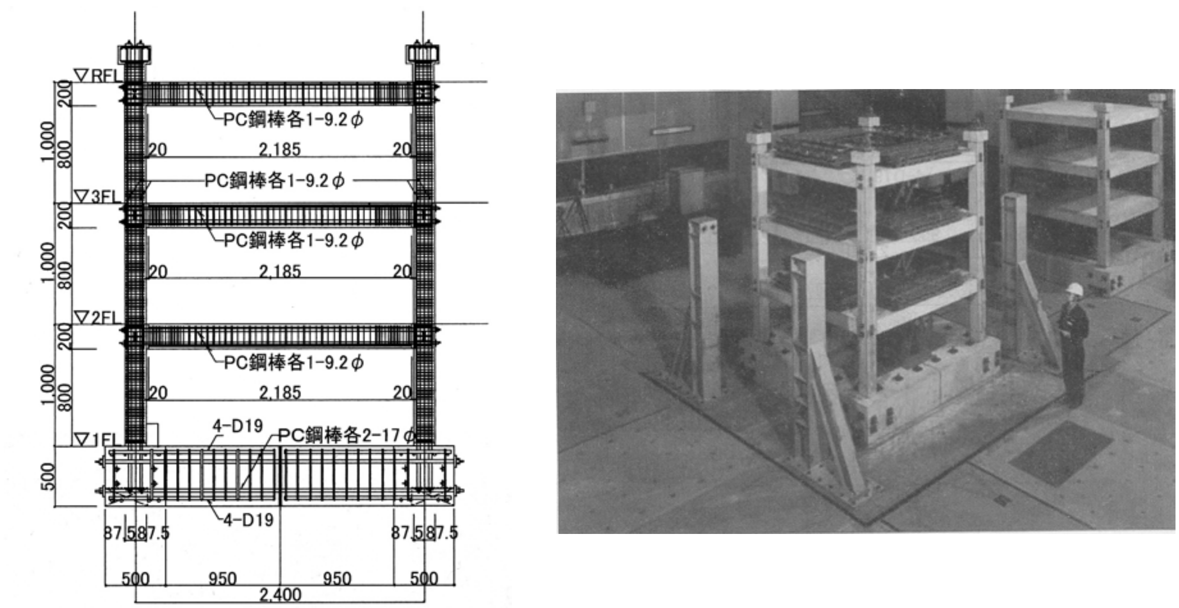

(a) (b)

Figure 1.1 Elevation of the longitudinal frame [Ikenaga et al. 2007].

In this study the PT concrete structure is denoted at the “PT Building.” The design of the building is based on typical Japanese practice, with grouted PT precast prestressed concrete structure for beams and columns and unbounded prestressed concrete shear walls to provide energy dissipation. To adequately compare the response of the RC Building and the PT Building, it was mandatory that the PT Building be designed such that the lateral force capacity of the PT specimen be close to that of RC specimen (for scientific interest); note that the Japanese code requires that the PT Building have slightly larger lateral strength than the RC Building. The PT Building also used high-quality, high-strength concrete. The innovative energy dissipative device utilized in the PT Building—the unbonded PT shear wall—has been investigated previously (see discussion above), but they have not been used in practice in either Japan or the U.S.

1.4.2.3 Reinforced Concrete Building - Moment Frame Direction

The conventional RC building system (RC Building) was designed to satisfy typical seismic design practice in Japan, with the quantity and arrangement of longitudinal and transverse reinforcement conforming to the Building Standard Law Enforcement Order and AIJ Standard. Typical materials were used to construct the test specimen. Preliminary analytical results presented by U.S. researchers at the October 2009 meeting in San Francisco and at the March 2010 meeting in Tokyo indicated that the design also reasonably represented U.S. Special Moment Frame (SMF) construction in California. A detailed assessment of the RC Building relative to U.S. code provisions is presented in Chapter 2.

Reinforced concrete special moment-resisting frames (SMRF) are commonly used in seismic regions, particularly for low- to mid-rise construction. Their behavior during seismic excitation depends on the behavior of individual members (e.g., columns, beams, joints, and slabs) and the interaction between members. Although numerous component tests have been performed on RC columns [Berry et al. 2004], beam-column joints and slab system tests that capture the interaction between these elements are rare [e.g., Ghannoum 2007; Panagiotou 2008]. Even less common are system tests that account for multi-directional dynamic loading effects. The E-Defense tests will help fill the knowledge gap in this area.

The influence of beam-column joint behavior on performance of the RC Building was identified as a topic of interest that could be assessed with the test buildings. Because test data within this range were not well represented in the literature and this range of strength ratios is common in Japan, Hiraishi et al. [1988] conducted quasi-static tests on beam-column joints with column-to-beam strength ratios between 1.0 and 2.0. The test results indicated that the beam-column joint specimens performed uniformly poor, with significant strength loss and severely pinched hysteresis behavior due to bar slip, even if the demand on the joint (from beam yielding) was less than the joint shear strength. Given this information, the RC Building was designed to have beam-column joints that satisfy the weak-beam strong-column concept, but with calculated column-to-beam strength ratios near 1.2 for interior joints and 1.6 for exterior joints, respectively. The objective was to assess the behavior of joints in a conventional design at full scale on the E-Defense shake table.

As the structural engineering field moves towards PBSD, it is increasingly important to accurately model the full nonlinear behavior of SMRFs. Many challenges arise in nonlinear dynamic simulation due to the complex interactions between members and the variability in member boundary conditions. Current key challenges in simulating the seismic behavior of SMRFs are summarized below:

(1) ***Evaluating the "elastic" stiffness of all members:*** Structural stiffness is crucial for obtaining the correct seismic demand. Member stiffness is variable during seismic excitation and largely depends on axial load and level of cracking [Elwood and Eberhard 2009]. Element interactions also play a vital role. For example, strain penetration of longitudinal bars of columns and beams into joints and foundations can affect the stiffness of a structure by as much as 40% [Sezen and Setzler 2008; Zhao and Sritharan 2007]. Strain penetration effects in joints are highly dependent on joint demands and confinement, which can only be obtained from system tests.

(2) ***Evaluating the strength of each member at which its behavior softens significantly:*** In SMRF that strength usually coincides with the yield strength. It is particularly critical to achieve a model with the correct ratios of member strengths so that correct mechanisms are determined. While member yield strength can be estimated with reasonable accuracy for individual columns and beams, it is quite difficult to assess that strength in complete structural systems, particularly for monolithic beam/slab systems and joint construction. Quantifying the contribution of the slab on beam and joint capacities as well as the effect of strain rate effect under dynamic excitation is an especially important challenge that requires full system tests.

(3) ***Simulating the post-"yield" response of each member:*** Dynamic tests that cycle a structural system to very large deformations are necessary to obtain information about post-yield behavior. Structural assessment for the collapse prevention performance objective requires the identification of the deformation at which strength degradation is initiated and the ensuing degrading behavior. Such degradation can be the result of bar buckling, loss of shear strength, and fracture of transverse reinforcement in SMRF. Loading history and load sharing between structural elements both affect the initiation and the propagation of damage in elements. If adjacent elements are able to redistribute loads the behavior of the failing elements is significantly altered [Ghannoum 2007; Elwood and Moehle 2008]. Component tests cannot capture such system effects.

(4) ***Simulating joint deformations and their progression during seismic excitation:*** As with strain penetration effects, joint deformations can significantly affect the lateral stiffness of a SMRF. The joint-softening effect is particularly high at large deformations where joint damage can be substantial. The difficulty in assessing joint behavior stems from the fact that slabs, beams, and columns affect their behavior substantially. The beam-to-column strength ratio has particular influence on joint behavior [Shiohara 2001] as does bi-axial loading.

(5) ***Assessing bi-axial loading effects on columns:*** very few column tests are performed under bi-axial loading and even fewer dynamically. Bi-axial loading affects column strength as well as strength degradation.

1.4.2.4 Reinforced Concrete and Post-tensioned Buildings - Shear Wall Directions

Common Japanese practice uses columns at wall boundaries that are wider than the wall web (so-called barbell-shape). Over the past twenty years in the U.S., however, it has become common practice to design walls with rectangular cross sections. (Based on test results available in the literature, the AIJ Standard for "Structural Calculations of Reinforced Concrete Buildings" was revised in 2010 to show RC walls with rectangular cross section.) Although the deformation capacity attributed to wall shear failure or wall bending compression failure can be estimated using the "AIJ Design Guide Lines for Earthquake

Resistant Reinforced Concrete Buildings Based on Inelastic Displacement Concept," these procedures can be applied to walls with rectangular cross sections. Therefore, walls with rectangular cross sections were used in both the RC and PT Buildings to assess wall behavior at full-scale under dynamic loading. Primary objectives of the tests were to assess the behavior and performance of shear walls with rectangular cross sections to provide data to assess common practice in the U.S. and to potentially change practice in Japan, as well as to enable a side-by-side comparison between the conventional RC walls and high-performance PT walls.

Behavior and modeling of shear walls has received increased attention in recent years because not only do shear wall systems provide substantial lateral strength and stiffness, they are resilient to complete collapse [Wallace et al. 2008; EERI Newsletter 2010]. Recent testing conducted within the NEES-Research program includes quasi-static testing at: (i) nees@UIUC on isolated cantilever walls with rectangular cross sections with and without lap splices by Lowes and Lehman; (ii) nees@Minnesota on isolated, cantilever walls with both rectangular and T-shaped cross sections subjected to uniaxial and biaxial loading by French and Sritharan, and (iii) nees@UCLA by Wallace and nees@Buffalo by Whittaker on low-to-moderate aspect ratio (one to two), isolated walls with rectangular cross sections. Shake table tests on very-large scale, eight-story walls with both rectangular and T-shaped cross sections subjected to uniaxial loading have been conducted at nees@UCSD (Panagiotos and Restrepo). Tests also have been conducted on PT walls (Sause and others). Therefore, the full-scale shake table tests on the RC and PT Buildings will provide a wealth of data, including information on shear wall systems (walls and frames) subjected to three-dimensional, dynamic loading.

Nonlinear modeling of shear walls has been the subject of much research in the last five years, with considerable attention has focused on modeling flexure-shear interaction, i.e., where yielding in shear is observed for relatively slender, isolated walls, with aspect ratios $\left(A_w = h_w/l_w\right)$ between 2.4 (PCA tests) and 3.0 (e.g., see Massone and Wallace [2004]), even though the computed nominal shear strength exceeds the shear demand. The RC Building tested at E-Defense will provide important results for system level tests of slender walls $\left(A_w = 4.8\right)$ coupled by a shallow beam to corner columns at low axial load. The tests will provide data for a case where flexure-shear interaction is expected to be minor. Quasi-static tests are currently being conducted to assess flexure-shear interaction for moderate aspect ratio walls $\left(A_w = 1.5 \text{ to } 2.0\right)$ and quasi-static loading [Tran and Wallace 2010]; future shake table testing is needed to further address this need.

Slightly different detailing has been provided within the yielding regions (plastic hinge regions) of the shear walls on the north and south sides of the conventional RC building to investigate the role of detailing on damageability, lateral strength degradation, and, potentially, the loss of axial load carrying capacity. Given the likely role of detailing on the observed damage in the recent M_w 8.8 February 27, 2010, earthquake in Chile, this aspect of the test is of significant interest.

The impact of modest coupling on lateral story displacements and wall shear forces has not yet been studied, particularly for dynamic loading of three-dimensional building systems. The E-Defense tests will provide a wealth of data to assess these issues, as well as the increase in wall shear with shaking intensity.

2 Test Buildings

Descriptions of the RC and PT buildings are provided in the following sections. Background information is provided on the E-Defense shake table and detailed information on overall geometry, member dimensions, and longitudinal and transverse reinforcement are presented for the RC and PT buildings.

2.1 BACKGROUND

The E-Defense shake table, the largest in the world, has plan dimensions of 20 m × 15 m (Figure 2.1). The table can produce a velocity of 2.0 m/sec and a displacement of 1.0 m in two horizontal directions, simultaneously, and accommodate specimens weighing up to 1200 metric tons. In this study, two four-story buildings were tested, one RC and one PT. The two buildings were almost identical in geometry and configuration, and were tested simultaneously, as shown in Figure 2.2. Each building weighed approximately 5900 kN; therefore the combined weight of the two buildings was 98% of E-Defense table capacity. The test buildings utilized different structural systems to resist lateral forces in the longitudinal and transverse directions. In the longitudinal direction, a two-bay moment frame system was used, whereas in the transverse direction, structural (shear) walls coupled to corner columns by slab-beams were used at each edge of the buildings (Figure 2.3). Story heights at all levels for both buildings were 3 m, for an overall height of 12 m. The plan dimensions of the buildings were 14.4 m in the *x*- or frame direction and 7.2 m in the *y*- or wall direction.

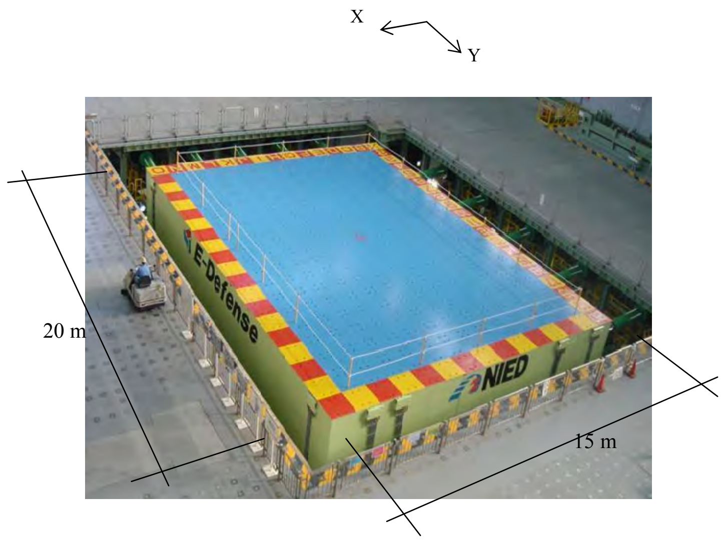

Figure 2.1 E-Defense shaking table.

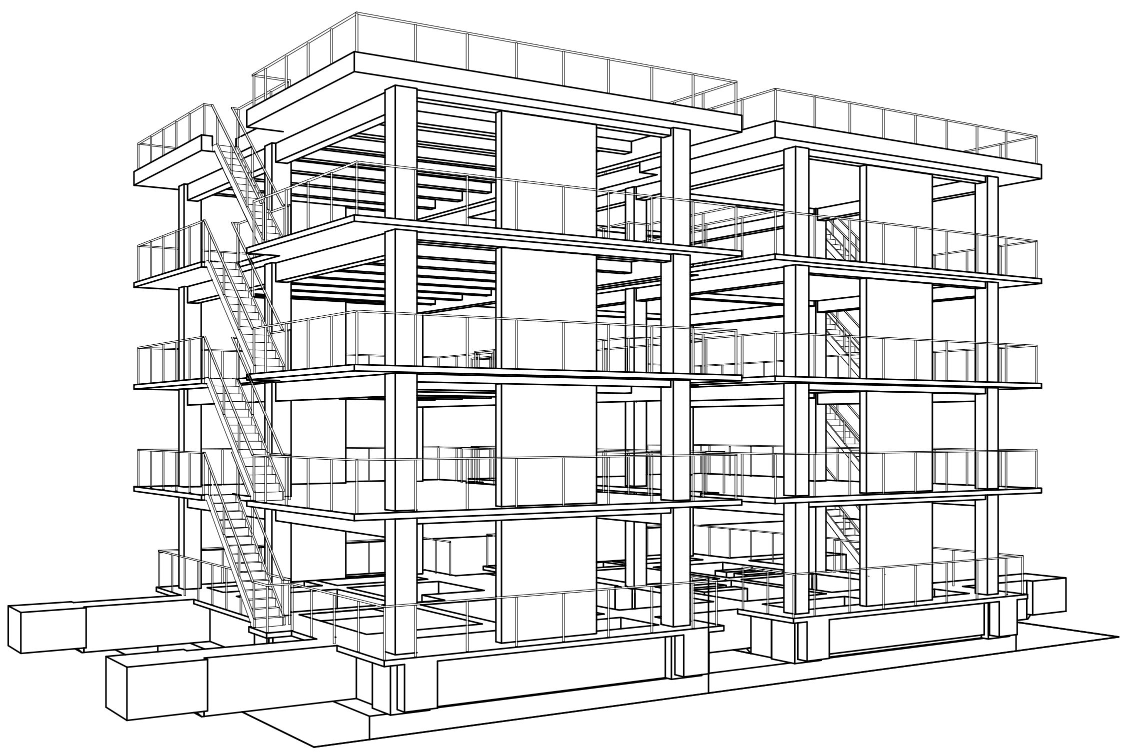

Figure 2.2 Overview of test set up on the shaking table.

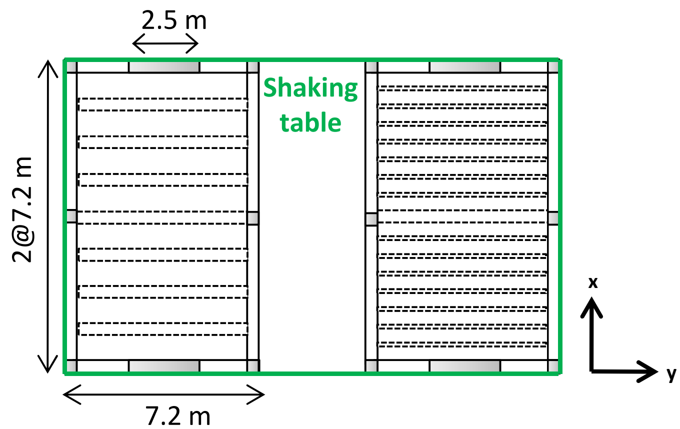

Figure 2.3 Plan view of specimens.

2.2 REINFORCED CONCRETE BUILDING

Plan and elevation views of the structure are shown in Figure 2.3 and Figure 2.4, respectively. Cross-section dimensions of columns were 500 mm × 500 mm, and walls were 250 mm × 2500 mm; beam cross-sections were 300 mm × 600 mm (width × depth) in the *x*-direction and 300 mm × 400 mm for interior beams and 300 mm × 300 mm for exterior beams in the *y*-direction. Additional beams with cross sections of 300 × 400 mm supported the floor slab at intervals of 1.5 m in the *y*-direction. A 130 mm-thick floor slab was used at floor levels 2 through 4 and at the roof level. Detailed information on member geometry and reinforcement used is given in Appendix A.2. Information on the building weight and material properties are contained in Table 2. and Table 2., respectively. Building weight was calculated based on the design, i.e. before the non-structural members were placed in the specimens. Floors 2 through 4 weighed about 900 kN, whereas the weight of the roof was 1000 kN; the remaining weight was in the foundation. The weight of the equipment is presented in Appendix A.1.

The design concrete compressive strength was 27 N/mm^2, with SD345 D19 and D22 bars used for primary longitudinal reinforcement. Information on the longitudinal and transverse reinforcement used in all members is provided in Table 2. and Figure 2.5. Typical concrete stress versus strain relations are given in Figure 2.6. See Appendix A.1 for detailed information on as-tested material properties.

Table 2.1 Weight of RC specimen.

Structural		RC			2.4	t/m^3
		RFL	4FL	3FL	2FL	Base
RC	Column	5.4	10.8	10.8	10.8	5.4
	Girder	16.4	16.4	16.4	16.4	216.2
	Wall	4.1	8.1	8.1	8.1	4.1
	Slab	44.1	43.7	43.3	42.8	10.6
	Beam	8.0	8.0	8.0	8.0	0.0
	Parapet	5.3	0.0	0.0	0.0	0.0
Steel	Temp. Girder	0.0	0.0	0.0	0.0	0.3
Sum	[t]	83.3	87.0	86.6	86.2	236.5
Non-Structural						
Steel	Stair	330	360	360	360	0
	Measurement	0	3000	1750	1690	1690
	Handrail	244	271	271	271	197
Machine	on the slab	4633	180	0	0	0
	under the slab	495	0	0	0	0
	RC Base	6042	346	0	0	0
Ceiling	under the slab	296	0	0	0	0
Sum	[kg]	12040	4157	2381	2321	1887
Total		RFL	4FL	3FL	2FL	Base
Sum		95.3	91.2	89.0	88.5	238.4
Whole Building [t]						602.4

Table 2.2 Design material properties.

(a) Concrete		(b) Steel Bar				
	σ_B (N/mm^2)		Grade	A_{normal} (mm^2)	σ_B (N/mm^2)	σ_B (N/mm^2)
Foundation	33	D22	SD345	387	345	490
Upper Part	27	D19	SD345	287	345	490
		D13	SD295	127	295	440
		D10	SD295	71	295	440
		D10	KSS785	71	785	930

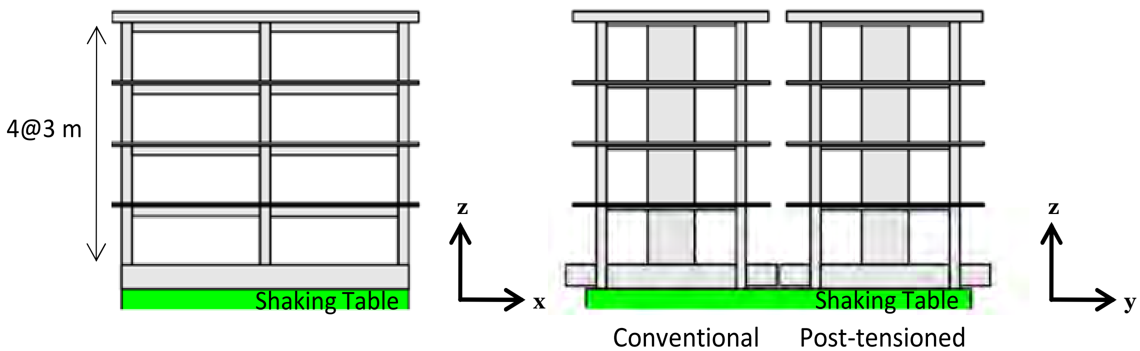

Figure 2.4 Elevation view of specimens.

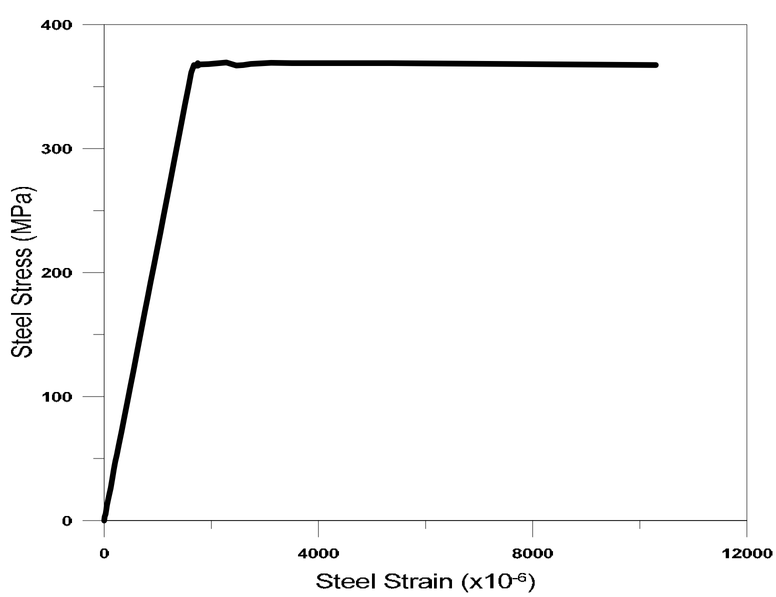

Figure 2.5 Reinforcement stress-strain relations.

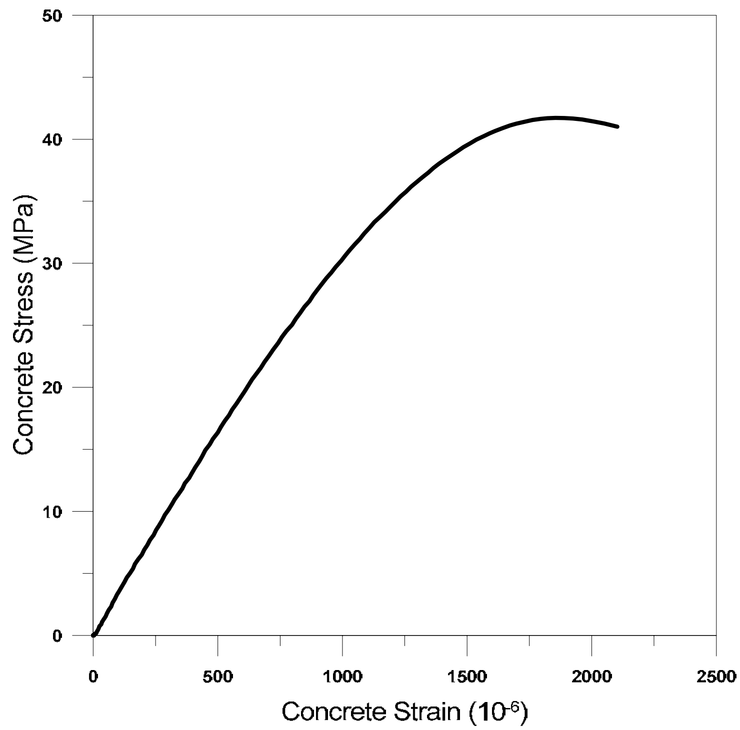

Figure 2.6 Concrete stress-strain relations.

2.2.1 Japanese Standard Law Provisions

The RC buildings were designed to conform to the Japanese Building Standard Law. The Japanese seismic design procedure consists of two stages design; allowable stress design for moderate earthquake level to guarantee the damage control performance, and lateral load capacity design for major to rare earthquake to guarantee the collapse prevention performance.

The base shear coefficient C_b for the allowable stress design is 0.20. The lateral force distribution shape is an A_i distribution, which is similar to inverted triangular where the lateral load at the`top-most stories is slightly larger. For the structural analysis, the building was modeled as linearly elastic. All member response was designed to not exceed the yielding level for reinforcing bars, and the concrete stress response was designed to not exceed the allowable compressive stress of concrete—two third of concrete design strength.

The design base shear coefficients C_b for the lateral load capacity at collapse mechanism of the conventional RC Building were 0.30 in the frame direction and 0.35 in the wall-frame direction, respectively, as all structural members were designed to perform at the highest possible ductility. The lateral capacity of the building was confirmed by pushover analysis that considered nonlinear material characteristics; the lateral force distribution shape A_i was used. Capacity design checks were carried out for shear failure of beams, columns, and shear walls, as well as shear failure of beam-column joints; note that there was no requirement regarding the column-to-beam strength ratio at the beam-column joints. Shear reinforcement provided in columns and beams (in the moment frame or x-direction) and walls (in the y-direction) had shear reinforcement in excess of that required by the Japanese Building Standard Law. Minimum requirements such as the spacing of the steel, anchorage detail, dimension of concrete section as well as concrete cover thickness were designed in accordance with the AIJ Standard for reinforced concrete structures. Thus the RC Building accurately represented a building that followed typical construction practices common in Japan.

2.2.2 Assessment of RC Building using ASCE 7-05 and ACI 318-08

A detailed assessment of the RC Building was conducted to assess whether the final design satisfied U.S. code provisions. This assessment is covered in two subsections—one for the shear wall direction and one for the moment frame direction—to provide the reader with information to help understand the measured responses and observed behavior once this information becomes available.

2.2.2.1 Shear Wall Direction

For the shear wall (y-) direction, the structural system was assumed to be a Building Frame System Special RC Shear Wall $\left(R = 6, C_d = 5\right)$ as the framing provided by the shallow beam and column at the building edge was insufficient for a Dual System designation. Based on this designation, all lateral forces are resisted by the shear wall. Given that the building system is relatively simple, the ASCE 7-05 S12.8 Equivalent (Static) Lateral Force Procedure was used, assuming that the building was located in a region where the mapped short period and 1-sec-period accelerations were 1.5 and 0.9, respectively; for Site Class B, design spectral acceleration parameters were 1.0 and 0.6 with $T_0 = 12$ and $T_S = 0.6$.

The seismic weight (ASCE 7-05, 12.7.2) of the building was taken as the combined dead and live loads as 3630 kN (see Table 2.1), i.e., the live load value includes permanent live load attached to the building. The fundamental period of the building was computed using a two-dimensional model of a single wall, i.e., a cantilever assuming an effective moment of inertia $I_{eff} = 0.51g$ over the full wall height and one-half the seismic weight at the floor levels. A fundamental period of $T = 0.58$ sec was computed from an eigenvalue analysis. According to ASCE 7-05 12.8.2, $T_a = 0.488(h_n = 12 \text{ m})^{0.75} = 0.315$ sec T_a and $T_u = C_u T_a = 1.4T_a = 0.0440$; therefore, $T = 0.44 = T_u$ was used to determine a base shear of $V = C_s = 0.167W = 302.5$ kN. Because only two shear walls were used—one at each end of the building—the redundancy factor (ASCE 7-05 12.3.4) was taken as 1.3. Therefore, $E_h = \rho Q_E = 1.3(302.5 \text{ kN}) = 393.3$ kN (ASCE 7-05 Equation 12.4-3). Vertical earthquake loading (E_V) was included in the load combinations (ASCE 7-05 12.4.2 and 12.4.2.3).

Strength Requirements for Walls: Dead and live loads for the wall were calculated by assuming the dead and live loads (see Table 2.1) were uniformly distributed based on a tributary area equal to the wall length (2.5 m) plus the beam clear length (2.5 m + 2.1 m) times one-half the joist spacing and the slab overhand (0.9 m + 0.8 m), or 7.82 m^2 (84.2 ft^2). Shown in Figure 2.7, the resulting story forces produce wall base moment $M_u = 3569$ kN-m and axial load $P_u = 285$ kN. Note that the axial load ratio is low $\left[P_u / A_g f'_c = 285 \text{ kN} / (0.25 \text{ m} \times 2.5 \text{ m})(27 \text{ MPa}) = 0.017 \right]$. Demands were compared with a wall P-M interaction diagram (see Figure 2.8), demonstrating that the wall P-M strength does not satisfy ASCE 7-05 12.8 requirements.

Capacity Design Checks: Wall shear strength was computed as $\phi V_n = 0.75 A_{cv} \left(\alpha_c \sqrt{f'_c} + \rho_t f_y \right) = 912$ kN, using the minimum horizontal web reinforcing ratio (2D10 @ 200 mm spacing for the wall at axis *C*, $t_w = 250$ mm; $\rho_t = 0.0031$; $\alpha_c = 0.167$; $f'_c = 27$ MPa; $f_y = 345$ MPa). Calculated shear strength $\phi V_n = 912$ kN is much greater than shear demand $V_u = 393$ kN, as would be expected given the relatively high wall aspect ratio $(12 \text{ m}/2.5 \text{ m} = 4.8)$. The wall shear strength at axis *A* is much larger as a result of the 125 mm spacing of the horizontal web reinforcement.

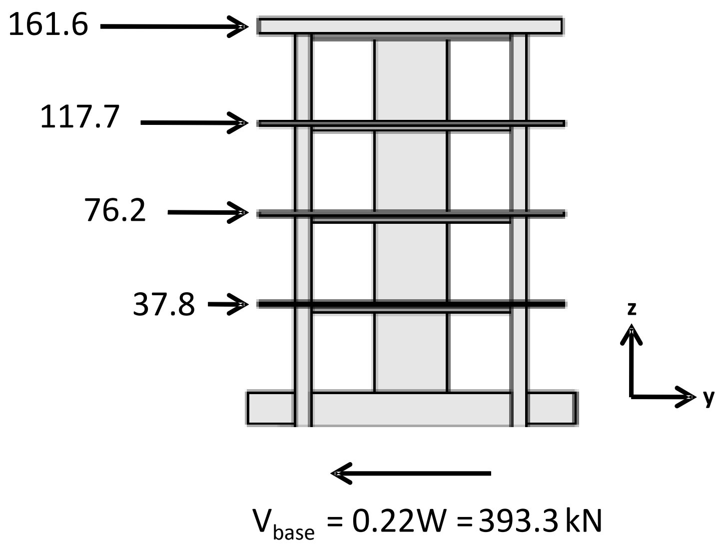

Figure 2.7 Equivalent lateral loads on the shear wall system.

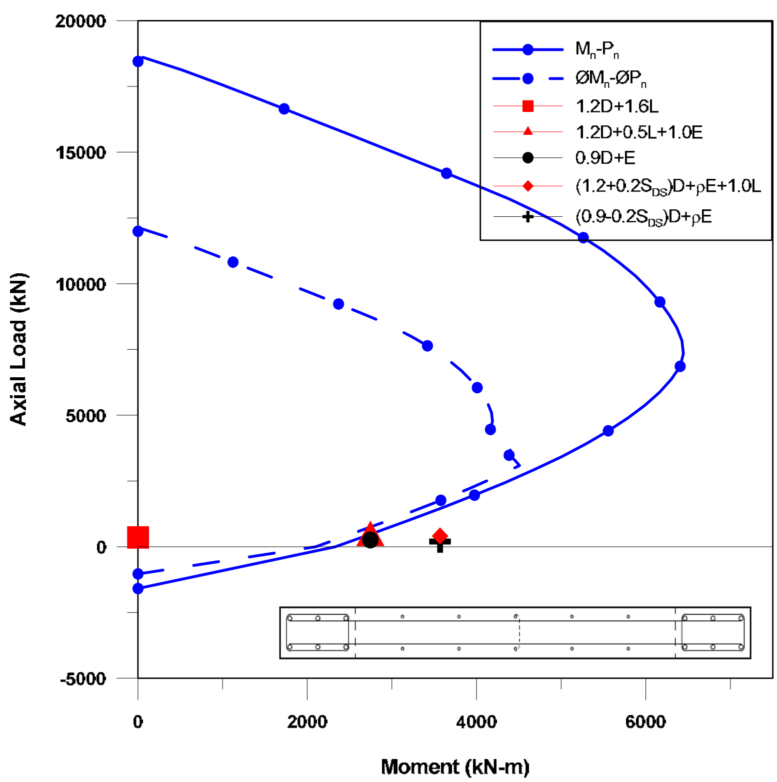

Figure 2.8 P-M interaction diagram for the wall.

Drift Requirements in the Wall: Lateral displacements and story drifts were computed according to ASCE 7-05 12.8.6 and compared to allowable story drift per Table 12.12-1 where $0.02h_{sx}/\rho = 1.3 = 0.0154\,h_{sx}$. Story drift ratios of 0.0045, 0.0113, 0.0151, and 0.0167 were computed (Figure 2.9). The drift ratio for the fourth level exceeded the ASCE 7-05 limit by 8% (0.0167/0.0154 = 1.08).

Detailing Requirements in the Wall: Detailing requirements at wall boundaries were checked using the displacement-based approach of ACI 318-08 21.9.6 (21.9.6.2); the roof drift ratio $\left(\delta_u/h_w = 0.142/12\text{ m} = 0.012\right)$ exceeded the minimum value of 0.007. Based on this value, the critical neutral axis depth using ACI 318-08 equation (21-8) is 352 mm. The neutral axis depth computed for the given wall cross section for an extreme fiber compression strain of 0.003 with $P_u = 285\text{ kN}$ is 244 mm; therefore, special boundary elements are not required per 21.9.6.2. The vertical reinforcing ratio of the boundary reinforcement [$\rho = 6A_b/h(2x+a) = 0.017$, with $A_b = 284\text{ mm}^2$, $h = 250\text{ mm}$, $\left(2x+a\right) = 400\text{ mm}$], exceeded $\rho = 2.3/f_y = 0.0067$, where $f_y = 345\text{ MPa}$; therefore, ACI 318-08 21.9.6.5(a) must be satisfied as a hoop spacing cannot exceed 203 mm. The configuration and the spacing used at the wall boundary satisfies the requirements of 21.9.6.5(a), since the spacing of hoops and crossties is 80 mm (axis *A*) and 100mm (axis C), and a hoop and a crosstie are provided (all 6 bars are supported) over a depth of almost 400 mm, which significantly exceeds the minimum depth required from 21.9.6.4(a) of one-half the neutral axis depth (244 mm/2).

If the "stress-based" approach of 21.9.6.3 is used, however, the extreme fiber compression stress of $f_c = M_u/s + P_u/A = 11.56\text{ MPa}$ ($M_u = 3569\text{ kN-m}$; $P_u = 285\text{ kN}$; $I_g/S = 0.26\text{ m}^3$; and $A_g = 0.625\text{ m}^2$) significantly exceeds the stress limit of $0.2f_c' = 5.4\text{ MPa}$, with 21.9.6.4 left to be satisfied and requiring special boundary elements. Based on a wall boundary zone with $b_{cx} = 160\text{ mm}$, $b_{cy} = 320\text{ mm}$, $A_{shx} = 2A_b$, $A_{shy} = 3A_b$, $A_b = 78.5\text{ mm}^2$, $s = 80\text{ mm}$ (axis *A*) or 100 mm (axis *C*), $f_c' = 27\text{ MPa}$, and $f_{yt} = 345\text{ MPa}$, the provided A_{sh} values are 1.39 and 2.09 times that required by ACI 318-08 Equation (21-5) for 100 mm spacing, satisfying 21.9.6.4. Note that the provided A_{sh} values are only 0.45 and 0.34 times that required by ACI 318-08 Equation (21-4).

In summary, the RC shear wall generally satisfies ASCE 7-05 and ACI 318-08 requirements for the assumed design spectrum, although the wall P-M strength does not meet the requirement and the interstory drift ratio in the top floor exceeds the limiting value by 8%. (see Figure 2.9).

2.2.2.2 Frame Direction

For the frame (x-) direction, the structural system was assumed to be a Special Reinforced Concrete Moment Frame $\left(R = 8, C_d = 5.5\right)$, whereby the lateral forces are resisted by a four-story, two-bay frame at the perimeter of the building.

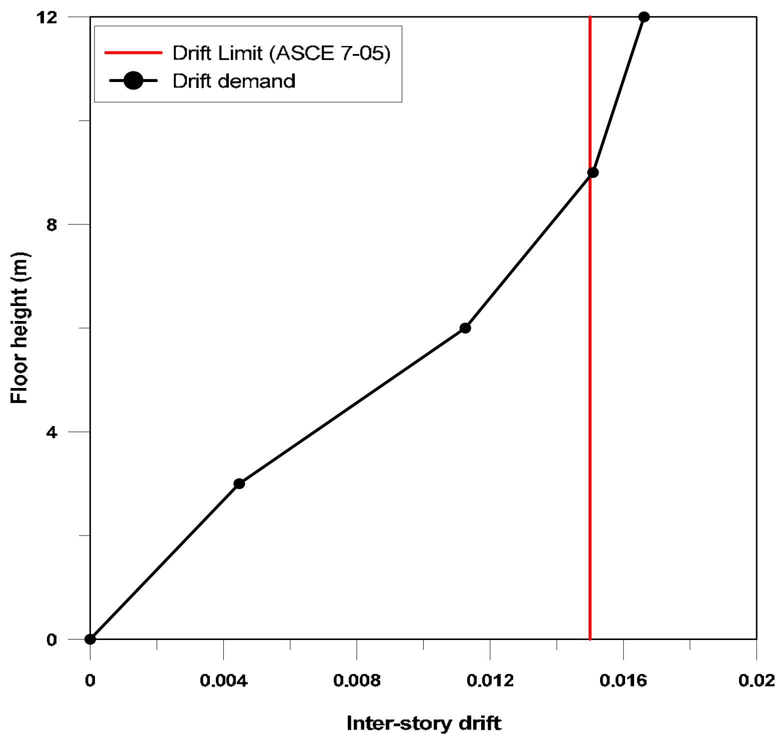

Figure 2.9 Interstory drift demands for the wall.

The fundamental period of the building was computed using a two-dimensional model of a single perimeter moment frame, assuming an effective moment of inertia $I_{eff} = 0.3I_g$ for beams and columns (based on ASCE-41) and one-half the seismic weight at the floor levels. A fundamental period of $T = 0.67$ sec was computed from an eigenvalue analysis. According to

ASCE 7-05 12.8.2, $T_a = 00466(h_n = 12\text{ m})^{0.9} = 0.44\text{ sec}$ and $T_u = C_u T_a = 1.4 T_a = 0.610$; therefore, $T = 0.56 = T_u$ was used to determine a base shear of $V = C_s W = 0.125W = 226.9\text{ kN}$. The redundancy factor (ASCE 7-05 12.3.4) was taken as 1.3, since the structure was expected to have an extreme torsional irregularity by loss of moment resistance at the beam-to-column connections at both ends of a single beam (which is the worst case scenario); therefore, $E_h = \rho Q_E = 1.3(226.9\text{ kN}) = 294.9\text{ kN}$ (ASCE 7-05 Equation 12.4-3). Vertical earthquake loading (E_y) was included in the load combinations (ASCE 7-05 12.4.2 and 12.4.2.3).

Strength Requirements for Beams and Columns*:* Dead and live loads for the beams and columns—calculated by assuming the dead and live loads (see Table 2.1)—were uniformly distributed based on a tributary area associated with the member, e.g., for the corner column this is equal to approximately one-eighth the entire floor plan minus one-half the wall tributary area, or 18.1 m^2 (81 ft^2) (see Figure 2.10). Using the same spectral acceleration parameters and seismic weight that were used in the shear wall system calculations, the ASCE 7-05 S12.8 Equivalent (Static) Lateral Force Procedure was used; the resulting story forces are shown in Figure 2.11. These forces were applied to the two-dimensional model to compute the member demands. At the base of the first story, columns values were computed to be M_u = 205 kN-m and axial load P_u = 772 kN for the corner columns (C1), and M_u = 200 kN-m and P_u = 1222 kN for the interior column (C2). Note that the axial load ratio was $P_u / A_g f_c' = P_u = 772\text{ kN}/(0.5\text{ m} \times 0.5\text{ m})(27\text{ MPa}) = 0.11$ for the corner columns and 0.18 for the interior column.

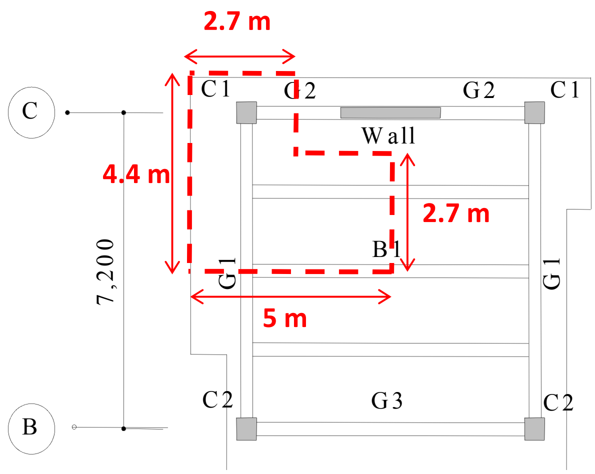

Figure 2.10 **Tributary area for corner column C1.**

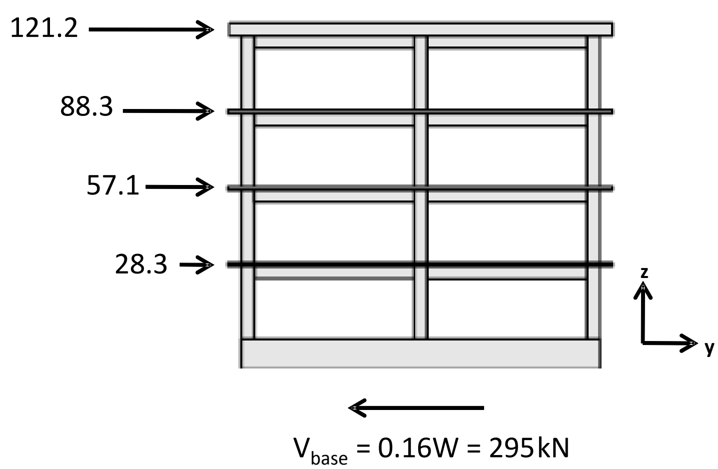

Figure 2.11 **Equivalent lateral loads on the frame system.**

Beam and column nominal moment capacities were computed, and the column, beam, and joint shear demands computed to assess if the system satisfied capacity design concepts that promote beam yielding. Slab effective widths were based on the provisions of ACI 318-08 8.12. Calculation details are provided in Appendix B. The concrete stress-strain relation was assumed to have a peak of 27 MPa (3.9 ksi) at 0.002 strain, and the steel stress-strain relation was assumed as an elastic-perfectly plastic behavior with a yield strength of 345 MPa (50 ksi) and an ultimate strength of 490 MPa (71 ksi). Moment and axial load demands of the columns were compared with a column P-M interaction diagram (Figure 2.12) and for the corner column (C1) (Figure 2.13) and the interior column (C2), respectively. The results demonstrate that the column P-M strengths satisfy ASCE 7-05 12.8 requirements.

In addition, beam moment demands were checked in accordance with the provisions of ACI 318-08 S21.5 such that $M^{+}_{n} > M^{-}_{n}/2$, and neither negative or positive moment strength at any section along the member length was less than one-fourth the maximum moment strength at the face of either joint. The amount of reinforcement in the beams was $A_{s,provided} = 1140\ \text{mm}^2$ ($\rho_{provided} = 0.007$), which is much greater than the minimum required reinforcement per ACI 318-08 S21.5.2, $A_{s,\min} = 654\ \text{mm}^2$, and less than the maximum allowed reinforcement ratio $\rho_{\max} = 0.025$. The reinforcement was continuous along the entire span, indicating that beam moment strengths satisfy the provisions of ACI 318-08 21.5.

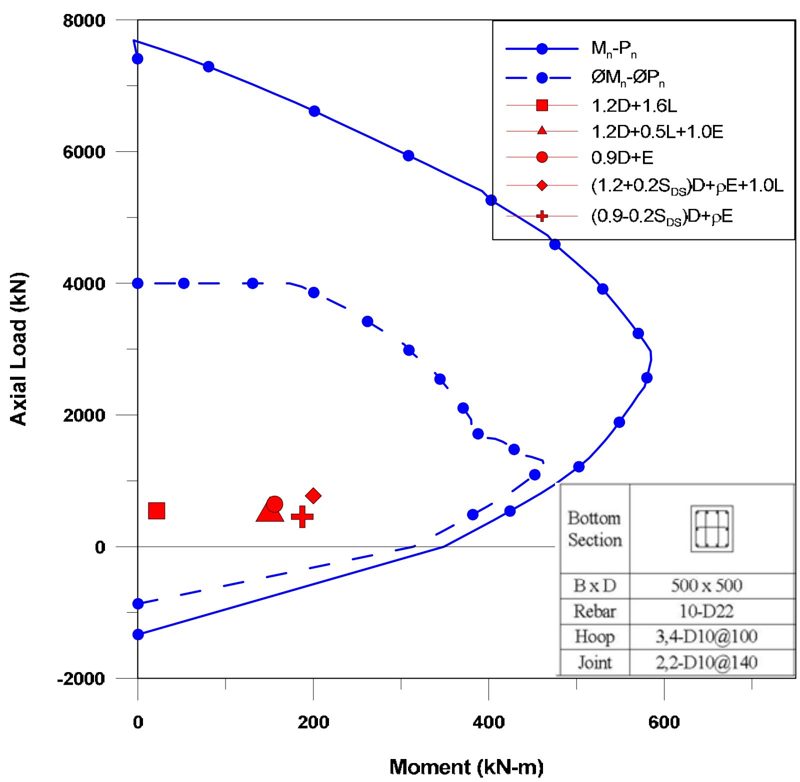

Figure 2.12 P-M interaction diagram for corner column C1.

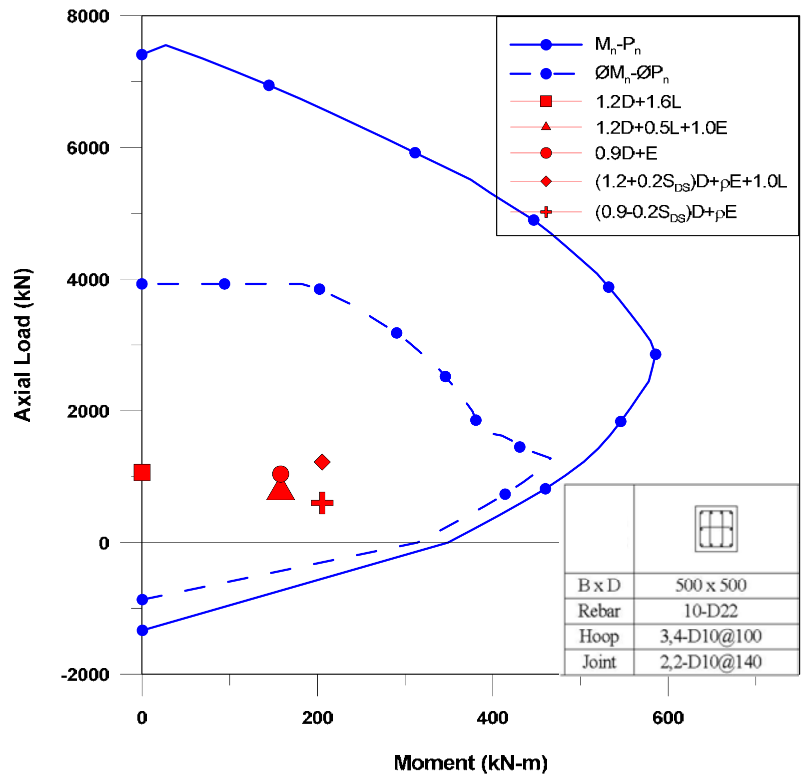

Figure 2.13 P-M interaction diagram for interior column C2.

Capacity Design Checks

<u>Columns Shear Strength (21.6.5):</u> Beam shear demands were determined as when beam probable moment strength was reached (calculated using f_s = 1.25 f_y), column shear when column probable moments were reached, and beam probable moments reached for the interior, first-story column [see Figure 2.14(a)] and a typical beam [Figure 2.14(b)]. Nominal shear strengths also are shown, demonstrating that beam and column shear strengths were sufficient to develop the beam probable moments, and the column shear strength was sufficient to resist the column shear developed at column probable moments.

<u>Beam Shear Strength (21.5.4):</u> ACI 318-08 requires that beams of special moment frames be designed such that flexural yielding occurs prior to shear failure. Therefore, beam shear strengths were checked to sufficient capacity to resist the shear that develops when the beam reaches its probable moment of flexural capacity at each end (see Figure 2.15). The demand calculation was based on the gravity loading on the beams and beam probable moments. Shear demand and capacity in the beams are also shown in Figure 2.15. Results of

this assessment are shown in Figure 2.13, demonstrating that beam shear strength satisfied ACI 318-08 requirements for a special moment frame.

Strong-Column Weak Beam (21.6.2): The strong column–weak beam provision of ACI 318-08 was checked at all floor levels; this requires that sum of column nominal moment strength $\sum M_{nc}$ be at least 1.2 times the sum of the beam nominal moment strengths $\sum M_{nb}$. Column flexural strengths were calculated with the factored axial force, resulting in the lowest strength [where $(0.9\text{-}0.2S_{DS})\ D + \rho E$)]. Beam nominal strengths were calculated including an effective slab width per ACI 318-08 8.12. Results presented in Figure 2.16 demonstrate that corner columns satisfy these requirements, whereas interior columns have the column-to-beam strength ratios about 1.0 (< 1.2). Note that the ratio at the roof level connections is smaller than 1.0, indicating that column yielding might occur at the roof level.

The design of beam-column joints was calculated according to ACI 318-08, Section 21.7, defined as: (1) joint shear demand V_u; (2) joint nominal shear strength ϕV_n; (3) required transverse reinforcement; and (4) required anchorage. Next, each of these parameters are assessed to determine whether or not the given requirements are satisfied for an interior connection (case 1: G1-C2-G1), and for an exterior connection (case 2: G1-C2). Additional details and information for other connections are provided in Appendix B.

$$M_{pr,col} = 1.25(M_{n,col} = 486) = 607kNm \qquad M^{+}{}_{pr,b} = 1.25(M^{+}{}_{n,b} = 386) = 483kNm$$

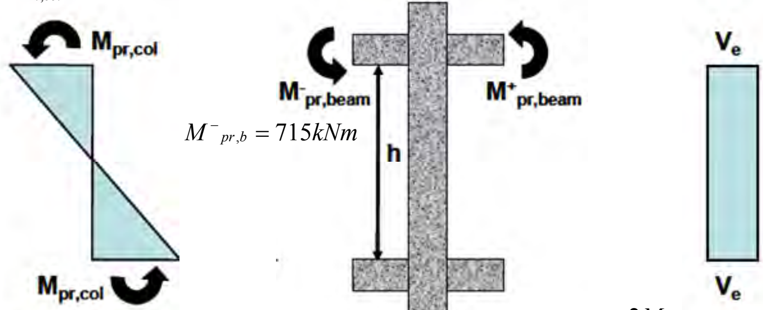

$$M^{-}{}_{pr,b} = 715kNm$$

$$M_{pr,col} = 1.25(M_{n,col} = 486) = 607kNm$$

$$V_E^{(1)} = \frac{2M_{pr,col}}{h} = \frac{2(607kNm)}{h = 2.4m} = 506kN$$

$$V_E^{(2)} = \frac{M^{+}{}_{pr,b} + M^{-}{}_{pr,b}}{h} = \frac{1198kNm}{h = 2.4m} = 499kN$$

$$\phi V_N = (0.75)(V_N = 675) = 506kN$$

Figure 2.14 Column shear strength demands.

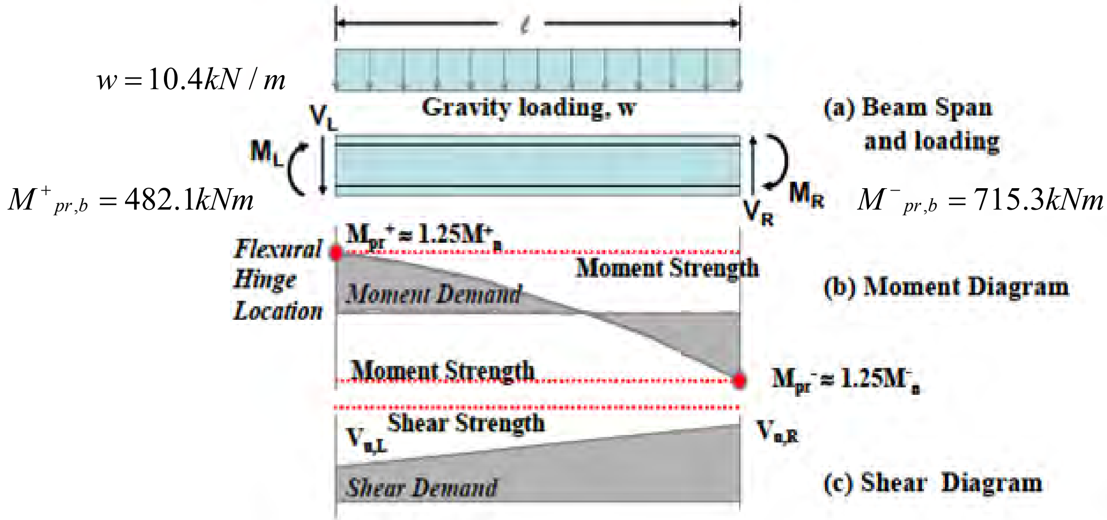

$$\left[V_{u,pr}\right]_R = \left[V_{u,pr}\right]_{\max} = \frac{M^+{}_{pr,b} + M^-{}_{pr,b}}{l} + \frac{w_g l}{2} = 214kN$$

$$\phi V_N = (0.75)(V_N = 289) = 217kN$$

Figure 2.15 Beam shear strength demands.

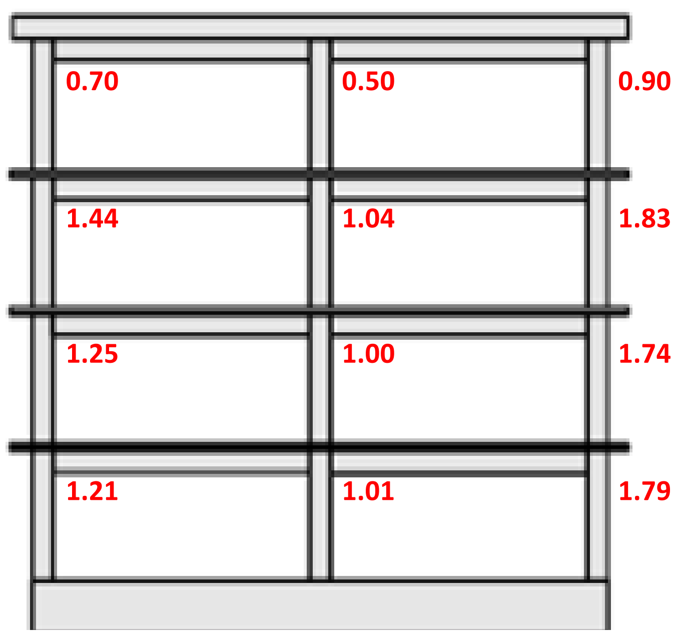

Figure 2.16 Column-to-beam strength ratios.

.

Given the weak-beam requirements and capacity design requirements for beam and column shear, beams that frame into beam-column joints are typically assumed to yield prior to the columns. Therefore, the demands on the joint are controlled by the quantity of longitudinal reinforcement used in the beams, as well as the stress developed in these bars. In ACI 318-08 S21.5.4, the probable moment is calculated for a minimum longitudinal reinforcement stress of $1.25f_y$. Joint shear demand for both cases was calculated using horizontal joint equilibrium (Figure 2.17) resulting in: $V_{u,joint,1} = 1.25A_{s,b1}f_y + 1.25A_{s,b2}f_y - V_{c1}$ for an interior connection (case 1), and $V_{u,joint,2} = 1.25A_{s,b2}f_y - V_{c1}$ for an exterior connection (case 2). Here, V_{c1} represents the column shear, which can be estimated as $V_{c1} = M_{c1}/(h_{clear}/2)$ where $M_{c1} = M_{c2} \approx (M_{pr,b1} + M_{pr,b2})/2$ for case 1, and $M_{c1} = M_{pr,b1}/2$ for case 2. According to Section 21.7.4, joint shear demands for case 1 and case 2 are $V_{c1,1}$ = 936 kN and $V_{c1,2}$ = 538 kN, respectively. Using values of $\phi_v = 0.85$, and $\gamma_v = 12$ (for both cases), the joint shear capacities calculated according to Section 21.7.4 are: $\phi V_{u,1} = \phi V_{u,2}$ = 1097 kN. Note that the nominal shear capacities are greater than shear demands.

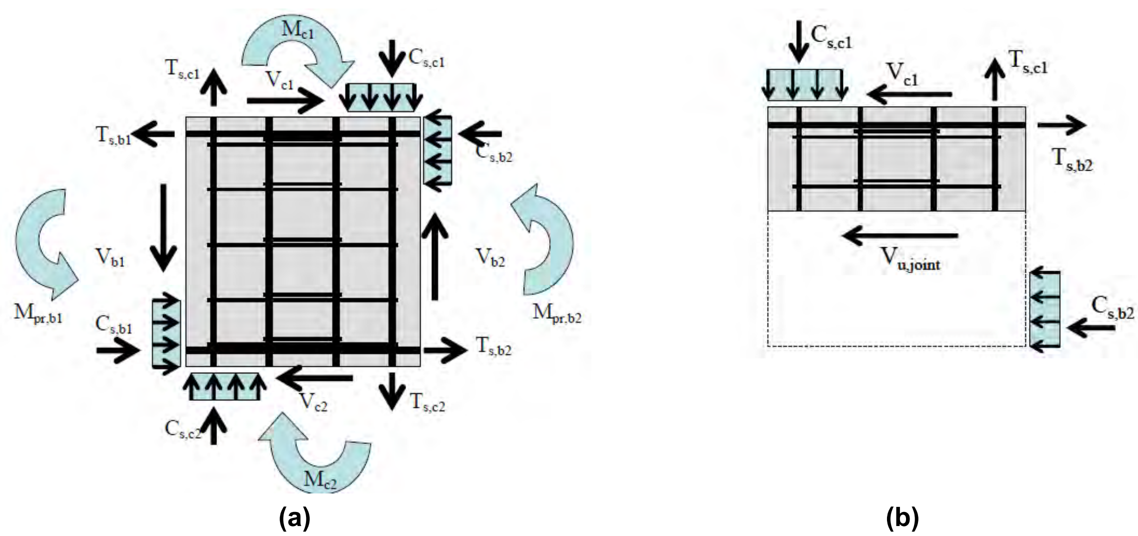

Figure 2.17 Free body diagrams for (a) interior and (b) exterior beam-column connection.

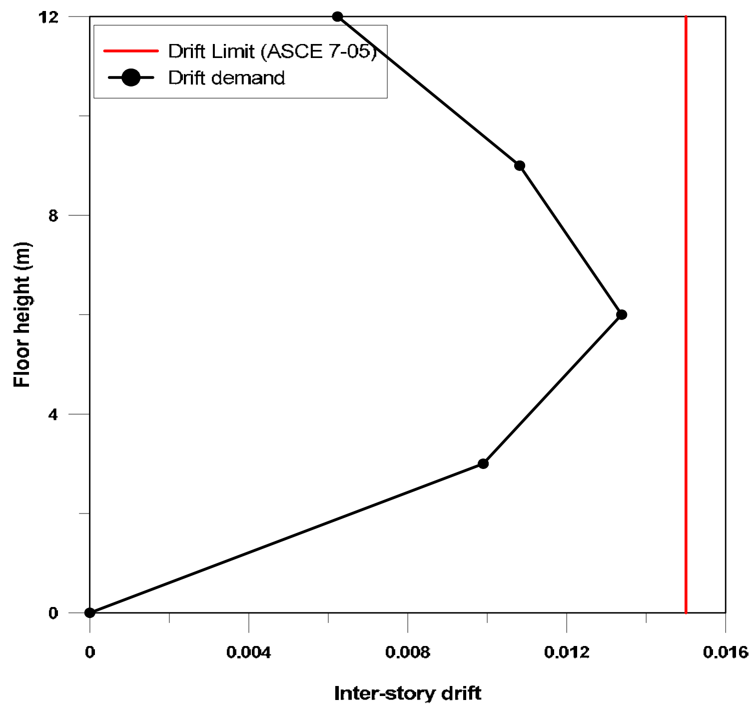

Figure 2.18 Interstory drift demands for the frame system.

Drift Requirements in the Frame: Lateral displacements and story drifts were computed according to ASCE 7-05 12.8.6 and compared to allowable story drift per ASCE 7-05 Table 12.12-1 of $0.02h_{sx} / \rho = 1.3 = 0.0154h_{sx}$. As was done to determine the fundamental period, effective moment of inertia values of $0.3I_g$ were used for the beams and columns based on ASCE 41-06 recommendations. Story drift ratios of 0.0099, 0.0134, 0.0108, and 0.0068 were computed, and, the drift ratios did not exceed the ASCE 7-05 limit (Figure 2.18).

Detailing Requirements: Detailing requirements for columns were compared with ACI 318-08 S21.6.4 provisions. Spacing of the transverse reinforcement in the columns was compared with the ACI 318-08 S21.6.4.3 provisions where the minimum required transverse reinforcement spacing is:

$$s_{\min} = \min(h/4 = 125 \text{ mm};\ 6d_{lb} = 132 \text{ mm};\ s_o = 140 \text{ mm};\ 6 \text{ in.} = 152.4 \text{ mm}) = 125 \text{ mm}$$

where $s_o = 4 + (14 - h_x/3)$ and $h_x = 240 \text{ mm}$ Using ACI 318-08 S21.6.4.4, the minimum required spacing was also calculated to provide the transverse reinforcement. For example, for the interior column at the base, transverse reinforcement quantity was obtained as $A_{sh} = 4A_b = 314 \text{ mm}^2$, where $A_b = 78.5 \text{ mm}^2$, $s_{\min} = 73 \text{ mm}$ (ACI 318 21-4) and $s_{\min}$=107 mm (ACI 318 21-5), where f_c = 27 MPa, f_y = 345 MPa, $b_c = 417 \text{ mm}$, $A_g = 250{,}000 \text{ mm}^2$, and $A_{ch} = 417^2 \text{ mm}^2$.

$$s_{\min} = \frac{A_{sh}}{0.3b_c \frac{f'_c}{f_y}\left[(\frac{A_g}{A_{ch}} - 1)\right]} = 73 \text{ mm} \qquad \text{Eq. (1) (ACI 318 21-4)}$$

$$s_{\min} = \frac{A_{sh}}{0.09b_c \frac{f'}{f_y}} = 107 \text{ mm} \qquad \text{Eq. (2) (ACI 318 21-5)}$$

Therefore, the spacing provided in the column (*s* = 100 mm) satisfies all spacing requirements except $s_{\min} = 73 \text{ mm}$ determined from (Eq .21-4). This spacing requirement is not satisfied either at the other floors or in the corner columns. Note that the required transverse reinforcement should be based on these limits within a height of l_o, which is $l_o = \min\,(h = 500 \text{ mm};\ 1/6h_{clear} = 400 \text{ mm};\ 18 \text{ in.} = 152.4 \text{ mm}) = 400 \text{ mm}$ (see Figure 2.19). Beyond l_o, ACI 318 limits the spacing to

$$s_{\min} = \min\,(6d_{lb} = 132 \text{ mm};\ 6 \text{ in.} = 152.4 \text{ mm}) = 132 \text{ mm}$$

therefore, beyond l_o (i.e., within the middle portion of the column height), ACI 318 requirements are satisfied because *s* = 100 mm is used.

Detailing requirements at the beams also were checked using ACI 318-08 S21.5.3. Hoops are required over a length equal to twice member depth (2*h* region = 1200 mm) (see Figure 2.19). Minimum required spacing in this region was calculated as

$$s_{\min} = \min\,(d/4 = 150 \text{ mm};\ 8\text{d}_{\text{bl}}{=}176;\ 24\text{d}_{\text{bt}}{=}240; 12 \text{ in.} = 304.8 \text{ mm}) = 150 \text{ mm}$$

which does not satisfy the provision, since the provided spacing is *s* = 200 mm. Beyond the 2*h* region, where hoops are not required by ACI 318, minimum spacing is defined as $s_{\min} = d/2 = 273 \text{ mm}$ and is satisfied.

Required transverse reinforcement in the beam-column joints is calculated according to Section 21.7.3.1. Since b_w < ¾ b_{col}, the required transverse reinforcement is 100% of A_{sh} computed for columns. This provision is not satisfied for the same reason as found in the case of columns (see detailed discussion in the previous section regarding this issue). Development length of bars in tension was calculated according to Section 21.7.5 [$l_{dh} = f_y\, d_b$ / (65 $(f'_c)^{0.5}$]. For both cases of joints this provision is satisfied since the actual development length is greater than the required value.

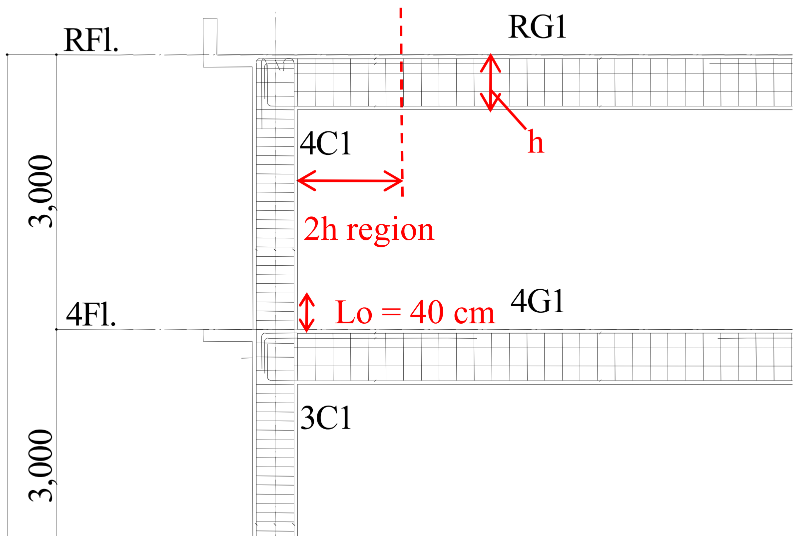

Figure 2.19   Locations where special hoop requirements are needed.

2.2.2.3   Collapse Mechanism

A collapse mechanism analysis was conducted for both the shear wall and moment frame directions using the code prescribed distribution of lateral forces over the building height. Four different collapse mechanisms were assumed for each direction: column yielding at the first, the second, the third, and the fourth floors. Figure 2.20 shows base shear calculated for each collapse mechanism assumption. For the moment frame, the expected collapse mechanism is beam hinging accompanied by hinging at the base of first floor columns and at the top of the second floor columns (Figure 2.21). For the shear wall direction, the mechanism involves beam hinging accompanied by yielding at the base of first floor walls (Figure 2.22). The actual strength coefficients are approximately 0.45 and 0.50 for the moment frame and wall-frame directions, respectively, or 3.6 and 3.0 times the values given in ASCE 7-05. Note that the overstrength factors given in ASCE 7-05 Table 12.2-2 are 3.0 and 2.5 for the moment frame and shear wall, respectively. Therefore, the computed overstrengths for the wall and moment frame are higher than expected (3.6 versus 3.0 for frame and 3.0 versus 2.5 for shear wall direction).

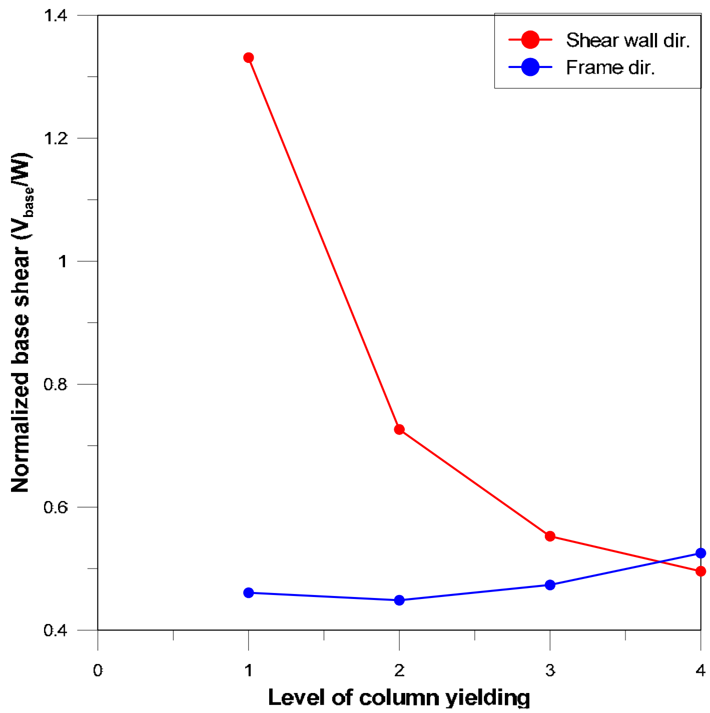

Figure 2.20 Collapse mechanism assessment-influence of column yielding level.

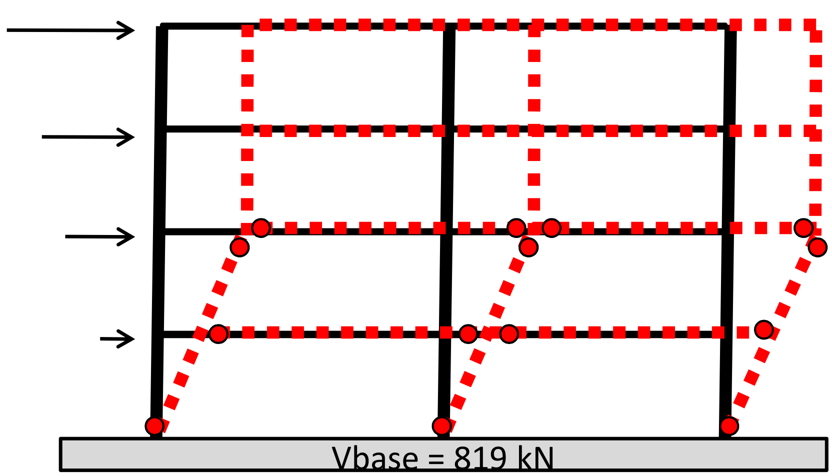

Figure 2.21 Controlling collapse mechanism in the frame direction.

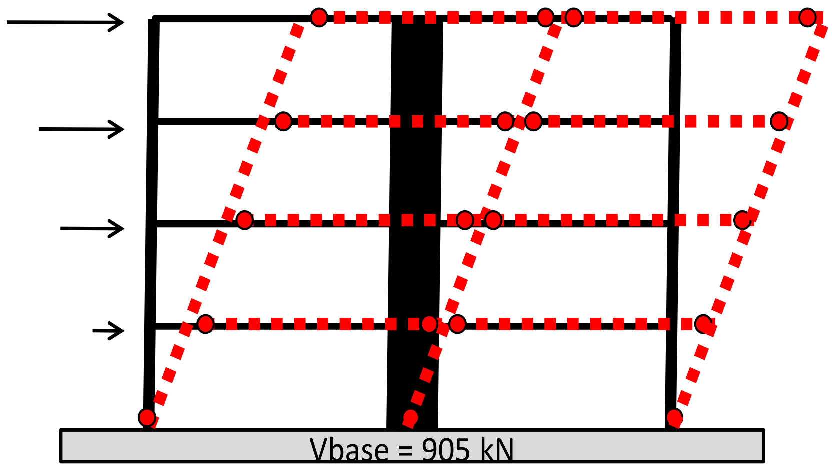

Figure 2.22 Controlling collapse mechanism in the wall direction.

2.3 POST-TENSIONED BUILDINGS

Table 2.3 details the weight and material properties of the specimen. The weight of each floor from the second to the fourth floor was about 900 kN and the weight of roof floor was 1000 kN. The weight above the foundation was about 3700 kN. The design strength of the precast concrete was 60 N/mm^2. The plan is shown in Figure 2.3 and the elevation in Figure 2.4. The columns were 450 mm x 450 mm square, the walls 250 mm x 2500 mm thick, and the beams 300 mm x 500 mm in the longitudinal direction. The beam of interior frame was 300 mm x 300 mm in the transverse direction, and the beam of exterior frame was 300 mm x 300 mm. The floor slab was 130 mm thick. Beams 300 x 300 mm square supported the floor slab at intervals of 1.0 m in the transverse direction.

Table 2. Design material properties of post-tensioned specimen.

STEEL		Grade	A_{normal} (mm^2)	σ_y (N/mm^2)	σ_t (N/mm^2)
	D22 (ED for wall base)	SD345	387	385	563
	PT bar ϕ21 (1-3Fl column)*	C	346.4	1198	1281
	PT bar ϕ21 (3-RFl column)*	C	346.4	1189	1273
	*σy of 0.2% offset				
		Grade	A_{normal} (mm^2)	F_y (kN)	F_t (kN)
	PT wire ϕ15.2 (ED of wall base)*		140.7	250	277
	PT wire ϕ15.2 (beam)*		140.7	255	279
	PT wire ϕ17.8 (beam)*		208.4	356	404
	PT wire ϕ19.3 (beam)*		243.7	429	481
	* F_y of 0.2% offset				

CONCRETE		F_c (N/mm^2)	σ_B (N/mm^2)
	Precast concrete (normal)	60	83.2
	Precast concrete (fiber)	60	85.5
	Top concrete	30	40.9

Grout

GROUT		F_c (N/mm^2)	σ_B (N/mm^2)
	Column base, wall base and beam end	60	135.6
	Wall base (fiber)	60	120.3
	PT duct of PT bar and PT wire	30	63.4

The specimen was designed with a typical Japanese PT frame structure in the longitudinal direction, but with a new type of unbonded PT wall-frame structure in the transverse direction. Table 2.4 lists the reinforcing details. Figure 2.23 shows details of the whole steel arrangement. Beam to column connection detail, details of wall, and the construction procedure are provided in Appendix A.3. The precast concrete members were assembled at the construction site, and then half-precast beams and half-precast slabs were fixed using topping concrete. The half-precast slabs were supported by pretensioned, prestressed beams at 1-m intervals. The design strength of the topping concrete was 30 N/mm^2. The design strength of the grout mortar was 60 N/mm^2. The PT reinforcement of the columns was a high-strength steel bar whose nominal strength was 1080 N/mm^2. The PT reinforcement of beams and walls was high-strength steel strands whose nominal strength was about 1600 N/mm^2. The PT tendons located in sheaths of columns and beams of the longitudinal direction were grouted. The PT tendons located in sheaths of walls and beams in the transverse direction were not grouted and remained unbonded from anchor to anchor. The normal steel bars cross the wall and foundation interface remained unbonded in half of the first story wall length. The nominal strength of the normal steel bar was 345 N/mm^2. The column, wall, and beam of the longitudinal direction contained the amount of shear reinforcement required by the Japanese Building Standard Law. In the transverse direction, the walls and beams were confined by high-strength steel bars. The nominal strength of the steel bar was 785 N/mm^2. In the first and second stories, one of two walls was additionally reinforced by steel fibers.

The corresponding grout beds were reinforced by steel fibers as well. The steel fiber for the wall concrete was 30 mm long with a nominal strength of 1000 N/mm^2. The steel fiber for grout bed was 10 mm long with a nominal strength of 1500 $N//mm^2$. The effective stress of the PT tendon was designed to be 0.6 times of the yield strength for the walls and beams in the exterior frame of the transverse direction. The effective stress of the PT tendon was designed to be 0.8 times of the yield strength for the others.

Table 2.4 Reinforcement details for PT building.

List of Column

		PC1
4Fl. 3Fl. 2Fl. 1Fl.	Section	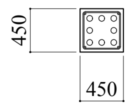
	Tendon	8-21mm(SBPR1080/1230)
	Rebar	4-D19
	Hoop	D10@100

List of Wall

		P Wall
4Fl. 3Fl. 2Fl.	Section	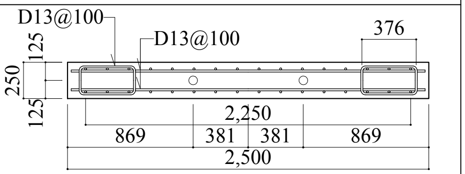
	Tendon	3-10-15.2mm(SWPR7B)
	V bar	D13@150(double)
	H bar	D13@100(double)
1Fl.	Top Section	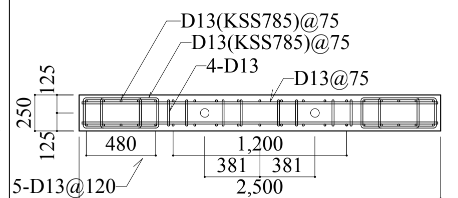
	Bottom Section	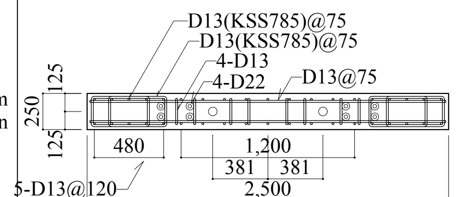
	Tendon	3-10-15.2mm(SWPR7B)
	V bar	
	H bar	

List of Girder

		PG1	
	Location	End	Center
RFl.	Section	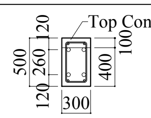	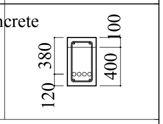
	Tendon	4C-1-15.2mm(SWPR7BL)	
	Top	2 - D19	
	Bottom	3 - D19	
	Stirrup	2-D10@150	2-D10@200
	Web	―	
4Fl.	Section	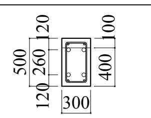	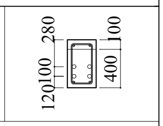
	Tendon	4C-1-19.3mm(SWPR7BL)	
	Top	2 - D19	
	Bottom	3 - D19	
	Stirrup	2-D10@100	2-D10@200
	Web	―	
3Fl. 2Fl.	Section	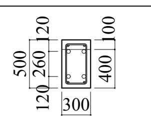	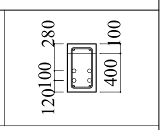
	Tendon	4C-3-15.2mm(SWPR7BL)	
	Top	2 - D19	
	Bottom	3 - D19	
	Stirrup	2-D10@90	2-D10@200
	Web	―	

List of Girder

		PG2	PG3
	Location		
All	Section	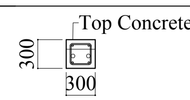	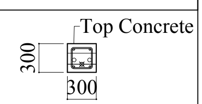
	Tendon	2C-1-17.8mm(SWPR19L)	2C-1-17.8mm(SWPR19L) 1C-17mm(SBPR930/1080)
	Top	2 - D19	2 - D19
	Bottom	2 - D19	2 - D19
	Stirrup	2-D10@100(KSS785)	2-D10@150
	Web	―	―

List of Slab Depth: 130mm

		Shorter direction	Longer direction
PS1		D10@200	D10@200
CS1	Top	D13@200	D10@250
	Bottom	D10@200	D10@250
CS2	Top	D10@200	D10@250
	Bottom	D10@200	D10@250
CS3	Top	D13@200	D13@200
	Bottom	D10@200	D10@200

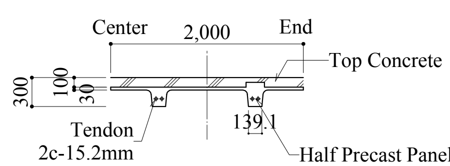

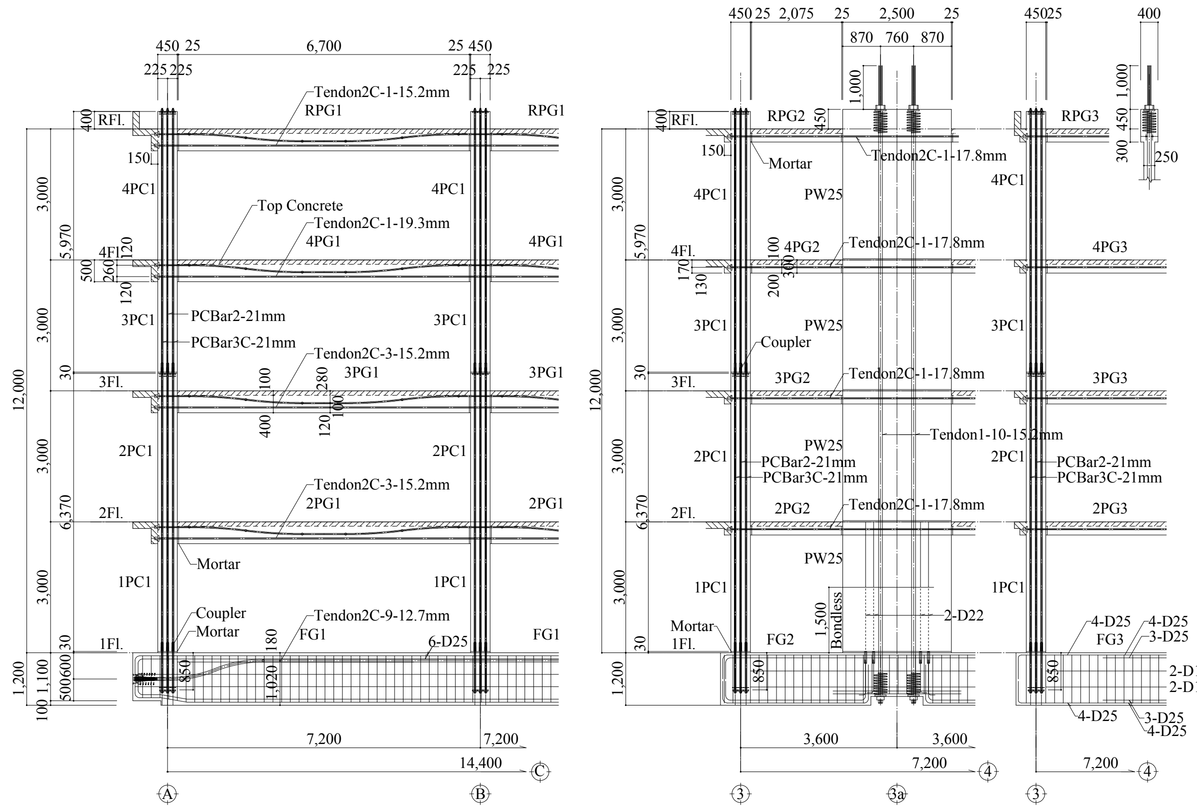

Figure 2.23 Configuration of the steel.

In designing the columns and beams in the longitudinal direction, more than 1.5 of the column-to-beam strength ratios was satisfied so that the complete mechanism was based on beam hinges. The strength capacity in the longitudinal direction was set to have the same value as defined in the Japanese Building Standard Law. The PT wall was designed referring to static parametric studies using a fiber model. The study focused primarily on the balance between the amounts of vertical PT tendons and the confinement reinforcements, as well as on the influence to capacity of the normal unbonded steel bars of the base. Basically, the walls satisfied the provisions of ACI ITG-5.2-09. Detailed information of unbounded post-tensioned concrete walls was as follows:

Unbonded Post-Tensioned Concrete Walls: The four-story unbounded post-tensioned (UPT) concrete walls were constructed using four precast concrete panels that were post-tensioned together along horizontal joints. The typical section for the wall panels was 2.5 m long by 250 mm thick with a cross-sectional aspect ratio (l_w / t_w) of 10. The first, second, and third story wall panels were 3 m high. The fourth story wall panel was extended 450 mm above the roof slab. The extended length of the fourth story wall panel was thickened to 400 mm in order to accommodate anchorage for the post-tensioning reinforcing. The assembled walls had a height-to-length aspect ratio (H_w / l_w) of 5.

The concrete panels for the North wall were fabricated using a high-performance fiber reinforced cement composite (FRCC). The South wall panels were fabricated using a conventional Portland cement concrete mix with a minimum specified compressive strength of 60 MPa (8.7 ksi). The vertical faces of the panels were reinforced with a two-way mesh of D13 SD295 reinforcing bars. Supplemental D13 SD295 transverse ties were added to prevent separation of the reinforcing mesh from the concrete core, a failure mechanism noted by Perez et al. [2004c]. The mild steel reinforcing was not developed across the panel joints.

The compression zones of the wall panels were reinforced with high-strength S13 KSS785 confinement hoops. In the base wall panel the compression zones were reinforced with two bundled, overlapping S13 KSS785 hoops at a vertical spacing of 75 mm. The confinement reinforcing ratios for the base wall panel, equal to the volumetric ratio of confinement reinforcing to the confined concrete core, were 1.7% for the length-wise direction (ρ_x), and 1.8% for the thickness direction (ρ_y). The overall confinement reinforcing ratio (ρ_s) for the base wall panel was 3.5%. In the upper story panels, the level of confinement was reduced to single S13 KSS785 hoop at 100 mm vertical spacing. The ratio of the total confinement length to the overall length of the wall (l_c / l_w) was 0.4.

Based on preliminary design results presented at planning meetings at PEER, a wall cross section 250 mm thick and 2500 mm long was selected. According to the AIJ Guidelines, the walls have deformation capacity of more than 2% drift angle for both shear failure and bending compression failure. In the PT Building, the wall was post-tensioned by unbonded strands extending over the full height of the building to provide a mechanism for energy dissipation at the interface of the wall and the foundation. Unbonded reinforcement also was placed across the interface of the wall base and the foundation to provide a mechanism for energy dissipation. The arrangement of the unbonded energy-dissipating reinforcement was selected based on numerical studies. These studies are briefly described in the following paragraph.

For both the RC and PT Buildings, preliminary analyses were conducted using fiber models to assist with design decisions. Two results are presented for the PT Building, one with two PT strands and no energy-dissipating bars, and the other with two PT strands and 8 energy-dissipating bars (Figure 2.24). Figure 2.25 compares relative strength, hysteretic energy dissipation, and concrete compressive strain for RC and PT walls. The energy dissipation capacity of the PT wall increased four times by providing the unbonded deformed reinforcement at the wall base (and embedded into the foundation). The concrete compressive strain was about four times higher in the PT wall compared with the RC wall. In addition to providing high-strength transverse reinforcement, as was done in the RC wall, steel-fiber reinforced concrete was used over the first two stories of the PT wall.

In order to enhance energy dissipation during seismic response, eight D22 SD345 mild steel reinforcing bars (four at each end) were included across the base panel-foundation interface. The energy-dissipating reinforcing bars were positioned within the central core of the wall (i.e., outside of the compression regions) and were unbonded over a length of 1.5 m within the base wall panel. In order to facilitate construction, the energy-dissipating bars were spliced within the foundation using a grouted coupler.

The post-tensioning in the walls consisted of two bundles of 10-D15.2 SWPR7B post tensioning strands, with a PT steel ratio $\left(\rho_{pt}\right)$ of 0.44%. The bundled strand groups were positioned symmetrically on either side of the centroidal axis of the wall with an eccentricity of 380 mm. The initial prestress (after release) in the strand groups was equal to 60% of the yield stress for the strand material $\left(f_{py}\right)$. The corresponding initial compressive stress in the wall due to post-tensioning $\left(f_{ci,pt}\right)$ was 4.3 MPa (0.62 ksi). Because the bundled strands were contained within ungrouted polyethylene ducts, they were unbonded from the concrete wall panels over the full wall height between mechanical anchorages at the top and bottom of the wall

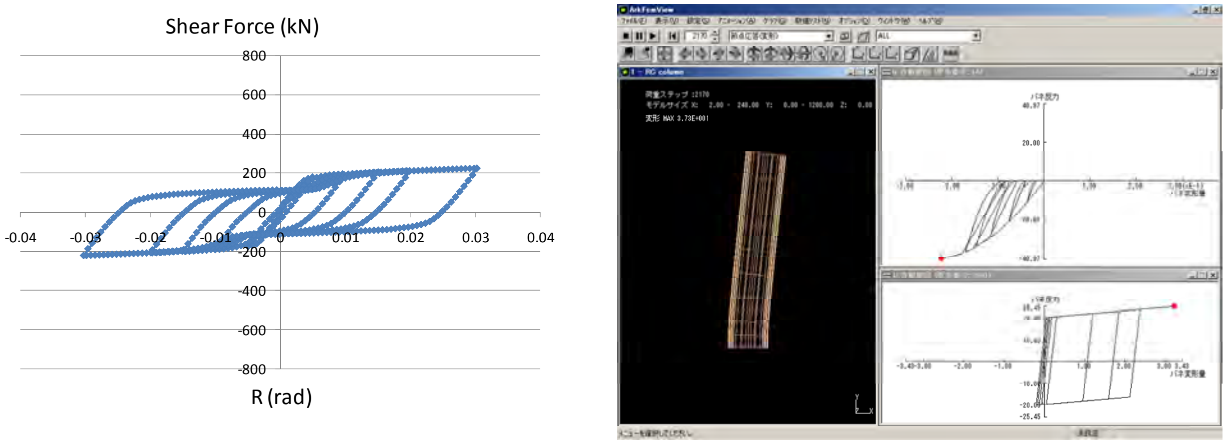

(1) RC Wall

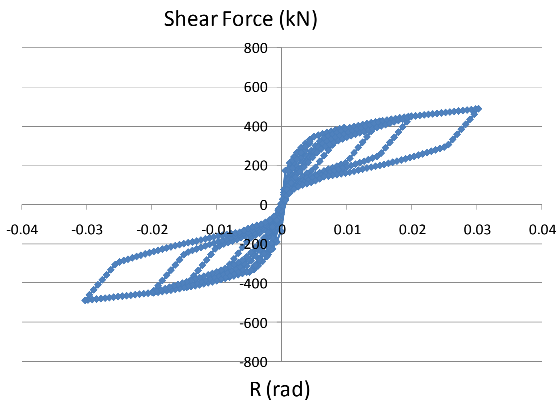

(2) PT Wall: 2 PT ducts- 8 energy dissipating bars

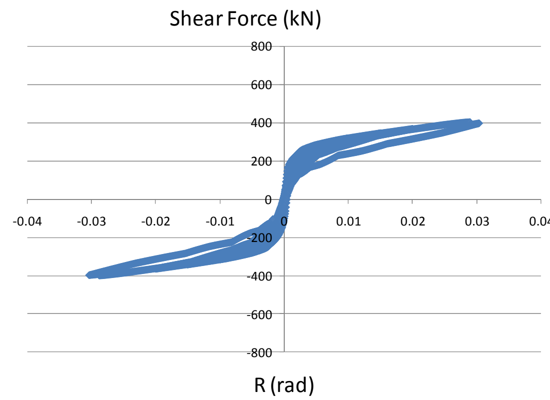

(3) PT Wall: 2 PT ducts- no energy dissipating bars

Figure 2.24 Hysteretic behavior of cantilever analyses.

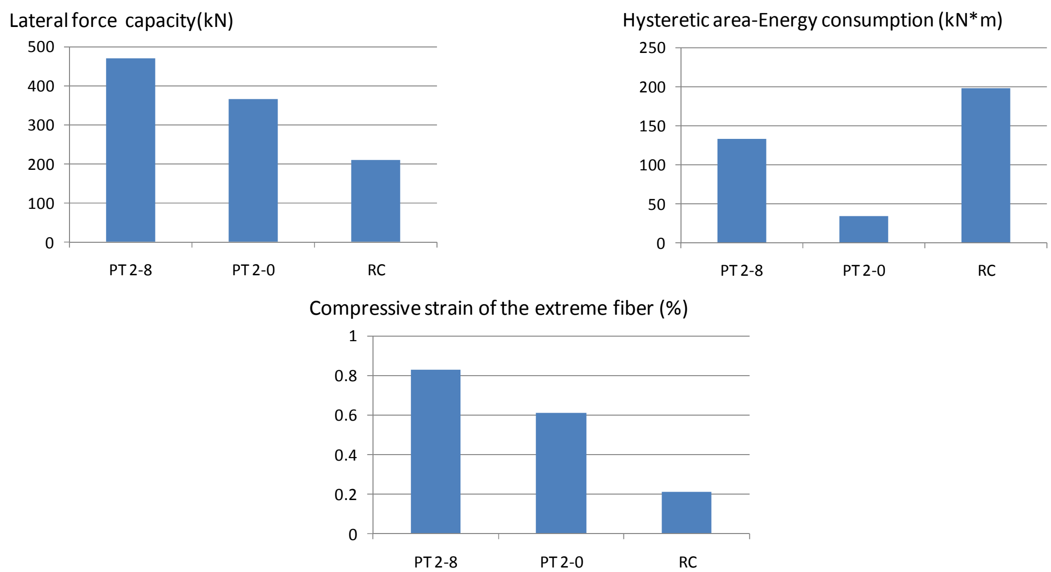

Figure 2.25 Strength, hysteresis, energy dissipation, and concrete compressive strain at 2% drift angle.

2.3.1 Design of Unbonded Post-tensioned Concrete Walls

2.3.1.1 Performance-Based Design

Details for the UPT concrete walls were developed using a performance-based design approach. For design purposes, the UPT concrete walls were conservatively analyzed as isolated lateral force resisting components, i.e., the contribution of the light PT frames and the interaction of the walls with the connecting UPT beams and composite floor system were neglected. Two analytical models were developed to characterize the lateral load response of the walls and to estimate design capacities and design demands: (1) an idealized tri-linear lateral load response model; and (2) a rigorous nonlinear finite element model (presented in Section 2.3).

Idealized Tri-Linear Lateral Load Response Model: Previous analytical and experimental studies [Kurama et al. 1996; 1997; 1999a; 1999b; Perez et al. 1998; 2004a; 2004b; 2004c; 2007; Keller and Sause 2010] have demonstrated that the lateral load response of UPT concrete walls can be characterized by the following limit states: (1) decompression (DEC), (2) effective linear limit (ELL), (3) yielding of the post-tensioning steel (LLP), (4) crushing of the confined concrete (CCC), and (5) fracture of the post-tensioning steel (FP). For well-designed and detailed UPT concrete walls, an idealized tri-linear pushover curve (Figure 2.26) can be developed using simplified predictions of response parameters for limit states 2 (ELL), 3 (LLP), and 4 (CCC). Comparisons of response predictions from the idealized tri-linear pushover model with results from previous large-scale experimental tests and detailed nonlinear finite element analyses are presented in Figure 2.27.

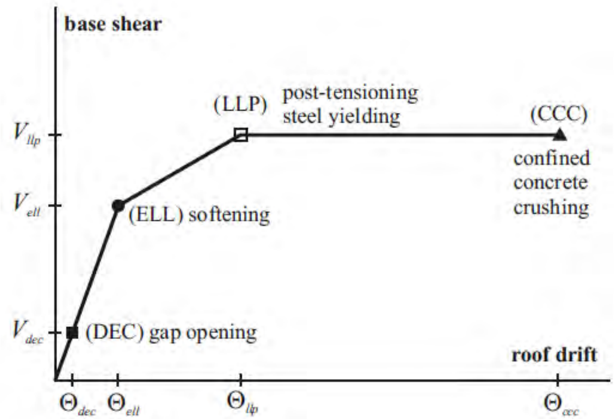

Figure 2.26 Idealized tri-linear lateral load response curve for UPT concrete walls [Perez et al. 2004a].

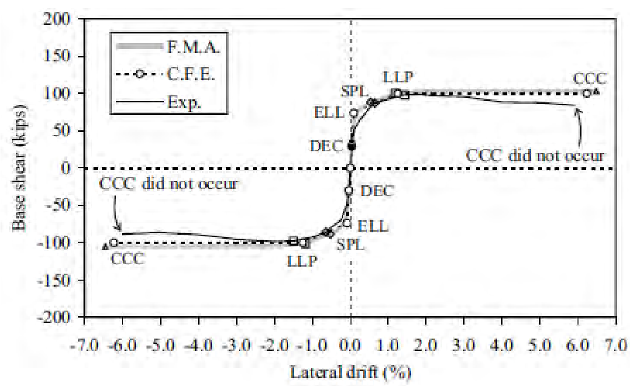

Table 8.8. Comparison of experimental and analytical results for TW5.

Result Type	Loading Direction	DEC		SPL		LLP		CCC	
		V_{dec} (kips)	Θ_{dec} (%)	V_{spl} (kips)	Θ_{spl} (%)	V_{llp} (kips)	Θ_{llp} (%)	V_{ccc} (kips)	Θ_{ccc} (%)
Exp.	Eastward	28.4	0.05	86.9	0.65	97.8	1.44	**	**
	Westward	-29.8	-0.04	-85.9	-0.65	-97.7	-1.50	**	**
F.M.A. (mono-tonic)	Eastward	33.2	0.04	88.1	0.54	99.9	1.19	102.7	6.49
	Westward	-33.3	-0.04	-88.3	-0.53	-101.1	-1.19	-105.3	-6.46
F.M.A. (cyclic)	Eastward	34.0	0.04	88.9	0.54	106.7	1.25	115.2	3.81
	Westward	-34.0	-0.04	-90.6	-0.54	-108.6	-1.28	-	-
C.F.E.	Eastward	29.6	0.04	-	-	99.7	1.26	99.7	6.24

** CCC was not reached.

Figure 2.27 Comparison of experimental and analytical results for test wall TW5 [Perez et al. 2004a].

LIMIT STATES FOR UPT CONCRETE WALLS:

Decompression (DEC)—Decompression (DEC) occurs when tensile strain demand at the base of the wall, due to overturning moment from lateral loading, equals the pre-compression strain due to post-tensioning and gravity loads. If reinforcing steel is not developed across the horizontal joint at the base of the wall, decompression is accompanied by the initiation of gap opening along the wall base-foundation interface. Under a specified lateral load distribution, decompression of the wall can be related to a specific level of base shear, V_{dec}, and roof drift, Θ_{dec}.

Effective Linear Limit (ELL)—The lateral load response of a UPT concrete wall is nearly linear elastic immediately after decompression. As drift levels increase, however, a substantial reduction in lateral stiffness occurs due to nonlinear softening of the concrete in compression and the progression of the gap opening along the horizontal joint at the base of the wall (geometric softening). The lateral stiffness decreases in a smooth and continuous manner, so the term effective linear limit is generally used to describe the point at which softening is apparent.The base shear and roof drift corresponding to the effective linear limit are V_{ell} and Θ_{ell}, respectively.

Yielding of the Post-Tensioning Steel (LLP)— The linear limit for the post-tensioning steel is calculated at the onset of yielding. For simplicity, the axial strain demand is calculated at the centroidal axis of a strand group, i.e., small discrepancies in strain within a group due to the relative eccentricity of the individual strands are neglected. The LLP limit state for the wall is reached when tensile strain demand in the critically stressed group reaches the linear limit for the strand material. The base shear and roof drift corresponding to yielding of the post-tensioning steel are denoted as V_{llp} and Θ_{llp}, respectively.

Crushing of the Confined Concrete (CCC) —Failure of the wall occurs when the confined concrete at the base fails in compression. Based on the confined concrete constitutive model developed by Mander et al. [1988a; 1988b], crushing of the confined concrete occurs at an ultimate concrete compressive strain, ε_{cu}, which is reached when the confinement reinforcement fractures. Significant loss of lateral load and gravity load resistance are expected to occur when the crushing limit state is reached. The base shear and roof drift corresponding to crushing of the confined concrete are denoted as V_{ccc} and Θ_{ccc}, respectively.

Fracture of the PT Steel (FP)—Fracture of the PT steel occurs when the tensile strain demand reaches the capacity of the strand material. The limit state is accompanied by a sudden and significant loss of lateral load resistance and self-centering capability. The base shear and roof drift corresponding to fracture of the post-tensioning steel are denoted as V_{fp} and Θ_{fp}, respectively.

DESIGN CRITERIA FOR UPT CONCRETE WALLS

The following design criteria were developed by Perez et al. [2004c] for UPT concrete walls:

Criterion 1: Softening—This design criterion controls softening of the lateral stiffness of the UPT concrete wall for the design level ground motion.

$$V_{ell} \geq \alpha_d \cdot V_d$$

where V_{ell} is the base shear at the effective linear limit, α_d is a factor applied to the design base shear demand to define the base shear at which softening is allowed to occur (recommended range: 0.65-1.0), and V_d is the design base shear demand.

Criterion 2: Base Moment Capacity—This design criterion controls the base moment capacity of the wall as governed by axial-flexural behavior.

$$\Phi_f V_{llp} \geq V_d$$

where Φ_f is a capacity reduction factor for flexural strength, and V_{llp} is the base shear corresponding to the initiation of yielding in the PT steel.

Criterion 3: Yielding of the Post-Tensioning Steel—This design criterion controls yielding of the PT steel, which has an adverse effect on drift control and self-centering capability.

$$\Theta_{llp} \geq \Theta_d$$

where Θ_{llp} is the roof drift corresponding to the initiation of yielding in the PT steel and Θ_d is the roof drift demand for the design level ground motion.

Criterion 4: Story Drift—This design criterion controls the maximum story drift for the design level ground motion.

$$\delta_{all} \geq \delta_d$$

where δ_{all} is the allowable story drift for the design level ground motion, and δ_d is the story drift demand for the design level ground motion.

Criterion 5: Crushing of the Confined Concrete—This design criterion controls the axial-flexural compression failure of the walls.

$$\Theta_{ccc} \geq \Theta_m$$

where Θ_{ccc} is the roof drift corresponding to crushing of the confined concrete, and Θ_m is the roof drift demand for the maximum considered ground motion.

Criterion 6: Fracture of the Post-Tensioning Steel—This design criterion ensures that fracture of the PT steel does not occur.

$$\Theta_{fp} \geq \Theta_{ccc}$$

where Θ_{fp} is the roof drift corresponding to fracture of the PT steel.

Criterion 7: Roof Drift Limit under the Maximum Considered Ground Motion—This design criterion limits the drift demand under the maximum considered ground motion to ensure stability of the gravity load system.

$$\Theta_g \geq \Theta_m$$

where Θ_g is the roof drift corresponding to failure of the gravity load resisting system.

ESTIMATION OF DESIGN CAPACITIES

Preliminary estimates of design capacities for the walls were based on the simplified tri-linear lateral load response model. Perez et al. [2004c] presents simplified expressions for estimating design capacities of UPT concrete walls. Final estimates of design capacities for the walls were based on nonlinear finite element pushover analyses (see Section 2.3).

ESTIMATION OF DESIGN DEMANDS

Design demands for the UPT concrete walls were based on three levels of seismic intensity. Seismic response coefficients (C_s) of 0.20 and 0.30 were used to represent the design-basis earthquake (DBE) and the MCE, respectively. In addition, the UPT concrete walls were designed to remain linear elastic up to a seismic response coefficient of 0.15. Preliminary estimates of deformation demands for the UPT concrete walls were estimated using the procedure outlined in Seo and Sause [2005], which accounts for the tangent stiffness of the wall after the effective linear limit (ELL) and hysteretic energy-dissipation characteristics. Nonlinear response history simulations (see Section 2.3) were used to evaluate deformation demands for the proposed test plan.

CONFORMANCE WITH CURRENT U.S. DESIGN PROVISIONS

The UPT concrete wall design satisfies the strength and detailing requirements of ACI ITG-5.2-09 with one notable exception. The PT reinforcing groups are offset from the centroid of the wall by 15% of the wall length. The ACI ITG-5.2-09 was developed for UPT concrete walls with PT reinforcing located within 10% of the wall length from the wall centroid. The experimental program described herein increased the eccentricity of the PT reinforcing steel to 15% to control drift demands, by way of increasing the post-decompression lateral stiffness. The two ground acceleration records selected for the experimental program, from the 1995 Great Hanshin Earthquake produce relatively large spectral acceleration demands in the elongated post-ELL period range of the structure, which significantly increases deformation demands in the structural system.

2.4 CONSTRUCTION

The buildings were constructed between July and October 2010 and moved onto the E-Defense shake table in November 2010. Instrumentation of building was primarily completed in November 2010. The construction process is depicted in Appendix C.

The specimen was constructed outside and then transferred onto the shake table, as shown in Appendix A. The specimen was suspended by two cranes and then set on the shaking table. The foundation beams were strongly fixed by one hundred and fifty post-tensioned PT bars. The foundation beams were constructed on the six concrete stubs, 1.4 m x 3 m x 1.5 m in configuration, to leave enough space for the carrier access beneath the specimen. The foundation beams were 1200 mm deep and designed for each phase of the test program, from the construction to set up, by using the supplementary PT tendons to prevent excessive cracks. The concrete was cast for the columns, walls, upper floor beams, and the floor slab. The main reinforcement of columns, beams, and the assumed column-zones of walls were connected by gas pressure welding. Lap joints were used for reinforcing the walls and floor slabs.

3 Test Plan and Instrumentation

The two test buildings were heavily instrumented to assess their performance when subjected to a range of shaking intensities for a range of post-test analytical studies. The table motions used for the testing and the instrumentation used for each of the two buildings are briefly described in the following sections. Additional information is provided in Appendix D.

3.1 TEST PLAN

The 1995 JMA-Kobe and JR-Takatori records were selected for this experimental program. Testing was conducted on December 13th and December 15th, subjecting the buildings to the JMA-Kobe record, and a third test was conducted using the JR-Takatori record on December 17th. The NS-direction acceleration, EW-direction acceleration, and vertical-direction acceleration were aligned with the transverse-direction (y), longitudinal direction (x), and vertical direction of the specimen (Figure 2.3). Natural periods 0.36 and 0.18 were computed for the models (see Chapter 2) for the shear wall (y) and moment frame (x) directions, respectively. In the tests the amplitude associated with the JMA-Kobe record was scaled to produce a range of shaking intensities; scale factors of 25 %, 50 %, and 100 % were used. The orbit of horizontal acceleration is shown in Figures 3.9-3.10. Based on preliminary analyses, the stronger NS-direction wave was input into the transverse-direction. The two tests run with the JR-Takatori record were scaled to 40% and 60%.

3.2 INSTRUMENTATION

3.2.1 General

A total of 609 channels of data were collected during the tests for RC and PT specimens, including 48 accelerometers, 202 displacement transducers, and 235 strain gauges. The accelerometers were placed on the foundation and on each floor slab to record accelerations in three directions. Displacement transducers were arranged to measure interstory displacements, beam end rotations, column end rotations, and base wall rotations. Strain gauges were glued to longitudinal and transverse reinforcement of beams, columns, and walls. Strain gauges were largely used for the RC specimen, whereas displacement transducers were used for the PT specimen (to measure member end rotations). Video cameras were used to record the tests and included overall views of the test specimens, as well as close up views of regions where yielding and damage were anticipated. Data acquisition was accomplished using 24 bit A/D converters using a sample rate of 0.001 sec (1000 Hz). Locations of instrumentation are shown in Appendix D.

3.2.2 Types of instrumentation

Figure 3.1 shows properties of the three different types of instrumentation that were used for the tests: accelerometers, displacement transducers, and strain gauges.

3.2.2.1 Accelerometers

Accelerometers were used to record accelerations at each floor. Figure 3.2 shows the locations of accelerometers. Detailed information is provided in Appendix D.

名称	写真	仕様等	名称	写真	仕様等
サーボ型加速度センサ		東京計器(株) TA-25E-10-1 (3方向セット) 定格:±98.07m/s^2	ポテンショメータ型変位センサ		(株)東京測器 DP-500D (ワイヤタイプ) 定格:±250mm
歪型加速度センサ		(株)共和電業 ASW-5AM36 (防水型) 定格:±49.03m/s^2	ポテンショメータ型変位センサ		(株)東京測器 DP-1000D (ワイヤタイプ) 定格:±500mm
レーザ型変位センサ		(株)KEYENCE LK-500 定格:±250mm	ポテンショメータ型変位センサ		(株)東京測器 DP-2000D (ワイヤタイプ) 定格:±1000mm
ポテンショメータ型変位センサ		(株)共和電業 DTP-D-300 (ワイヤタイプ) 定格:±150mm	歪ゲージ型変位センサ		(株)共和電業 DTH-A-100 (バネタイプ) 定格:±50mm
ポテンショメータ型変位センサ		(株)共和電業 DTP-D-2KS (ワイヤタイプ) 定格:±1000mm	歪ゲージ型変位センサ		(株)東京測器 CDP-100 (バネタイプ) 定格:±50mm
ポテンショメータ型変位センサ		(株)共和電業 DTP-D-5KS (ワイヤタイプ) 定格:±2500mm	ブリッジボックス		(株)共和電業 DBB-120A (10ch用)

Figure 3.1 Properties of the instrumentation used in the specimens.

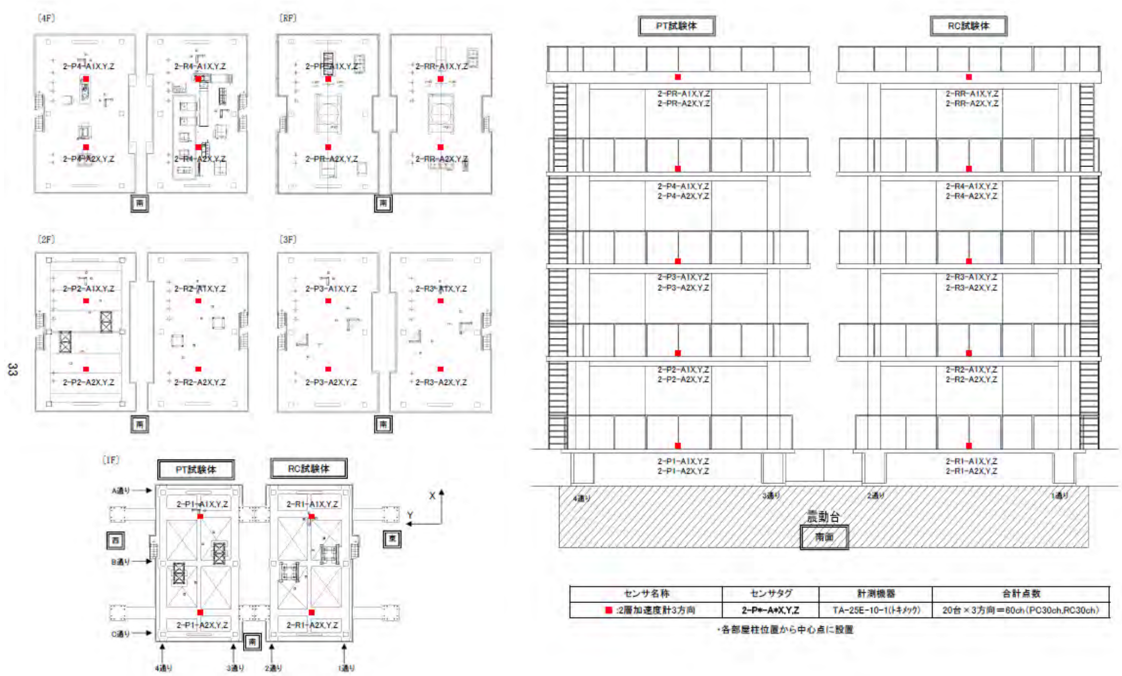

Figure 3.2 Locations of the accelerometers.

3.2.2.2 Displacement Transducers

A total of 202 displacement transducers were used for the tests, including wire potentiometers, laser-type displacement transducers, and linear variable differential transducers (LVDTs). The transducers were attached to the test specimens to measure horizontal and vertical displacements, lateral story displacements and drifts, average concrete strains over gauge lengths, pullout/gapping at member ends, and sliding at the base of the shear walls. Locations of wire and laser transducers are shown in Figures 3.3 and 3.4.

A majority of the LVDTs were provided by NIED; however, some of the displacements transducers were provided by NEES@UCLA, IOWA State University, and the Earthquake Research Institute at the University of Tokyo; this enabled more detailed measurements of wall deformations (Figures 3.5 and 3.6). Four transducers were used over a gauge length of 540 mm at the base of the walls to enable the curvature along the wall length (depth) to be determined (Figure 3.5); additional displacement transducers were provided at each wall boundary over the entire height of the building (Figure 3.5). Two pairs of diagonally-oriented displacement transducers were used over the first story height to enable the determination of shear deformations. Photographs showing the displacement transducers over the first story height of the RC building are shown in Figure 3.7. Further information is provided in Appendix D.

Strain Gauges: Reinforcement strains were measured at 235 locations using strain gauges. Figure 3.8 shows the locations of the strain gauges in horizontal and vertical reinforcement in RC building at the first and second floor. More detailed information is provided in Appendix D.

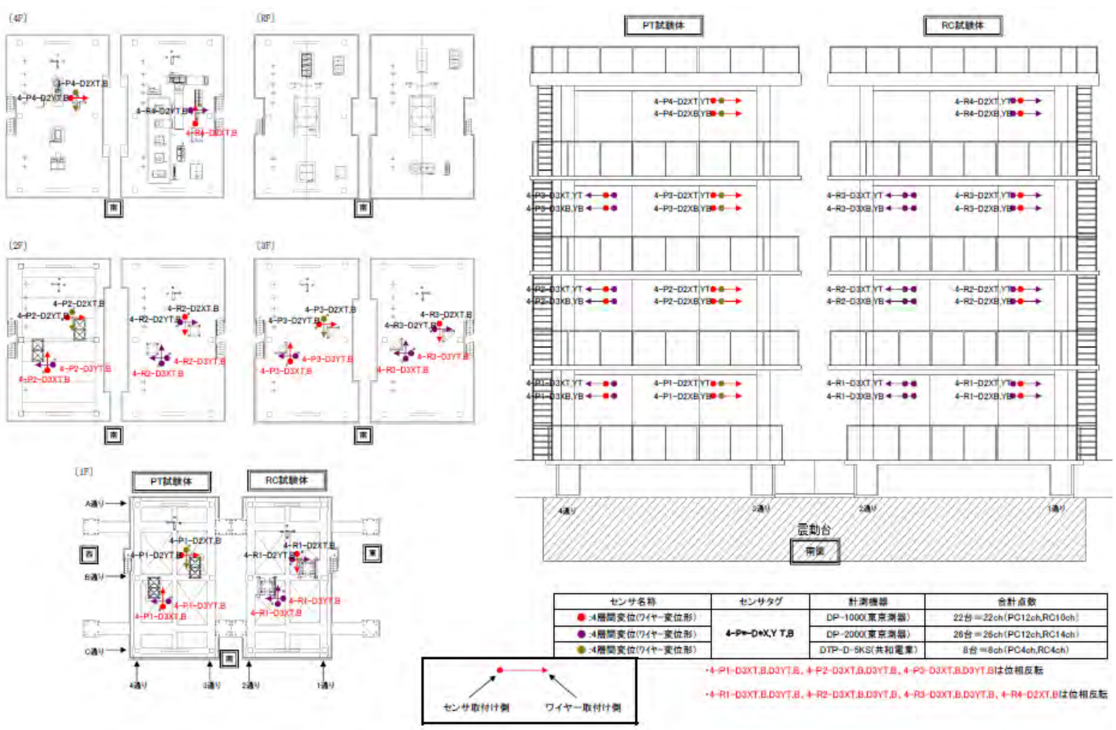

Figure 3.3 Locations of the wire-type displacement transducers.

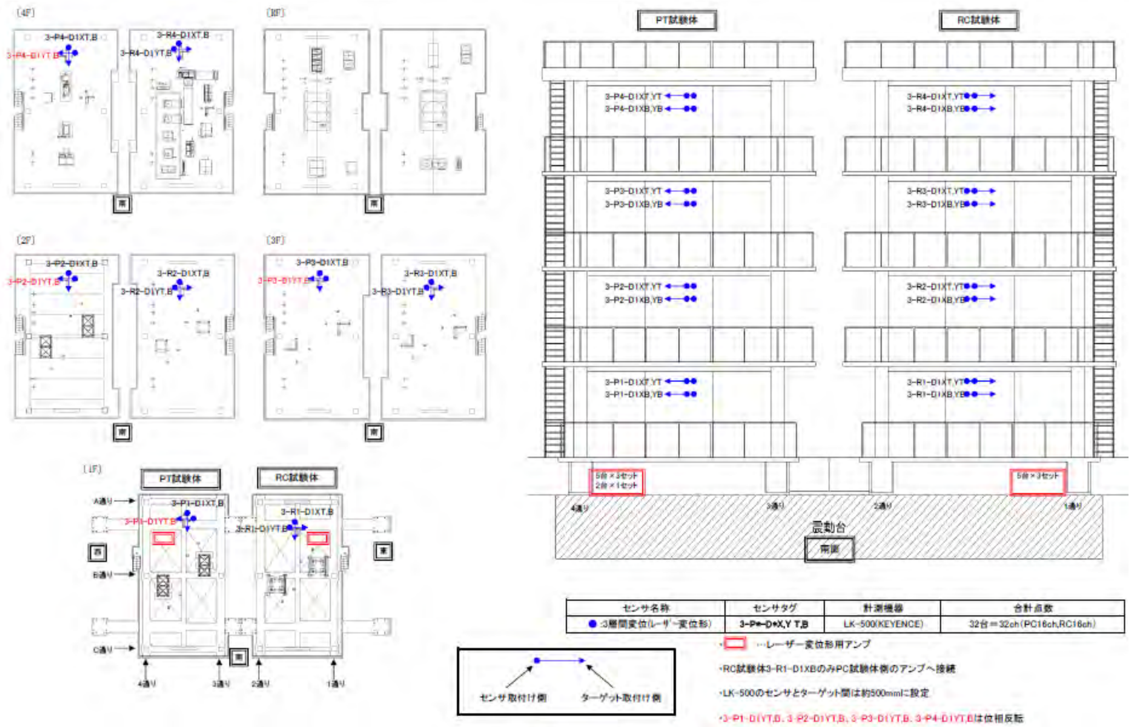

Figure 3.4 Locations of the laser-type displacement transducers.

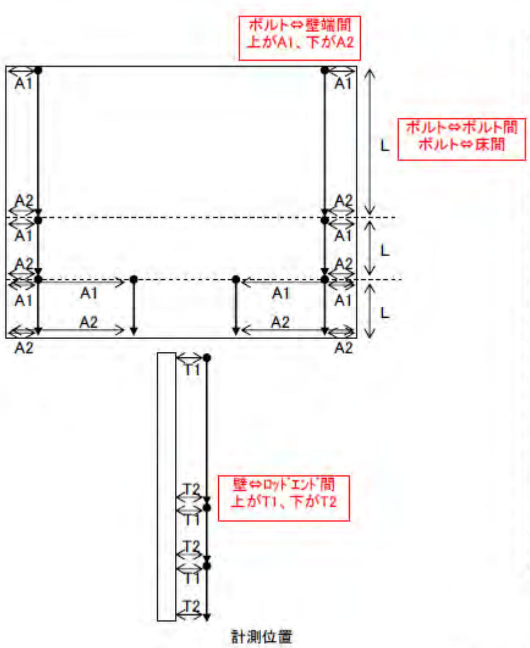

センサータグ	寸法計測点				
	L	T1	T2	A1	A2
A1-R1N-D1	245		76		135
A1-R1N-D2	245		73		130
A1-R1N-D3	545	104	100	104	96
A1-R1N-D4	542	100	102	1020	1020
A1-R1N-D5	545	102	100	1030	1020
A1-R1N-D6	550	104	104	100	105
A1-R1N-D7	483	37	40	98	102.5
A1-R1N-D8	497	42	40	104	100
A1-R1N-D9	1850	69	67	124	98
A1-R1N-D10	1845	69	70	130	104
A1-R2N-D11	2815	70	72	128	120
A1-R2N-D12	2820	73	67	127	128
A1-R3N-D13	2805	75	70	130	125
A1-R3N-D14	2815	78	72	135	135
A1-R4N-D15	2855	70	67	130	125
A1-R4N-D16	2855	68	65	130	130
A1-R1S-D1	252		90		135
A1-R1S-D2	250		93		110
A1-R1S-D3	554	105	105	99	98
A1-R1S-D4	560	98	100	1027	1015
A1-R1S-D5	550	105	107	1024	1019
A1-R1S-D6	550	106	105	100	102
A1-R1S-D7	510	43	40	98	96
A1-R1S-D8	505	41	40	100	100
A1-R1S-D9	2830	64	70	134	98
A1-R1S-D10	2850	64	70	128	100

A1-2 RC棟壁変形計測

Figure 3.5 Vertical LVDT configuration (first floor).

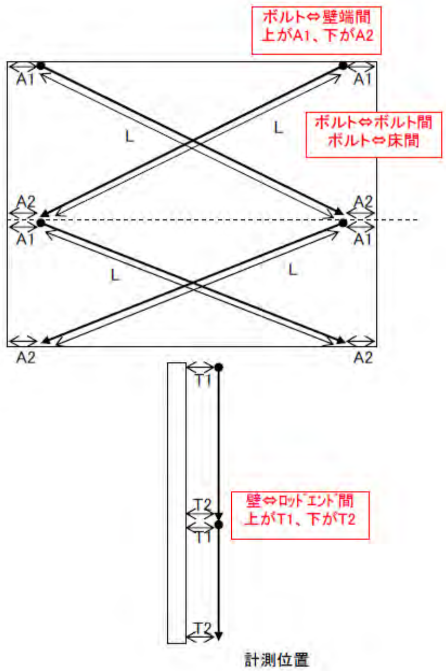

センサータグ	寸法計測点				
	L	T1	T2	A1	A2
A2-P1S-D1	2530	85	120	100	70
A2-P1S-D2	2470	40	70	100	130
A2-P1S-D3	2970	110	90	80	100
A2-P1S-D4	2930	70	40	130	100
A2-R1S-D1	2528	80	115	103	65
A2-R1S-D2	2475	78	68	95	130
A2-R1S-D3	2975	120	78	75	95
A2-R1S-D4	2920	77	33	110	103

A2 壁せん断変形

Figure 3.6 Diagonal LVDT configuration (first floor).

013_10-R1-DC1aNW_1

013_10-R1-DC1aSE_1

Figure 3.7 Instrumentation on the RC wall.

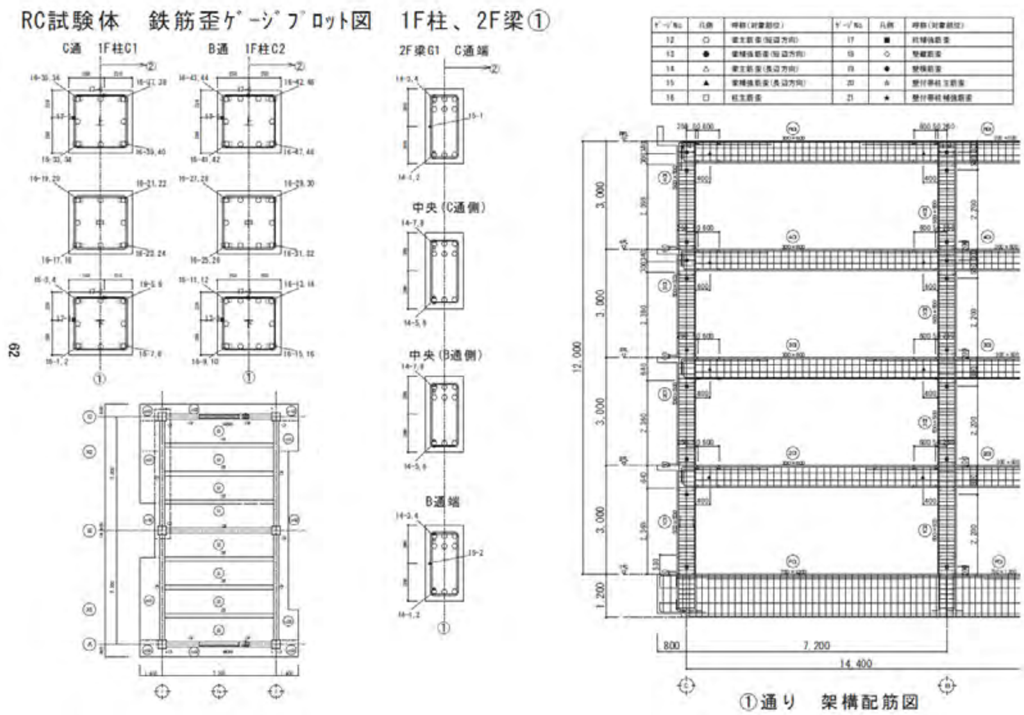

(a)

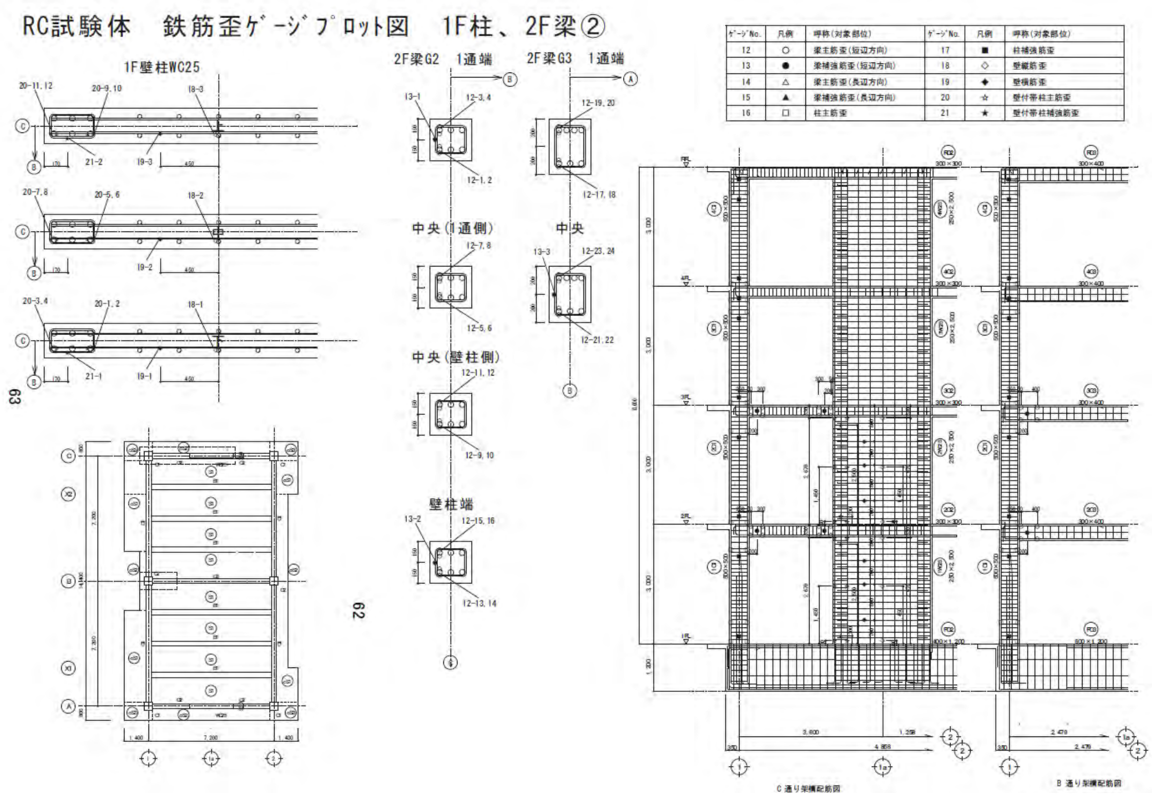

(b)

Figure 3.8　Strain gauge locations in horizontal and vertical directions at the first floor (RC).

3.3 GROUND MOTIONS

Two different table motions at various intensities were used: JMA-Kobe (25%, 50%, and 100%) and Takatori (40% and 60%). The testing was planned over five days: low-to-moderate intensity JMA-Kobe (25% and 50%) on December 13, 2010, 100% JMA-Kobe on December 15, 2010, and Takatori (40% and 60%) on December 17, 2010.

Pseudo acceleration spectra of the JMA-Kobe ground motions are presented in Figures 3.9 and 3.10 for the *x*- (frame) direction and *y*- (shear wall) directions, respectively. The broken lines show the target spectrum, whereas solid lines illustrate the actual spectra determined form measurements. Peak spectral accelerations observed on the shaking table were 0.58g at 25%, 1.18g at 50% and 2.79g at 100% JMA-Kobe in the frame direction; and 0.89g at 25%, 1.58g at 50% and 3.42g at 100% JMA-Kobe in the shear wall direction.

Pseudo acceleration spectra of the Takatori ground motions were also plotted (see Figures 3.11 and 3.12). At 40%, the Takatori record had a peak spectral acceleration of 1.11g and 0.99g in the frame and shear wall directions, respectively. At 60%, the Takatori record had a peak spectral acceleration of 1.72g in the frame direction and 1.51g in the shear wall directions, respectively.

Displacement spectra are shown in Figures 3.13-3.16. Peak spectral displacements were observed as 10.5 cm at 25%, 20.9 cm at 50%, and 41.8 cm at 100% JMA-Kobe; and 40.3 cm at 40%, and 60.2 cm at the 60% Takatori in the frame direction. In the other direction, the peak displacements were 11.6 cm at 25%, 23 cm at 50%, and 46 cm at the 100% JMA-Kobe record; and 48.1 cm at the 40%, and 72.3 cm at the 60%Takatori records.

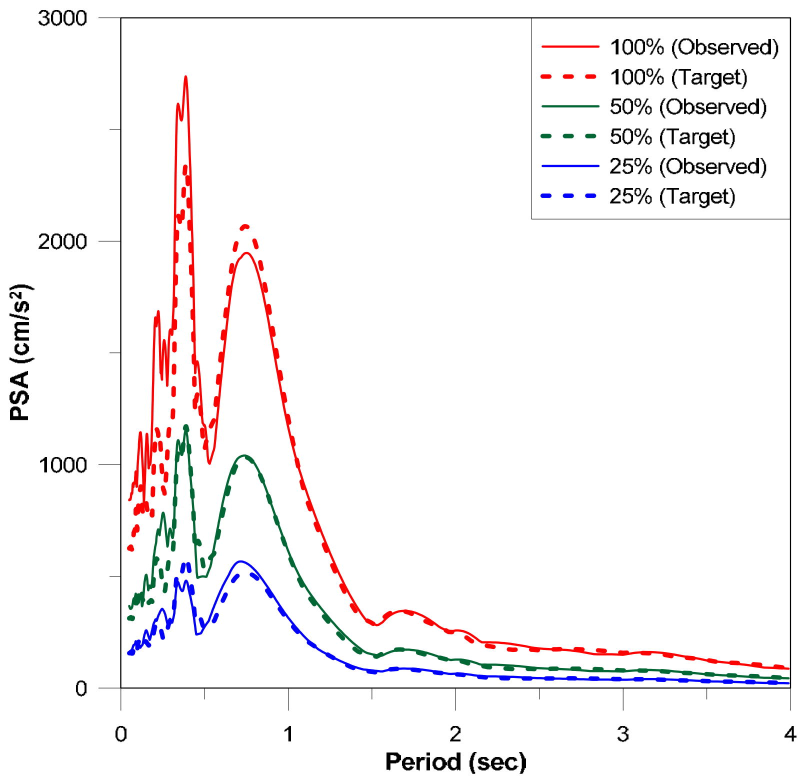

Figure 3.9 Acceleration spectra for JMA-Kobe ground motion (*x*-direction).

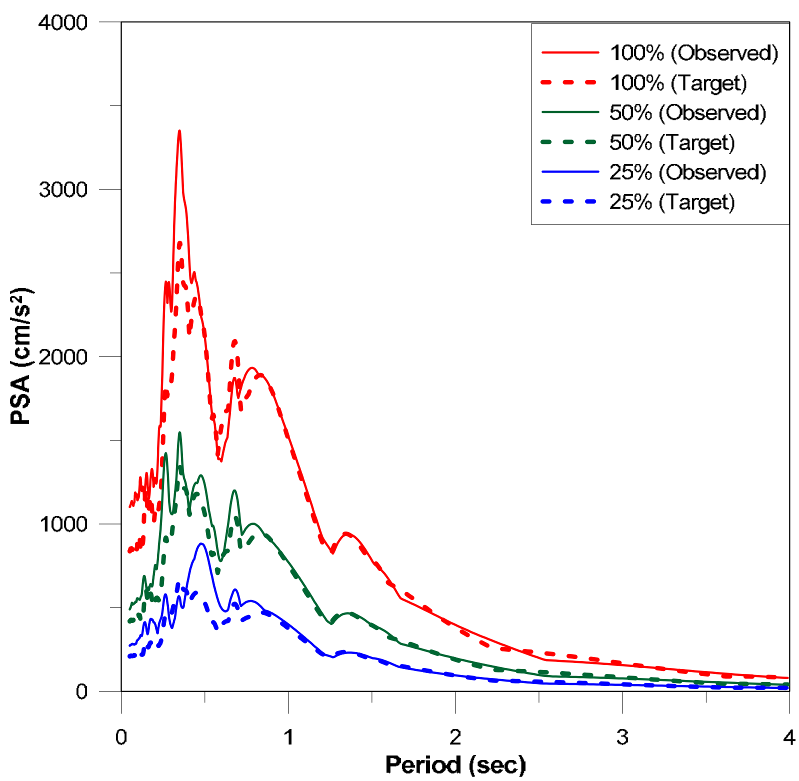

Figure 3.10 Acceleration spectra for JMA-Kobe ground motion (*y*-direction).

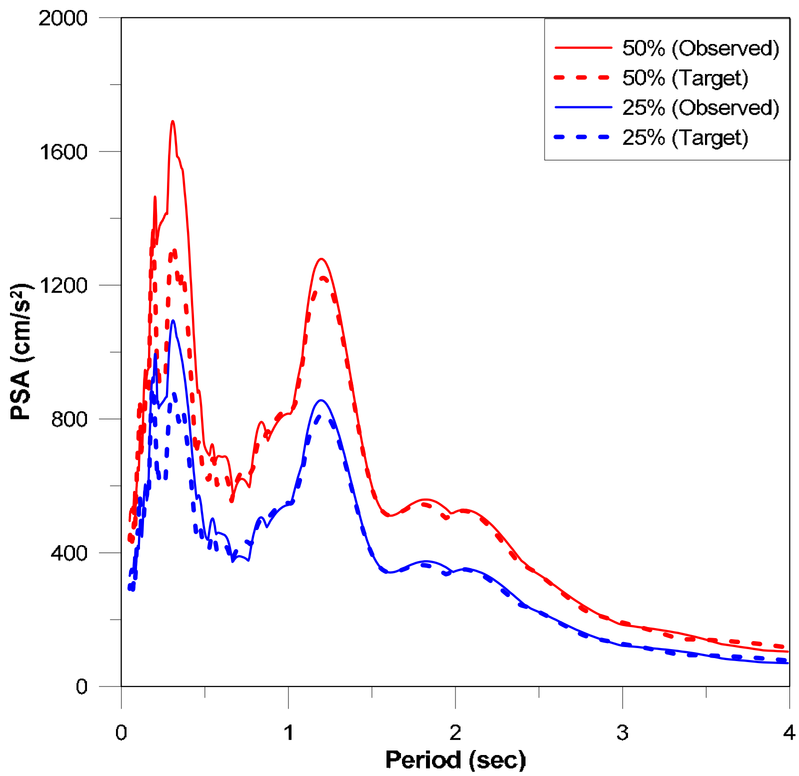

Figure 3.11 Acceleration spectra for Takatori ground motion (*x*-direction).

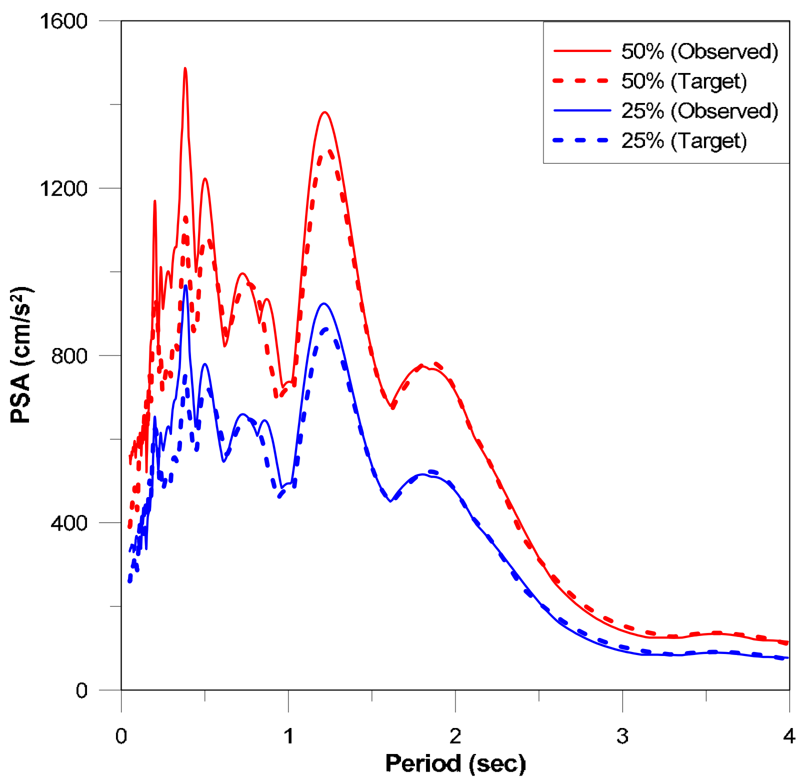

Figure 3.12 Acceleration spectra for Takatori ground motion (*y*-direction).

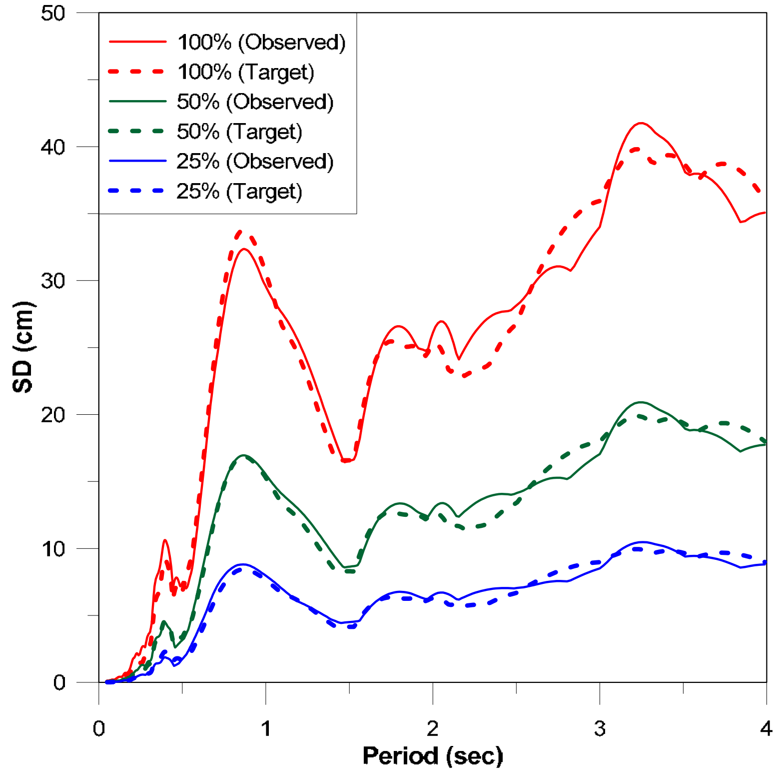

Figure 3.13 Displacement spectra for the Kobe ground motion (*x*-direction).

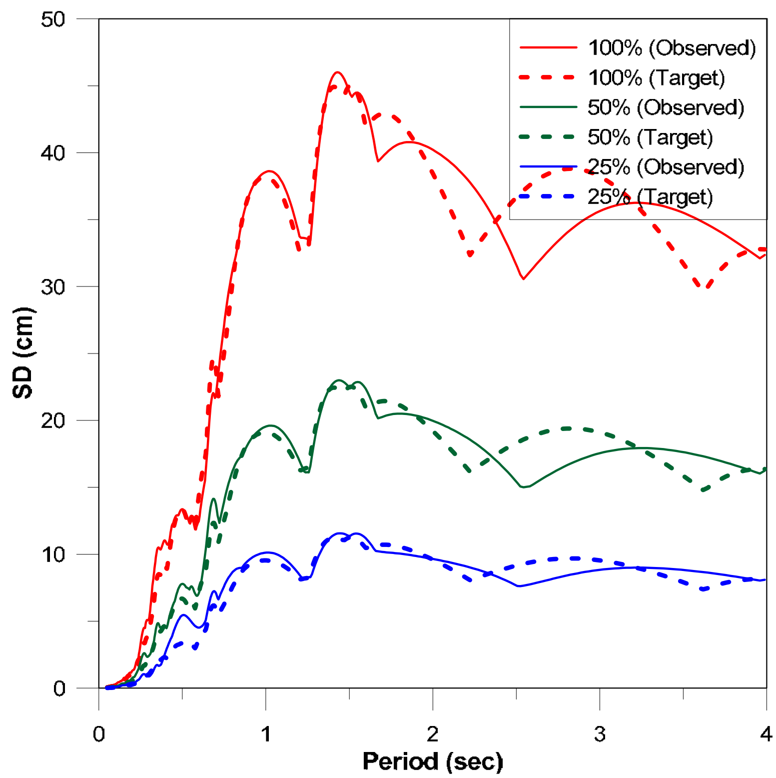

Figure 3.14 Displacement spectra for the Kobe ground motion (*y*-direction).

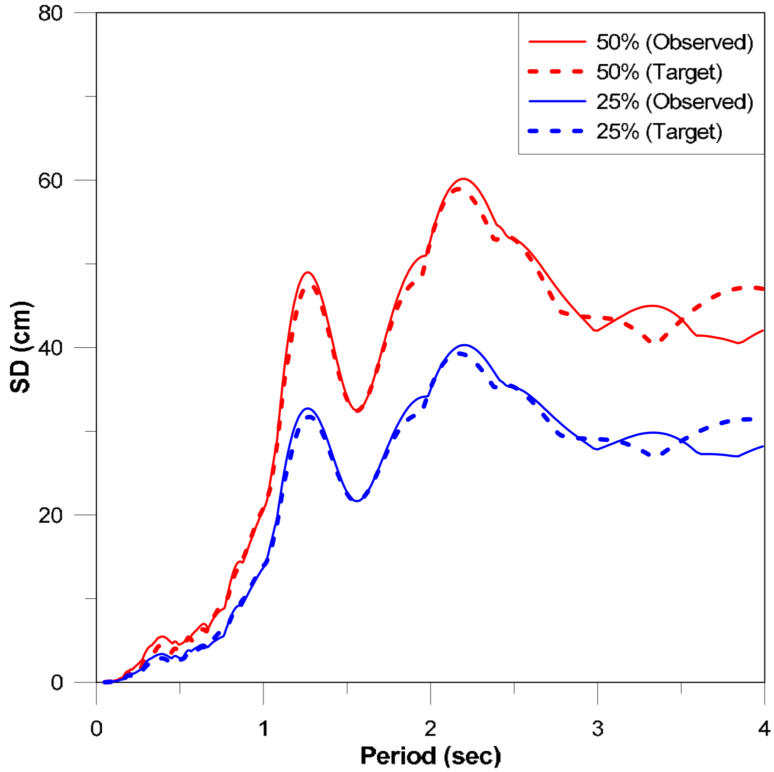

Figure 3.15 Displacement spectra for the Takatori ground motion (*x*-direction).

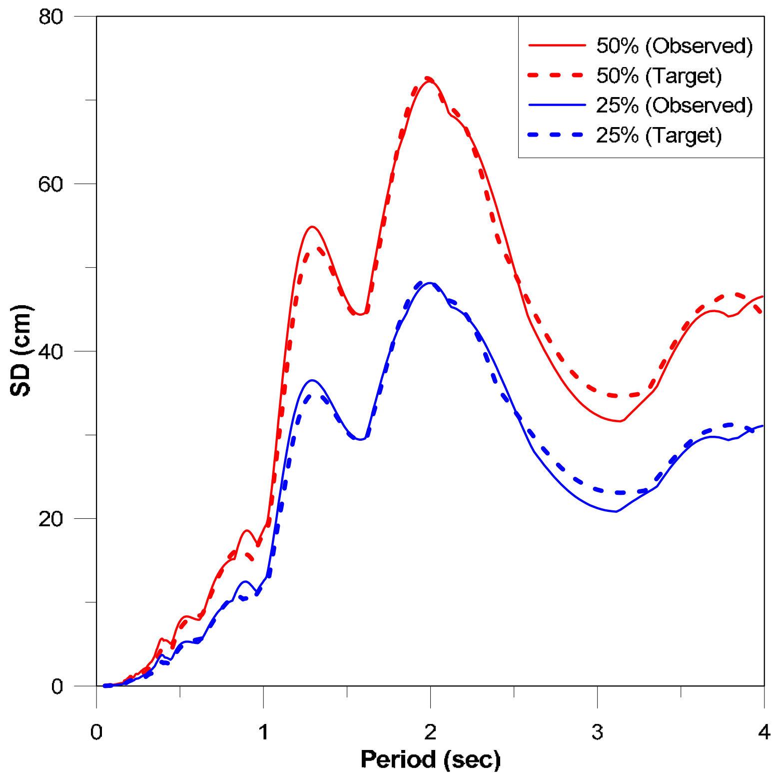

Figure 3.16 Displacement spectra for the Takatori ground motion (*y*-direction).

4 Summary, Conclusions, and Future Work

4.1 SUMMARY

Detailed information related to the December 2010 tests of two, full-scale, four-story buildings that were tested on the NIED E-Defense shake table are presented. Substantial collaboration between U.S. and Japan researchers over a period of nearly two years preceded the shake table testing. The goal of the collaboration was to produce test buildings that would provide vital data on behavior and response over a spectrum on shaking intensities, including near-collapse, for research efforts in both the U.S. and Japan.

The tests were successfully completed during the week of December 13-17, 2010. The large number of instruments placed, including video cameras, will provide a wealth of data that will enable both Japanese and U.S. researchers to improve our understanding of the behavior of these systems. Papers that summarize the overall results are being prepared for submittal to AIJ and a U.S. journal by mid-summer 2011.

Support has been provided by NEEScomm to conduct a blind prediction study associated with the RC and PT Building tests. The data in this report are intended to provide background information to support this effort.

4.2 FUTURE STUDIES

A subsequent report will be prepared that provides an overview of the test results and pre-test analytical studies, as well as post-test studies.

REFERENCES

Applied Technology Council (2007). ATC-58, Guidelines for Seismic Performance Assessment of Buildings, 50% Draft, Redwood City, CA.

Berry, M.P., Parrish, M., and Eberhard, M.O. (2004). PEER Structural Performance Database User's Manual, Pacific Earthquake Engineering Research Center, http://nisee.berkeley.edu/spd/.

EERI (2010). "The Mw 8.8 Chile Earthquake of February 27, 2010," EERI Special Earthquake Report, Earthquake Engineering Research Institute, June. (http://www.eeri.org/site/images/eeri_newsletter/2010_pdf/Chile10_insert.pdf)

Elwood, K.J., and Moehle, J.P. (2008). Dynamic shear and axial-load failure of reinforced concrete columns, *J. Struct. Engrg.,* 134(7):1189–1198.

Elwood, K.J., and Eberhard, M.O. (2009). Effective Stiffness of Reinforced Concrete Columns, *ACI Struct. J.*, 106(4):476–484.

Englekirk, R.E. (2002). Design-construction of the Pamamount–A 39-story precast prestressed concrete apartment building, *PCI J*., 47(4):56–71.

Ghannoum, W. M. (2007). Experimental and analytical dynamic collapse study of a reinforced concrete frame with light transverse reinforcements, PhD Dissertation, Dept. of Civil and Environmental Engineering, University of California, Berkeley, CA.

Hiraishi H. et al. (1988). Experimental study on seismic performance of multistory shear walls with flanged cross section, *Proceedings*, 9th World Conf. Earthq. Engrg., Vol. IV, Tokyo-Kyoto, Japan.

Ichioka Y., Kono S., Nishiyama M., and Watanabe F. (2009). Hybrid System Using Precast Prestressed Frame with Corrugated Steel Panel Damper, *Journal of Advanced Concrete Technology*, Vol. 7 No. 3, 297-306.

Ikenaga, M., Nagae, T., Nakashima, M., and Suita, K. (2007). Cyclic loading test of self-centering column bases developed for reduction of residual deformations, Architectural Institute of Japan, *J. Struct. Construct. Engrg.*, No. 612:223–230.

Keller, W.J., and Sause, R. (2010). Analysis and design of unbonded post-tensioned concrete walls for the 2010 E-Defense post-Tensioned concrete test structure, Center for Advanced Technology for Large Structural Systems (ATLSS) Report No. 10-04, Lehigh University, Bethlehem, PA.

Kurama, Y. C., Pessiki, S., Sause, R., Lu, L.-W., and El-Sheikh, M. (2006). Analytical Modeling and Lateral Load Behavior of Unbonded Post-Tensioned Precast Concrete Walls, Center for Advanced Technology for Large Structural Systems (ATLSS) Report, No. EQ-96-02, Lehigh University, Bethlehem, PA, 191 pp.

Kurama, Y.C. (1997). Seismic analysis, behavior, and design of unbonded post-tensioned precast concrete walls, PhD Dissertation, Department of Civil and Environmental Engineering, Lehigh University, Bethlehem, PA.

Kurama, Y.C., Pessiki, S., Sause, R., and Lu, L.-W. (1999a). Seismic behavior and design of unbonded post-Tensioned precast concrete walls, *PCI J*., 44(3):72–93.

Kurama, Y.C., Sause, R., Pessiki, S., and Lu, L.-W. (1999b). Lateral load behavior and seismic design of unbounded post-tensioned precast concrete walls, *ACI Struct. J*., 96(4):622–632.

Mander, J.B., Priestley, M.J.N., and Park, R. (1988a). Theoretical stress–strain model for confined concrete. ASCE, *J. Struct. Engrg*., 114(8):1804–1826.

Mander, J. B., Priestley, M.J.N., and Park, R. (1988b). Observed stress–strain model of confined concrete. ASCE, *J. Struct. Engrg*., 114(8):1827–1849.

Maruta, M. and Hamada, K. (2010). Shaking table tests on three story precast prestressed concrete frame, Architectural Institute of Japan, *J. Struct. Construct. Engrg*., 75(648):405–413.

Massone, L.M., and Wallace, J.W. (2004). Load–deformation responses of slender reinforced concrete walls, *ACI Struct. J*., 101(1):103–113.

Niwa, N. et al. (2005). Seismic response control of precast prestressed concrete frames by dampers at beam's end, Architectural Institute of Japan, Summaries of Technical Papers of Annual Meeting Architectural Institute of Japan. C-2, Structures IV, pp. 749–750.

Pampanin S. (2005). Emerging solutions for high seismic performance of precast/prestressed concrete buildings, *J. Advanced Concr. Tech*., 3(2):207–223.

Pampanin S., Amaris, A. and Palermo, A. (2006). Implementation and testing of advanced solutions for jointed ductile seismic resisting frames, *Proceedings*, 2nd International fib Congress, ID8-20, Naples, Italy.

Panagiotou, M. (2008). Seismic design, testing and analysis of reinforced concrete wall buildings, PhD Dissertation, Dept. of Civil Engineering, University of California, San Diego, CA.

Perez, F.J. (1998). Lateral load behavior and design of unbonded post-tensioned precast concrete walls with ductile vertical joint connectors, M.S. Thesis, Department of Civil and Environmental Engineering, Lehigh University, Bethlehem, PA.

Perez, F.J., Pessiki, S., and Sause, R. (2004a). Seismic design of unbonded post-tensioned precast concrete walls with vertical joint connectors, *PCI J*.,49(1):58–79.

Perez, F.J., Pessiki, S., and Sause, R. (2004b). Lateral load behavior of unbonded post-tensioned precast concrete walls with vertical joints, *PCI J*., 49(2):48–65.

Perez, F.J., Pessiki, S., and Sause, R. (2004c). Experimental and analytical lateral load response of unbonded post-tensioned precast concrete walls, *Center for Advanced Technology for Large Structural Systems (ATLSS) Report No. 04-11,* Lehigh University, Bethlehem, PA.

Perez, F.J., Pessiki, S., and Sause, R. (2007). Analytical and experimental lateral load behavior of unbonded post-tensioned precast concrete walls, ASCE, *J. Struct. Engrg*., 133(11):1531–1540.

Priestley, M.J.N. (1991). Overview of the PRESSS research program, *PCI J.,* 36(4):50–57.

Priestley, M.J.N. (1996). The PRESSS program current status and proposed plans for phase III, *PCI J.,* 41(2):22–40.

Priestley, M.J.N., Sritharan, S., Conley, J.R., and Pampanin, S. (1999). Preliminary results and conclusions from the PRESSS five-storey precast concrete test building, *PCI J.,* 44(6):42–67.

Seo, C.Y., and Sause, R. (2005). Ductility demands on self-centering systems under earthquake loading, *ACI Struct. J*., 102(2):275–285.

Sezen, H., and Setzler, E.J. (2008). Reinforcement slip in reinforced concrete columns, *ACI Struct. J*., 105(3):280–289.

Shiohara, H. (2001). New model for shear failure of RC interior beam-column connections, *J. Struct. Engrg*., 127(2):152–160.

Sugata, M. and Nakatsuka, T. (2004). Experimental study for load-deflection characteristics of precast prestressed flexural members with unbonded tendon and mild steel, Architectural Institute of Japan, *J. Struct. Construct. Engrg*, No. 584:153–159.

Sugata, M. and Nakatsuka, T. (2005). Study for flag shaped hysteresis model of precast prestressed flexural member with unbonded tendons and mild steels, Architectural Institute of Japan, *J. Struct. Construct. Engrg*, No. 598:133–140.

Tran, T.A., and Wallace, J.W. (2010). Lateral load behavior and modeling of low-rise RC walls for performance-based design, PhD Qualifying Exam, Department. of Civil and Environmental Engineering, University of California, Los Angeles. CA.

Wallace, J.W., Elwood, K.J., and Massone L.M. (2008). An axial load capacity model for shear critical RC wall piers, ASCE, *J. Struct. Engrg*., 134(9):1548–1557.

Zhao, J., and Sritharan, S. (2007). Modeling of strain penetration effects in fiber-based analysis of reinforced concrete structures, *ACI Struct. J*., 104(2):133–141.

Appendix A

A.1 MATERIAL PROPERTIES

Actual material properties for RC specimen

Steel

	Grade	A_{normal} (mm^2)	σ_y (N/mm^2)	σ_t (N/mm^2)
D22	SD345	387	370	555
D19	SD345	287	380	563
D13	SD295	127	372	522
D10	SD295	71	388	513
D10*	SD295	71	448	545
D10*	KSS785	71	952	1055

*σy of 0.2% offset (shear reinforcement)

Concrete

	F_c (N/mm^2)	σ_B (N/mm^2)	Age (Days)
1st - 2nd floor	27	39.6	91
2nd - 3rd floor	27	39.2	79
3rd - 4th floor	27	30.2	65
4th - roof floor	27	41.0	53

Actual material properties for PT specimen

Steel

	Grade	A_{normal} (mm^2)	σ_y (N/mm^2)	σ_t (N/mm^2)
D22 (ED for wall base)	SD345	387	385	563
PT bar ϕ21 (1-3Fl column)*	C	346.4	1198	1281
PT bar ϕ21 (3-RFl column)*	C	346.4	1189	1273

*σy of 0.2% offset

	Grade	A_{normal} (mm^2)	F_y (kN)	F_t (kN)
PT wire ϕ15.2 (ED of wall base)*		140.7	250	277
PT wire ϕ15.2 (beam)*		140.7	255	279
PT wire ϕ17.8 (beam)*		208.4	356	404
PT wire ϕ19.3 (beam)*		243.7	429	481

* Fy of 0.2% offset

Concrete

	Fc (N/mm^2)	σ_B (N/mm^2)
Precast concrete (normal)	60	83.2
Precast concrete (fiber)	60	85.5
Top concrete	30	40.9

Grout

	Fc (N/mm^2)	σ_B (N/mm^2)
Column base, wall base and beam end	60	135.6
Wall base (fiber)	60	120.3
PT duct of PT bar and PT wire	30	63.4

A.2 MEMBER GEOMETRY AND REINFORCEMENT OF THE RC SPECIMEN

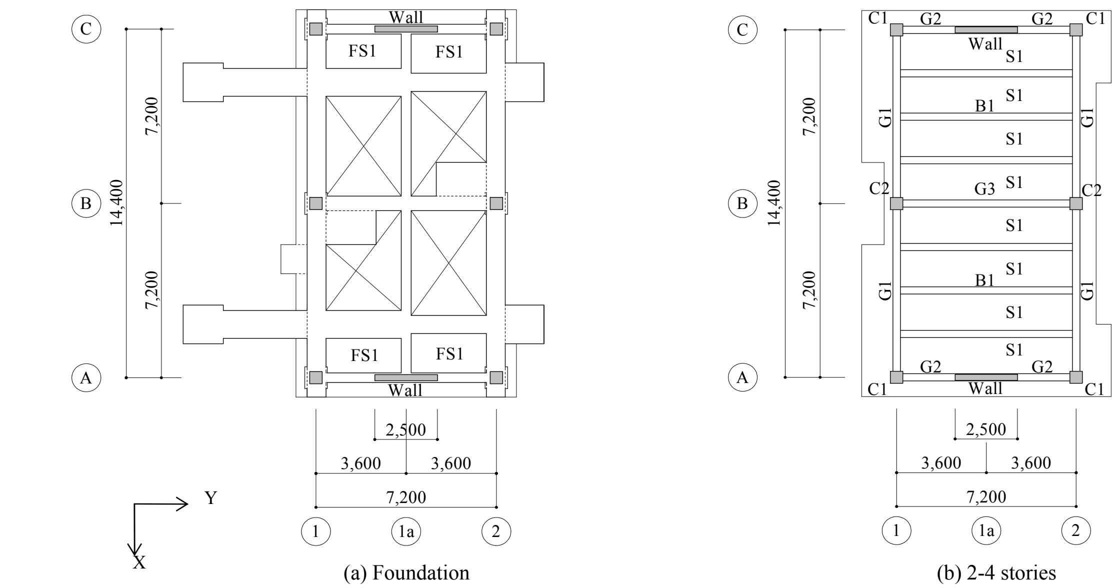

Figure A.1 Floor plan of the RC specimen.

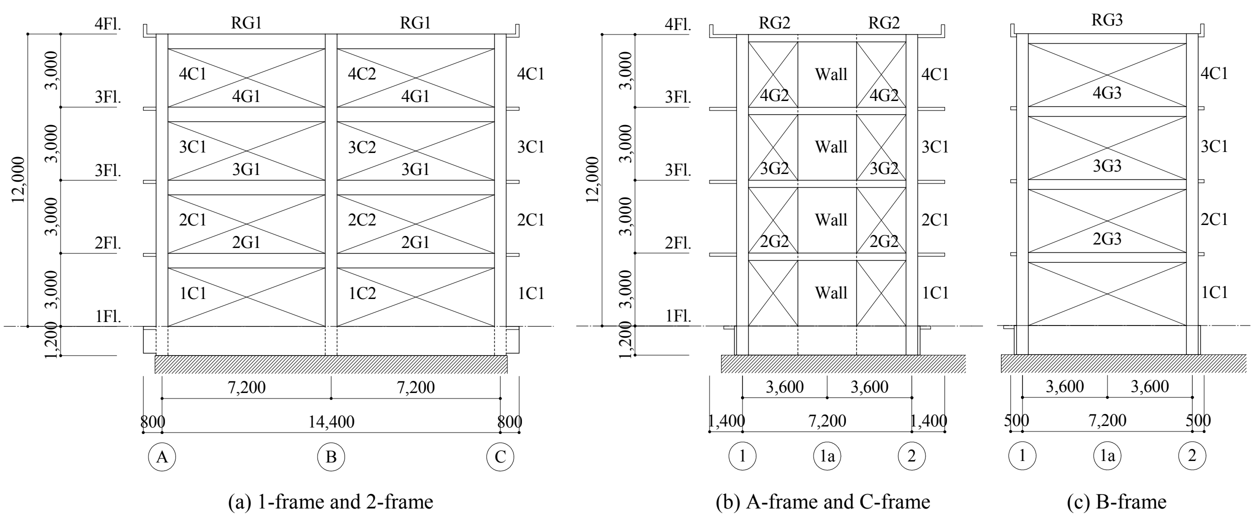

Figure A.2 Elevation of the RC specimen.

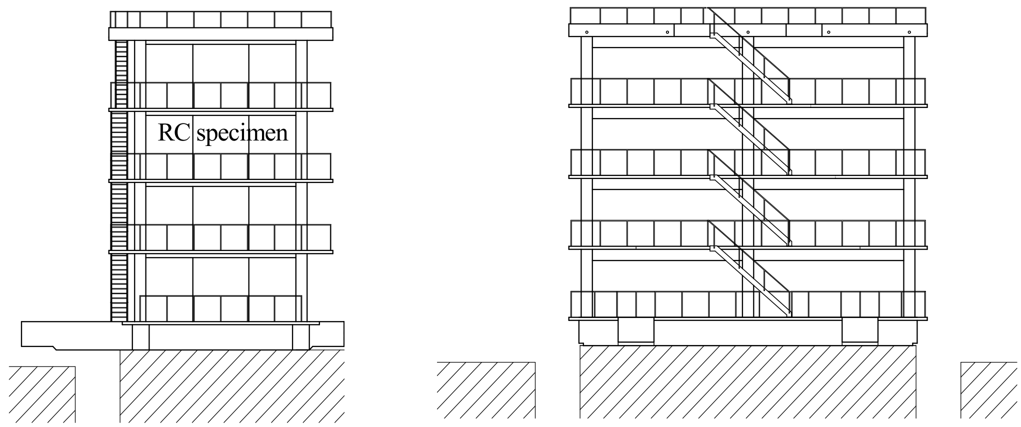

Figure A.3 Overview of the RC specimen.

Table A.1 List of steel reinforcement

List of Column

		C1	C2
4Fl. 3Fl.	Section	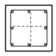	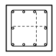
	B x D	500 x 500	500 x 500
	Rebar	8-D22	10-D22
	Hoop	2,2-D10@100	2,2-D10@100
	Joint	2,2-D10@140	2,2-D10@140
2Fl.	Section	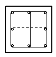	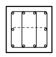
	B x D	500 x 500	500 x 500
	Rebar	8-D22	10-D22
	Hoop	2,3-D10@100	2,4-D10@100
	Joint	2,2-D10@140	2,2-D10@140
1Fl.	Top Section	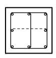	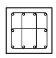
	B x D	500 x 500	
	Rebar	8-D22	
	Hoop	2,3-D10@100	
	Joint	2,2-D10@140	
	Bottom Section	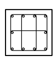	
	B x D	500 x 500	500 x 500
	Rebar	10-D22	10-D22
	Hoop	3,4-D10@100	3,4-D10@100
	Joint	2,2-D10@140	2,2-D10@140

List of Wall

		Wall				
4Fl. 3Fl. 2Fl.	Section	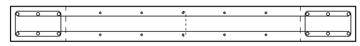				
	B x D	2,500 x 250				
	Rebar		2 x 6-D19	Vertical		D13@300 (W)
	Hoop		2,2-D10@100	Horizontal	A	D10@125 (W)
					C	D10@200 (W)
	Joint	2,2-D10@150				
1Fl.	Section	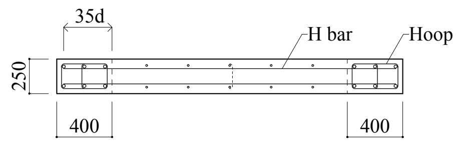				
	B x D	2,500 x 250				
	Rebar		2 x 6-D19	Vertical		D13@300 (W)
	Hoop	A	2,3-D10@80	Horizontal	A	D10@125 (W)
		C	2,3-D10@100		C	D10@200 (W)
	Joint	2,2-D10@150				

List of Slab Depth: 130mm

		Shorter direction	Longer direction
S1	Top	D10@200	D10@250
	Bottom	D10@200	D10@250
CS1	Top	D10,D13@200	D10@250
	Bottom	D10@200	D10@250
CS2	Top	D10@200	D10@250
	Bottom	D10@200	D10@250
CS3	Top	D10,D13@200	D10,D13@200
	Bottom	D10@200	D10@200

List of Girder

		G1		
	Location	End	Center	End
RFl. 4Fl.	Section	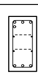	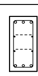	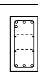
	B x D	300 x 600		
	Top	4-D22	3-D22	4-D22
	Bottom	3-D22	3-D22	3-D22
	Web	4-D10		
	Stirrup	2-D10@200		
3Fl.	Section	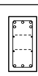	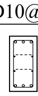	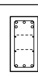
	B x D	300 x 600		
	Top	5-D22	3-D22	5-D22
	Bottom	3-D22	3-D22	3-D22
	Web	4-D10		
	Stirrup	2-D10@200		
2Fl.	Section	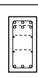	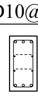	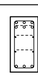
	B x D	300 x 600		
	Top	6-D22	3-D22	6-D22
	Bottom	3-D22	3-D22	3-D22
	Web	4-D10		
	Stirrup	2-D10@200		

List of Girder

		G2	
	Location	End	Center
RFl.	Section		
	B x D	300 x 300	
	Top	3-D19	3-D19
	Bottom	2-D19	3-D19
	Web	-	
	Stirrup	2-D10@100(KSS785)	
4Fl. 3Fl. 2Fl.	Section		
	B x D	300 x 300	
	Top	3-D19	4-D19
	Bottom	3-D19	3-D19
	Web	-	
	Stirrup	2-D10@100(KSS785)	

List of Girder

		G3	
	Location	End	Center
4Fl. 3Fl. 2Fl.	Section	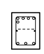	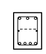
	B x D	300 x 400	
	Top	5-D19	3-D19
	Bottom	3-D19	4-D19
	Web	2-D10	
	Stirrup	2-D10@200	
1Fl.	Section	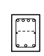	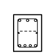
	B x D	300 x 400	
	Top	4-D19	3-D19
	Bottom	3-D19	4-D19
	Web	2-D10	
	Stirrup	2-D10@200	

List of beam

		B1	
	Location	End	Center
All	Section	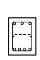	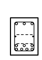
	B x D	300 x 400	
	Top	3-D19	3-D19
	Bottom	4-D19	7-D19
	Web	2-D10	
	Stirrup	2-D10@200	

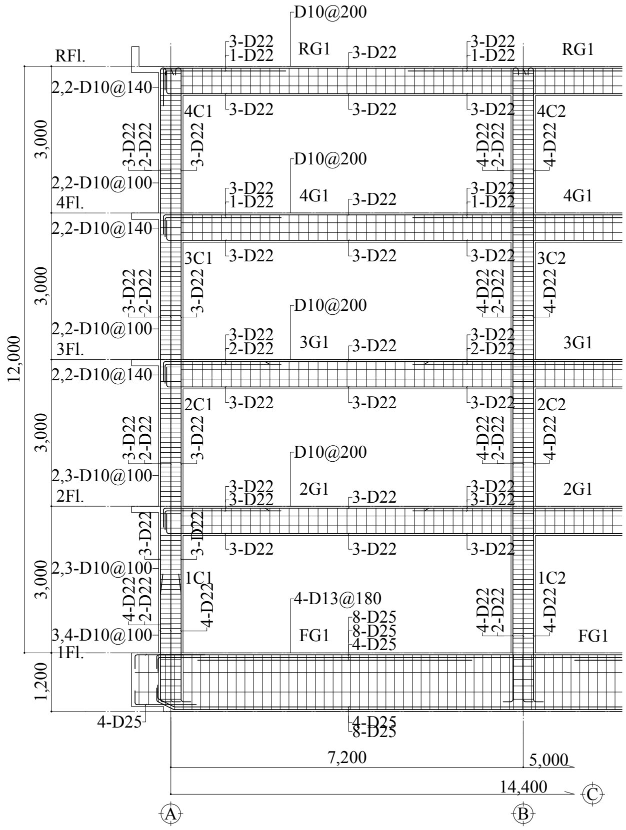

(a) 1-frame and 2-frame

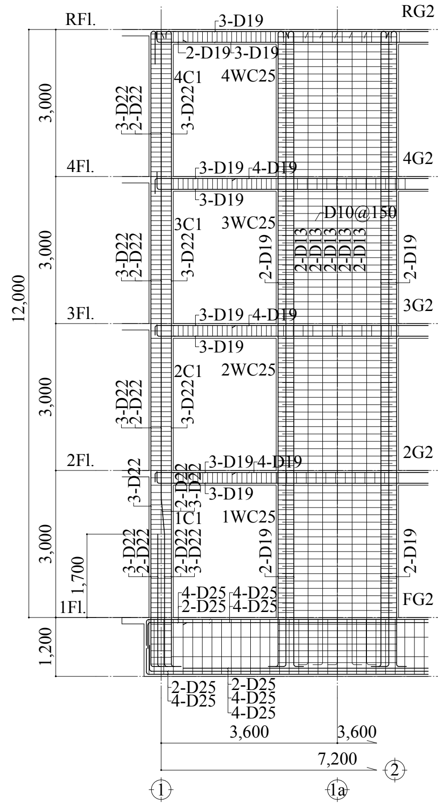

(b) A-frame and C-frame

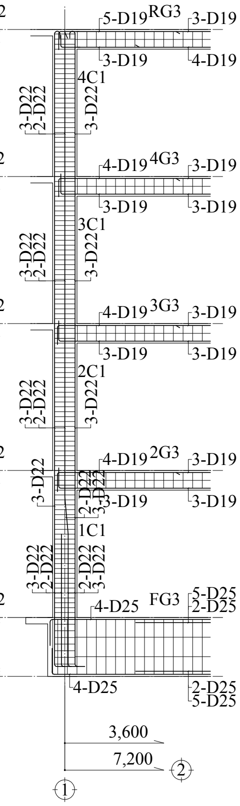

(c) B-frame

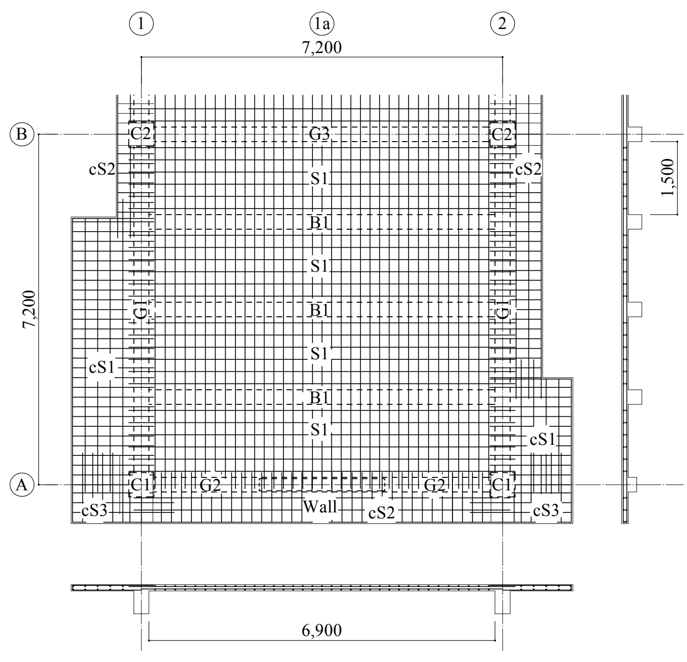

(d) Floor slab

Figure A.4 Details of RC specimen.

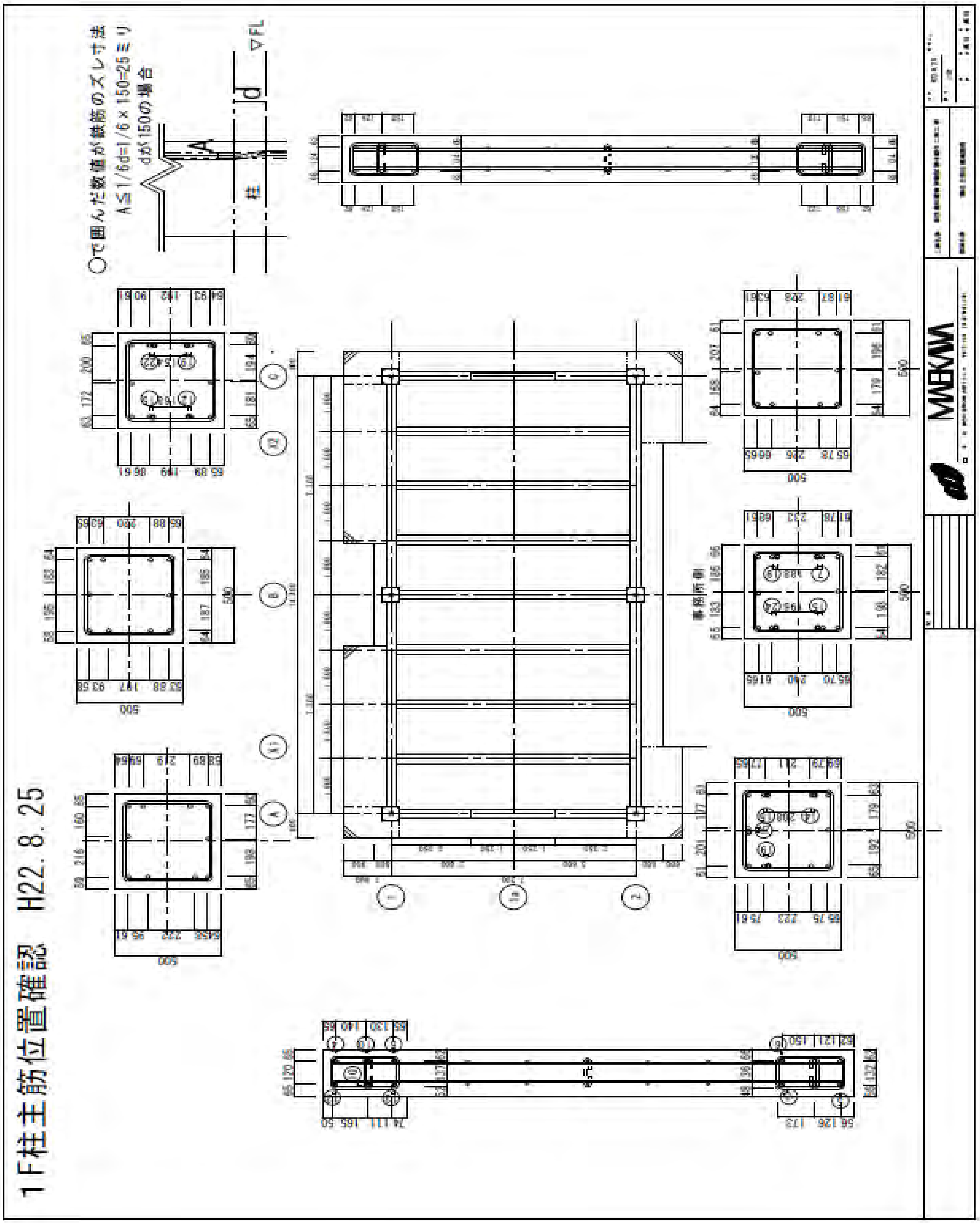

Figure A.5   Steel locations at floor 1F.

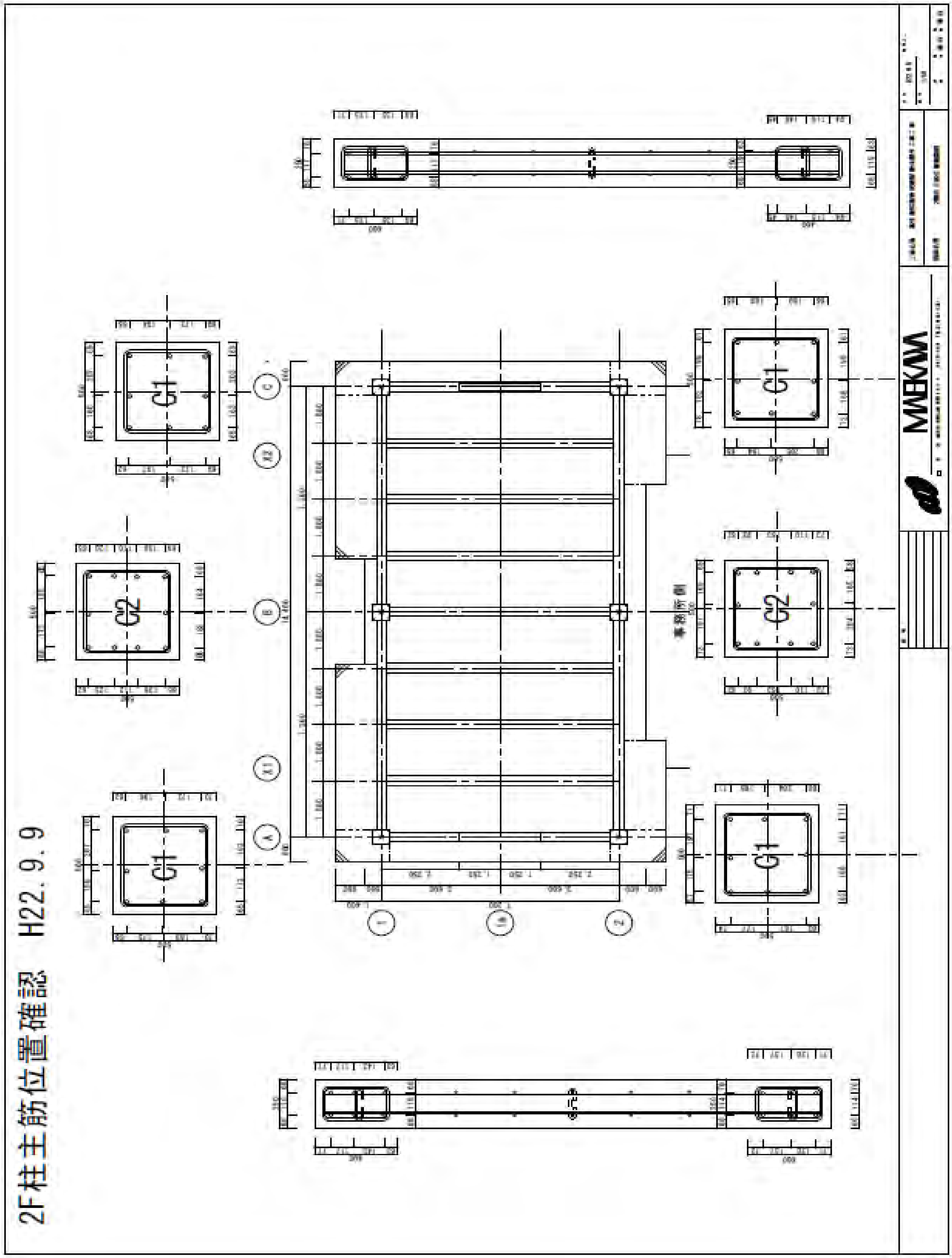

Figure A.6 Steel locations at floor 2F.

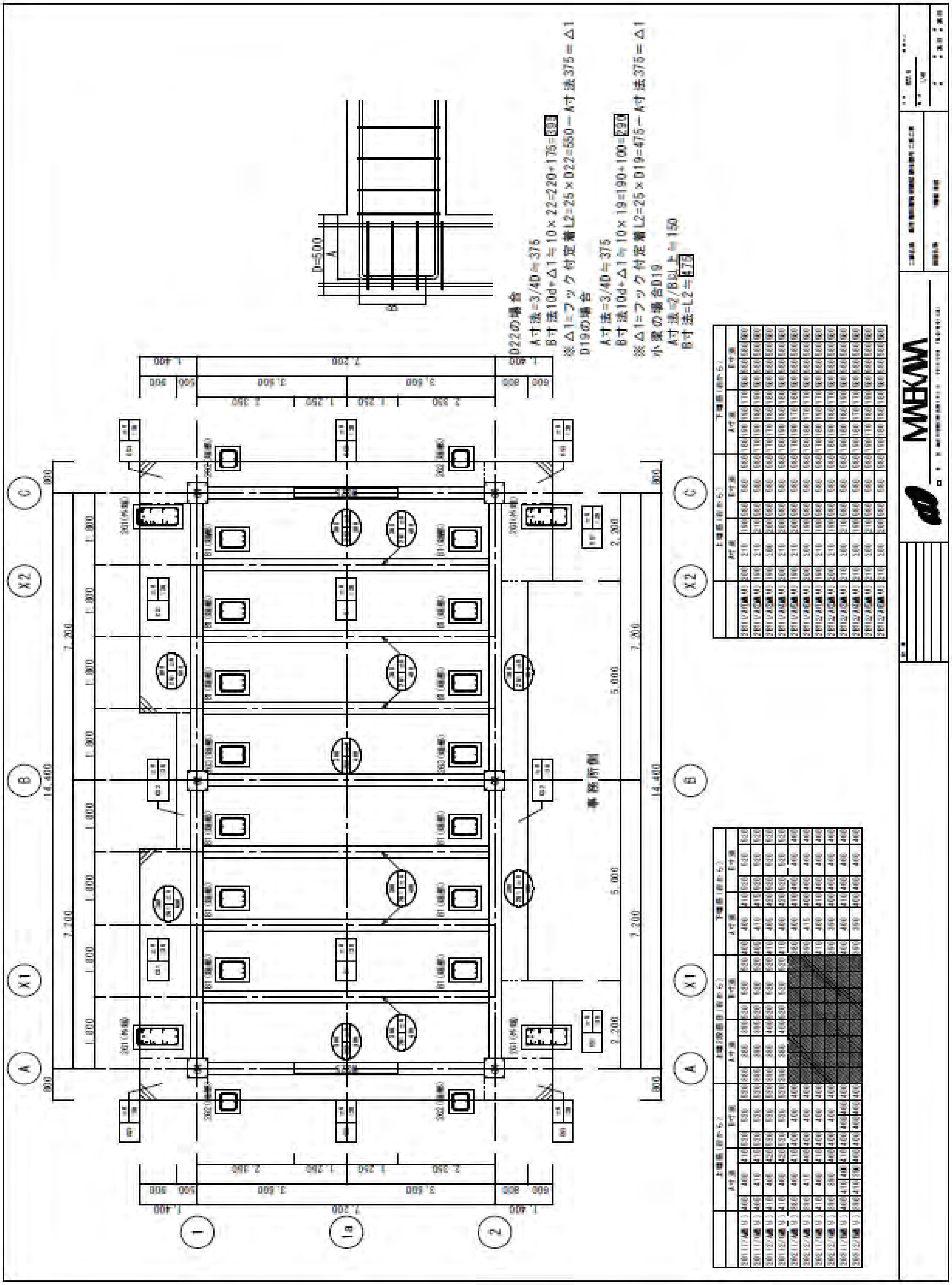

Figure A.7 Steel locations at floor 2F.

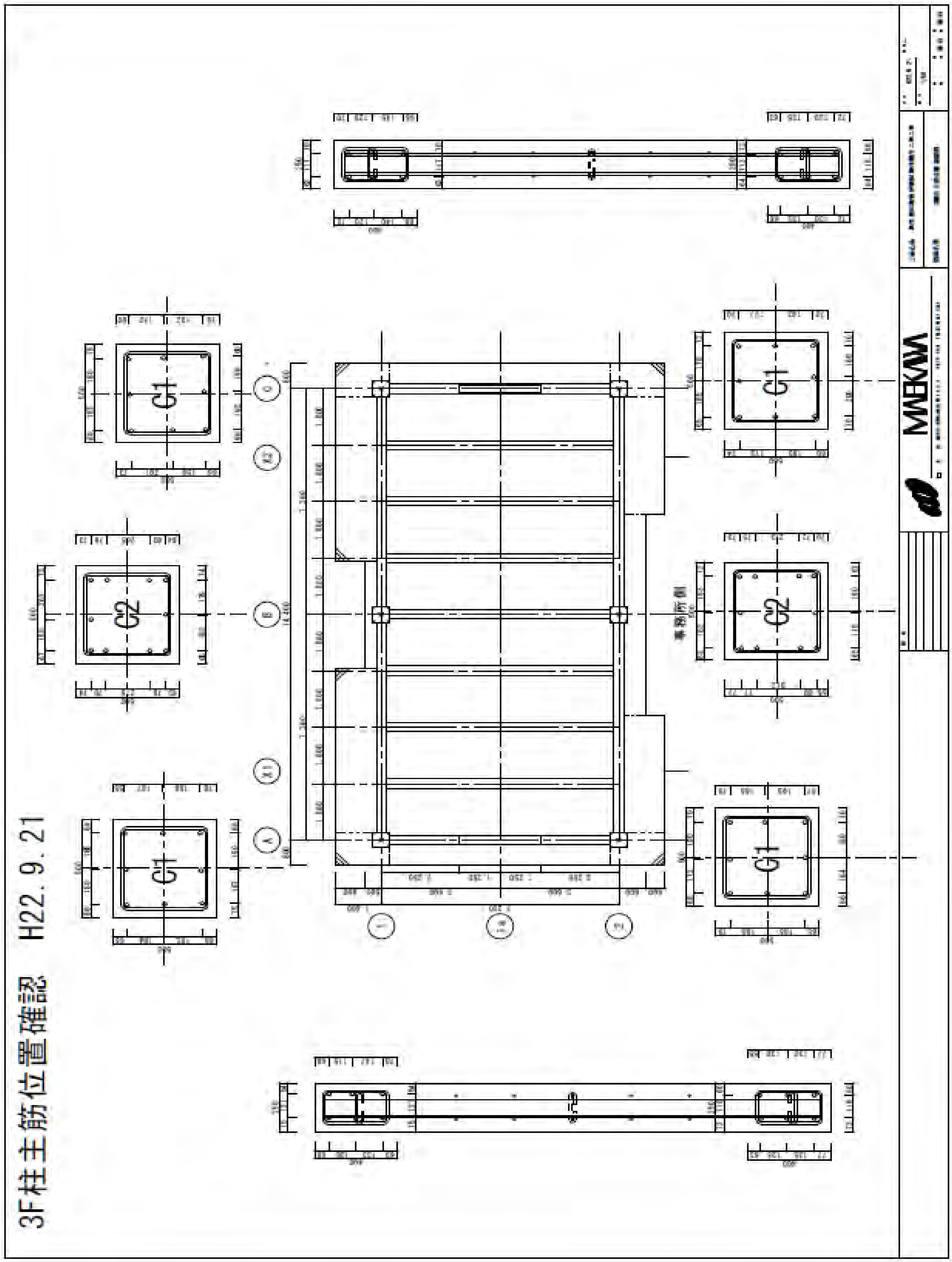

Figure A.8   Steel locations at floor 3F.

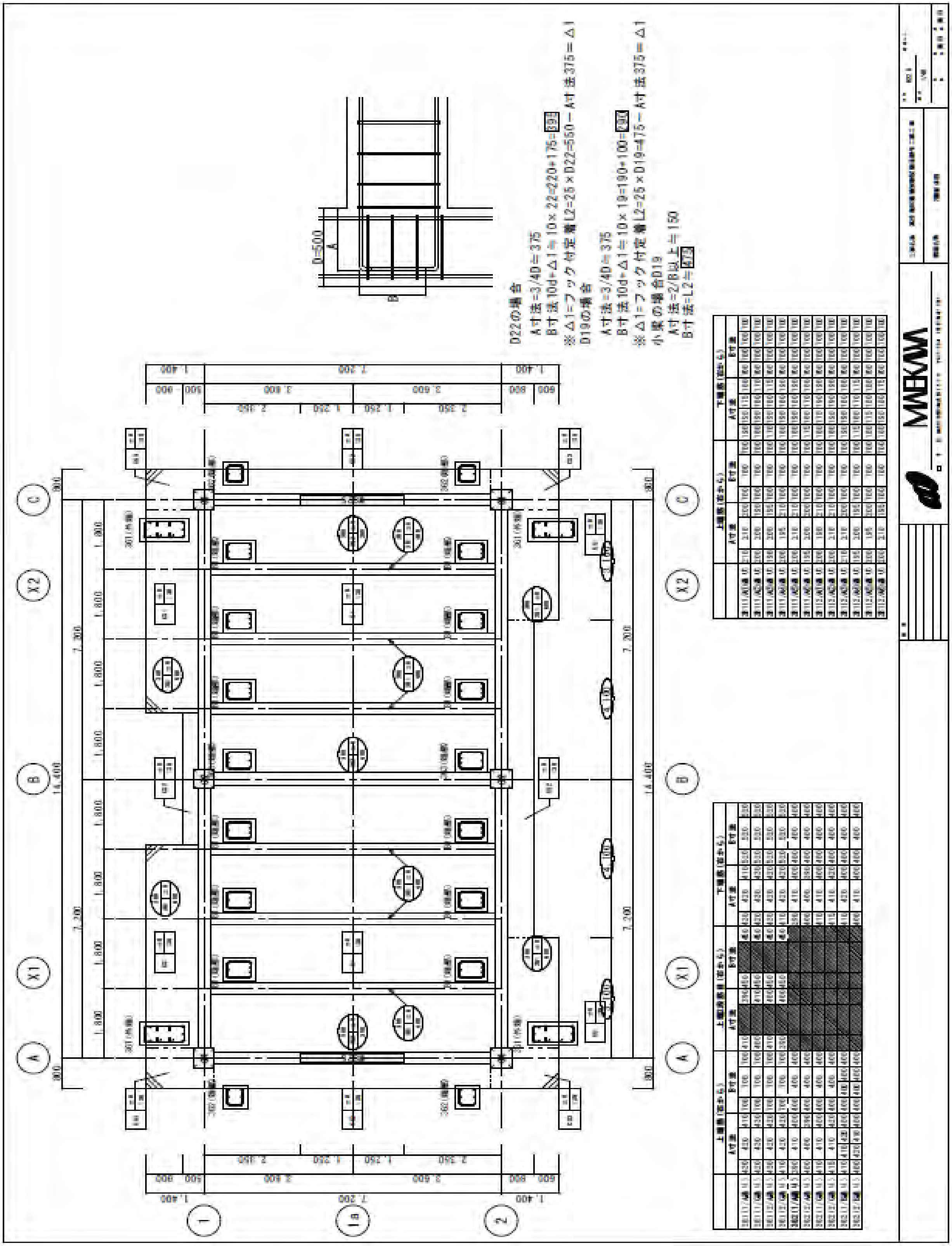

Figure A.9 Steel locations at floor 3F.

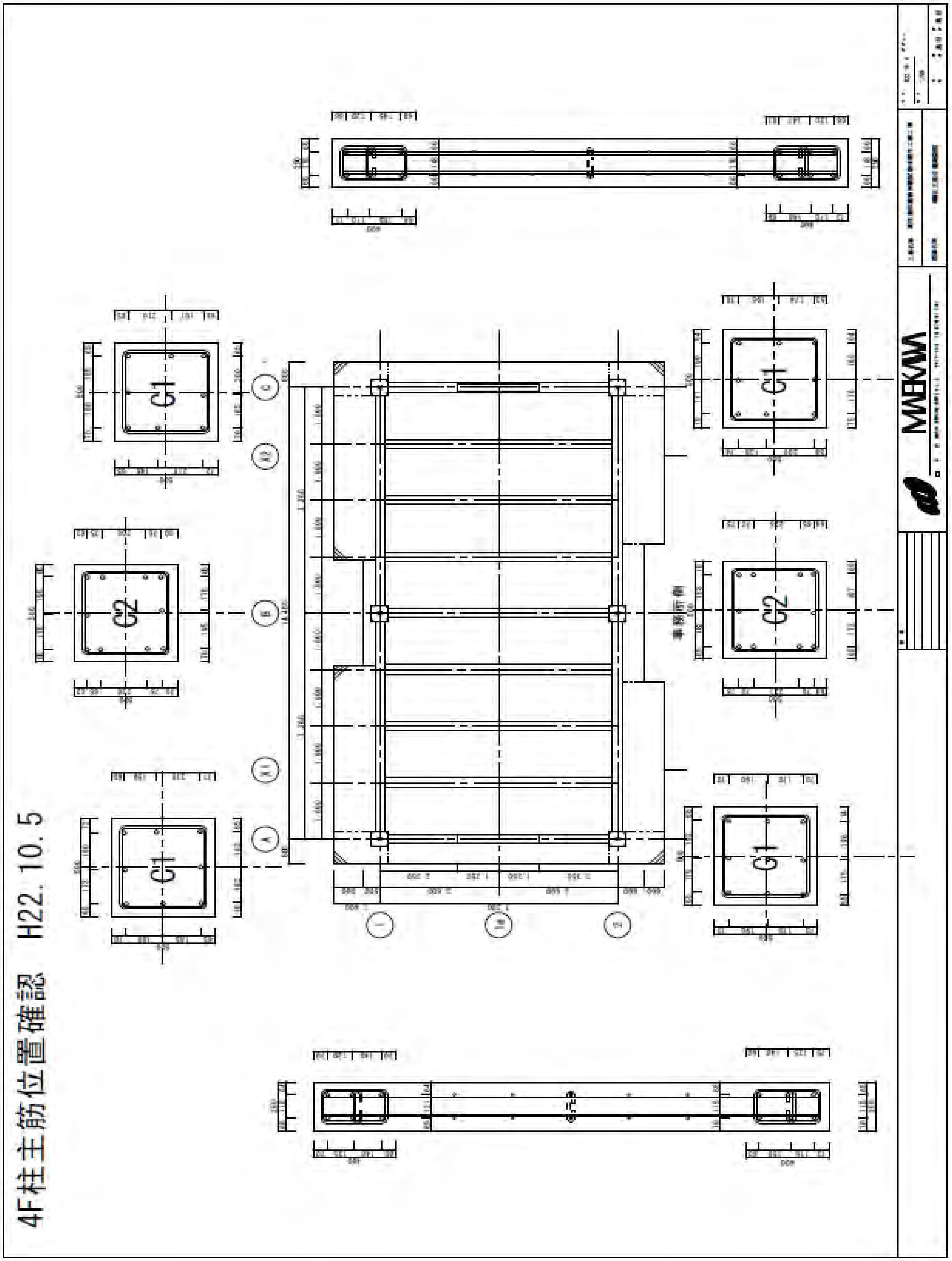

Figure A.10　Steel locations at floor 4F.

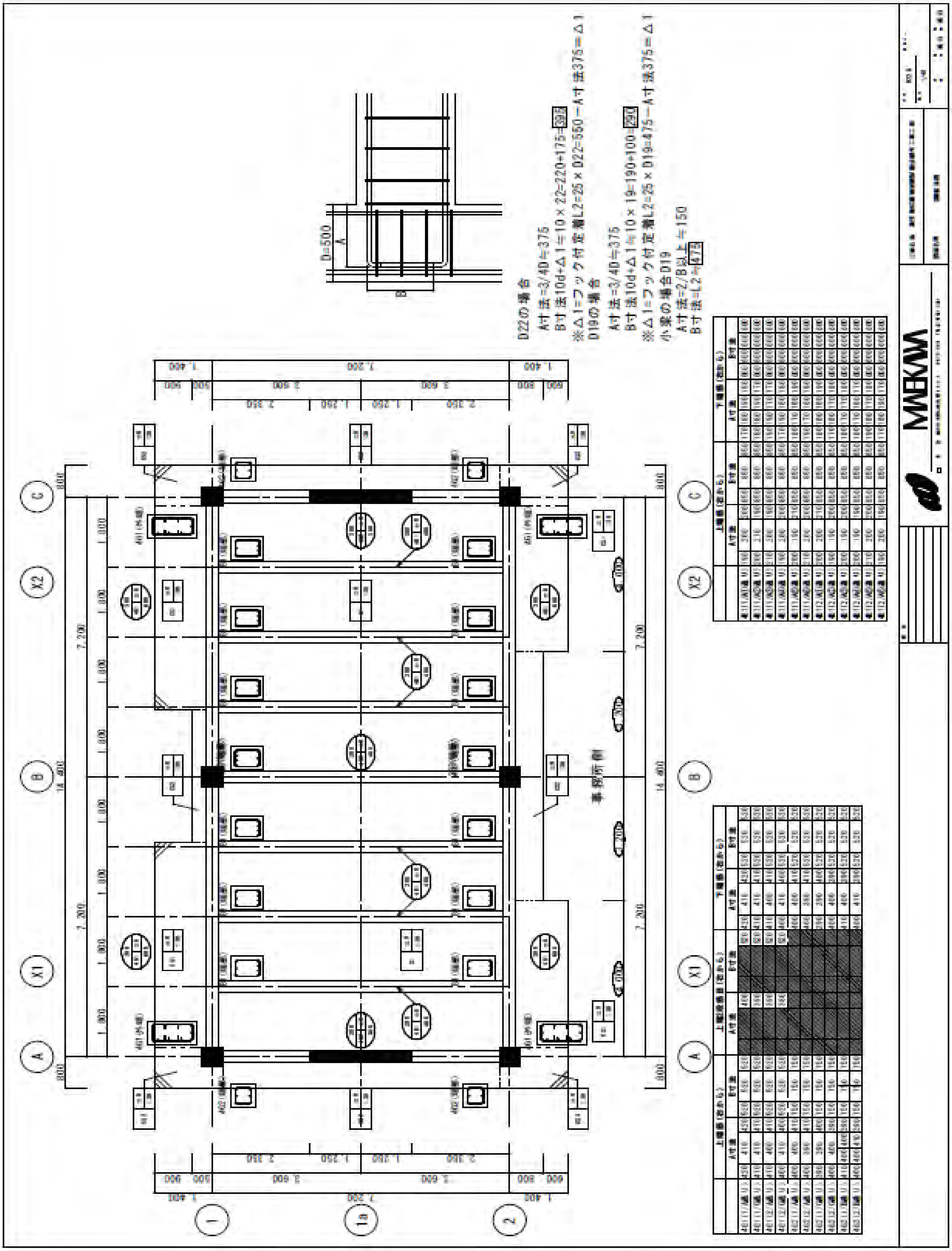

Figure A.11 Steel locations at floor 4F.

A.2 MEMBER GEOMETRY AND REINFORCEMENT OF THE PT SPECIMEN

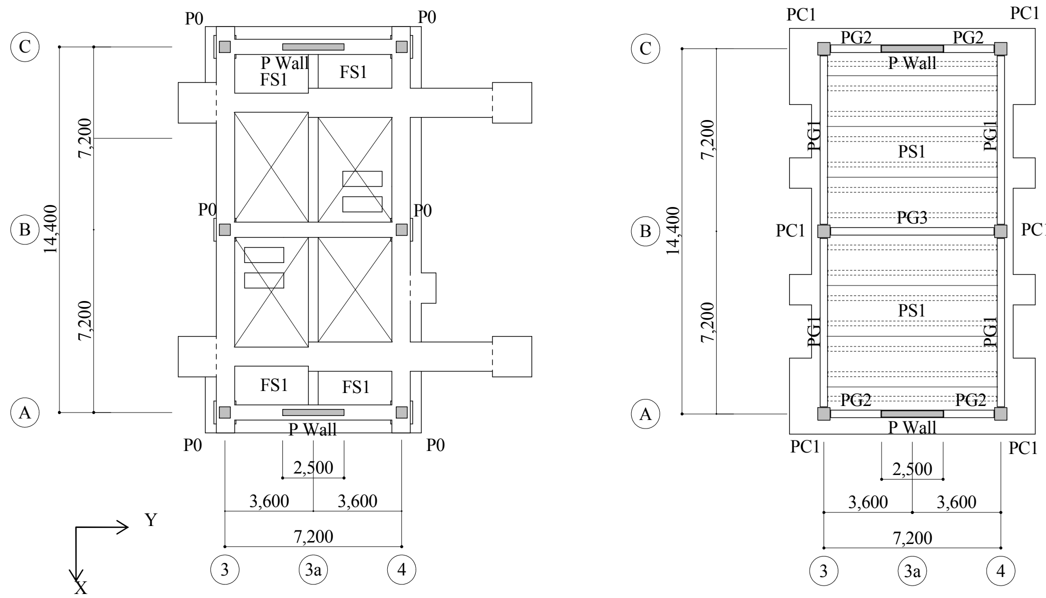

(a) Foundation (b) 2-4 stories

Figure A.12 Floor plan of the PT specimen.

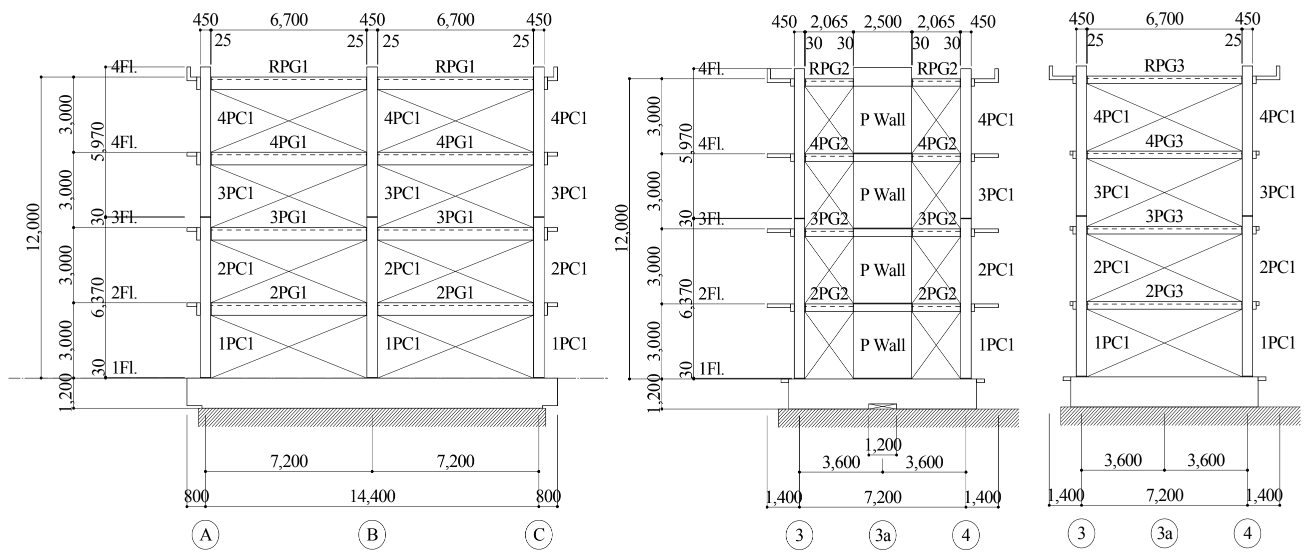

(a) 3-frame and 4-frame (b) A-frame and C-frame (c) B-frame

Figure A.13 Elevation of the PT specimen.

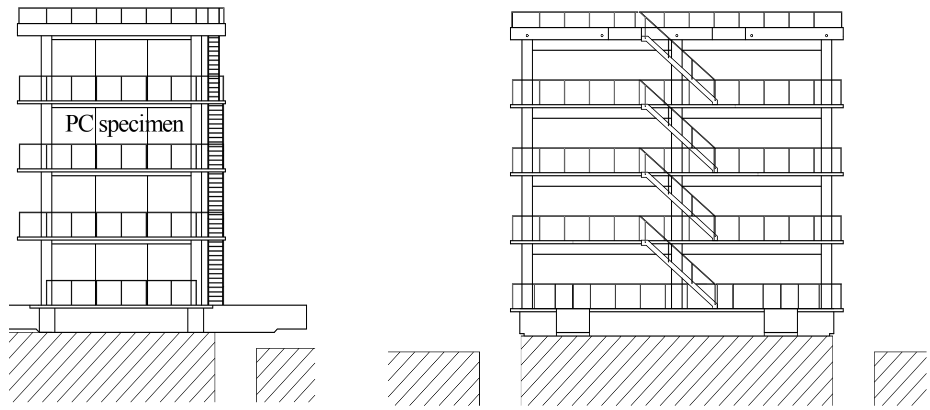

Figure A.14   Overview of the PT specimen.

Table A.2 List of steel reinforcement.

List of Column		
		PC1
4Fl. 3Fl. 2Fl. 1Fl.	Section	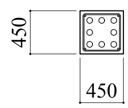
	Tendon	8-21mm(SBPR1080/1230)
	Rebar	4-D19
	Hoop	D10@100

List of Girder			
		PG1	
	Location	End	Center
RFl.	Section	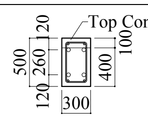	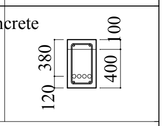
	Tendon	4C-1-15.2mm(SWPR7BL)	
	Top	2 - D19	
	Bottom	3 - D19	
	Stirrup	2-D10@150	2-D10@200
	Web	————	
4Fl.	Section	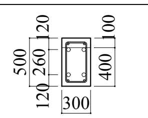	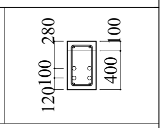
	Tendon	4C-1-19.3mm(SWPR7BL)	
	Top	2 - D19	
	Bottom	3 - D19	
	Stirrup	2-D10@100	2-D10@200
	Web	————	
3Fl. 2Fl.	Section	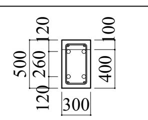	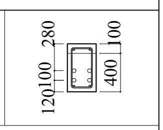
	Tendon	4C-3-15.2mm(SWPR7BL)	
	Top	2 - D19	
	Bottom	3 - D19	
	Stirrup	2-D10@90	2-D10@200
	Web	————	

List of Wall		
		P Wall
4Fl. 3Fl. 2Fl.	Section	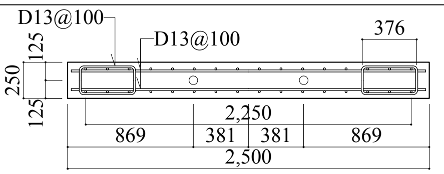
	Tendon	3-10-15.2mm(SWPR7B)
	V bar	D13@150(double)
	H bar	D13@100(double)
1Fl.	Top Section	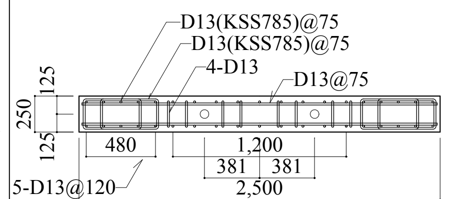
	Bottom Section	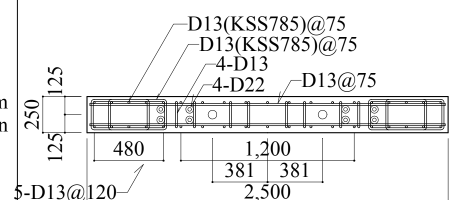
	Tendon	3-10-15.2mm(SWPR7B)
	V bar	
	H bar	

List of Girder			
		PG2	PG3
	Location		
All	Section	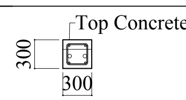	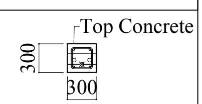
	Tendon	2C-1-17.8mm(SWPR19L)	2C-1-17.8mm(SWPR19L) 1C-17mm(SBPR930/1080)
	Top	2 - D19	2 - D19
	Bottom	2 - D19	2 - D19
	Stirrup	2-D10@100(KSS785)	2-D10@150
	Web	————	————

List of Slab	Depth: 130mm			
		Shorter direction	Longer direction	
PS1		D10@200	D10@200	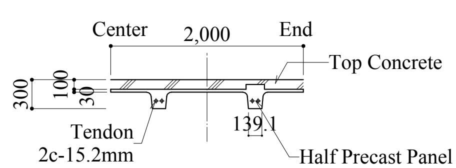
CS1	Top	D13@200	D10@250	
	Bottom	D10@200	D10@250	
CS2	Top	D10@200	D10@250	
	Bottom	D10@200	D10@250	
CS3	Top	D13@200	D13@200	
	Bottom	D10@200	D10@200	

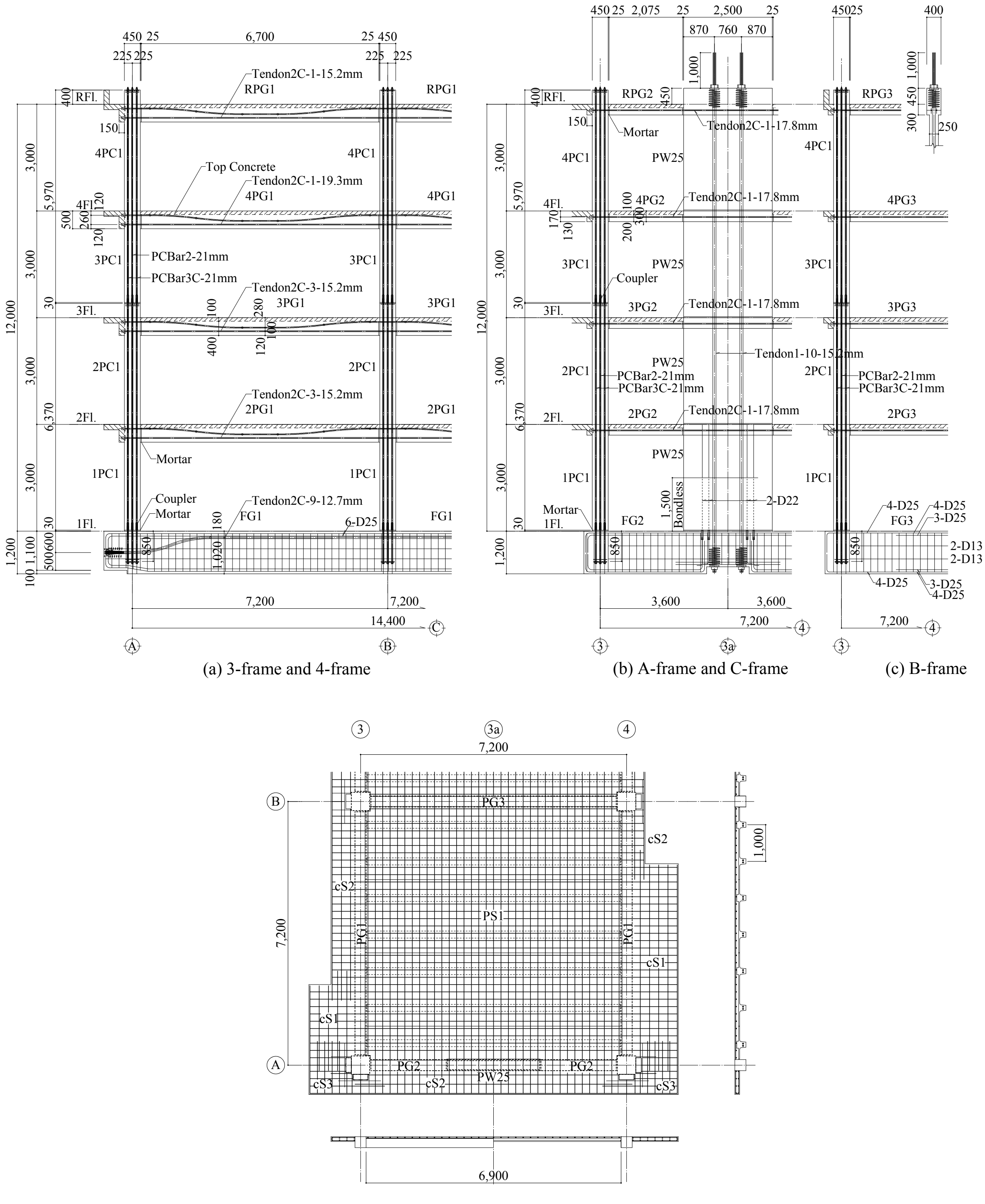

Figure A.15 Details of PT specimen.

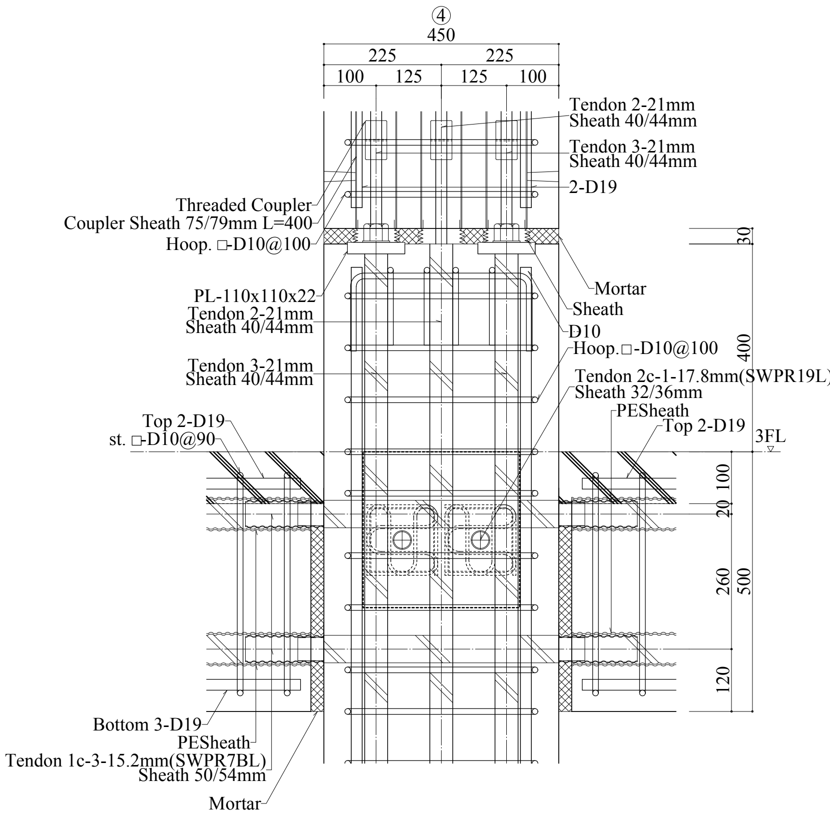

Figure A.16 Details of PT beam column joint.

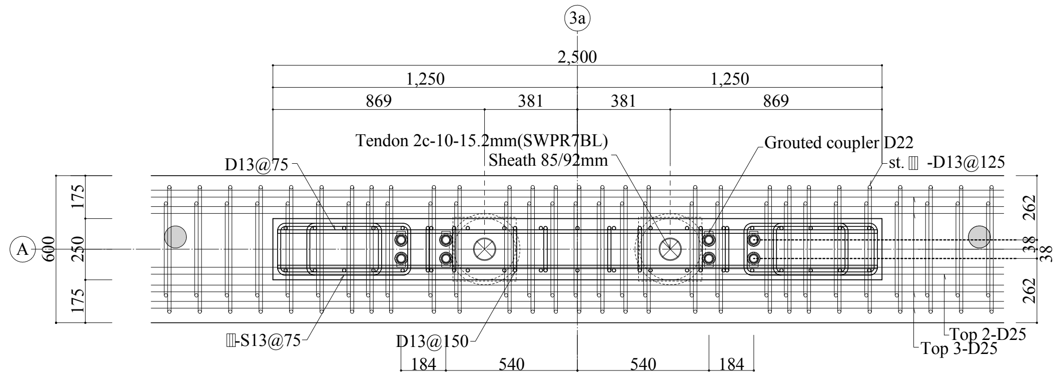

Plan

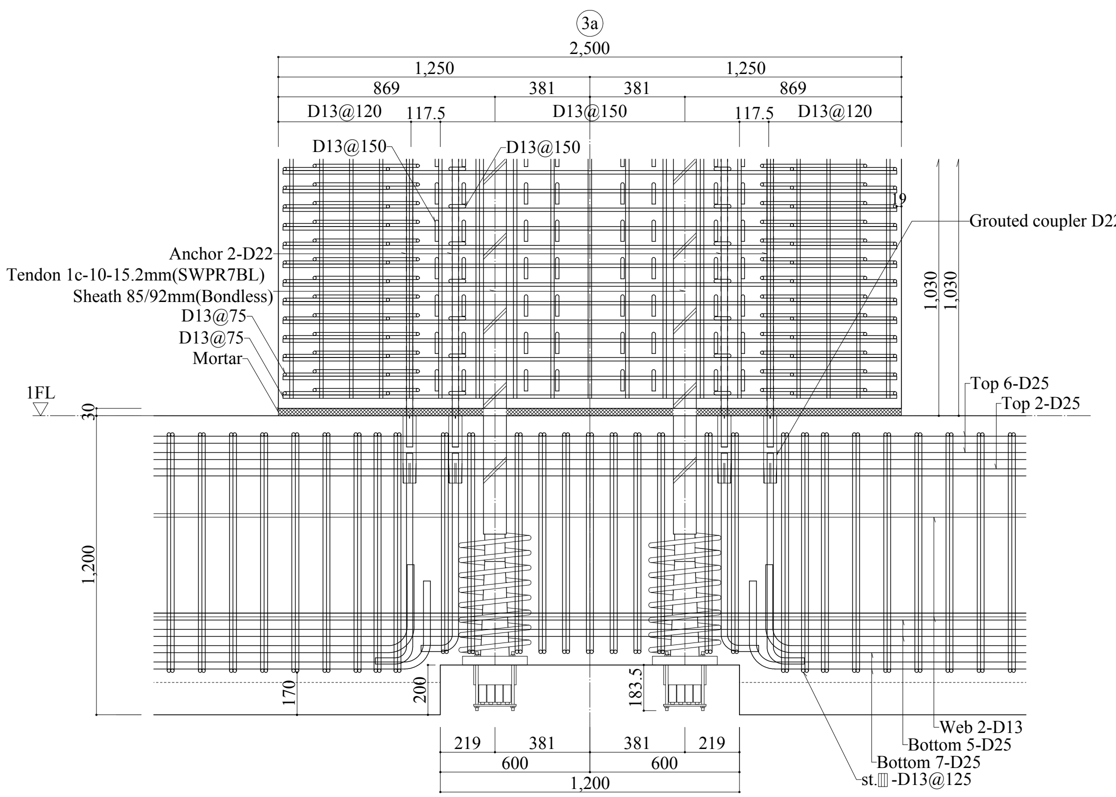

Figure A.17 Details of PT wall base and foundation.

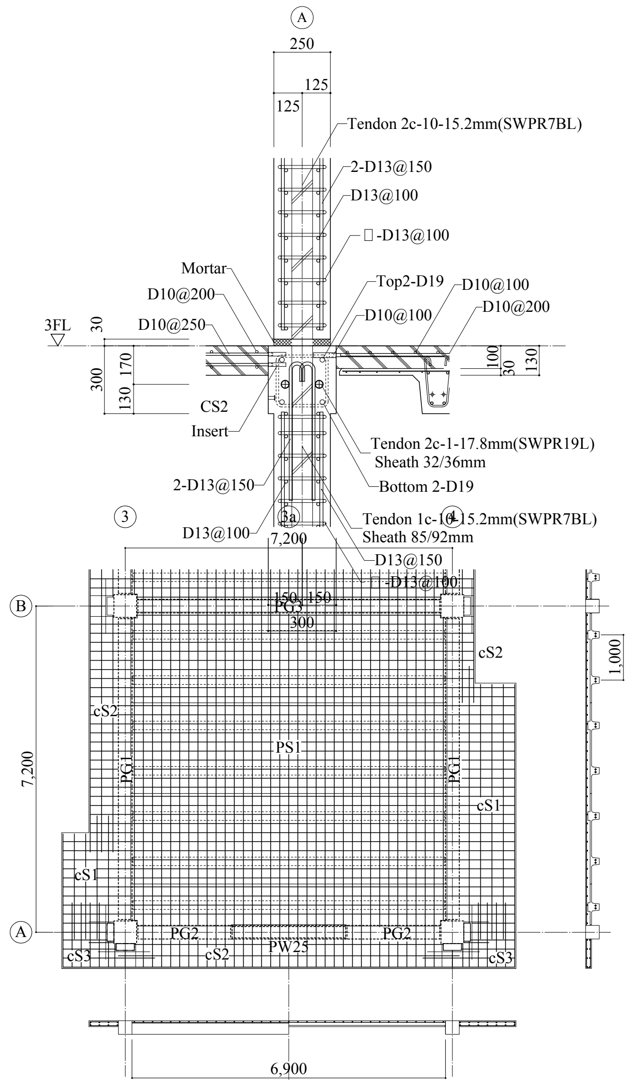

Figure A.18 Details of PT wall floor slab interface

A.3 SETUP AND PLACEMENT OF THE SPECIMENS

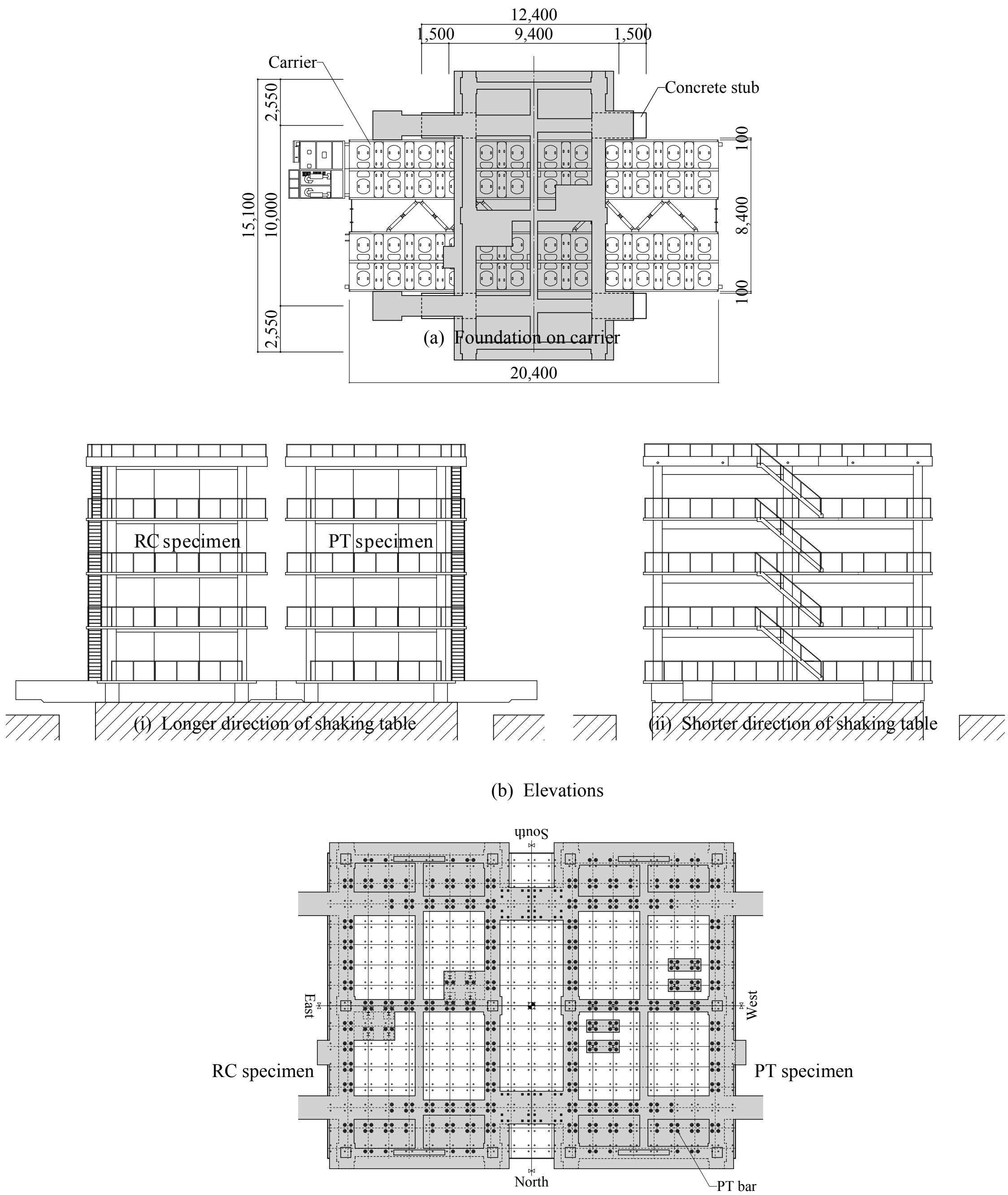

(c) Fixed foundations on shaking table

Figure A.19 Set up of the specimens.

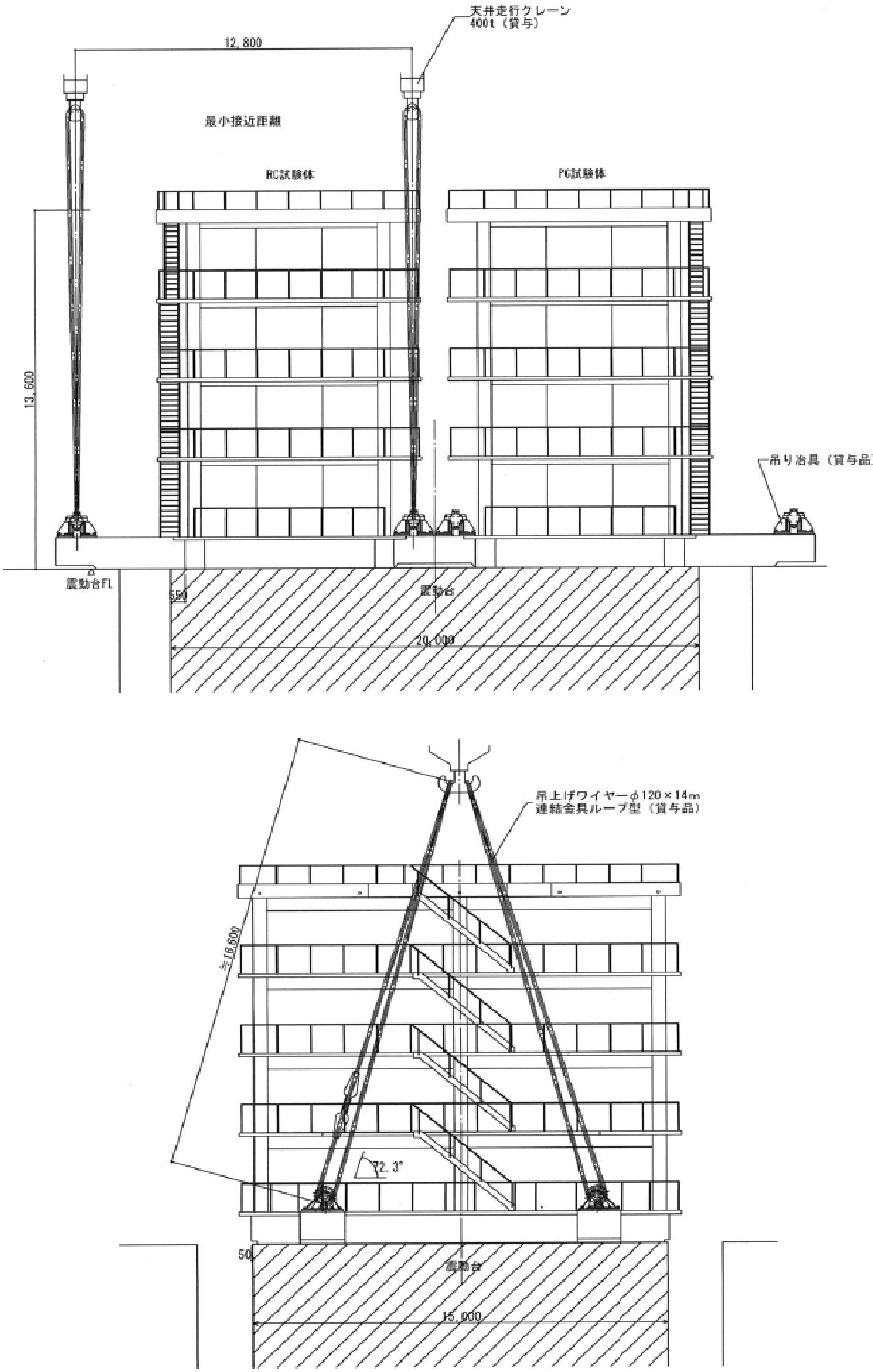

Figure A.20 Placement of the specimens on the shaking table.

The specimens can be weighted when they are carried on the shaking table.

Photo 1. Specimen on Carrier car

Photo 2. Specimen Hanging on Cranes

Photo 3. RC Specimen Hanging on Cranes (248+365-25=588 t)
(Total weight of hanging wires is 25 t)

Photo 4. Weight of PT Specimen Hanging on Cranes: 335+236-25=546 t
(Total weight of hanging wires is 25 t)

Table 1. Summary of Weight of Specimen

	Measured	Estimated (Vol.×2.4 [t/m^3] + Machines)	Ratio (Estimated/ Measured)
RC	588 t	595.9 t	101.3 %
PT	546 t	558.8 t	102.3 %

Figure A.21 Measuring weight of the specimens.

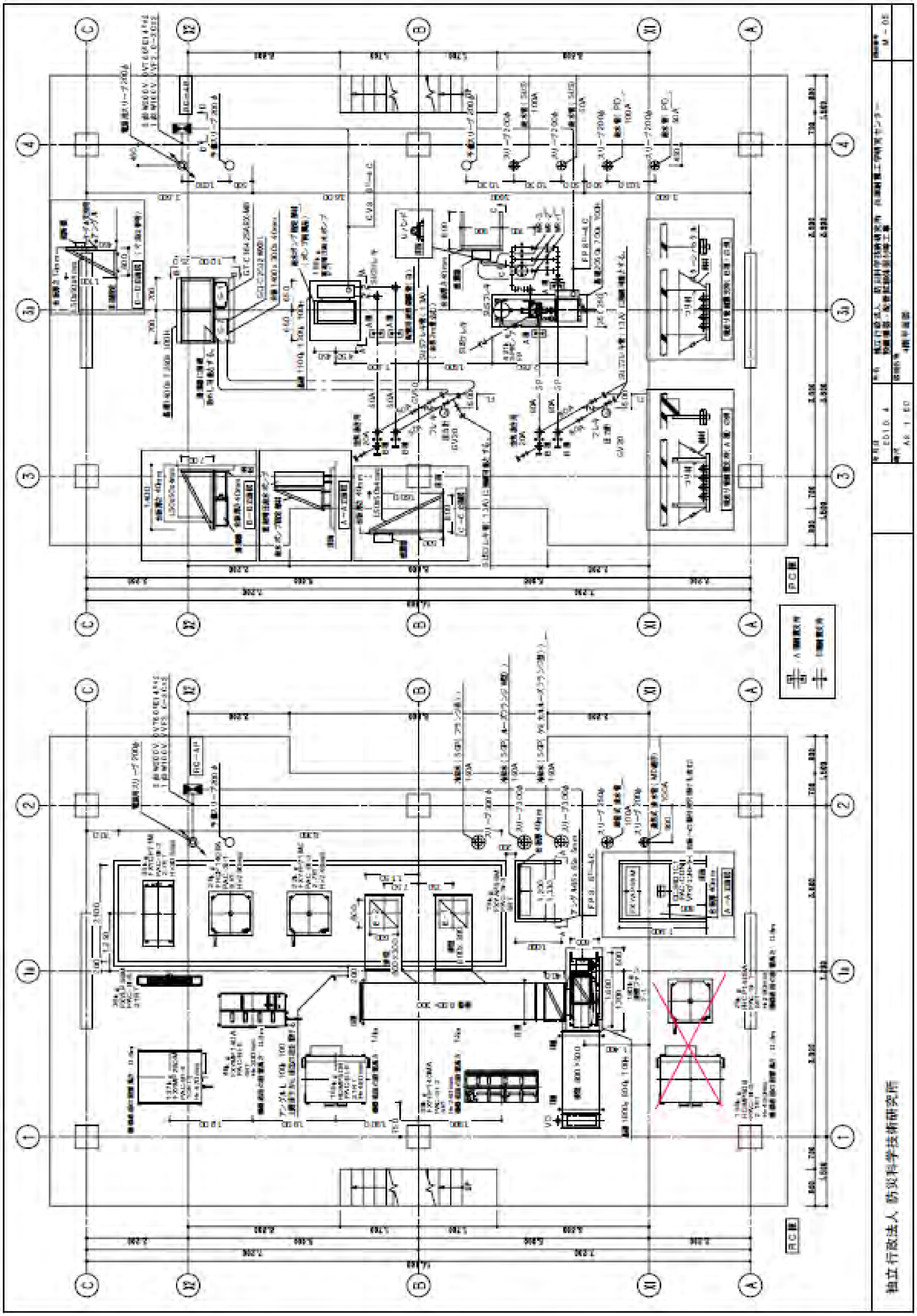

Figure A.22 Weights of equipment on the buildings at the third level

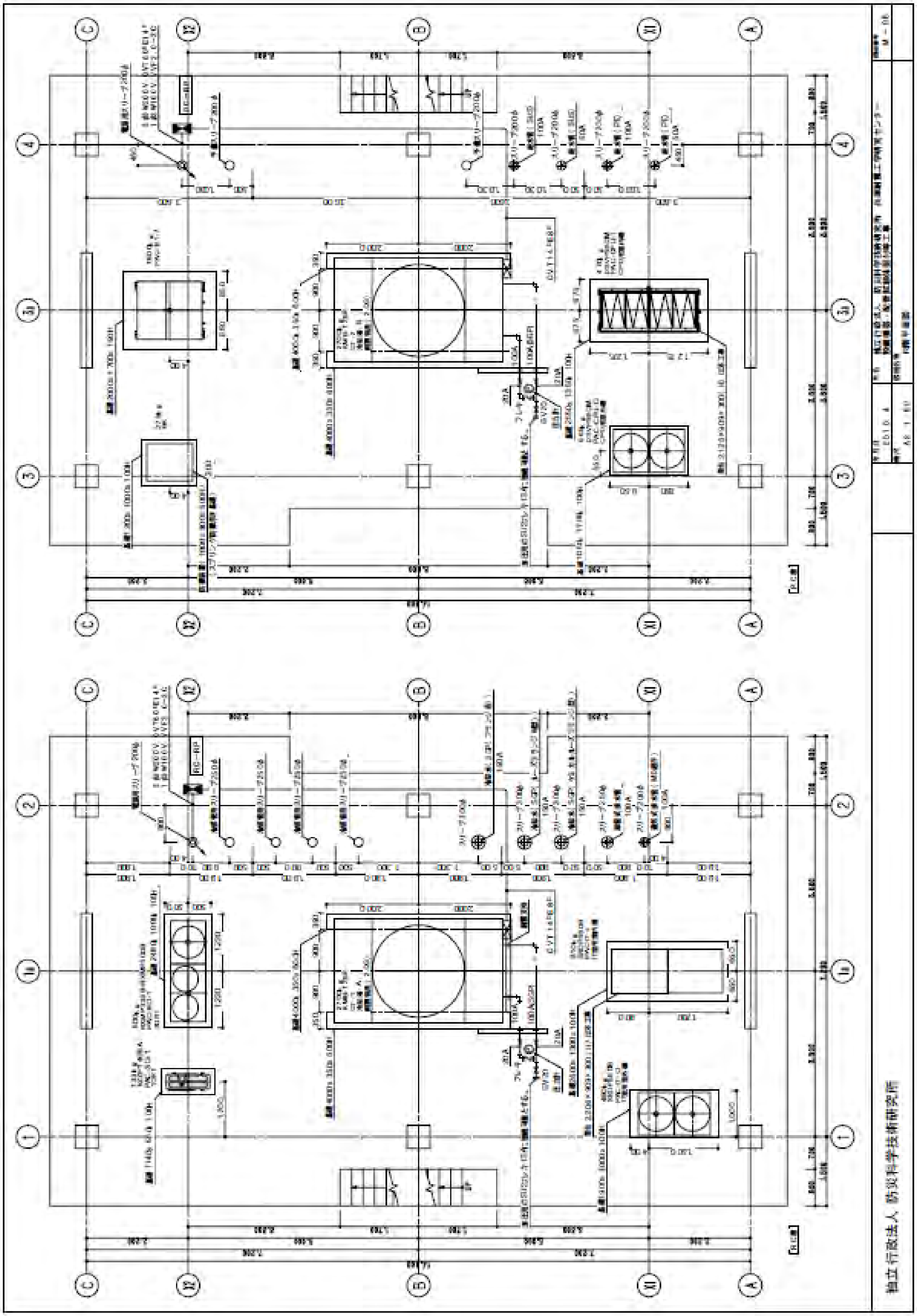

Figure A.23 Weights of equipment on the buildings at roof level.

Appendix B

B.1 EQUIVALENT LATERAL LOAD PROCEDURE (ASCE 7-05)

SHEAR WALL DIRECTION

Mapped MCE spectral response accelerations:

	S_s (g) =	1.5	At short periods		
	S_1 (g) =	0.9	At 1 s.		
Site coefficients:					
	F_a =	1			
	F_v =	1			
Importance factor:	I =	1			
Response modification factor:	R =	6			
Story height:	h_i =	3	m	9.84	ft
Number of stories:	n =	4			

Design spectral response acceleration parameters:

S_{MS} (g) =	1.5	S_{DS} (g) =	1	T_s (sec)	0.6
S_{M1} (g) =	0.9	S_{D1} (g) =	0.6	T_0 (sec)	0.12

Period Calculations:

Eigenvalue analysis:		T_{eigen}=	0.58	sec
Approximate period:				
	Table 12.8-2:	C_t =	0.0488	(for metric)
		h_n =	12	m
		x =	0.75	
	ASCE 7-05 (12.8): $C_t*(h_n)^x$	T_a (sec)=	0.315	
	ASCE 7-05 (12.8): 0.1N	T_a (sec)=	0.4	

C_u =	1.4 (S_{D1}>0.6)
$T_{limit} = C_uT_a$=	0.44
T (sec)=	**0.440**

Seismic Response Coefficient:

Cs (12.8-2)	**Cs_{max} (12.8-3)**	**Cs_{min} (12.8-5)**	**Cs_{min} (12.8-6)**	**Weight (kN)**	**V_{base} = Cs*W**	**k**
0.167	0.23	0.01	0.075	1815	302.50	1

Story forces:

	i	wi (kN)	Cvi	Fi (kN)	Mi(kN-m)
	1	441	0.096	29.1	2745
	2	444.5	0.194	58.6	1838
	3	458	0.299	90.6	1017
	4	471.5	0.411	124.3	373
Total weight:		1815			
			V_{base}=	302.5	

** Weight is half the full weight to find the forces per shear wall system.

Redundancy Factor ρ= 1.3

Story forces with redundancy factor

$E_h=\rho Q_E$	i	Fi (kN)	Mi(kN-m)	
	1	37.8	**3569**	**Mu,base**
	2	76.2	2389	
	3	117.7	1323	
	4	161.6	485	

Eh= V*ρ =	**393.3**	kN
% of weight=	21.67	%

FRAME DIRECTION

Mapped MCE spectral response accelerations:

	S_s (g) =	1.5	At short periods
	S_1 (g) =	0.9	At 1 s.
Site coefficients:			
	F_a =	1	
	F_v =	1	
Importance factor:	I =	1	
Response modification factor:	R =	8	
Story height:	h_i =	3	m 9.84 ft
Number of stories:	n =	4	

Design spectral response acceleration parameters:

S_{MS} (g) =	1.5	S_{DS} (g) =	1	T_s (sec)	0.6
S_{M1} (g) =	0.9	S_{D1} (g) =	0.6	T_0 (sec)	0.12

Period Calculations:

Eigenvalue analysis: T_{eigen}= 0.67 sec

Approximate period:

Table 12.8-2:	C_t =	0.0466	(for metric)
	h_n =	12	m
	x =	0.9	
ASCE 7-05 (12.8): $C_t*(h_n)^x$	T_a (sec)=	0.44	
ASCE 7-05 (12.8): 0.1N	T_a (sec)=	0.4	
	C_u =	1.4	(S_{D1}>0.6)
	T_{limit} = C_uT_a=	0.56	
	T (sec)=	**0.56**	

Seismic response Coefficient:

Cs (12.8-2)	**Cs_{max} (12.8-3)**	**Cs_{min} (12.8-5)**	**Cs_{min} (12.8-6)**	**Weight (kN)**	**V_{base} = Cs*W**	**k**
0.125	0.13	0.01	0.05625	1815	226.88	1.015

Story forces:

	i	wi (kN)	Cvi	Fi (kN)	Mi(kN-m)
	1	441	0.093	21.1	2067
	2	444.5	0.192	43.5	1387
	3	458	0.300	68.0	769
	4	471.5	0.415	94.2	283
Total weight:		1815			
			V_{base}=	226.9	

** Weight is half the full weight to find the forces per special moment frame.

Redundancy Factor ρ= 1.3

Story forces with redundancy factor

	i	Fi (kN)	Mi(kN-m)
$E_h = \rho Q_E$			
	1	27.5	2687
	2	56.5	1803
	3	88.5	1000
	4	122.5	367

Eh= V*ρ =	**294.9**	kN
% of weight=	16.25	%

B.2 CALCULATIONS BASED ON ACI 318-08 PROVISIONS

BEAMS

Materials

Concrete:	f'_c =	27	MPa	3.9	ksi
Steel:	f_y =	345	MPa	50.0	ksi

2G1 (Frame direction)

Cross-section

	hi=	3000	mm	118.11	in
	Total height =	12000	mm	472.44	in
	bw=	300	mm	11.81	in
	h=	600	mm	23.62	in
	Ag =	180000	mm^2	279.00	in^2
	Diahoop=	10	mm	0.39	in
	Ahoop=	78.54	mm^2	0.12	in^2
	spacing=	200	mm	7.87	in
	d=	545.5	mm	21.48	in
	DiaBar =	22	mm	0.87	in
	Abar=	380.13	mm^2	0.59	in^2
	DiaWeb =	10	mm	0.39	in
	AWeb=	78.54	mm^2	0.12	in^2
slab thickness	ts=	130	mm	5.12	in
slab reinforcement		D10 @ 250			

Strength check:

Flexural strength

effective beam width:

ln=	6700	mm	263.78	in

S.8.12.2 : beff=min(ln/4,bw+2*[8ts],bw+2*[1/2(clear dist. to the next web)]

clear dist to the next web =	6900	mm	271.65	in

	overhanging =	1400	mm	55.12	in

Max total length from:

1) Total length <= ln/4	beff=	1675	mm	65.94	in
2) Each side <= 8ts	beff=	2380	mm	93.70	in
3) Each side <= lc/2	beff=	7200	mm	283.46	in
	beff=	**1675**	**mm**	**65.94**	**in**

M_n^+ =	385.70	kN-m
M_n^- =	572.20	kN-m
$M_{n,center}$=	424.60	kN-m
M_n^{max} =	572.20	kN-m

S21.5.2.2	M_n^+ =	385.70	>	M_n^- /2=	286	OK
mid-span	M_n^+ =	385.70	>	M_n^{max} /4 =	143	OK
	M_n^- =	572.20	>	M_n^{max} /4 =	143	OK

S21.5.2.1 As,min = 3sqrt(f'c)/fy*bw*d
not less than 200bw*d/fy

As,min =	614.07	mm^2	0.95	in^2
200bw*d/fy=	654.27	mm^2	1.01	in^3

Try 3,6

# of bars=	3			
current As=	1140.40	mm^2	1.77	in^3

current As =	1140.40	>	As,min =	654	OK

check reinf. Ratio ρt = 0.0070

ρt =	0.0070	<	ρt ,max=	0.0250	OK

Shear strength

Vc=2*sqrt(f'c)*bw*d	Vc =	141.19	kN	31.74	kips
	# of hoops=	2			
	Av =	157.08	mm^2	0.24	in^3
Vs = Av*fy*d/s	Vs=	147.76	kN	33.22	kips

Vn=	Vc+Vs =	288.96	kN	64.96	kips

Vu,pr due to moments

$M_{n,pr}^{+}$ =	482.13	kN-m		
$M_{n,pr}^{-}$ =	715.25	kN-m		
wg =	10.40	N/mm		
Vn=	288.96	kN	64.96	kips
Vu,pr=	214	kN	48.01	kips

ΦV_n = 217 > Vu = 214 **OK**

Detailing:

Transverse reinforcement

S21.5.3.1: hoops shall be provided in 2h

2h =	1200	mm	47.24	in
current region length =	-	mm	-	in

S21.5.3.2: max spacing in 2h:

s = min(d/4; 8d_b; 24d_{hoop}; 12") =	136.38	mm	5.37	in
current spacing=	200	mm	7.87	in

current spacing= 200 > s,min = 136 **NOT OK**

beyond 2h:

s<=d/2=	272.75	mm	10.74	in
current spacing=	200	mm	7.87	in

current spacing= 200 < s,min = 273 **OK**

3G1 (Frame direction)

Cross-section

hi=	3000	mm	118.11	in
Total height =	12000	mm	472.44	in
bw=	300	mm	11.81	in
h=	600	mm	23.62	in

A_g =	180000	mm^2	279.00	in^2
Diahoop=	10	mm	0.39	in
Ahoop=	78.54	mm^2	0.12	in^2
spacing=	200	mm	7.87	in
d=	545.5	mm	21.48	in
DiaBar =	22	mm	0.87	in
Abar=	380.13	mm^2	0.59	in^2
DiaWeb =	10	mm	0.39	in
AWeb=	78.54	mm^2	0.12	in^2

slab thickness	ts=	130	mm	5.12	in
slab reinforcement		D10 @ 250			

<u>Strength check:</u>

<u>Flexural strength</u>

effective beam width:

ln=	6700	mm	263.78	in

S.8.12.2 : beff=min(ln/4,bw+2*[8ts],bw+2*[1/2(clear dist. to the next web)]

clear dist to the next web =	6900	mm	271.65	in
overhanging =	1400	mm	55.12	in

Max total length from:

1) Total length <= ln/4	beff=	1675	mm	65.94	in
2) Each side <= 8ts	beff=	2380	mm	93.70	in
3) Each side <= lc/2	beff=	7200	mm	283.46	in
	beff=	**1675**	**mm**	**65.94**	**in**

M_n^+ =	380.30	kN-m
M_n^- =	526.90	kN-m
$M_{n,center}$=	424.60	kN-m
M_n^{max} =	526.90	kN-m

S21.5.2.2	M_n^+ =	380.30	>	M_n^- /2=	263	OK
mid-span	M_n^+ =	380.30	>	M_n^{max} /4 =	132	OK
	M_n^- =	526.90	>	M_n^{max} /4 =	132	OK

S21.5.2.1 As,min = 3sqrt(f'c)/fy*bw*d

not less than 200bw*d/fy

As,min =	614.07	mm^2	0.95	in^2
200bw*d/fy=	654.27	mm^2	1.01	in^3

Try 3,5

# of bars=	3			
current As=	1140.40	mm^2	1.77	in^3

current As =	1140.40	>	As,min =	654	**OK**

check reinf. Ratio

		ρt =	0.0070		
ρt =	0.0070	<	ρt ,max=	0.0250	**OK**

Shear strength

Vc=2*sqrt(f'c)*bw*d	Vc =	141.19	kN	31.74	kips
	# of hoops=	2			
	Av =	157.08	mm^2	0.24	in^3
Vs = Av*fy*d/s	Vs=	147.76	kN	33.22	kips
Vn=	Vc+Vs =	288.96	kN	64.96	kips

Vu,pr due to moments

$M_{n,pr}^{+}$ =	475.38	kN-m		
$M_{n,pr}^{-}$ =	658.63	kN-m		
wg =	10.40	N/mm		
Vn=	288.96	kN	64.96	kips
Vu,pr=	204	kN	45.88	kips

ΦV_n =	217	>	Vu =	204	**OK**

Detailing:

Transverse reinforcement

S21.5.3.1: hoops shall be provided in 2h

2h =	1200	mm	47.24	in

current region length =	-	mm	-	in

S21.5.3.2: max spacing in 2h:

s = min(d/4; 8d_b; 24d_{hoop}; 12") =	136.38	mm	5.37	in
current spacing=	200	mm	7.87	in

current spacing= 200 > s,min = 136 **NOT OK**

beyond 2h:

s<=d/2=	272.75	mm	10.74	in
current spacing=	200	mm	7.87	in

current spacing= 200 < s,min = 273 **OK**

4G1,RG1 (Frame direction)

Cross-section

hi=	3000	mm	118.11	in
Total height =	12000	mm	472.44	in
bw=	300	mm	11.81	in
h=	600	mm	23.62	in
Ag =	180000	mm^2	279.00	in^2
Diahoop=	10	mm	0.39	in
Ahoop=	78.54	mm^2	0.12	in^2
spacing=	200	mm	7.87	in
d=	545.5	mm	21.48	in
DiaBar =	22	mm	0.87	in
Abar=	380.13	mm^2	0.59	in^2
DiaWeb =	10	mm	0.39	in
AWeb=	78.54	mm^2	0.12	in^2

slab thickness	ts=	130	mm	5.12	in
slab reinforcement		D10 @ 250			

Strength check:

Flexural strength

effective beam width:

ln=	6700	mm	263.78	in

S.8.12.2 : beff=min(ln/4,bw+2*[8ts],bw+2*[1/2(clear dist. to the next web)]

	clear dist to the next web =	6900	mm	271.65	in
	overhanging =	1400	mm	55.12	in

Max total length from:

1) Total length <= ln/4	beff=	1675	mm	65.94	in
2) Each side <= 8ts	beff=	2380	mm	93.70	in
3) Each side <= lc/2	beff=	7200	mm	283.46	in
	beff=	**1675**	**mm**	**65.94**	**in**

M_n^+ =	372.80	kN-m
M_n^- =	475.40	kN-m
$M_{n,center}$=	424.60	kN-m
M_n^{max} =	475.40	kN-m

S21.5.2.2	M_n^+ =	372.80	>	M_n^- /2=	238	OK
mid-span	M_n^+ =	372.80	>	M_n^{max} /4 =	119	OK
	M_n^- =	475.40	>	M_n^{max} /4 =	119	OK

S21.5.2.1 As,min = 3sqrt(f'c)/fy*bw*d
not less than 200bw*d/fy

As,min =	614.07	mm^2	0.95	in^2
200bw*d/fy=	654.27	mm^2	1.01	in^3

Try 3,4

# of bars=	3			
current As=	1140.40	mm^2	1.77	in^3

current As =	1140.40	>	As,min =	654	OK

check reinf. Ratio

		ρt = 0.0070			
ρt =	0.0070	<	ρt ,max=	0.0250	OK

Shear strength

Vc=2*sqrt(f'c)*bw*d

Vc =	141.19	kN	31.74	kips
# of hoops=	2			
Av =	157.08	mm^2	0.24	in^3

Vs = Av*fy*d/s	Vs=	147.76	kN	33.22	kips
Vn=	Vc+Vs =	288.96	kN	64.96	kips

Vu,pr due to moments

	$M_{n,pr}^{+}$ =	466.00	kN-m		
	$M_{n,pr}^{-}$ =	594.25	kN-m		
	wg =	10.40	N/mm		
	Vn=	288.96	kN	64.96	kips
	Vu,pr=	193	kN	43.41	kips

ΦV_n =	217	>	Vu =	193	OK

Detailing:

Transverse reinforcement

S21.5.3.1: hoops shall be provided in 2h

2h =	1200	mm	47.24	in
current region length =	-	mm	-	in

S21.5.3.2: max spacing in 2h:

s = min(d/4; $8d_b$; $24d_{hoop}$; 12") =	136.38	mm	5.37	in
current spacing=	200	mm	7.87	in

current spacing=	200	>	s,min =	136	NOT OK

beyond 2h:

s<=d/2=	272.75	mm	10.74	in
current spacing=	200	mm	7.87	in

current spacing=	200	<	s,min =	273	OK

CORNER COLUMNS

Materials

Concrete:	f'_c =	27	MPa	3.9	ksi
Steel:	f_y =	345	MPa	50.0	ksi

1C1 (Frame Direction) -- Corner Column

Cross-section

	hi=	3000	mm	118.11	in
	Total height	12000	mm	472.44	in
	Hc =	500	mm	19.69	in
	Bc =	500	mm	19.69	in
	Ag=	250000	mm^2	387.50	in^2
	Diahoop=	10	mm	0.39	in
	Ahoop=	78.54	mm^2	0.12	in^2
	spacing=	100	mm	3.94	in
	d=	445.5	mm	17.54	in
	DiaBar =	22	mm	0.87	in
	Abar=	380.13	mm^2	0.59	in^2
Beam(s) Connected:					
2G1	bw=	300	mm	11.81	in
	h=	600	mm	23.62	in
	hclear=	2400	mm	94.49	in
	R=	8			
	I=	1			
	Cd=	5.5			

Strength check:

Flexural strength

Column strength:	$M_{n,col}^{top}$ =	346	kN-m
	$M_{n,col}^{bottom}$ =	429	kN-m
	Mu=	200	kN-m

ΦM_n = 225 > Mu = 200 **OK**

Beam(s) strength:		$M_{n,beam}^{+}$ =	386	kN-m		
		$M_{n,beam}^{-}$ =	572	kN-m		

S21.6.3.1

Ast>=0.01Ag		# of bars=	10			
		Ast =	3801.33	mm^2	5.89	in^2

Ast =	3801.33	>	0.01Ag =	2500.000	OK

Axial Force ratio

Ptotal=	772.02	kN	173.57	kips
P/f'cAg=	0.114			

Shear strength

1) Ve = 2*Mpr,col/h	$M_{pr,col}^{top}$ =	432.51	kN-m		
2) Ve = (Mpr,beam(+)+Mpr,beam(-))/h	$M_{pr,col}^{bottom}$ =	536.75	kN-m		
	$V_e^{(1)}$ =	403.86	kN	90.80	kips
@ one axis	$V_e^{(2)}$ =	200.89	kN	45.16	kips
@ the other axis	$V_e^{(2)}$ =	298.02	kN	67.00	kips
	V_u =	98.31	kN	22.10	kips

If Ve/Vu > 0.5 & P<Agf'c/20 --> ignore Vc

current Ve/Vu =	2.04	>	limit Ve/Vu =	0.5	OK
P =	772.02	>	Agf'c/20 =	337.5	NOT OK

Bottom section

	Vc =	192.18	kN	43.21	kips
	# of hoops=	4			
Vs = Av*fy*d/s	Vs=	482.85	kN	108.56	kips
Vn= Vc+Vs		675.04	kN	151.76	kips

ΦV_n =	506	>	Ve =	298.02	OK

if Vs< 4(bd)sqrt(f'c) ; s < (d/2 ; 24")
if Vs< 4(bd)sqrt(f'c) ; s < (d/4 ; 12")

check if Vs< 4(bd)sqrt(f'c)

Vs=	109	>		4sqrt(f'c)bd =	86	**s < (d/4 ; 12)**
	s = min(d/2; 24") =	111.38	mm		4.38	in
	current spacing=	100	mm		3.94	in
current spacing=	100	<		s,min =	111	**OK**

Vsmax = 8(bd)sqrt(f'c)

Vs=	109	<	8sqrt(f'c)bd =	173	**OK**

Top section

	Vc =	192.18	kN	43.21	kips
	# of hoops=	3			
Vs = Av*fy*d/s	Vs=	362.14	kN	81.42	kips
Vn=	Vc+Vs	554.32	kN	124.62	kips
ΦV_n =	416	>	Ve =	298.02	**OK**

if Vs< 4(bd)sqrt(f'c) ; s < (d/2 ; 24")
if Vs< 4(bd)sqrt(f'c) ; s < (d/4 ; 12")

check if Vs< 4(bd)sqrt(f'c)

Vs=	81	<		4sqrt(f'c)bd =	86	**s < (d/2 ; 24)**
	s = min(d/2; 24") =	222.75	mm		8.77	in
	current spacing=	100	mm		3.94	in
current spacing=	100	<		s,min =	223	**OK**

Vsmax = 8(bd)sqrt(f'c)

Vs=	81	<	8sqrt(f'c)bd =	173	**OK**

Detailing:

S21.6.4

# of hoops =	4			
Ash =	314.16	mm^2	0.49	in^2

bc =	417	mm	16.42	in
Ach =	173889	mm^2	269.53	in^2
hx =	226	mm	8.90	in
so =	144.8	mm	5.70	in

S21.6.4.1

*lo <= min (member depth; 1/6*clear height; 18")*

	l_o =	400.00	mm	15.75	in
spacing same everywhere-->	current lo=	2400	mm	94.49	in

current lo= 2400 > lo,min = 400 **OK**

Within lo:

s <= min (h/4; 6db; so; 6")	*s = min (h/4; 6db; so; 6")*	125	mm	4.92	in
	current spacing=	100	mm	3.94	in

current spacing= 100 < s,min = 125 **OK**

S21.6.4.4

s (1) <= A_{sh} / (0.3 b_c f'_c/f_y (A_g/A_{ch} - 1))

s (2) <= A_{sh} / (0.09 b_c f'_c/f_y)

$s^{(1)}$ =	73.31	mm	2.89	in
$s^{(2)}$ =	106.96	mm	4.21	in

current spacing= 100 > s,min = 73 **NOT OK**

Beyond lo:

s = min (6db; 6")	132	mm	5.20	in
current spacing=	100	mm	3.94	in

current spacing= 100 < s,min = 132 **OK**

Drift check: (ASCE7-05 12.12)

Δs shall be <= $0.02/\rho$ = 0.015

Floor	h (mm)	δ_{xe} (mm)	δx (mm)	Δi	
4	12000	22.30	122.65	0.0068	**OK**
3	9000	18.60	102.3	0.0108	**OK**
2	6000	12.70	69.85	0.0134	**OK**
1	3000	5.40	29.7	0.0099	**OK**

Δtotal= 0.0102 **OK**

INTERIOR COLUMNS

Materials

Concrete:	f'_c =	27	MPa	3.9	ksi
Steel:	f_y =	345	MPa	50.0	ksi

1C2 (Frame Direction) -- Interior Column

Cross-section

	hi=	3000	mm	118.11	in
	Total height=	12000	mm	472.44	in
	Hc =	500	mm	19.69	in
	Bc =	500	mm	19.69	in
	Ag=	250000	mm^2	387.50	in^2
	Diahoop=	10	mm	0.39	in
	Ahoop=	78.54	mm^2	0.12	in^2
	spacing=	100	mm	3.94	in
	d=	445.5	mm	17.54	in
	DiaBar =	22	mm	0.87	in
	Abar=	380.13	mm^2	0.59	in^2
Beam(s) Connected:					
2 x 2G1	bw=	300	mm	11.81	in
	h=	600	mm	23.62	in
	hclear=	2400	mm	94.49	in
	R=	8			
	I=	1			
	Cd=	5.5			

Strength check:

Flexural strength

Column strength:	$M_{n,col}^{top}$ =	486	kN-m
	$M_{n,col}^{bottom}$ =	486	kN-m
	Mu=	205	kN-m

ΦM_n = 316 > Mu = 205 **OK**

Beam(s) strength:	$M_{n,beam}^{+}$ =	386	kN-m

		$M_{n,beam}^{-}$ =	572	kN-m		
S21.6.3.1						
Ast>=0.01Ag		# of bars=	10			
		Ast =	3801.33	mm^2	5.89	in^2
Ast =	3801.33		>	0.01Ag =	2500.000	OK

Axial Force ratio

P_{total}=	1222.22	kN	274.78	kips
P/f'_cA_g=	0.181			

Shear strength

1) Ve = 2*Mpr,col/h
2) Ve = (Mpr,beam(+)+Mpr,beam(-))/h

$M_{pr,col}^{top}$ =	607.38	kN-m		
$M_{pr,col}^{bottom}$ =	607.38	kN-m		
$V_e^{(1)}$ =	506.15	kN	113.79	kips
$V_e^{(2)}$ =	498.91	kN	112.16	kips
V_u =	98.31	kN	22.10	kips

If Ve/Vu > 0.5 & P<Agf'c/20 --> ignore Vc

current Ve/Vu =	5.07	>	Ve/Vu lim=	0.5	OK
P =	1222.22	>	Agf'c/20 =	337.5	NOT OK

	Vc =	192.18	kN	43.21	kips
	# of hoops=	4			
	Vc =	192.18	kN	43.21	kips
Vs = Av*fy*d/s	Vs=	482.85	kN	108.56	kips
Vn=	Vc+Vs	675.04	kN	151.76	kips
ΦV_n =	506	>	Ve =	498.91	OK

if Vs< 4(bd)sqrt(f'c) ; s < (d/2 ; 24")
if Vs< 4(bd)sqrt(f'c) ; s < (d/4 ; 12")

check if Vs< 4(bd)sqrt(f'c)

Vs=	109	>	4sqrt(f'c)bd	86	s < (d/4 ; 12)
s = min(d/2; 24") =	111.38	mm		4.38	in

	current spacing=	100	mm		3.94	in

current spacing=	100	<	s,min =	111	OK

Vsmax = 8(bd)sqrt(f'c)

Vs=	109	<	8sqrt(f'c)bd	173	OK

Detailing:

S21.6.4

# of hoops =	4			
Ash =	314.16	mm^2	0.49	in^2
bc =	417	mm	16.42	in
Ach =	173889	mm^2	269.53	in^2
hx =	240	mm	9.45	in
so =	140.1	mm	5.52	in

S21.6.4.1

*lo <= min (member depth; 1/6*clear height; 18")*

	l_o =	400.00	mm	15.75	in
spacing same everywhere-->	current lo=	2400	mm	94.49	in

current lo=	2400	>	lo,min =	400	OK

Within lo:

S21.6.4.3

s <= min (h/4; 6db; so; 6")	*s = min (h/4; 6db; so; 6")*	125	mm	4.92	in
	current spacing=	100	mm	3.94	in

current spacing=	100	<	s,min =	125	OK

S21.6.4.4

s (1) <= A_{sh} / (0.3 b_c f'_c/f_y (A_g/A_{ch} - 1))

s (2) <= A_{sh} / (0.09 b_c f'_c/f_y)

$s^{(1)}$ =	73.31	mm	2.89	in
$s^{(2)}$ =	106.96	mm	4.21	in

current spacing=	100	>	s,min =	73	NOT OK

Beyond lo:

s = min (6db; 6")	132	mm	5.20	in
current spacing=	100	mm	3.94	in

current spacing=	100	<	s,min =	132	OK

2C2 (Frame Direction) -- Interior Column

Cross-section

	hi=	3000	mm	118.11	in
	Total height	12000	mm	472.44	in
	Hc =	500	mm	19.69	in
	Bc =	500	mm	19.69	in
	Ag=	250000	mm^2	387.50	in^2
	Diahoop=	10	mm	0.39	in
	Ahoop=	78.54	mm^2	0.12	in^2
	spacing=	100	mm	3.94	in
	d=	445.5	mm	17.54	in
	DiaBar =	22	mm	0.87	in
	Abar=	380.13	mm^2	0.59	in^2
Beam(s) Connected:					
2 x 3G1	bw=	300	mm	11.81	in
	h=	600	mm	23.62	in
	hclear=	2400	mm	94.49	in
	R=	8			
	I=	1			
	Cd=	5.5			

Strength check:

Flexural strength

Column strength:	$M_{n,col}^{top}$ =	456	kN-m
	$M_{n,col}^{bottom}$ =	456	kN-m
	Mu=	187	kN-m

ΦM_n =	296	>	Mu =	187	OK

Beam(s) strength:	$M_{n,beam}^{+}$ =	380	kN-m
	$M_{n,beam}^{-}$ =	527	kN-m

S21.6.3.1

Ast>=0.01Ag	# of bars=	10			
	Ast =	3801.33	mm^2	5.89	in^2

Ast =	3801.33	>		0.01Ag =	2500.000	OK

Axial Force ratio

P_{total}=	919.65	kN	206.76	kips
P/f'_cA_g=	0.136			

Shear strength

1) Ve = 2*Mpr,col/h
2) Ve = (Mpr,beam(+)+Mpr,beam(-))/h

$M_{pr,col}^{top}$ =	569.80	kN-m		
$M_{pr,col}^{bottom}$ =	569.80	kN-m		
$V_e^{(1)}$ =	474.84	kN	106.75	kips
$V_e^{(2)}$ =	472.50	kN	106.23	kips
V_u =	89.01	kN	20.01	kips

If Ve/Vu > 0.5 & P<Agf'c/20 --> ignore Vc

current Ve/Vu =	5.31	>	limit Ve/Vu	0.5	OK
P =	919.65	>	Agf'c/20 =	337.5	NOT OK

	Vc =	192.18	kN	43.21	kips
	# of hoops=	4			
Vs = Av*fy*d/s	Vs=	482.85	kN	108.56	kips
Vn= Vc+Vs		675.04	kN	151.76	kips

ΦV_n =	506	>	Ve =	472.50	OK

if Vs< 4(bd)sqrt(f'c) ; s < (d/2 ; 24")
if Vs< 4(bd)sqrt(f'c) ; s < (d/4 ; 12")

check if Vs< 4(bd)sqrt(f'c)

Vs=	109	>	4sqrt(f'c)bd	86	s < (d/4 ; 12)

s = min(d/2; 24") =	111.38	mm	4.38	in
current spacing=	100	mm	3.94	in

current spacing=	100	<	s,min =	111	OK

Vsmax = 8(bd)sqrt(f'c)

Vs=	109	<	8sqrt(f'c)bd	173	OK

Detailing:

S21.6.4

# of hoops =	4			
Ash =	314.16	mm^2	0.49	in^2
bc =	407	mm	16.02	in
Ach =	165649	mm^2	256.76	in^2
hx =	163	mm	6.42	in
so =	165.8	mm	6.53	in

S21.6.4.1

*lo <= min (member depth; 1/6*clear height; 18")*

	l_o =	400.00	mm	15.75	in
spacing same everywhere-->	current lo=	2400	mm	94.49	in

current lo=	2400	>	lo,min =	400	OK

Within lo:

s <= min (h/4; 6db; so; 6")

s = min (h/4; 6db; so; 6")	125	mm	4.92	in
current spacing=	100	mm	3.94	in

current spacing=	100	<	s,min =	125	OK

S21.6.4.4

s (1) <= A_{sh} / $(0.3\ b_c\ f'_c/f_y\ (A_g/A_{ch} - 1))$

s (2) <= A_{sh} / $(0.09\ b_c\ f'_c/f_y)$

$s^{(1)}$ =	64.56	mm	2.54	in
$s^{(2)}$ =	109.59	mm	4.31	in

current spacing=	100	>	s,min =	65	NOT OK

Beyond lo:

s = min (6db; 6")	132	mm	5.20	in
current spacing=	100	mm	3.94	in

current spacing=	100	<	s,min =	132	OK

3C2 (Frame Direction) -- Interior Column

Cross-section

	hi=	3000	mm	118.11	in
	Total height	12000	mm	472.44	in
	Hc =	500	mm	19.69	in
	Bc =	500	mm	19.69	in
	Ag=	250000	mm^2	387.50	in^2
	Diahoop=	10	mm	0.39	in
	Ahoop=	78.54	mm^2	0.12	in^2
	spacing=	100	mm	3.94	in
	d=	445.5	mm	17.54	in
	DiaBar =	22	mm	0.87	in
	Abar=	380.13	mm^2	0.59	in^2
Beam(s) Connected:					
2 x 4G1	bw=	300	mm	11.81	in
	h=	600	mm	23.62	in
	hclear=	2400	mm	94.49	in
	R=	8			
	I=	1			
	Cd=	5.5			

Strength check:

Flexural strength

Column strength:	$M_{n,col}^{top}$ =	442	kN-m
	$M_{n,col}^{bottom}$ =	442	kN-m
	Mu=	153	kN-m

ΦM_n =	287	>	Mu =	153	OK

Beam(s) strength:	$M_{n,beam}^{+}$ =	373	kN-m
	$M_{n,beam}^{-}$ =	475	kN-m

S21.6.3.1

Ast>=0.01Ag		# of bars=	10				
		Ast =	3801.33	mm^2		5.89	in^2
Ast =	3801.33	>		0.01Ag =	2500.000	OK	

Axial Force ratio

P_{total}=	620.64 kN	139.53	kips
P/f'_cA_g=	0.092		

Shear strength

1) Ve = 2*Mpr,col/h
2) Ve = (Mpr,beam(+)+Mpr,beam(-))/h

$M_{pr,col}^{top}$ =	552.85	kN-m		
$M_{pr,col}^{bottom}$ =	552.85	kN-m		
$V_e^{(1)}$ =	460.71	kN	103.58	kips
$V_e^{(2)}$ =	441.77	kN	99.32	kips
V_u =	70.07	kN	15.75	kips

If Ve/Vu > 0.5 & P<Agf'c/20 --> ignore Vc

current Ve/Vu =	6.30	>	limit Ve/Vu	0.5	OK
P =	620.64	>	Agf'c/20 =	337.5	NOT OK

Vc =	192.18	kN	43.21	kips
# of hoops=	2			

Vs = Av*fy*d/s

		Vs=	241.43	kN	54.28	kips
Vn=	Vc+Vs		433.61	kN	97.48	kips
ΦV_n =	325	<		Ve =	441.77	NOT OK

if Vs< 4(bd)sqrt(f'c) ; s < (d/2 ; 24")
if Vs< 4(bd)sqrt(f'c) ; s < (d/4 ; 12")

check if Vs< 4(bd)sqrt(f'c)

Vs=	54	<	4sqrt(f'c)bd	86	s < (d/2 ; 24)

s = min(d/2; 24") =	222.75	mm	8.77	in

	current spacing=	100	mm	3.94	in
current spacing= 100	<	s,min =	223	**OK**	

Vsmax = 8(bd)sqrt(f'c)

Vs= 54	<	8sqrt(f'c)bd	173	**OK**

Detailing:

S21.6.4

# of hoops =	2			
Ash =	157.08	mm^2	0.24	in^2
bc =	409	mm	16.10	in
Ach =	167281	mm^2	259.29	in^2
hx =	210	mm	8.27	in
so =	150.1	mm	5.91	in

S21.6.4.1

*lo <= min (member depth; 1/6*clear height; 18")*

	l_o =	400.00	mm	15.75	in
spacing same everywhere-->	current lo=	2400	mm	94.49	in

current lo= 2400	>	lo,min =	400	**OK**

Within lo:

s <= min (h/4; 6db; so; 6")

s = min (h/4; 6db; so; 6")	125	mm	4.92	in
current spacing=	100	mm	3.94	in

current spacing= 100	<	s,min =	125	**OK**

S21.6.4.4

s (1) <= A_{sh} / (0.3 b_c f'_c/f_y (A_g/A_{ch} - 1))

s (2) <= A_{sh} / (0.09 b_c f'_c/f_y)

$s^{(1)}$ =	33.08	mm	1.30	in
$s^{(2)}$ =	54.53	mm	2.15	in

current spacing= 100	>	s,min =	33	**NOT OK**

Beyond lo:

s = min (6db; 6")	132	mm	5.20	in
current spacing=	100	mm	3.94	in

current spacing=	100	<	s,min =	132	OK

Beam Column Joint - G1-C2-G1 - frame direction (case 1)

Materials

Concrete:	f'_c =	3.9	ksi
Steel:	f_y =	50	ksi

Cross-section

B_{slab} =	66	in
B =	11.81	in
d =	22.10	in

Nominal Moment Capacity of Beams - G1

$M_n^{\pm}$	#7 bars	n =	3	
		$A_{s,1}$ =	0.60	in^2
		A_s =	1.8	in^2
		$a = A_s f_y / (0.85 f'_c B)$ =	0.41	in
		M_n^+ =	1970.49	in-kip
		M_n^+ =	164.21	ft-kip

M_n^-	#7 bars	n =	4	
		$A_{s,1}$ =	0.6	in^2
		A_s =	2.4	in^2
		$a = A_s f_y / (0.85 f'_c B)$ =	3.07	in
		M_n^- =	2468.09	in-kip
		M_n^- =	205.67	ft-kip

$M_{n,pr}^+$ =	205.26	ft-kip
$M_{n,pr}^-$ =	257.09	ft-kip

Interior Connection G1-C2-G1

h_{column} =	19.68	in
b_{col} =	19.68	in
b_w =	11.81	in
x =	3.94	in
b_{eff} =	19.68	in

Long beam bars: #7 bars

d_b =	0.875	in
$A_{sb,1}$ =	1.8	in^2
$A_{sb,2}$ =	2.4	in^2
f'_c =	3900	psi
γ_V =	12	

(beams frame into three faces of a column but
the beam width is less than 3/4 of the column width)

$M_{pr,b1}$ =	257.09	ft-kip
$M_{pr,b2}$ =	205.26	ft-kip
h_{clear} =	8.86	in
$M_{C1} = M_{C2} = M_C = (M_{pr,b1} + M_{pr,b2})/2$ =	231.18	ft-kip
$V_{C1} = M_{C1} / (h_{clear}/2)$ =	52.19	kip

Joint Shear Demand

$V_{u,joint} = 1.25\, f_y\, A_{sb,1} + 1.25\, f_y\, A_{sb,2} - V_{C1}$ =	210.31	kip
A_j =	387.30	in^2
θ_V =	0.85	
$\theta_V V_n = \theta_V \gamma_V (fc')^{0.5} A_j$ =	246.71	ksi

$V_{u,joint}$ < $\theta_V V_n$ => **OK**

Joint Detailing Requirements

b_w =	11.81	<	3/4 b_{col} =	14.76	

=> ***Required transferse reinforcement = 100% Ash***

<u>Column - C2</u>	3 #3 bars	A_{sh} =	0.33	in^2
		A_{ch} =	216.97	in^2
		A_g =	387.30	in^2
		b_c =	14.56	in
		h_x =	7.905	in
longitudial column bars:	#7	$d_{b,col}$ =	0.875	in
		s_o =	6.03	in
		$s < A_{sh} / (0.3\ b_c\ f'_c/f_y\ (A_g/A_{ch} - 1))$ =	1.23	in
		$s = \min(b/4;\ 6d_b;\ s_o;\ 6")$ =	4.92	in
Actual spacing in the structure:		s_A =	5.52	in

<u>Joint Anchorage Requirements</u>

M_n^+ / M_n^- = 0.80 **> 0.5, OK**

Beam longitudial reinforcement should be extended to the far face of the confined column and anchored in tension.

$l_{dh} = f_y\ d_b / (65\ (f'_c)^{0.5})$ =	10.78	> 8 db =	7.0	or 6"
$l_{dh,req}$ =	6 "	$l_{dh,act}$ =	14	"

OK

<u>Beam Column Joint - G1 - C1 - frame direction (case 2)</u>

<u>Materials</u>

Concrete: f'_c = 3.9 ksi

Steel: f_y = 50 ksi

Cross-section

B_{slab} =	66	in
B =	11.81	in
d =	22.10	in

Nominal Moment Capacity of Beams - G1

$M_n^{\pm}$ — #7 bars

n =	3	
$A_{s,1}$ =	0.60	in^2
A_s =	1.80	in^2
$a = A_s f_y / (0.85 f'_c B)$ =	0.41	in
M_n^+ =	1970.49	in-kip
M_n^+ =	164.21	ft-kip

M_n^- — #7 bars

n =	4	
$A_{s,1}$ =	0.60	in^2
A_s =	2.4	in^2
$a = A_s f_y / (0.85 f'_c B)$ =	3.07	in
M_n^- =	2468.09	in-kip
M_n^- =	205.67	ft-kip
$M_{n,pr}^+$ =	205.26	ft-kip
$M_{n,pr}^-$ =	257.09	ft-kip

Exterior Connection G1 - C1

h_{column} =	19.68	in
b_{col} =	19.68	in
b_w =	11.81	in
x =	3.94	in
b_{eff} =	19.68	in

Long beam bars: #7 bars

d_b =	0.875	in
$A_{sb,2}$ =	2.40	in^2
f'_c =	3900	psi
γ_V =	12	

(beams frame into two faces of a column)

$M_{pr,b1}$ =	257.09	ft-kip
h_{clear} =	8.86	in
$M_{C1} = M_{C2} = M_C = (M_{pr,b})/2$ =	128.55	ft-kip
$V_{C1} = M_{C1} / (h_{clear}/2)$ =	29.02	kip

Joint Shear Demand

$V_{u,joint} = 1.25\ f_y A_{sb,2} - V_{C1}$ =	120.98	kip
A_j =	387.30	in^2
θ_V =	0.85	
$\theta_V V_n = \theta_V \gamma_V (fc')^{0.5} A_j$ =	246.71	ksi

$V_{u,joint}$ < $\theta_V V_n$ => **OK**

Joint Detailing Requirements

b_w = 11.81 < 3/4 b_{col} = 14.76

=> ***Required transferse reinforcement = 100% Ash***

Column - C1 — 3 #3 bars

A_{sh} =	0.33	in^2
A_{ch} =	216.97	in^2
A_g =	387.30	in^2
b_c =	14.56	in
h_x =	7.905	in
longitudial column bars: #7 — $d_{b,col}$ =	0.875	in
s_o =	6.03	in
$s < A_{sh} / (0.3\ b_c\ f'_c/f_y\ (A_g/A_{ch} - 1))$ =	1.23	in
$s = \min(b/4;\ 6d_b;\ s_o;\ 6'')$ =	4.92	in
Actual spacing in the structure: s_A =	5.52	in

Joint Anchorage Requirements

$M_n^+ / M_n^- =$ 0.80 **> 0.5, OK**

- beam longitudial reinforcement should be extended to the far face of the confined column and anchored in tension.

$l_{dh} = f_y\, d_b / (65\, (f'_c)^{0.5}) =$ 10.78 > 8 db = 7.0 or 6"

$l_{dh,req} =$ 10.78 " $l_{dh,act} =$ 14 "

OK

WALLS

Materials

Concrete:	f'_c =	27	MPa	3.9	ksi
Steel:	f_y =	345	MPa	50.0	ksi

Cross-section

hi=	3000	mm	118.11	in
hw=	12000	mm	472.44	in
Lw =	2500	mm	98.43	in
tw=	250	mm	9.84	in
Acv=	625000	mm^2	968.75	in^2
Diahoop=	10	mm	0.39	in
Ahoop=	78.54	mm^2	0.12	in^2
hoop spacing=	100	mm	3.94	in
web transverse spacing (AXIS A)=	125	mm	4.92	in
web transverse spacing (AXIS C)=	200	mm	7.87	in
boundary width =	400	mm	15.75	in
# of bars in the boundary=	6			
Diabar=	19	mm	0.75	in
Abar=	283.53	mm^2	0.44	in^2
R=	6			
I=	1			
Cd=	5			

Strength check:

Flexural strength

M_n = 2884 kN-m

Mu= 3569 kN-m

ΦM_n = 2595.4 < Mu = 3569 **NOT OK**

Shear strength

AXIS A

αc= 2

# of hoops= 2

(transverse reinforcement ratio) ρt= 0.0050

ρt= 0.0050 > ρ_{min}= 0.0025 **OK**

Vn= 1622.74 kN 364.83 kips

Vu= 393 kN-m

	ΦV_n =	1217		>		Vu = 393	**OK**

AXIS C

	αc=	2				
	# of hoops=	2				
(transverse reinforcement ratio)	ρt=	0.0031				
ρt= 0.0031		>		ρmin=	0.0025	**OK**
	Vn=	1216.42	kN	273.48	kips	
	Vu=	393	kN-m			
ΦV_n = 912		>		Vu =	393	**OK**

Axial Force ratio

P_{total}=	284.86	kN	64	kips
P/f'_cA_g=	0.017			

Detailing:

Need for special boundary elements:

At design-based earthquake DBE

(elastic displacement)	δxe=	28.46	mm	1.12	in
	δu=	142.32	mm	5.60	in
$\delta u/hw$ shall not be less than 0.007-->	**$\delta u/hw$=**	0.0119			

check if c>=lw/600(δu/hw)

	lw/600(δu/hw)=	351.33	mm	13.83	in
(from BIAX)	c=	243.50	mm	9.59	in

c= 244	<	Climit =	351	**BE NOT NEEDED**

At maximum considered earthquake MCE

(elastic displacement)	δxe=	42.69	mm	1.68	in
	δu=	213.47	mm	8.40	in
$\delta u/hw$ shall not be less than 0.007-->	**$\delta u/hw$=**	0.0178			

check if c>=lw/600(δu/hw)

	lw/600(δu/hw)=	234.22	mm	9.22	in
	c=	243.50	mm	9.59	in

c= 244	>	lw/600(δu/hw) =	234	**BE NEEDED**

--> *if boundary elements are needed, length of BE:*

c'=larger of {c-0.1lw,c/2}	c'=	121.75	mm
	current BE length =	400	mm

--> *if not needed, satisfy 21.9.6.5*

21.9.6.5(a): if ρ> 400/fy ; satisfy 21.6.4.2 and 21.9.6.4(a); s<8"

		400/fy=	0.0080		
ρ=	0.0170		>	400/fy=	0.0080
			-> 21.6.4.2 and 21.9.6.4(a) ; s<8		

-- 21.9.6.4(a) : c'=larger of {c-0.1lw,c/2}

c'=	121.75	mm
current BE length =	400	mm

-- 21.6.4.2: hx<14"

1st floor		hx =	183.0	mm	7.20	in	
current hx =	183.0		<	hx_{limit} =	355.6		**OK**
upper floors		hx=	275.0	mm	10.83	in	
current hx =	275.0		<	hx_{limit} =	355.6		**OK**

-- check spacing: s < 8db ;8"

		s=	100	mm		
current s =	100		<	8 in=	203.2	**OK**
current s =	100		<	8db=	152	**OK**

Hoop reinforcement A_{sh}:

in x-dir:

# of hoops=	2			
bc=	163	mm	6.42	in
Ach =	51345	mm^2	79.58	in^2
Ag =	100000	mm^2	155.00	in^2

	current Ash=	157	mm^2	0.24	in^2

(eq.21-4) A_{sh} >= 0.3 s b_c f'_c / f_y (A_g/A_{ch} - 1)

	min Ash =	363	mm^2	0.56	in^2
current Ash= 157		<	min Ash =	362.65	NOT OK

(eq. 21-5) A_{sh} >= 0.09 s b_c f'_c/f_y

	min Ash =	115	mm^2	0.18	in^2
current Ash= 157		>	min Ash =	114.81	OK

in y-dir:

# of hoops=	3			
bc=	315	mm	12.40	in
current Ash=	236	mm^2	0.37	in^2

(eq.21-4) A_{sh} >= 0.3 s b_c f'_c / f_y (A_g/A_{ch} - 1)

	min Ash =	701	mm^2	1.09	in^2
current Ash= 236		<	min Ash =	700.82	NOT OK

(eq. 21-5) A_{sh} >= 0.09 s b_c f'_c/f_y

	min Ash =	115	mm^2	0.18	in^2
current Ash= 236		>	min Ash =	114.81	OK

<u>Drift check: (ASCE7-05 12.12)</u>

Δs shall be <= 0.02/ρ = 0.015

Floor	h (mm)	δxe (mm)	δx (mm)	Δi	
4	12000	28.46	142.32	0.0166	NOT OK
3	9000	18.49	92.45	0.0151	OK
2	6000	9.44	47.19	0.0113	OK
1	3000	2.68	13.42	0.0045	OK

Δtotal= 0.0119 OK

NOTE: Member capacities are calculated based on SD345 strength for all reinforcement.

Appendix C

C.1 CONSTRUCTION PROCESS

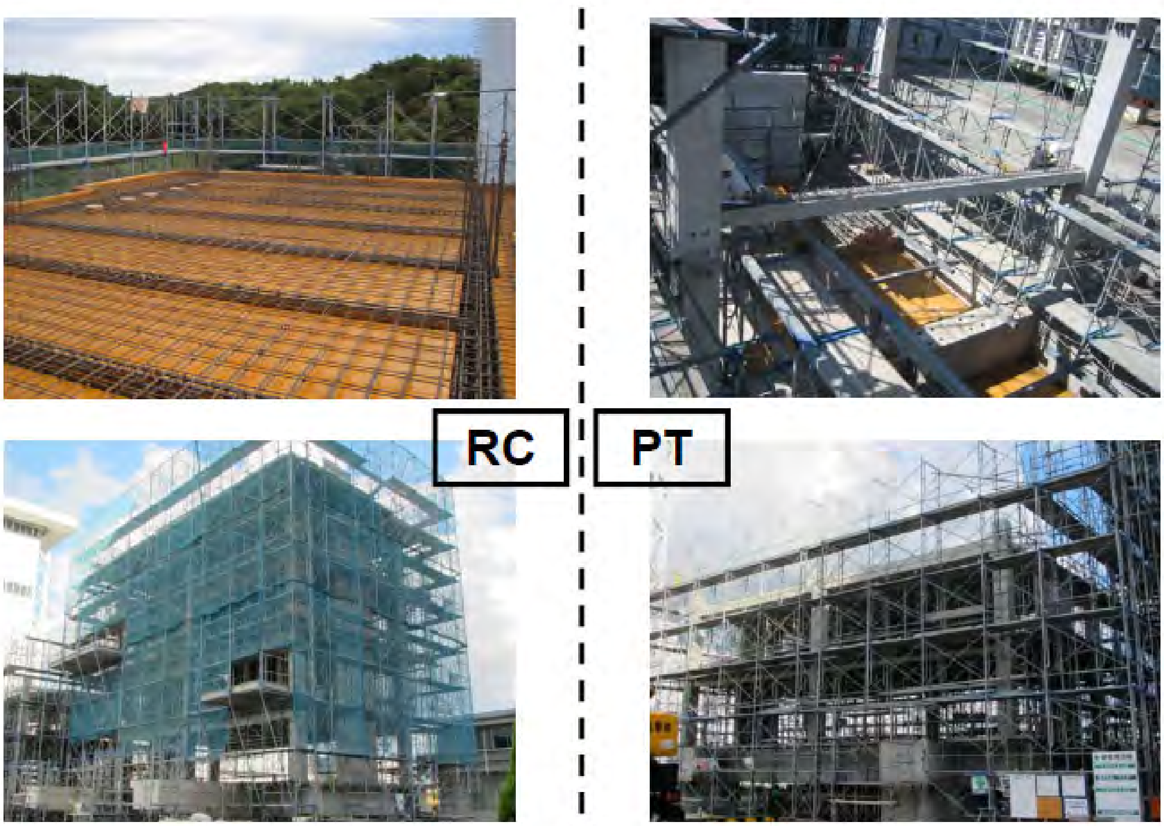

Figure C.1 Construction of RC specimen versus PT specimen.

(a) Gas pressure welding

(b) Steel arrangement of wall

(c) Steel arrangement of column

(d) Preparation for forms

(e) Supported forms

(f) Floor placing steel bars

(g) Concrete cast

(f) Specimen after whole concrete cast

Figure C.2 Construction of RC specimen.

(a) Anchorage of PT bars in foundation

(b) Steel arrangement of foundation

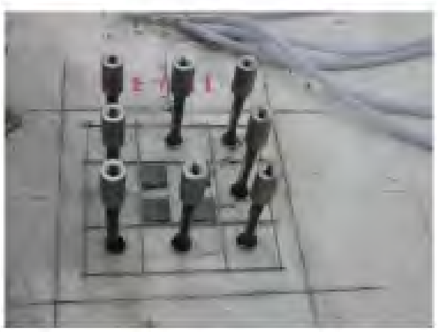

(c) Threaded couplers above foundation

(e) Lift-up of the precast concrete column

(f) Joint of PT bars

(g) Grouted column bed (mortar)

Figure C.3 Construction of PT specimen (column).

(a) Placing half precast concrete beam

(b) Bracket supporting beam end

(c) Grouted beam end (mortar)

(d) Half precast concrete floor panel

(e) Steel arrangement for top slab

(f) Cast of top concrete

(g) Beam prestressed after concrete cast

(h) Steel arrangement for corner slab

Figure C.4 Construction of PT specimen (beam and slab).

(a) Preparation for concrete cast of foundation

(b) Couplers for energy dissipating element (D22)

(c) Foundation before wall-set (holes for PT wires and D22)

(d) Erection of wall

(e) Grouted coupler (injection of mortar)

(f) Overflow of grout from coupler

(g) Mixture of steel fiber and mortar

(h) Fiber mortar for wall bed

Figure C.5 Construction of PT specimen (walls).

(a) Joint of wall and inside slab

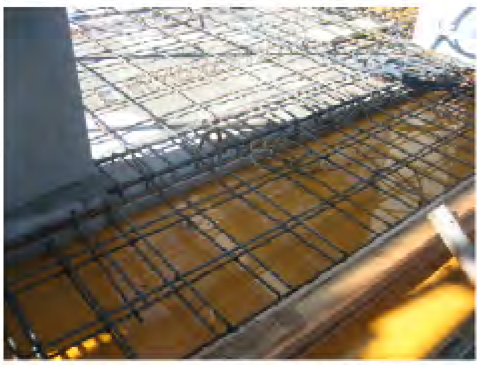

(b) Steel arrangement around Half precast beam

(c) Concrete cast around wall

(e) Preparation for prestressing the multi-story wall

(f) Anchorage of PT wires beneath foundation

(g) Pump and jack prestressing PT wire

Figure C.6 Construction of PT specimen (walls).

Appendix D

D.1 INSTRUMENTATION

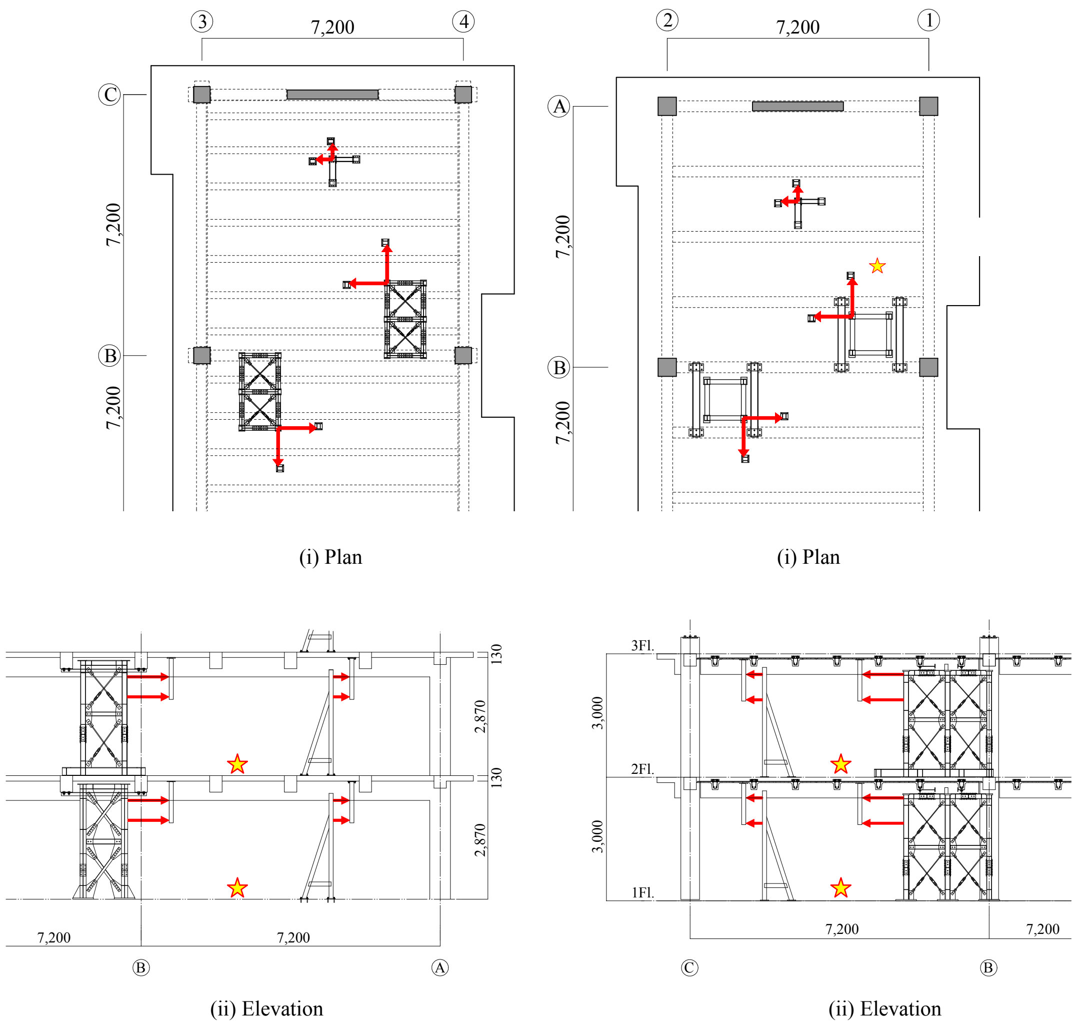

(a) RC specimen

(b) PC specimen

Displacement transducer

Accelerometer

Figure D.1 Measurements.

	呼称(対象部位)		対象建築		計測器	計測数量		数量の内訳							
						点数	ch数		計算	棟	層	部材	部材あたりの箇所・断面	1箇所あたりの計測数	計測面数
1	壁ワイヤ	荷重		PT	センターホールロードセル	2	2	=	1*1*1*2*1	1棟(PT)	1層(RF)	1枚の壁(C-3a)		ワイヤー2本	各1面
2	層加速度	加速度	RC	PT	加速度計	48	48	=	2*4*2*3*1	2棟(RC, PT)	4層(2F~RF)	各層2箇所		3方向(XYZ)	各1面
3	層間変位(レーザー)	変形	RC	PT	ロングレンジレーザー変位計	32	32	=	2*4*1*2*2	2棟(RC, PT)	4層(1F~4F)	各層1箇所	2段	2方向(X, Y)	各1面
3.2	層間鉛直変位	変形	RC	PT	CDP変位計	16	16	=	2*4*2*1*1	2棟(RC, PT)	4層(1F~4F)	各層2箇所		1方向(Z)	各1面
4	層間変位(ワイヤー)	変形	RC	PT	ワイヤー式変位計	56	56	=	2*(3*2+1*1)*2*2*1	2棟(RC, PT)	4層(1F~4F)	各層2箇所(4Fのみ1箇所)	2段	2方向(X, Y)	各1面
5.1	PT梁端変形(長辺方向)	変形		PT	CDP変位計	16	16	=	1*4*2*2*1*1	1棟(PT)	4層(2F~RF)	梁端2箇所(1通りB-C間の両端2箇所)	2箇所(梁上面、梁下面)	1方向	各1面
5.2	PT梁端変形(短辺方向)	変形		PT	ワイヤー式変位計	24	24	=	1*4*3*2*1*1	1棟(PT)	4層(2F~RF)	梁端3箇所(C通り2箇所、B通り1箇所)	2箇所(梁上面、梁下面)	1方向	各1面
6	PT柱脚変形	変形		PT	ワイヤー式変位計	8	8	=	1*1*2*4*1*1	1棟(PT)	1層(1F)	2本の柱(C-1柱, B-1柱)	4箇所	1方向	各1面
7	PT壁脚部変形	変形		PT	ワイヤー式変位計	16	16	=	1*4*1*4*1*1	1棟(PT)	4層(1F~4F)	1枚の壁(C-3a)	4箇所	1方向	各1面
8	PT壁端滑り	変形		PT	CDP変位計	4	4	=	1*4*1*1*1*1	1棟(PT)	4層(1F~4F)	1枚の壁(C-3a)	1箇所	1方向	各1面
9.1	RC梁端変形(長辺方向)	変形	RC		ワイヤー式変位計	4	4	=	1*1*2*2*1*1	1棟(RC)	1層(3F)	梁端2箇所(1通りB-C間の両端2箇所)	2箇所(梁上面、梁下面)	1方向	各1面
9.2	RC梁端変形(短辺方向)	変形	RC		ワイヤー式変位計	6	6	=	1*1*3*2*1*1	1棟(RC)	1層(3F)	梁端3箇所(C通り2箇所、B通り1箇所)	2箇所(梁上面、梁下面)	1方向	各1面
10	RC壁脚部変形	変形	RC		ワイヤー式変位計	4	4	=	1*1*1*4*1*1	1棟(RC)	1層(1F)	1枚の壁(C-1a)	4箇所	1方向	各1面
11	基礎滑り	変形	RC	PT	CDP変位計	6	6	=	2*1*3*1*1	2棟(PT, RC)	1層(台上)	3箇所(X方向各1, Y方向各2)		1方向	各1面
11.2	基礎浮上がり(壁下)	変形	RC	PT	CDP変位計	4	4	=	2*1*2*1*1	2棟(PT, RC)	1層(台上)	2箇所		1方向	各1面
12	梁主筋歪(短辺方向)	鉄筋の歪	RC		1軸歪ゲージ	48	24	=	1*2*3*2*2*2	1棟(RC)	2層(2F, 3F)	梁端3箇所(C通り2箇所、B通り1箇所)	梁端1部位あたり2断面(0D, 1D位置)	1断面あたり主筋2本	鉄筋の表裏
13	梁補強筋歪(短辺方向)	鉄筋の歪	RC		1軸歪ゲージ	6	6	=	1*2*3*1*1*1	1棟(RC)	2層(2F, 3F)	梁端3箇所(C通り2箇所、B通り1箇所)	梁端1部位あたり1断面(0.5D位置)	1断面あたり補強筋1本	鉄筋の片面
14	梁主筋歪(長辺方向)	鉄筋の歪	RC		1軸歪ゲージ	64	32	=	1*4*2*2*2*2	1棟(RC)	4層(1~4F)	梁端2箇所(1通りB-C間の両端2箇所)	梁端1部位あたり2断面(0D, 1D位置)	1断面あたり主筋2本	鉄筋の表裏
15	梁補強筋歪(長辺方向)	鉄筋の歪	RC		1軸歪ゲージ	8	8	=	1*4*2*1*1*1	1棟(RC)	4層(1~4F)	梁端2箇所(1通りB-C間の両端2箇所)	梁端1部位あたり1断面(0.5D位置)	1断面あたり補強筋1本	鉄筋の片面
16	柱主筋歪	鉄筋の歪	RC		1軸歪ゲージ	144	72	=	1*2*(2*3+3)*4*2	1棟(RC)	4層(1~4F)	2本の柱(C-1柱, B-1柱)	2~4F上下2断面、1F3断面	1断面あたり主筋4本	鉄筋の表裏
17	柱補強筋歪	鉄筋の歪	RC		1軸歪ゲージ	32	32	=	1*4*2*2*2*1	1棟(RC)	4層(1~4F)	2本の柱(C-1柱, B-1柱)	1~4Fの上下2断面	1断面あたり補強筋2本	鉄筋の片面
18	壁縦筋歪	鉄筋の歪	RC		1軸歪ゲージ	6	6	=	1*2*1*3*1*1	1棟(RC)	2層(1F, 2F)	1枚の壁(C-1a)	各階3断面(上中下)	1断面あたり縦筋1本	鉄筋の片面
19	壁横筋歪	鉄筋の歪	RC		1軸歪ゲージ	6	6	=	1*2*1*3*1*1	1棟(RC)	2層(1F, 2F)	1枚の壁(C-1a)	各階3断面(1/4位置、中、3/4位置)	1断面あたり横筋1本	鉄筋の片面
20	壁付帯柱主筋歪	鉄筋の歪	RC		1軸歪ゲージ	28	14	=	1*1*(4+3)*2*2	1棟(RC)	(1F, 2F)	1枚の壁(C-1a)の片側の柱	1F4断面、2F3断面	1断面あたり主筋2本	鉄筋の表裏
21	壁付帯柱補強筋歪	鉄筋の歪	RC		1軸歪ゲージ	4	4	=	1*1*(1+3)*1*1	1棟(RC)	2層(1F, 2F)	1枚の壁(C-1a)の片側の柱	1F1断面、2F3断面	1断面あたり補強筋1本	鉄筋の片面
22	PT壁脚部鉄筋	鉄筋の歪		PT	1軸歪ゲージ	4	4	=	1*1*1*2*1*2	1棟(PT)	1層(1F)	1枚の壁(C-1a)	1Fの2断面	1断面あたり鉄筋1本	鉄筋の表裏
23	PT壁脚主筋	鉄筋の歪		PT	1軸歪ゲージ	4	2	=	1*1*1*2*1*2	1棟(PT)	1層(1F)	1枚の壁(C-1a)	1Fの2断面	1断面あたり鉄筋1本	鉄筋の表裏
24	PT壁補強筋	鉄筋の歪		PT	1軸歪ゲージ	2	2	=	1*1*1*2*1*1	1棟(PT)	1層(1F)	1枚の壁(C-1a)	1Fの2断面	1断面あたり鉄筋1本	鉄筋の片面
25	RC柱梁接合部	鉄筋の歪		PT	1軸歪ゲージ	4	4	=	1*1*2*2*1*1	1棟(RC)	1層(4F)	2本の柱(C-1柱, B-1柱)	1断面	1断面あたり鉄筋2本	鉄筋の片面
26	RF梁主筋	鉄筋の歪	RC		1軸歪ゲージ	12	6	=	1*1*1*2*3*2	1棟(RC)	1層(RF)	1箇所	2断面	1断面あたり鉄筋3本	鉄筋の表裏
27	RF梁補強筋	鉄筋の歪	RC		1軸歪ゲージ	1	1	=	1*1*1*1*1*1	1棟(RC)	1層(RF)	1箇所	1断面	1断面あたり鉄筋1本	鉄筋の片面
28	スラブ筋	鉄筋の歪	RC		1軸歪ゲージ	12	12	=	1*1*1*2*6*1	1棟(RC)	1層(RF)	1箇所	2段(上段筋、下段筋)	1段あたり鉄筋6本	鉄筋の片面
29	カメラ(第1系統)	映像	RC	PT	移動カメラ 固定カメラ	18	18								
30	カメラ(第2系統)	映像	RC	PT	CCDカメラ	20	20								
31	設備計測(加速度)	加速度	RC	PT	加速度計	60	60								
32	設備計測(歪)	歪	RC	PT	1軸歪ゲージ	29	29								
33	設備計測(変位)	変位	RC	PT	変位計	1	1								
					合計	759	609								

センターホールロードセル	2	2
加速度計	48	48
変位計(層間変位)	104	104
変位計(部材接続)	92	92
1軸歪ゲージ	385	235
移動カメラ・固定カメラ	18	18
CCDカメラ	20	20
加速度計(設備計測)	60	60
歪ゲージ(設備計測)	29	29
変位計(設備計測)	1	1
合計	759	609

22番以外は
鉄筋の表裏に貼ったゲージは
ブリッジを組んで平均をとる

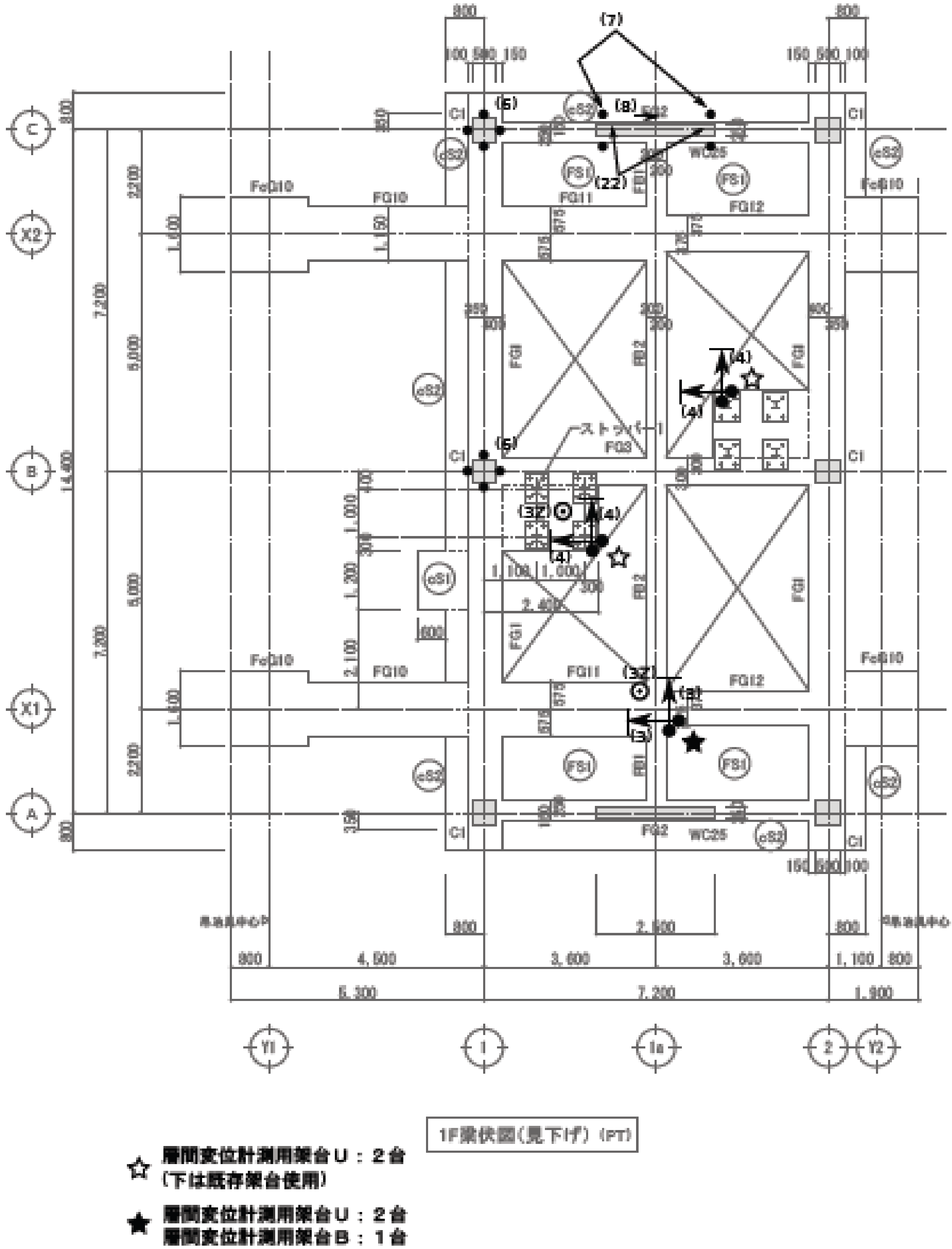
1F梁伏図（見下げ）（PT）
☆ 層間変位計測用架台U：２台
（下は既存架台使用）
★ 層間変位計測用架台U：２台
層間変位計測用架台B：１台

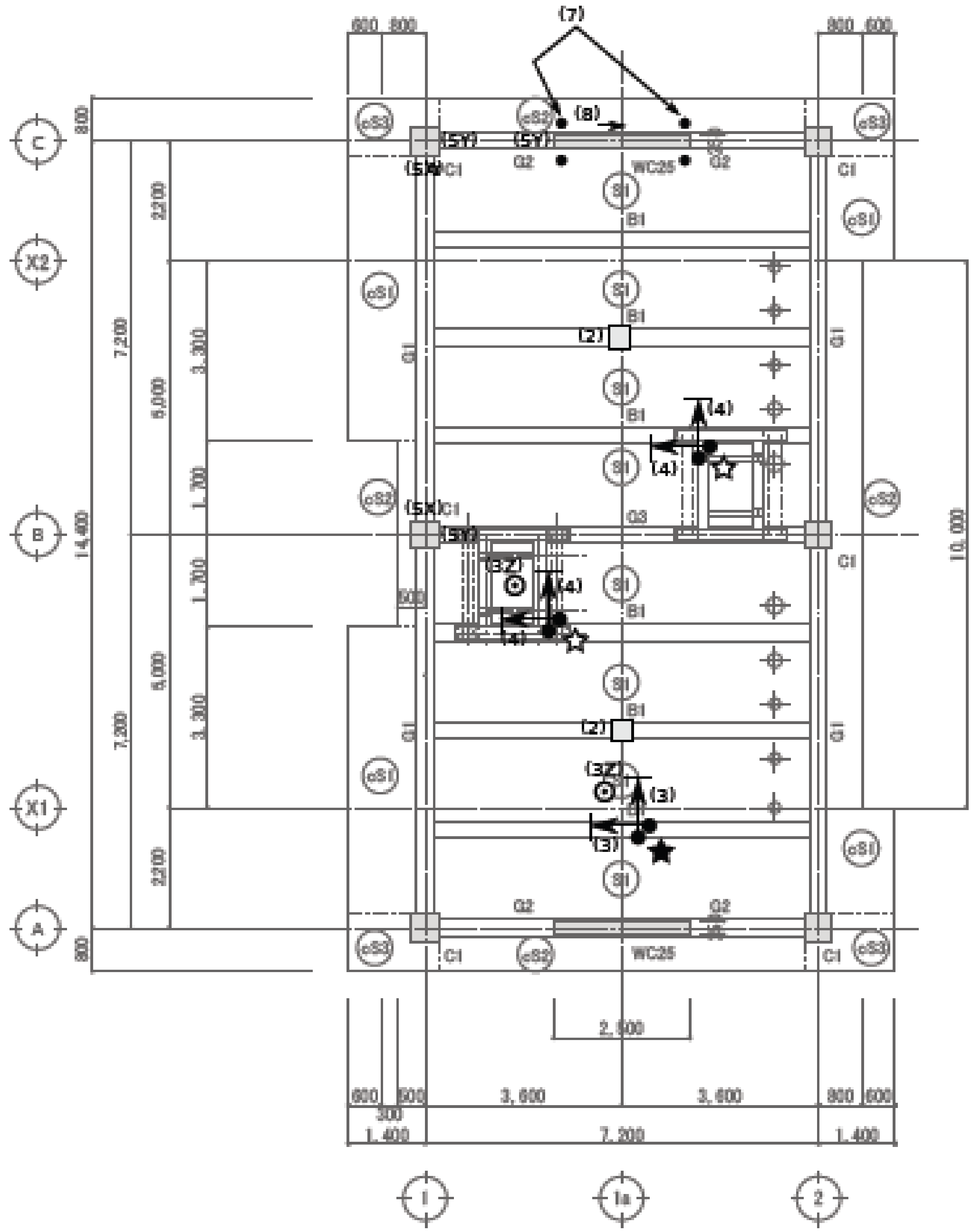

2F梁伏図（見下げ） (PT)

☆ 層間変位計測用架台U：２台
（下は既存架台使用）

★ 層間変位計測用架台U：２台
層間変位計測用架台B：１台

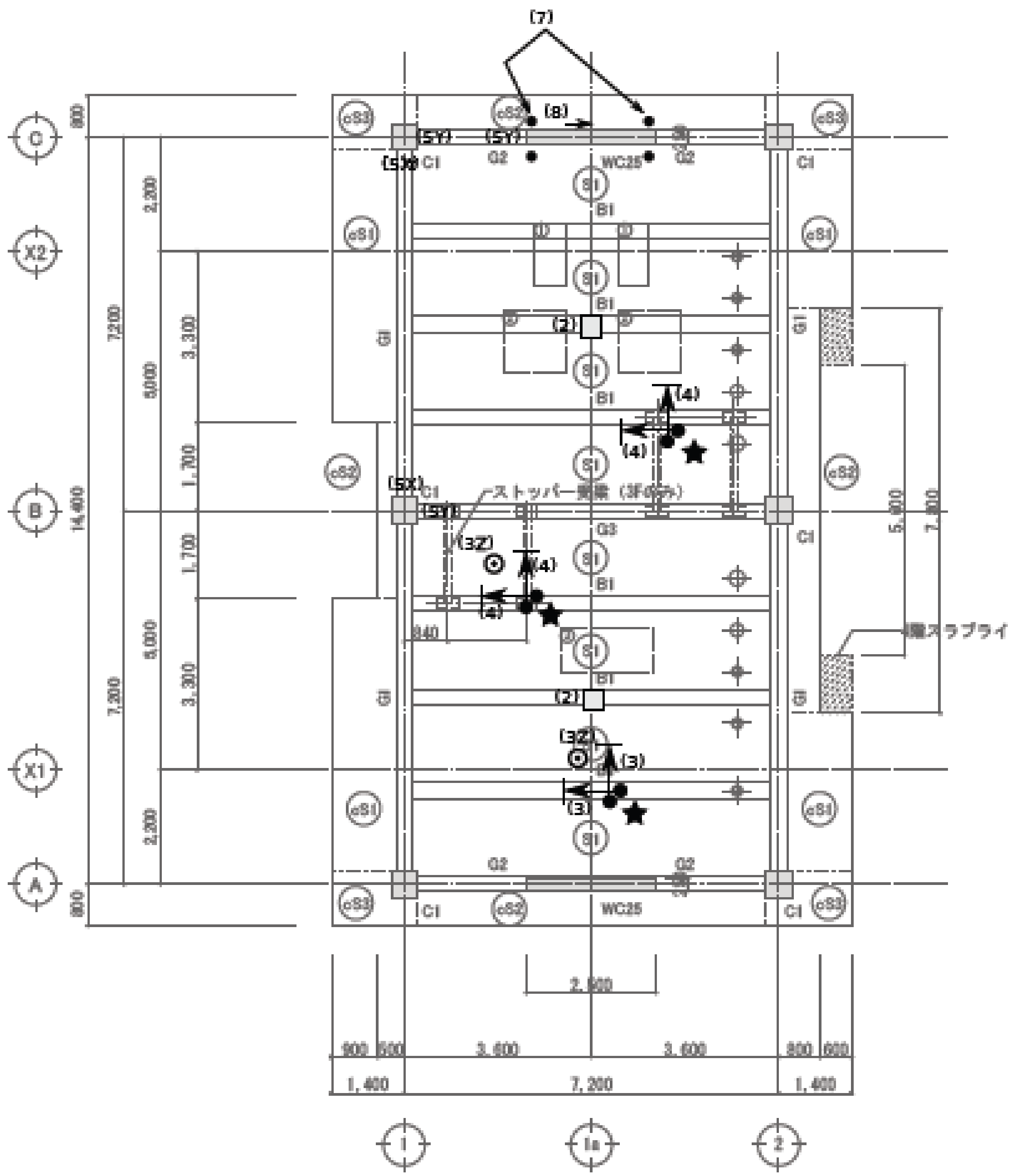

☆ 層間変位計測用架台Ｕ：２台
（下は既存架台使用）

★ 層間変位計測用架台Ｕ：２台
層間変位計測用架台Ｂ：１台

3　F梁伏図（見下げ）(PT)

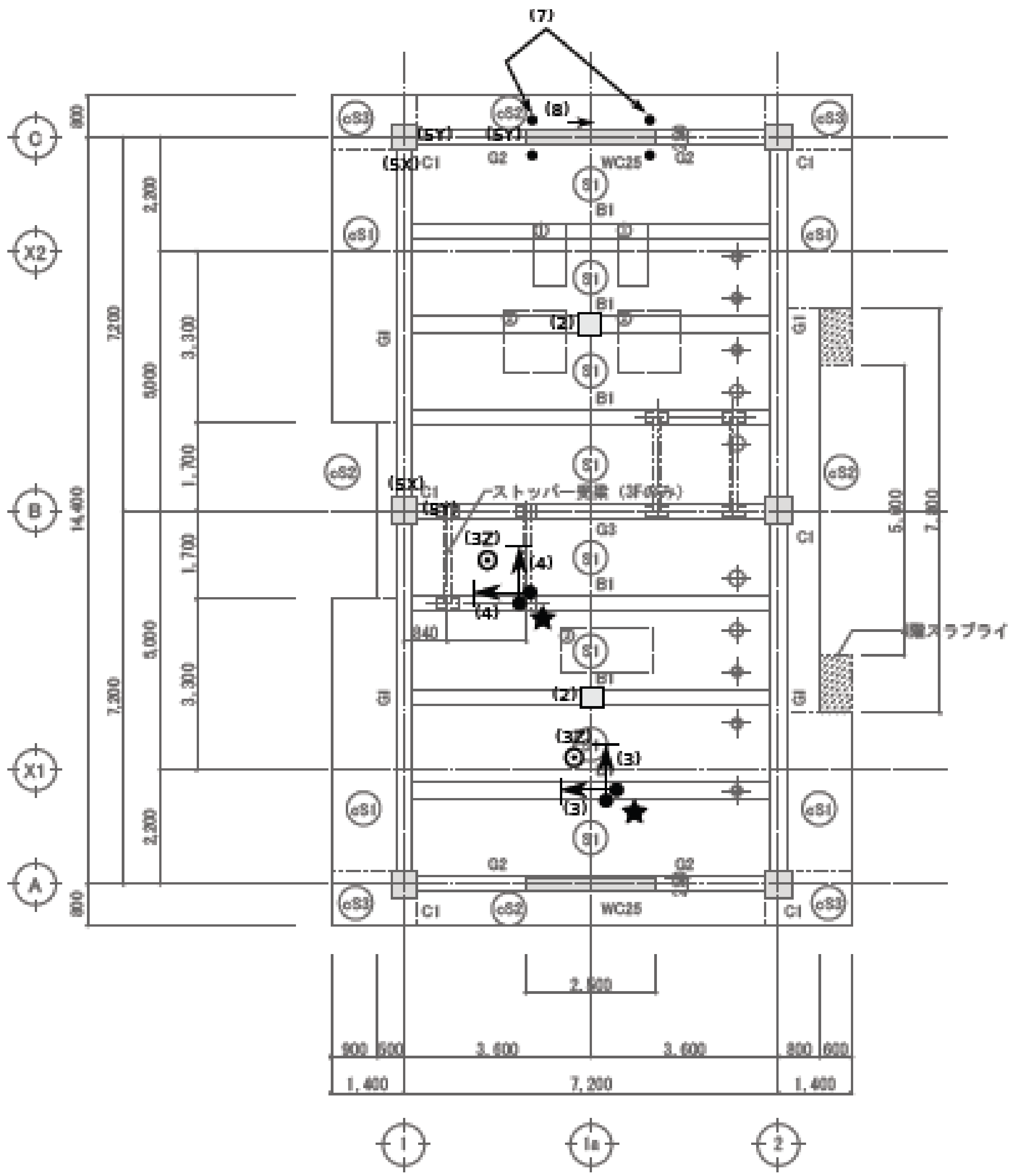

☆ 層間変位計測用架台U：２台
(下は既存架台使用)

★ 層間変位計測用架台U：２台
層間変位計測用架台B：１台

4F梁伏図（見下げ）（PT）

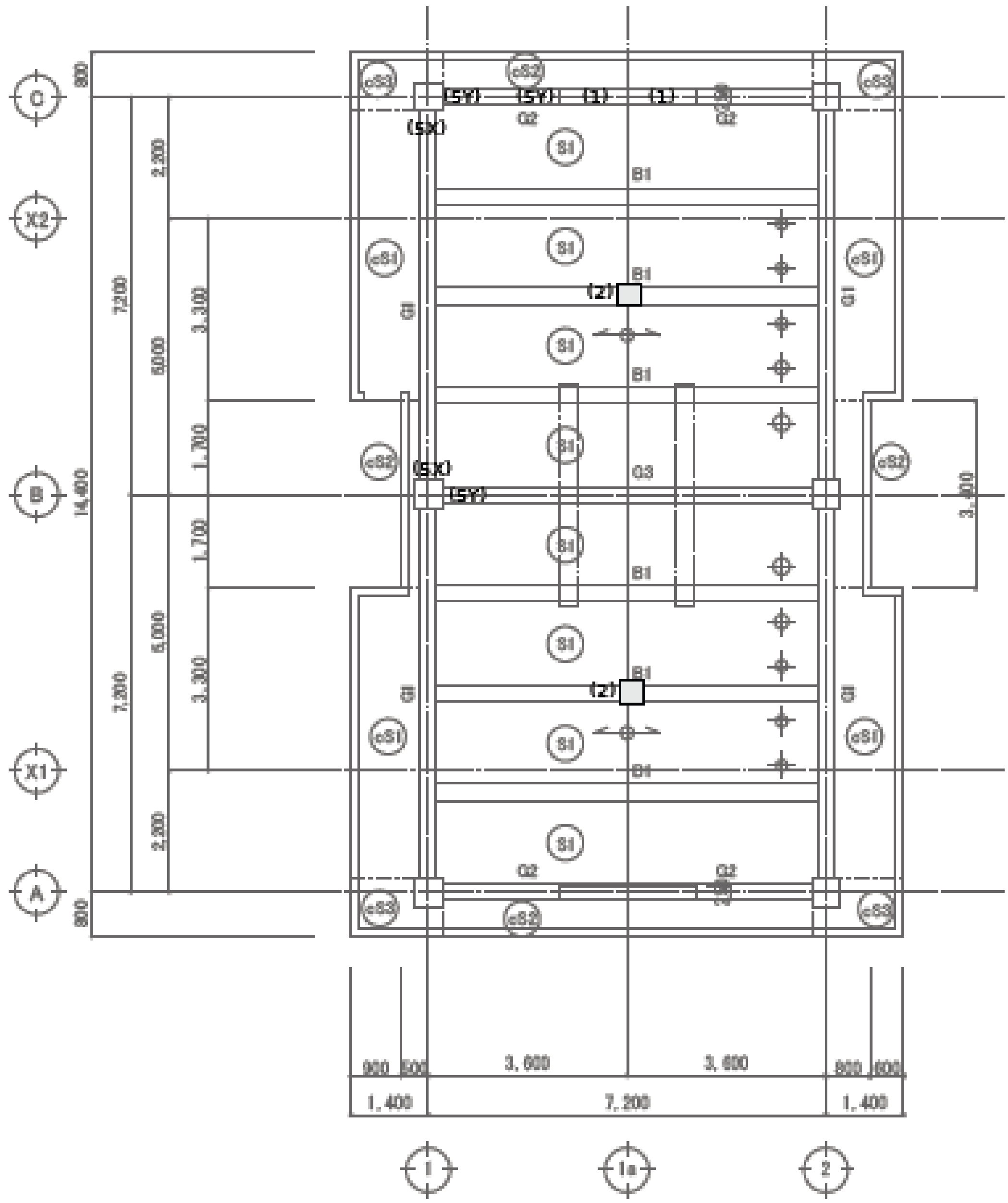
C
X2
B
X1
A
1
1a
2
800
2,200
7,200
5,000
3,300
1,700
14,400
3,400
900
500
3,600
800
600
1,400
7,200
G1
G2
G3
B1
S1
cS1
cS2
cS3
(SX)
(SY)
(1)
(Z)

RF梁伏図 （見下げ）（PT）

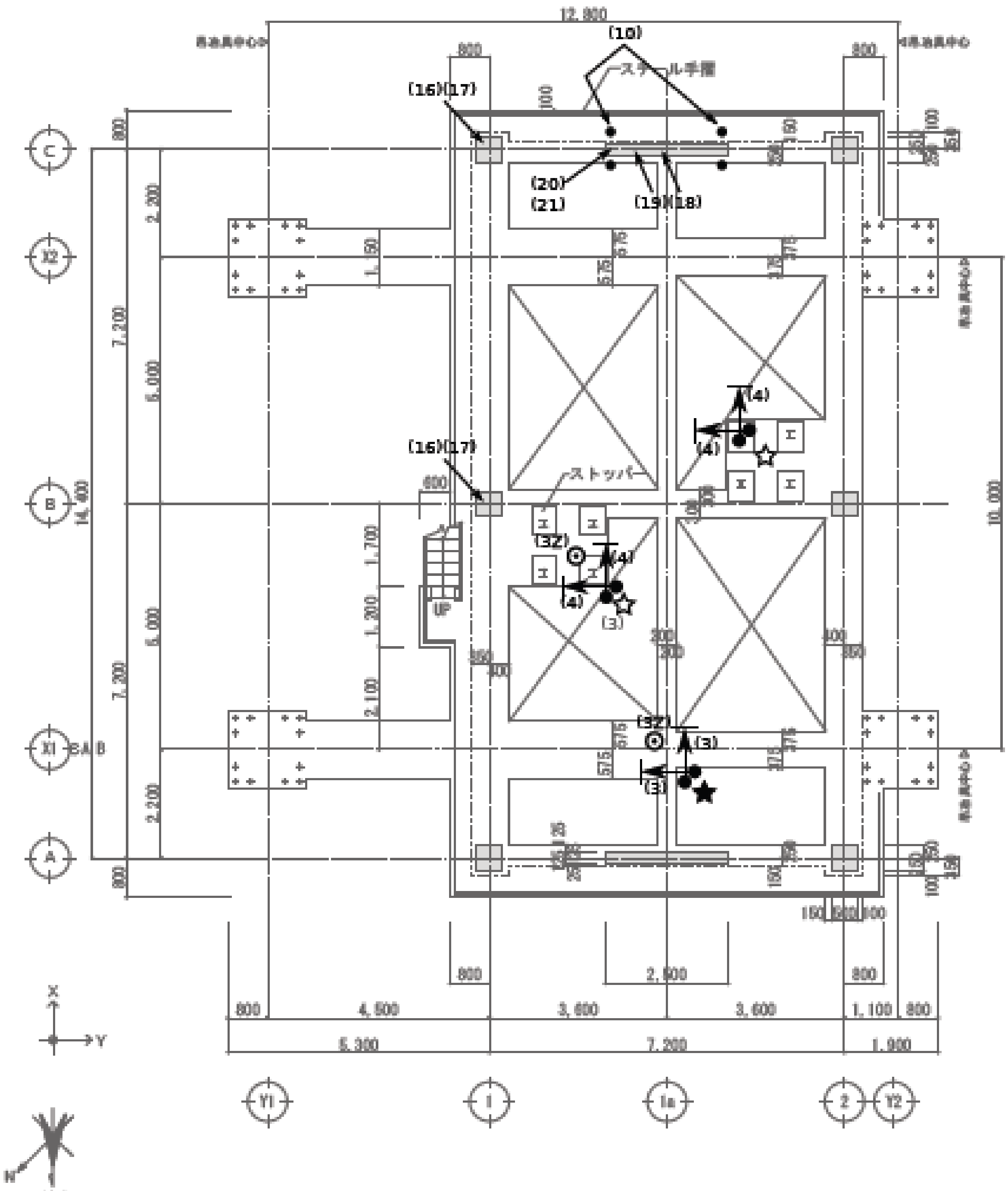

☆ 層間変位計測用架台Ｕ：２台
（下は既存架台使用）

★ 層間変位計測用架台Ｕ：２台
層間変位計測用架台Ｂ：１台

1F平面図（RC） S=1/100

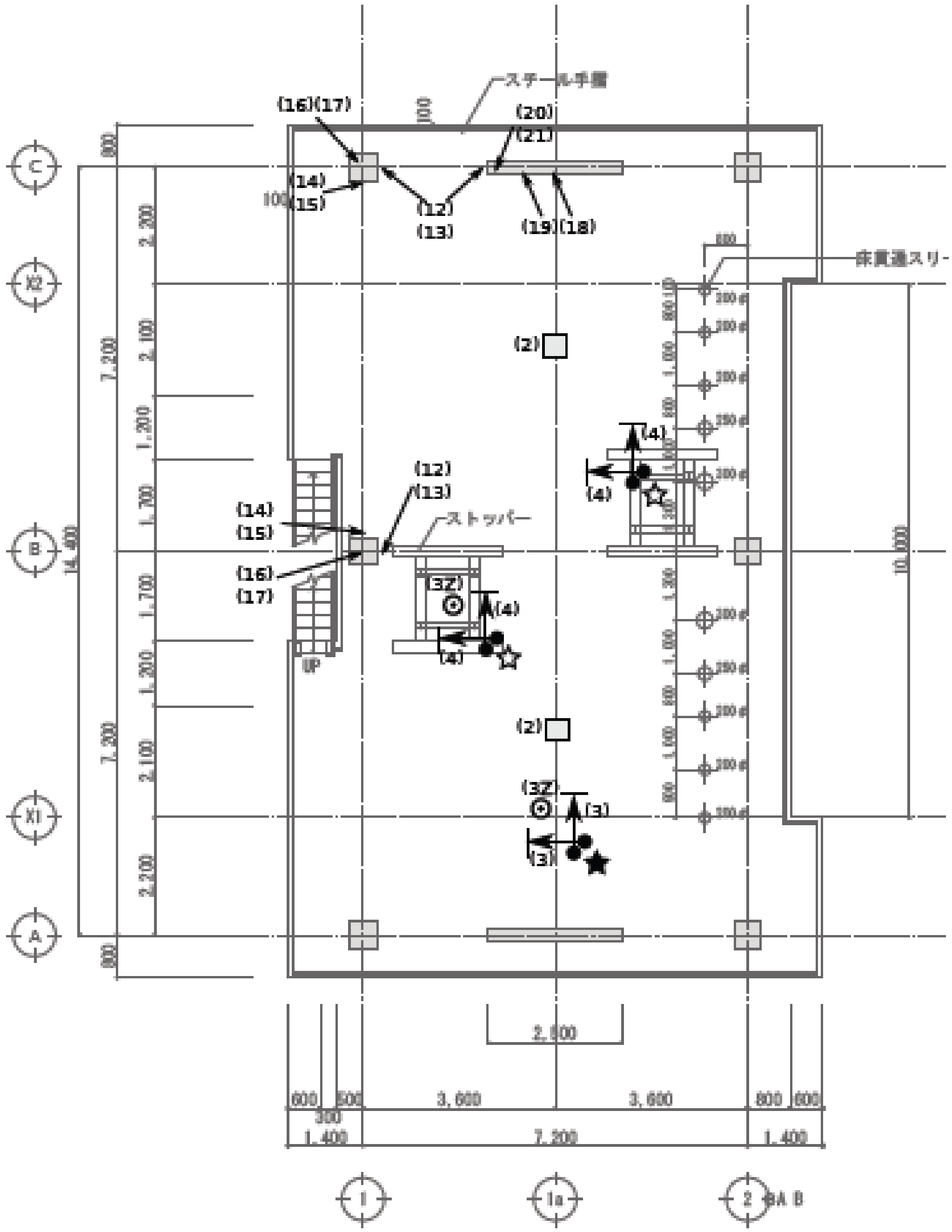

☆ 層間変位計測用架台Ｕ：２台
（下は既存架台使用）

★ 層間変位計測用架台Ｕ：２台
層間変位計測用架台Ｂ：１台

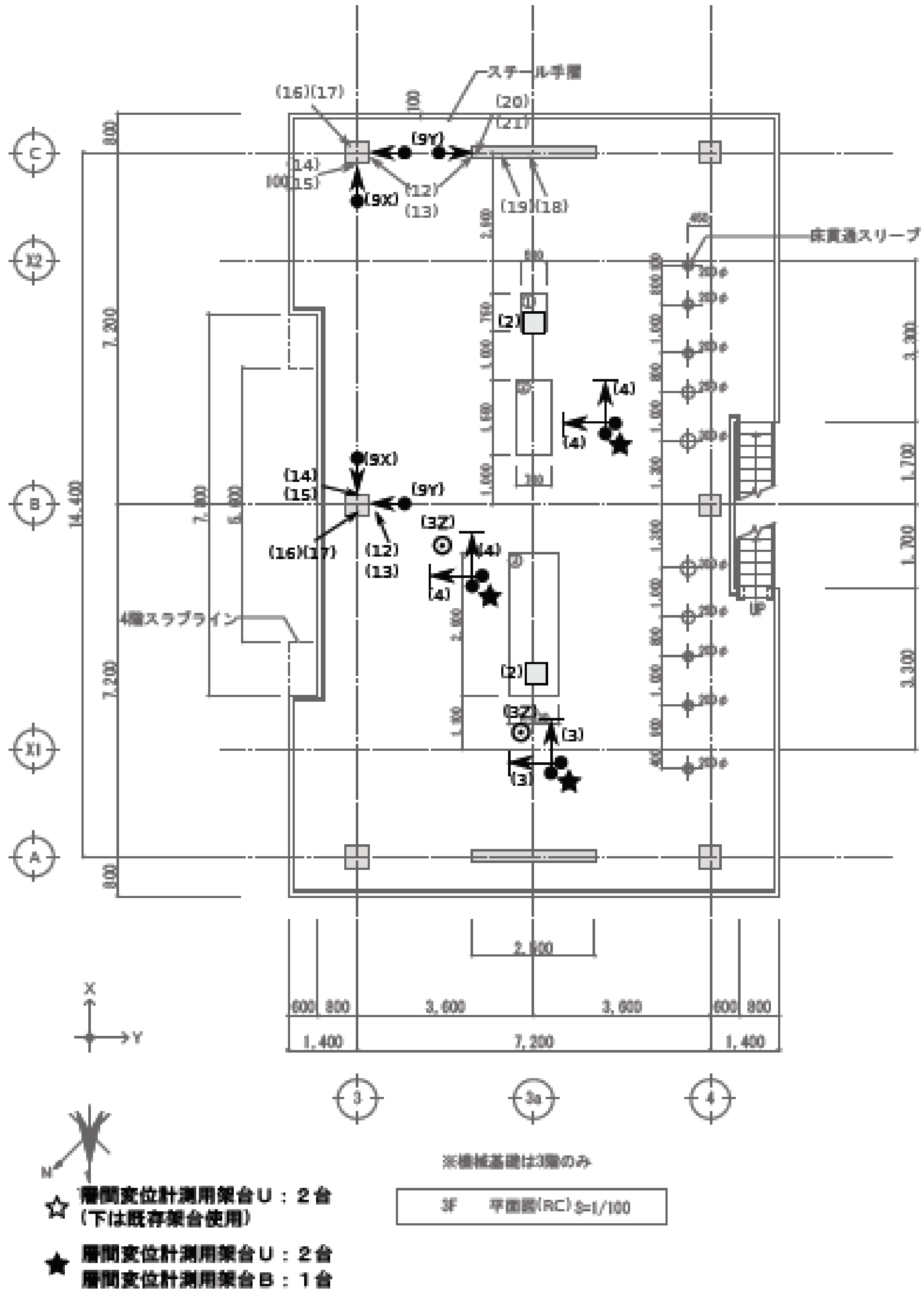

床貫通スリーブ
4階スラブライン
UP
X
Y
N
※機械基礎は3階のみ
3F 平面図(RC) S=1/100
☆ 層間変位計測用架台Ｕ：２台
(下は既存架台使用)
★ 層間変位計測用架台Ｕ：２台
層間変位計測用架台Ｂ：１台

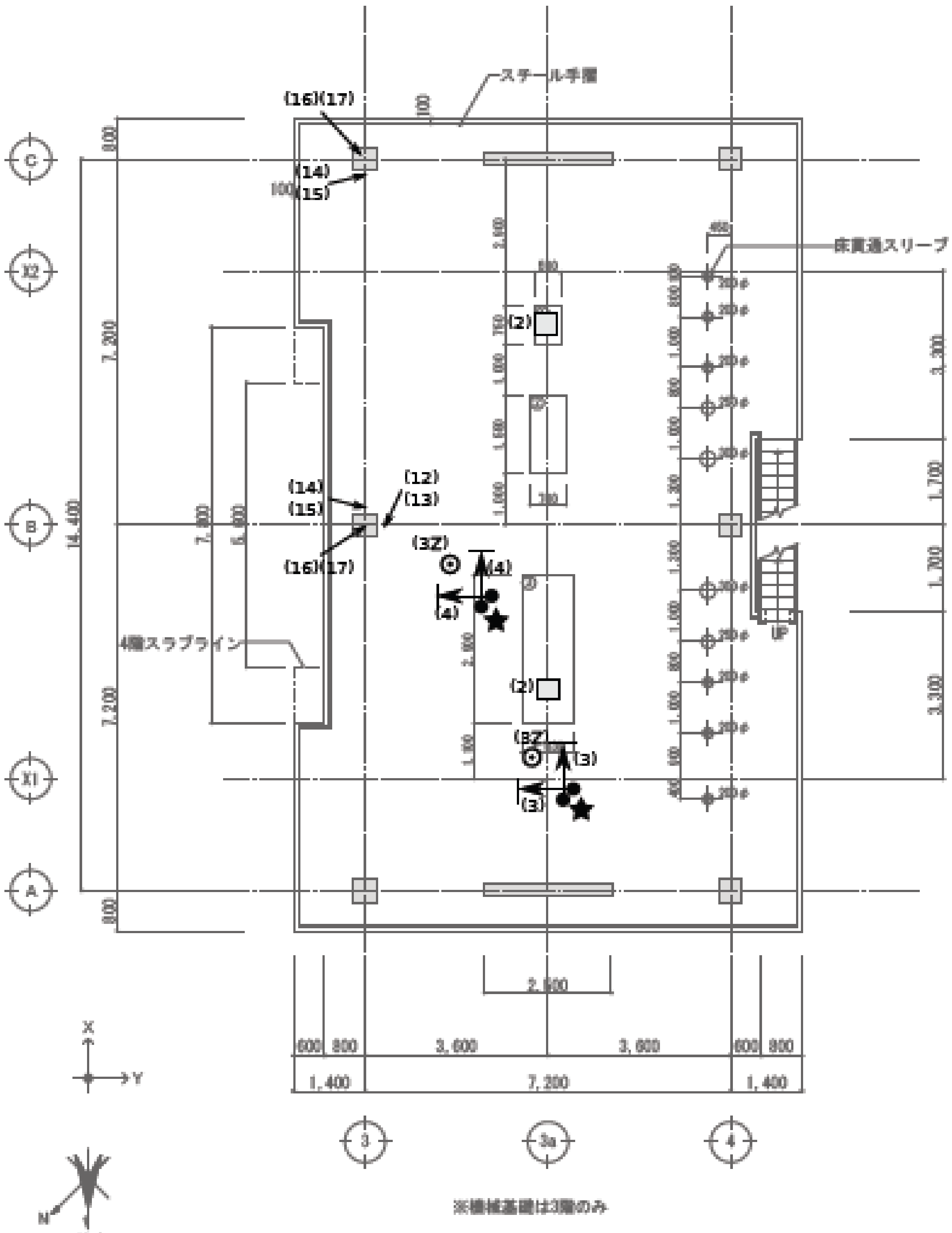

4F平面図(RC) S=1/100

☆ 層間変位計測用架台Ｕ：２台
(下は既存架台使用)

★ 層間変位計測用架台Ｕ：２台
層間変位計測用架台Ｂ：１台

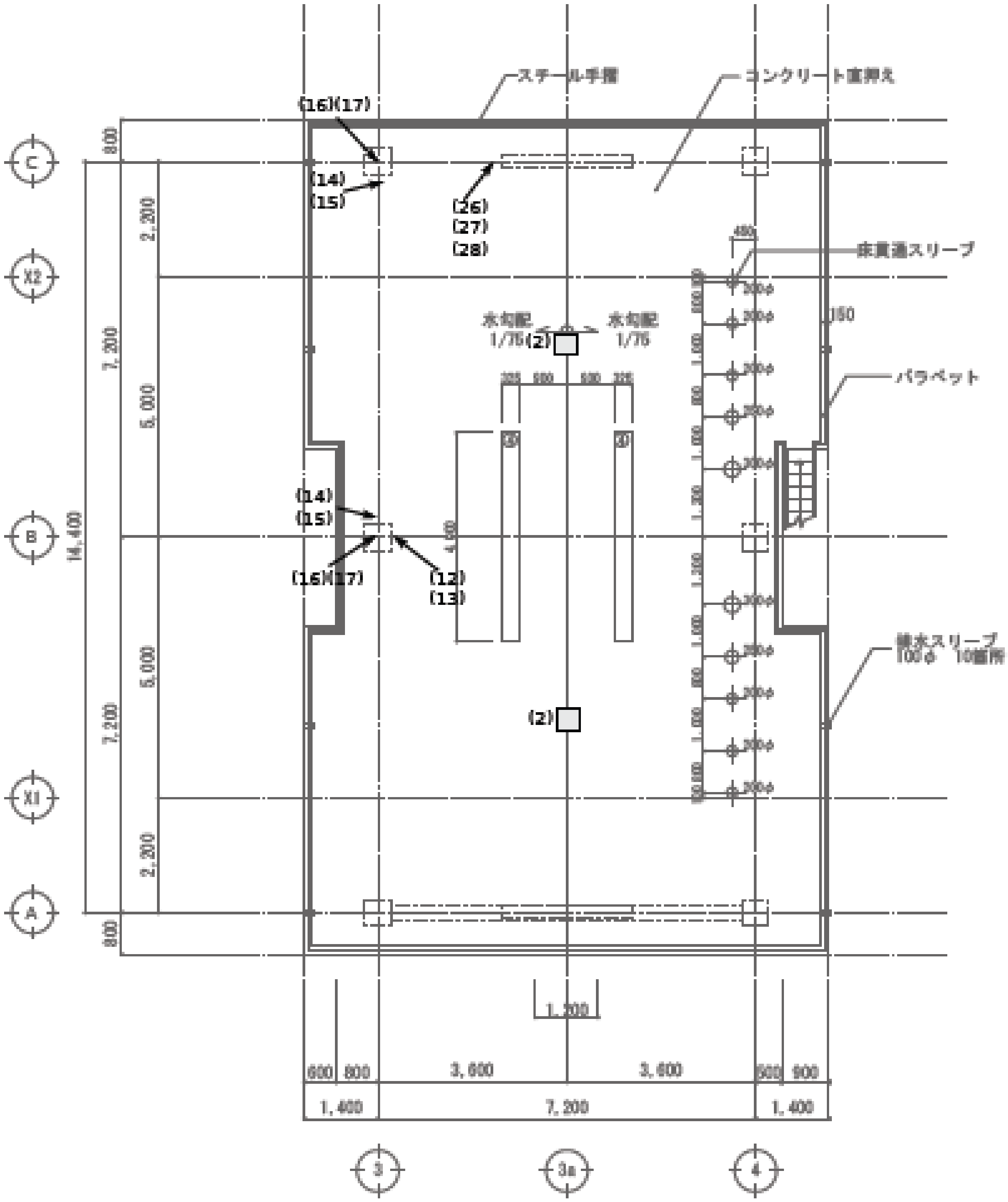

屋上平面図（RC） S=1/100

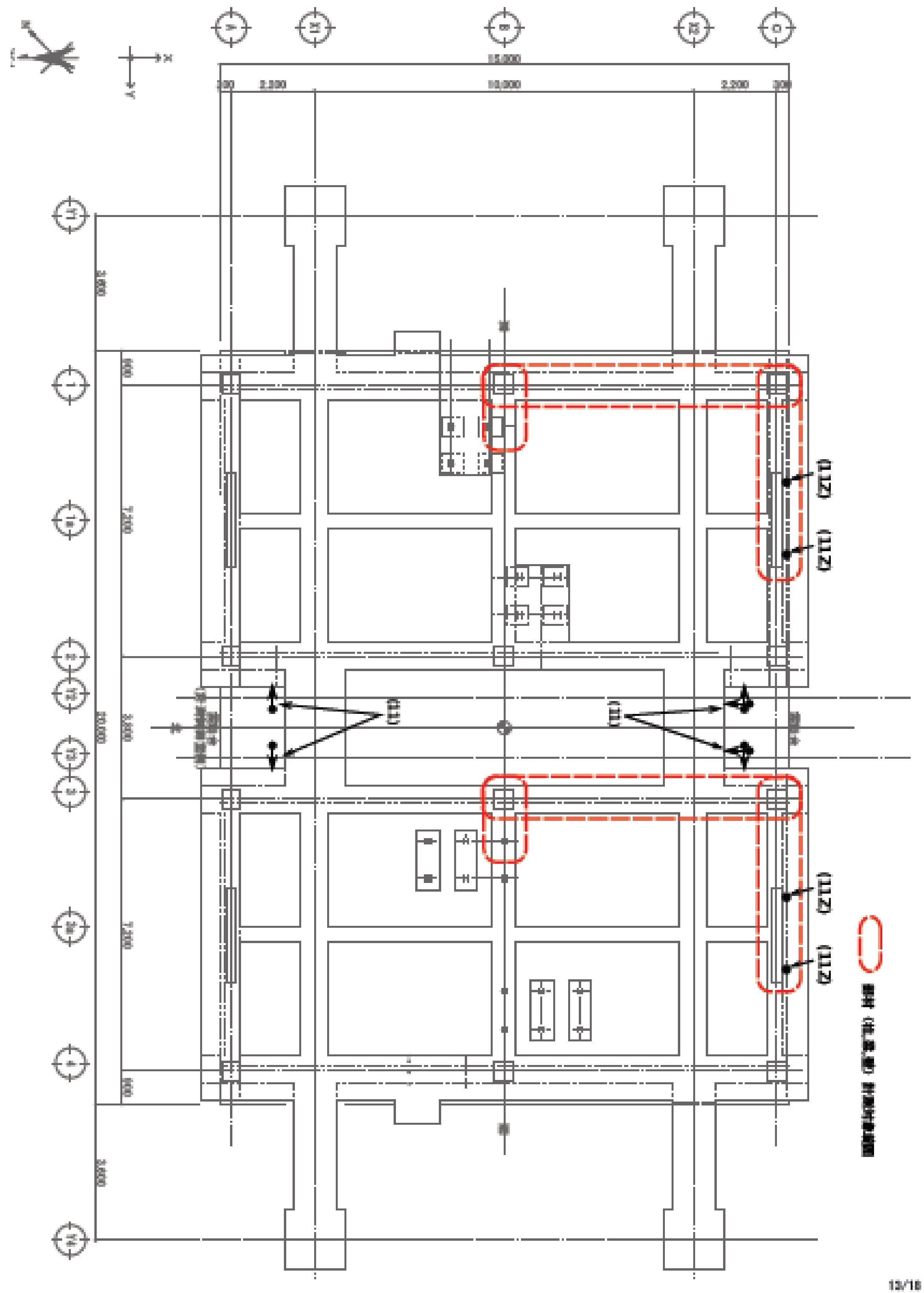

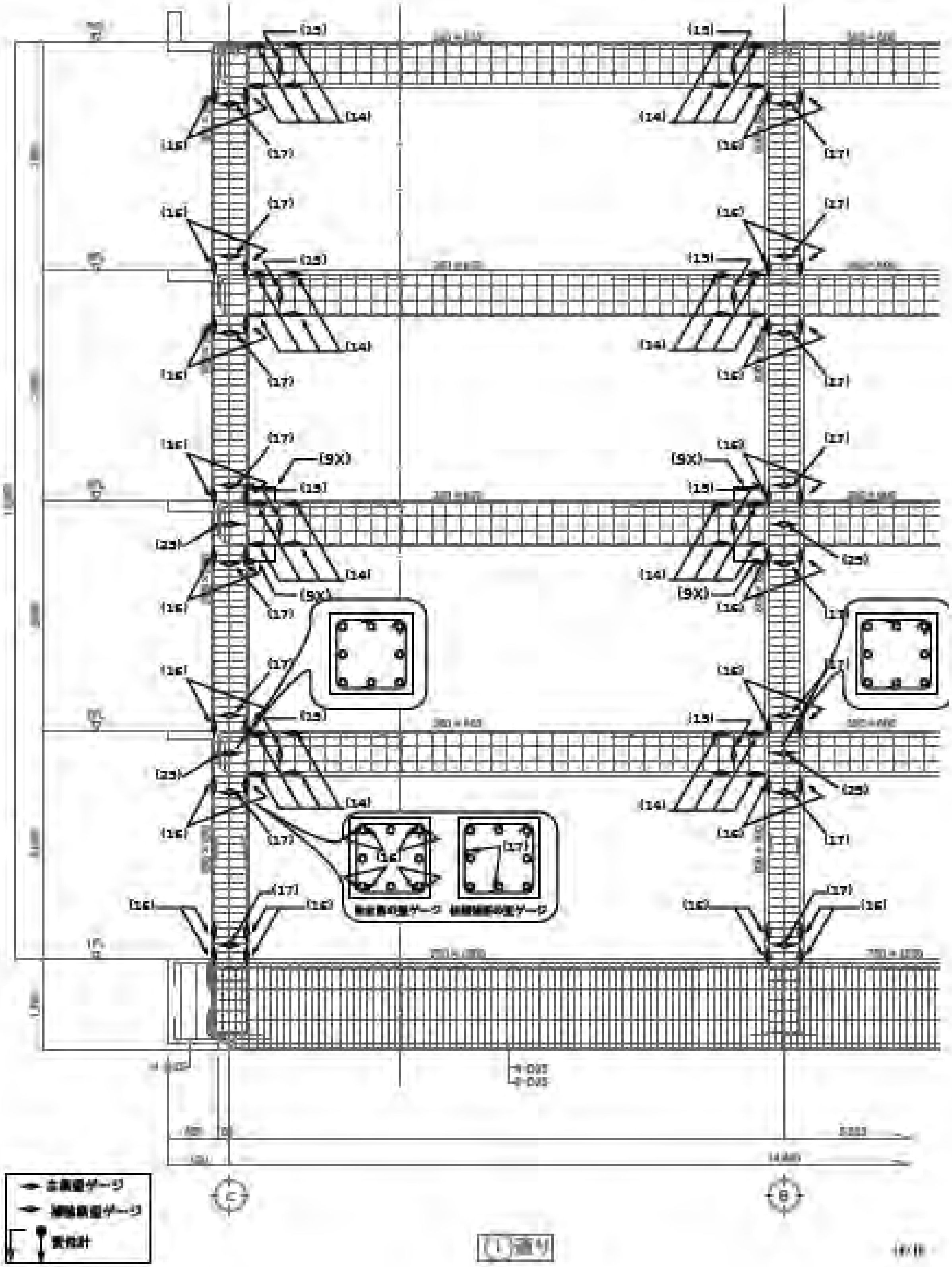
(14)
(15)
(16)
(17)
(9X)
(25)

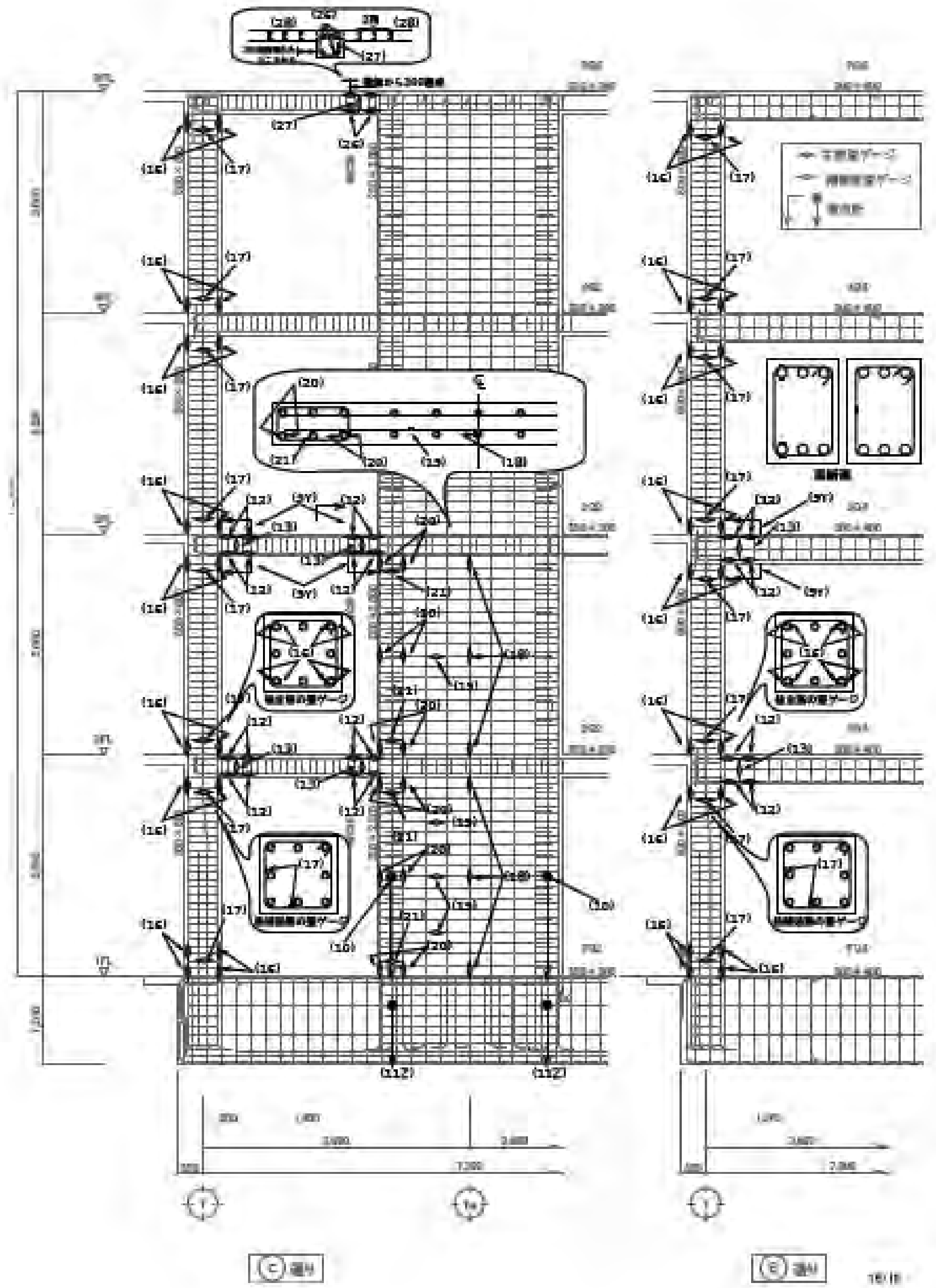

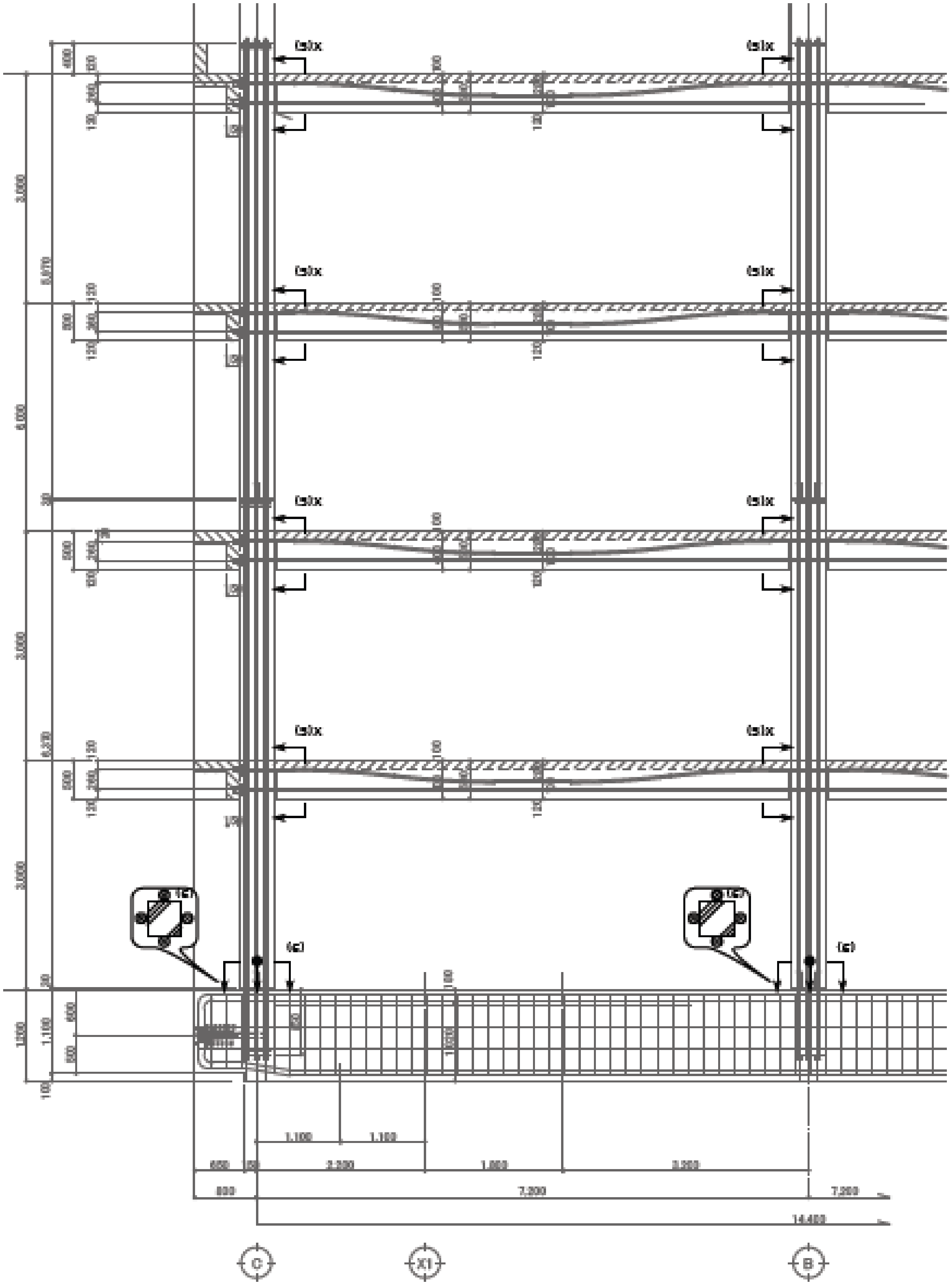

③ 通り

16/16

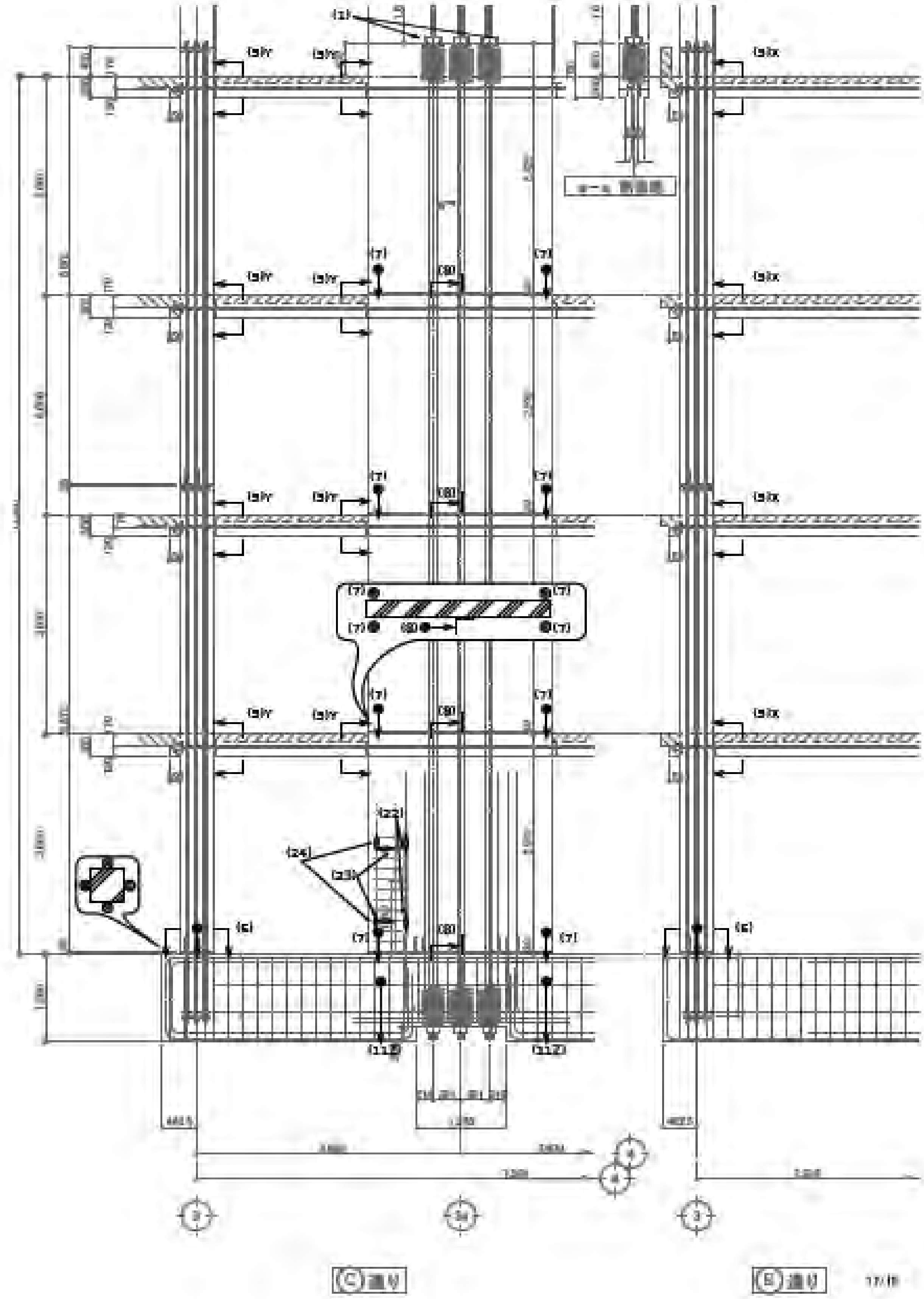

1　概要

独立行政法人防災科学技術研究所殿がE-ディフェンスにて実施する「高性能RC建物実験

において、実験データ収集のための計測準備作業（計測機器設置撤去・カメラ設置撤去）

についての作業を行った。

本資料は、加振実験前に実施する詳細計画、センサ等の取付け、ケーブル配線、

ラインチェック、ノイズ確認、信号確認、カメラ設置確認・実験終了後の撤収作業を

実施した報告書である。

2　実施場所

〒673-0515　兵庫県三木市志染町三津田西亀屋1501-21

独立行政法人　防災科学技術研究所　兵庫耐震工学研究センター(E-ディフェンス)

3　実施工程

実施工程表をページ3に示し、加振実験日を下表に示す。

表1　加振試験日

試験日		加振内容
1日目	12月13日	JMA神戸波10%・25%・50%
2日目	12月15日	JMA神戸波100%　公開試験
3日目	12月17日	JR鷹取波40%・60%　プレス公開試験

試験体設置状況

4　実施体制及び安全留意事項

実施体制図及び緊急連絡先をページ4に、作業上の安全留意事項をページ5に示す。

5　実施内容

(1) 計測に必要なセンサ機器類を倉庫から搬出し、員数確認やケーブル伸ばし等の事前準備を行った。

(2) 計測センサ及び小物治具類を指定された箇所に取付け、ケーブルをｼﾞｬﾝｸｼｮﾝﾎﾞｯｸｽ

(JB)まで配線接続した。(カメラ類も同様である)

(3) 計測センサの取付け状態や、配線の状態が適正であるかを判断するために、信号の確認を行った。

(4) カメラの設置を行い、映像集録までの確認を行った。

(5) 実験終了後、計測センサや機器類を取外し、整理の上所定の箇所に返納した。

6　詳細資料

(1) 震動台の方向と位置関係及びジャンクションボックス(JB)の様子をページ6に示す。

(2) ジャンクションボックス(JB)の配置図をページ7に示す。

(3) 計測点数一覧表をページ8に示す。

(4) 計測センサー一覧及びカメラ一覧をページ9～10に示す。

(5) 計測ブロック線図をページ11～16に示す。

(6) 計測センサチャンネルリスト一覧をページ17～18に示す。

(7) 計測センサチャンネルリスト(各JB)をページ19～31に示す。

(8) センサの設置位置図をページ32～41に示す。

(9) センサの寸法計測図をページ42～55に示す。

(10) カメラの設置位置図をページ56～58に示す。

(11) ブリッジボックス接続表をページ59～61に示す。

(9)と対応している歪ゲージプロット図(作成:前川建設)を62～68に添付する。

(12) ブリッチボックス設置位置図をページ69に示す。

(13) ケーブル準備表をページ70～73に示す。

(14) ケーブル配線ルート図をページ74～85に示す。

(15) 試験体定点写真を添付1に示す。

(16) センサー写真・作業風景写真・試験体写真を添付2に示す。

(17) 層間変位計測架台の製作・設置・撤去及び使用材料試験の実施結果を添付3に示す。(後日

実施工程表

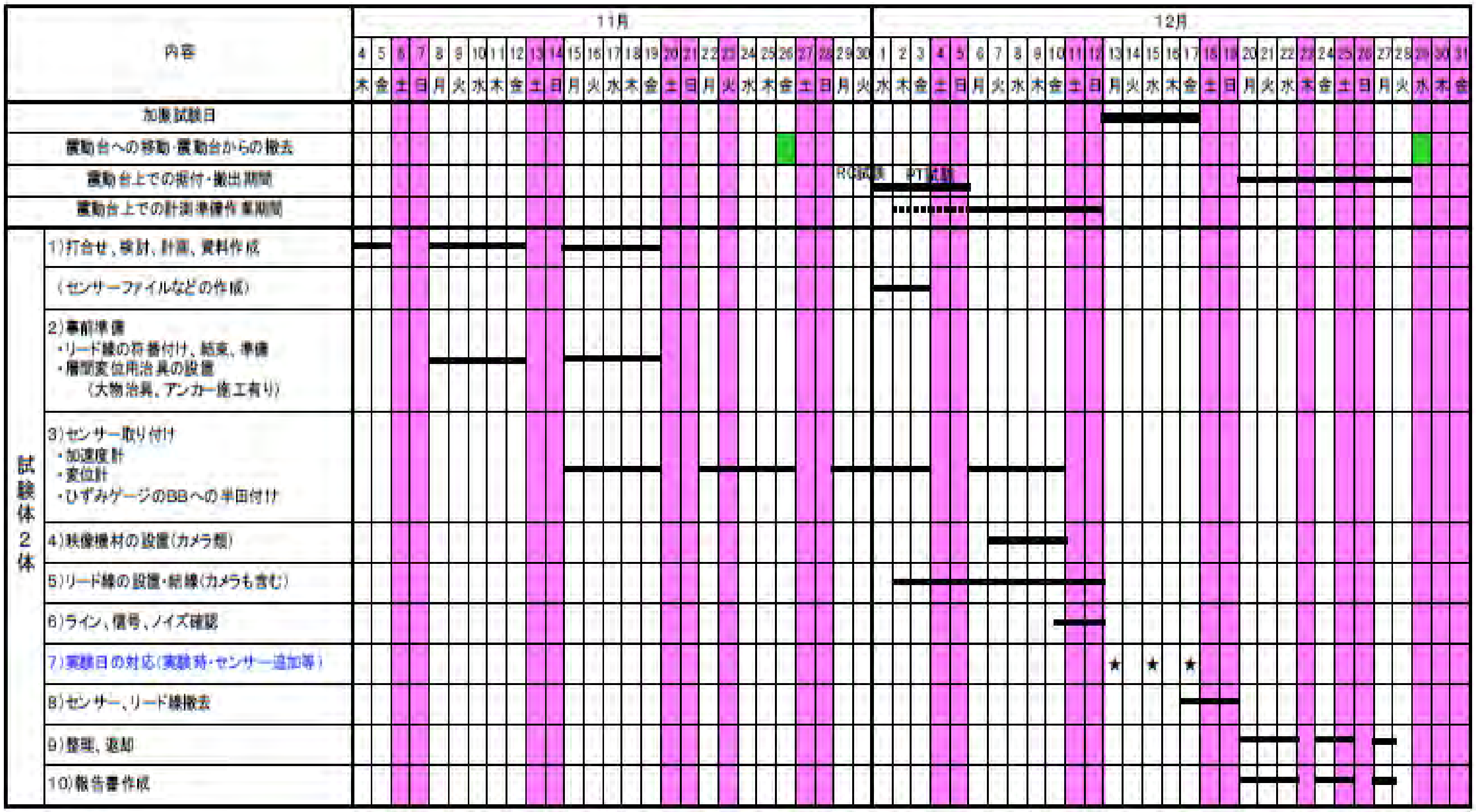
内容
11月
12月
加振試験日
震動台への移動・震動台からの撤去
震動台上での据付・搬出期間
震動台上での計測準備作業期間
RC試験
PT試験
試験体2体
1)打合せ、検討、計画、資料作成
（センサーファイルなどの作成）
2)事前準備
・リード線の符番付け、結束、準備
・層間変位用治具の設置
（大物治具、アンカー施工有り）
3)センサー取り付け
・加速度計
・変位計
・ひずみゲージのBBへの半田付け
4)映像機材の設置（カメラ類）
5)リード線の設置・結線（カメラも含む）
6)ライン、信号、ノイズ確認
7)実験日の対応（実験枠・センサー追加等）
8)センサー、リード線撤去
9)整理、返却
10)報告書作成

実施体制表および緊急連絡先

実施体制表

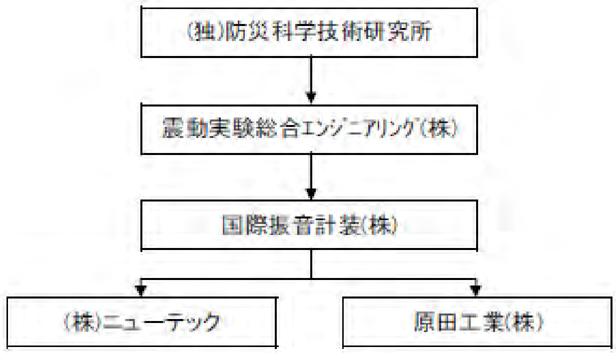

緊急連絡先

(独)防災科学技術研究所　E-Defense	0794-85-7654
震動実験総合エンジニアリング(株)	0794-87-8305
国際振音計装(株)	079-443-2617
(株)ニューテック	079-436-6200
原田工業(株)	079-442-4297
三木警察署	0794-82-0110
三木消防署	0794-82-0119
加古川労働基準監督	079-422-5001

安全留意事項

1) 作業開始時には安全教育を必ず受講し、決められた事を遵守すること。

2) 毎朝朝礼に参加し、TBMを行うこと。

3) 火気を使用する場合は火気使用届けを提出する。(消火器等用意する)

4) 電源ドラム、電動工具等電気機器類は点検を受けた物を使用する。

5) 決められたコンセントボックスを使用する。

6) 1.5m以上の高所作業では必ず安全帯を使用する。

7) 安全帯のフックは腰より高い位置に掛ける。

8) 玉掛作業時は吊荷の下に入らないこと。

9) 上下作業は同時並行的に行わない。

10) 一人作業は行わない。

11) 喫煙所以外の場所では喫煙を行わない。

12) ハンダゴテ等、火気使用時は、火気使用後30分以上経過後に残火の再確認をする。

13) 手元足元の状況を確認し、作業を行う。(周囲の確認)

14) 照明を確保し、明るい場所で作業を行うこと。

15) 作業場所の整理整頓清掃は進んで行うこと。

16) 決められた交通ルールを遵守すること。

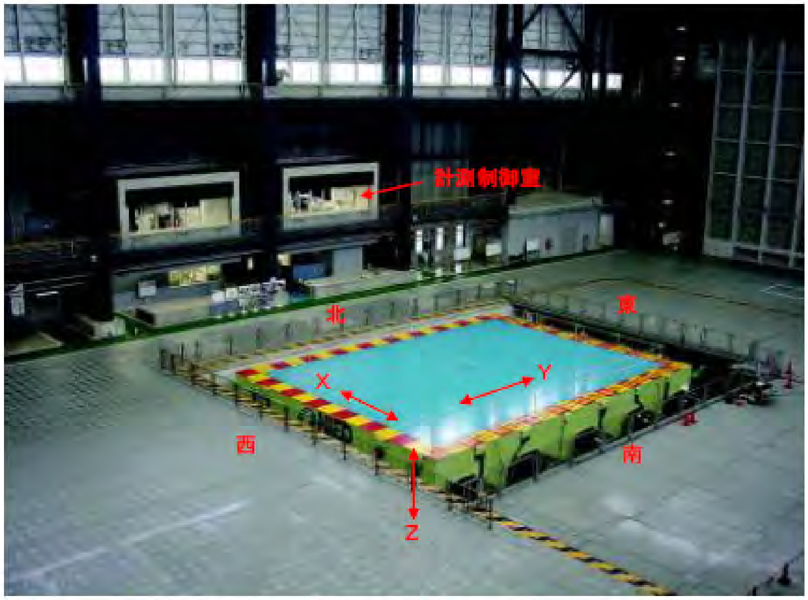

震動台の方向と位置関係


ジャンクションボックス(JB)の様子

JBチャンネル数	
No	数
JB01	64ch (ﾏﾙﾁｱﾝﾌﾟ)
JB02	64ch (ﾏﾙﾁｱﾝﾌﾟ)
JB03	64ch (ﾏﾙﾁｱﾝﾌﾟ)
JB04	64ch (ﾏﾙﾁｱﾝﾌﾟ)
JB05	64ch (ﾏﾙﾁｱﾝﾌﾟ)
JB06	64ch (ﾏﾙﾁｱﾝﾌﾟ)
JB07	64ch (ﾏﾙﾁｱﾝﾌﾟ)
JB08	64ch (ﾏﾙﾁｱﾝﾌﾟ)
JB09	64ch (ACｱﾝﾌﾟ)
JB10	64ch (ﾏﾙﾁｱﾝﾌﾟ)
JB11	64ch (ﾏﾙﾁｱﾝﾌﾟ)
JB12	64ch (ﾏﾙﾁｱﾝﾌﾟ)
JB13	64ch (ﾏﾙﾁｱﾝﾌﾟ)
JB14	32ch (ﾏﾙﾁｱﾝﾌﾟ)
JB15	64ch (DCｱﾝﾌﾟ)
JB16	32ch (高速ｱﾝﾌﾟ)

注意）サーボ型加速度計は各JBに対して
20ch以内の接続にすること

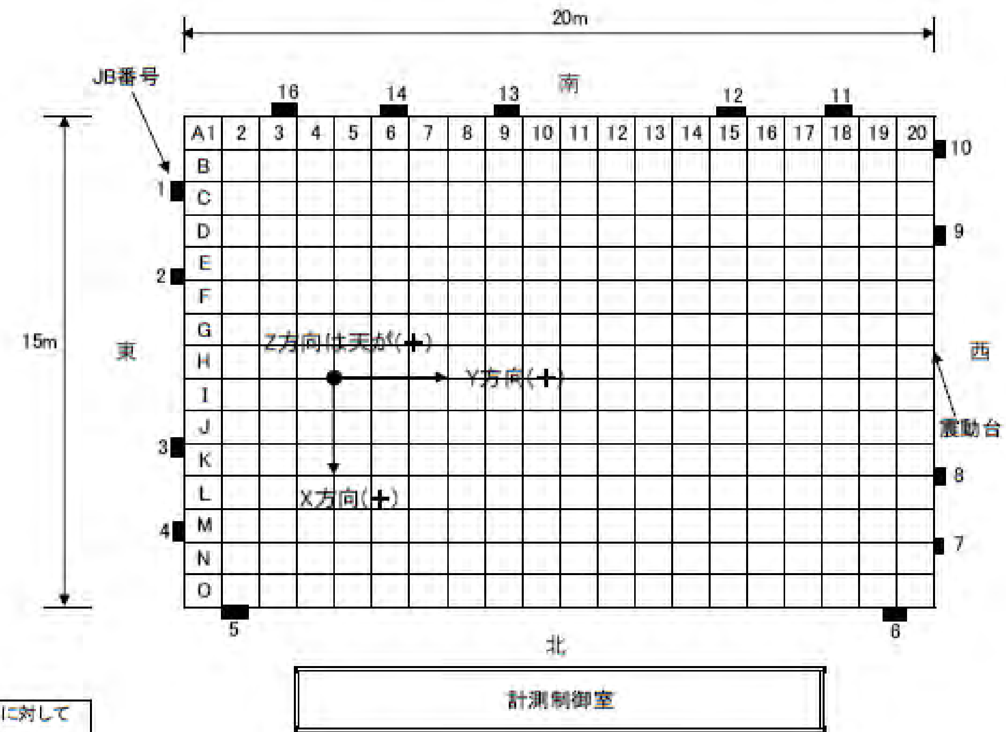

ジャンクションボックス(JB)の配置図

計測点数一覧表

計測	計測図	センサ	計測点	ロードセル	加速度		変位										ゲージ	小計	
				センターホール	サーボ型	歪型	レーザ型	CDP型			ワイヤ型						歪ゲージ		
				ロードセル	±10G	±5G	±250mm	±50mm	±12.5mm	±50mm	±250mm	±500mm	±1000mm	±150mm	±1000mm	±2500mm			
項目	記号	タグ	名称	東京測器	トキメック	共和電業	KEYENCE	共和電業	東京測器	東京測器	東京測器	東京測器	東京測器	共和電業	共和電業	共和電業	東京測器		
				KCM-3MNA	TA-25E-10-1	ASW-5AM36	LK-500	DTH-A-100	CDP-25	CDP-100	DP-500	DP-1000	DP-2000	DTP-D-300	DTP-D-2KS	DTP-D-5KS		ch数	点数
ロードセル	1	L	壁ワイヤ	2														2	2
加速度	2	A	層加速度		60													60	60
変位	3	D	層間変位(レーザ)				32											32	32
	3Z	D	層間鉛直変位					16										16	16
	4	D	層間変位(ワイヤ)									22	26			8		56	56
	5X	D	FT梁端変形(長辺)					16										16	16
	5Y	D	FT梁端変形(短辺)								24							24	24
	6	D	FT柱脚変形								8							8	8
	7	D	FT壁脚部変形											16				16	16
	8	D	FT壁端滑り					5		1								6	6
	9X	D	RC梁端変形(長辺)								4							4	4
	9Y	D	RC梁端変形(短辺)												6			6	6
	10	D	RC壁脚部変形											4				4	4
	11	D	基礎滑り					6										6	6
	11Z	D	基礎浮上がり					2	2									4	4
歪ゲージ	12	S	梁主筋歪(短辺)														24	24	48
	13	S	梁補強筋歪(短辺)														6	6	6
	14	S	梁主筋歪(長辺)														32	32	64
	15	S	梁補強筋歪(長辺)														8	8	8
	16	S	柱主筋歪														72	72	144
	17	S	柱補強筋歪														32	32	32
	18	S	壁縦筋歪														6	6	6
	19	S	壁横筋歪														6	6	6
	20	S	壁付帯柱主筋歪														12	12	24
	21	S	壁付帯柱補強筋歪														4	4	4
	22	S	FT壁脚部鉄筋														4	4	4
	23	S	FT壁柱主筋														2	2	4
	24	S	FT壁補強筋														2	2	2
設備計測	31		設備計測(加速度)			70												70	70
	32		設備計測(歪)														51	51	51
	33		設備計測(変位)							1								1	1
小計				2	60	70	32	45	2	2	36	22	26	20	6	8	261	592ch	734点

計測項目		CCD		デジタル	小計
29 移動カメラ	実験棟フロアー	1			8
29 CCDカメラ	試験体内部		16		16
30 デジタルカメラ	試験体内部			20	20
小計		1	16	20	44

合計＝ 636 ch

名称	写真	仕様等	名称	写真	仕様等
サーボ型加速度センサ		東京計器(株) TA-25E-10-1 (3方向セット) 定格:±98.07m/s^2	ポテンショメータ型変位センサ	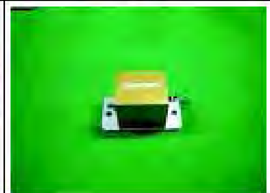	(株)東京測器 DP-500D (ワイヤタイプ) 定格:±250mm
歪型加速度センサ		(株)共和電業 ASW-5AM36 (防水型) 定格:±49.03m/s^2	ポテンショメータ型変位センサ		(株)東京測器 DP-1000D (ワイヤタイプ) 定格:±500mm
レーザ型変位センサ		(株)KEYENCE LK-500 定格:±250mm	ポテンショメータ型変位センサ	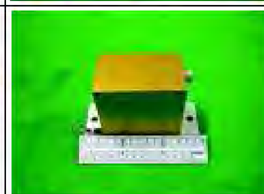	(株)東京測器 DP-2000D (ワイヤタイプ) 定格:±1000mm
ポテンショメータ型変位センサ		(株)共和電業 DTP-D-300 (ワイヤタイプ) 定格:±150mm	歪ゲージ型変位センサ	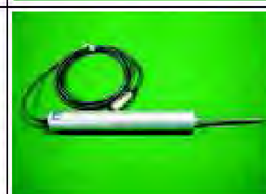	(株)共和電業 DTH-A-100 (バネタイプ) 定格:±50mm
ポテンショメータ型変位センサ		(株)共和電業 DTP-D-2KS (ワイヤタイプ) 定格:±1000mm	歪ゲージ型変位センサ		(株)東京測器 CDP-100 (バネタイプ) 定格:±50mm
ポテンショメータ型変位センサ		(株)共和電業 DTP-D-5KS (ワイヤタイプ) 定格:±2500mm	ブリッジボックス		(株)共和電業 DBB-120A (10ch用)

名称	写真	仕様等
移動カメラ一式		松下電器産業 AW-E300A ケーブル長20m
CCDカメラ1		TESCOM TBC-407S 38万画素
CCDカメラ2		SONY SSC-DC690 /2-SS259 38万画素

名称	写真	仕様等
デジタルカメラ		MOSWELL MS-265U 38万画素
バリフォーカルレンズ1		PENTAX CCTV LENSES H1212E(WX) 3.5×8mm
バリフォーカルレンズ2		TAMRON 13VG308AS 3×8mm

サーボ型加速度センサのブロック線図

歪型加速度センサのブロック線図

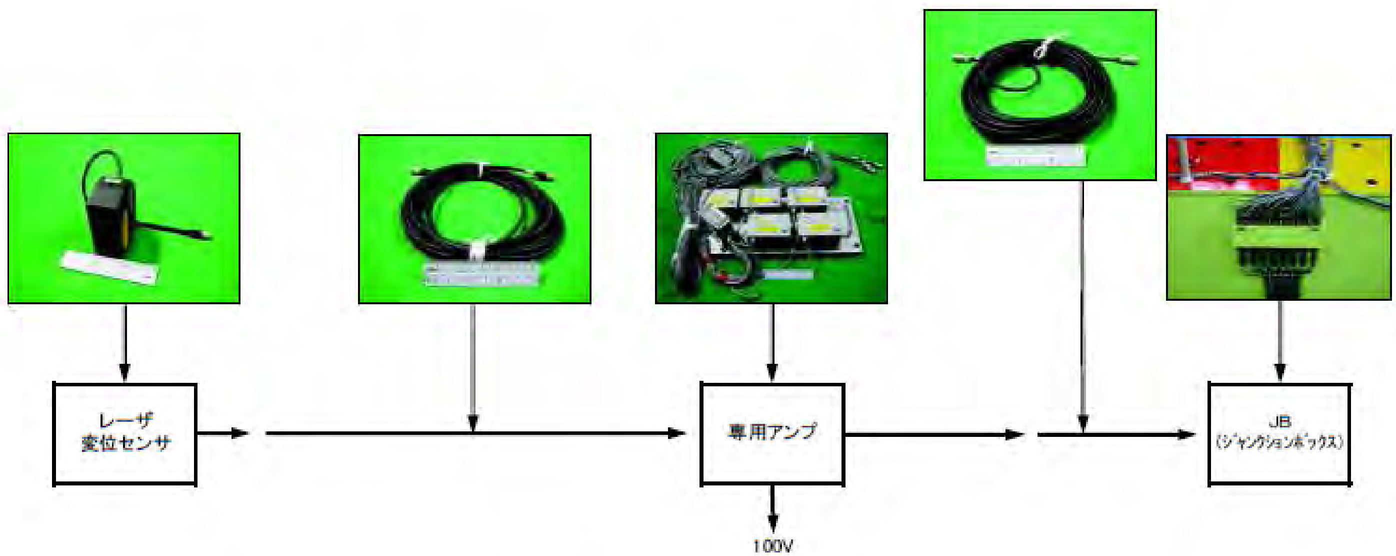

レーザ変位センサのブロック線図

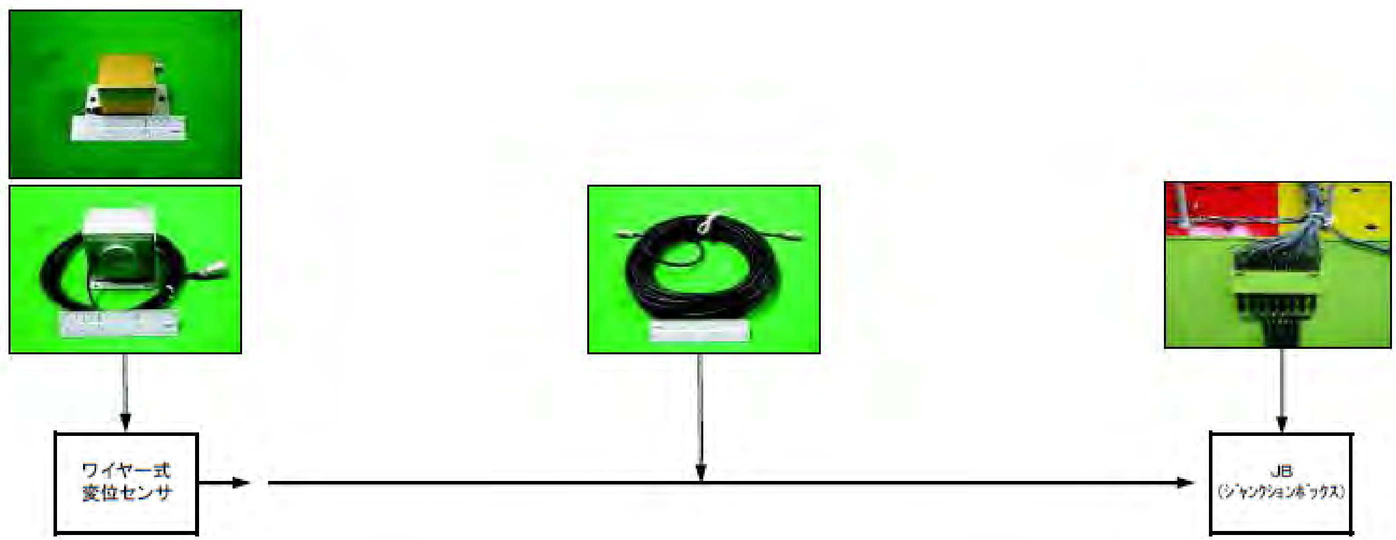

ワイヤー式変位センサのブロック線図

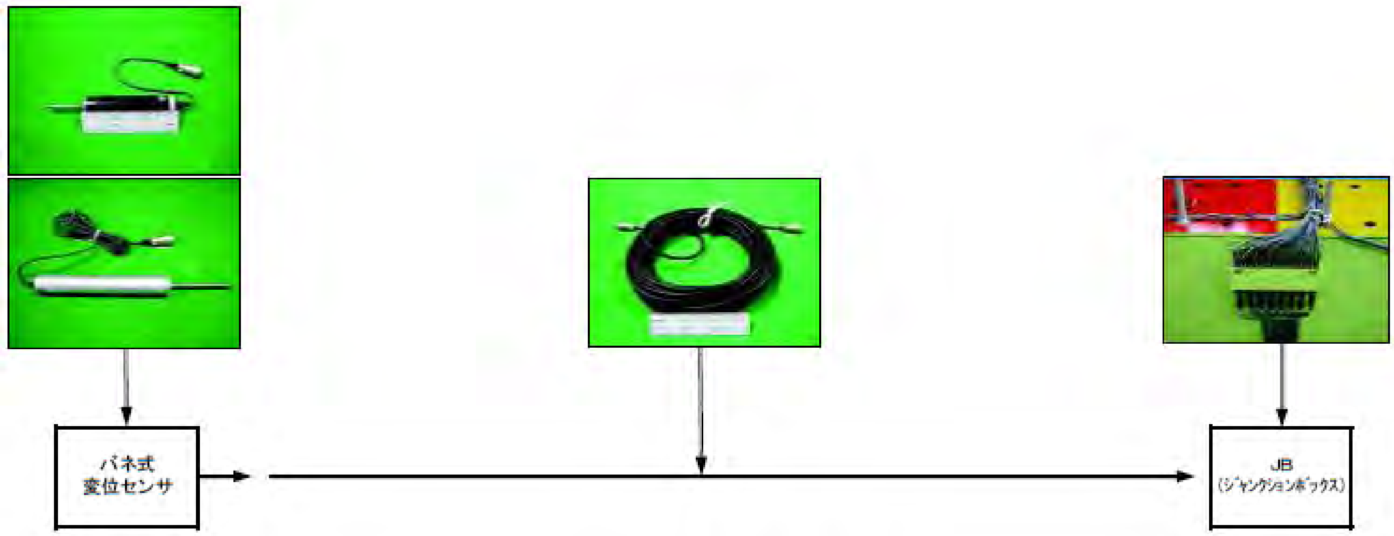

バネ式変位センサのブロック線図

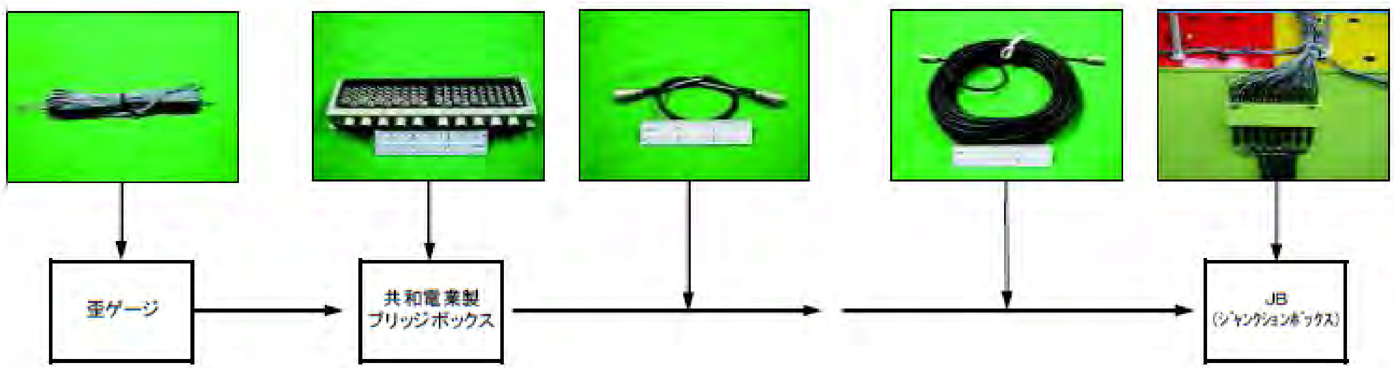

歪ゲージ(共和電業製ブリッジボックス)のブロック線図

計測センサチャンネルリスト一覧

青字：PT試験体用センサー
赤字：RC試験体用センサー

チャンネル	JB01		JB02		JB03		JB04		JB05	
	マルチアンプ		マルチアンプ		マルチアンプ		マルチアンプ		マルチアンプ	
	名称	長さ	名称	長さ	名称	長さ	名称	長さ	名称	長さ
1ch	12-R-S1	30	15-R-S1	30	16-R-S41	30	18-R-S1	30	2-R2-A1X	30
2ch	12-R-S2	30	15-R-S2	30	16-R-S42	30	18-R-S2	30	2-R2-A1Y	30
3ch	12-R-S3	30	15-R-S3	30	16-R-S43	30	18-R-S3	30	2-R2-A1Z	30
4ch	12-R-S4	30	15-R-S4	30	16-R-S44	30	18-R-S4	30	2-R3-A1X	30
5ch	12-R-S5	30	15-R-S5	40	16-R-S45	30	18-R-S5	30	2-R3-A1Y	30
6ch	12-R-S6	30	15-R-S6	40	16-R-S46	30	18-R-S6	30	2-R3-A1Z	30
7ch	12-R-S7	30	15-R-S7	40	16-R-S47	30	19-R-S1	30	2-R4-A1X	40
8ch	12-R-S8	30	15-R-S8	40	16-R-S48	30	19-R-S2	30	2-R4-A1Y	40
9ch	12-R-S9	30	25-R-S1	40	16-R-S49	30	19-R-S3	30	2-R4-A1Z	40
10ch	12-R-S10	30	25-R-S2	40	16-R-S50	30	19-R-S4	30	2-RR-A1X	40
11ch	12-R-S11	30	25-R-S3	40	16-R-S51	30	19-R-S5	30	2-RR-A1Y	40
12ch	12-R-S12	30	25-R-S4	40	16-R-S52	30	19-R-S6	30	2-RR-A1Z	40
13ch	12-R-S13	30	25-R-S5	40	16-R-S53	30	20-R-S1	30	3-R1-D1XT	10×1
14ch	12-R-S14	30	25-R-S6	40	16-R-S54	30	20-R-S2	30	3-R1-D1XB	10×1
15ch	12-R-S15	30	25-R-S7	40	16-R-S55	30	20-R-S3	30	3-R1-D1YT	10×1
16ch	12-R-S16	30	25-R-S8	40	16-R-S56	30	20-R-S4	30	3-R1-D1YB	10×1
17ch	12-R-S17	30	16-R-S1	30	16-R-S57	40	20-R-S5	30	3-R2-D1XT	10×3
18ch	12-R-S18	30	16-R-S2	30	16-R-S58	40	20-R-S6	30	3-R2-D1XB	10×3
19ch	12-R-S19	30	16-R-S3	30	16-R-S59	40	20-R-S7	30	3-R2-D1YT	10×3
20ch	12-R-S20	30	16-R-S4	30	16-R-S60	40	20-R-S8	30	3-R2-D1YB	10×3
21ch	12-R-S21	30	16-R-S5	30	16-R-S61	40	20-R-S9	30	3-R3-D1XT	10×3
22ch	12-R-S22	30	16-R-S6	30	16-R-S62	40	20-R-S10	30	3-R3-D1XB	10×3
23ch	12-R-S23	30	16-R-S7	30	16-R-S63	40	20-R-S11	30	3-R3-D1YT	10×3
24ch	12-R-S24	30	16-R-S8	30	16-R-S64	40	20-R-S12	30	3-R3-D1YB	10×3
25ch	13-R-S1	30	16-R-S9	30	16-R-S65	40	21-R-S1	30	3-R4-D1XT	10×3
26ch	13-R-S2	30	16-R-S10	30	16-R-S66	40	21-R-S2	30	3-R4-D1XB	10×3
27ch	13-R-S3	30	16-R-S11	30	16-R-S67	40	21-R-S3	30	3-R4-D1YT	10×3
28ch	13-R-S4	30	16-R-S12	30	16-R-S68	40	21-R-S4	30	3-R4-D1YB	10×3
29ch	13-R-S5	30	16-R-S13	30	16-R-S69	40			32-R1-D1Z	30
30ch	13-R-S6	30	16-R-S14	30	16-R-S70	40			32-R1-D2Z	30
31ch	14-R-S1	30	16-R-S15	30	16-R-S71	40	AI-R1N-D1	20	32-R2-D1Z	30
32ch	14-R-S2	30	16-R-S16	30	16-R-S72	40	AI-R1N-D2	20	32-R2-D2Z	30
33ch	14-R-S3	30	16-R-S17	30	17-R-S1	30	AI-R1N-D3	20	32-R3-D1Z	30
34ch	14-R-S4	30	16-R-S18	30	17-R-S2	30	AI-R1N-D4	20	32-R3-D2Z	40
35ch	14-R-S5	30	16-R-S19	30	17-R-S3	30	AI-R1N-D5	20	32-R4-D1Z	40
36ch	14-R-S6	30	16-R-S20	30	17-R-S4	30	AI-R1N-D6	20	32-R4-D2Z	40
37ch	14-R-S7	30	16-R-S21	30	17-R-S5	30	AI-R1N-D7	20	4-R1-D2XT	30
38ch	14-R-S8	30	16-R-S22	30	17-R-S6	30	AI-R1N-D8	20	4-R1-D2XB	30
39ch	14-R-S9	30	16-R-S23	30	17-R-S7	30	AI-R1N-D9	20	4-R1-D2YT	30
40ch	14-R-S10	30	16-R-S24	30	17-R-S8	30	AI-R1N-D10	20	4-R1-D2YB	30
41ch	14-R-S11	30	16-R-S25	30	17-R-S9	30	AI-R2N-D11	20	4-R1-D3XT	30
42ch	14-R-S12	30	16-R-S26	30	17-R-S10	30	AI-R2N-D12	20	4-R1-D3XB	30
43ch	14-R-S13	30	16-R-S27	30	17-R-S11	30	AI-R3N-D13	20	4-R1-D3YT	30
44ch	14-R-S14	30	16-R-S28	30	17-R-S12	30	AI-R3N-D14	20	4-R1-D3YB	30
45ch	14-R-S15	30	16-R-S29	30	17-R-S13	30	AI-R4N-D15	30	4-R2-D2XT	30
46ch	14-R-S16	30	16-R-S30	30	17-R-S14	30	AI-R4N-D16	30	4-R2-D2XB	30
47ch	14-R-S17	40	16-R-S31	30	17-R-S15	30			4-R2-D2YT	30
48ch	14-R-S18	40	16-R-S32	30	17-R-S16	30			4-R2-D2YB	30
49ch	14-R-S19	40	16-R-S33	30	17-R-S17	30			4-R2-D3XT	30
50ch	14-R-S20	40	16-R-S34	30	17-R-S18	30			4-R2-D3XB	30
51ch	14-R-S21	40	16-R-S35	30	17-R-S19	30	A3-R1-D1	20	4-R2-D3YT	30
52ch	14-R-S22	40	16-R-S36	30	17-R-S20	30	A3-R1-D2	20	4-R2-D3YB	30
53ch	14-R-S23	40	16-R-S37	30	17-R-S21	30	A3-R2-D3	30	4-R3-D2XT	40
54ch	14-R-S24	40	16-R-S38	30	17-R-S22	30	A3-R2-D4	30	4-R3-D2XB	40
55ch	14-R-S25	40	16-R-S39	30	17-R-S23	30	A3-R3-D5	30	4-R3-D2YT	40
56ch	14-R-S26	40	16-R-S40	30	17-R-S24	30	A3-R3-D6	30	4-R3-D2YB	40
57ch	14-R-S27	40			17-R-S25	40	A3-R3-D7	30	4-R3-D3XT	40
58ch	14-R-S28	40			17-R-S26	40	A3-R3-D8	30	4-R3-D3XB	40
59ch	14-R-S29	40			17-R-S27	40	A3-R4-D9	40	4-R3-D3YT	40
60ch	14-R-S30	40			17-R-S28	40	A3-R4-D10	40	4-R3-D3YB	40
61ch	14-R-S31	40			17-R-S29	40			4-R4-D2XT	40
62ch	14-R-S32	40			17-R-S30	40			4-R4-D2XB	40
63ch			8-R1-DA1aY	20	17-R-S31	40			4-R4-D2YT	40
64ch			8-R1-DC1aY	20	17-R-S32	40			4-R4-D2YB	40

チャンネル	JB06		JB07		JB10		JB11		JB12	
	マルチアンプ		マルチアンプ		マルチアンプ		マルチアンプ		マルチアンプ	
	名称	長さ	名称	長さ	名称	長さ	名称	長さ	名称	長さ
1ch	AI-P1N-D1	10	2-P2-A1X	30	31-P-A1	40	2-P2-A2X	30	5X-P1-DB3T	30
2ch	AI-P1N-D2	10	2-P2-A1Y	30	31-P-A2	40	2-P2-A2Y	30	5X-P2-DB3B	30
3ch	AI-P1N-D3	10	2-P2-A1Z	30	31-P-A3	40	2-P2-A2Z	30	5X-P2-DB3T	30
4ch	AI-P1N-D4	10	2-P3-A1X	30	31-P-A4	40	2-P3-A2X	30	5X-P3-DB3B	30
5ch	AI-P1N-D5	10	2-P3-A1Y	30	31-P-A5	40	2-P3-A2Y	30	5X-P3-DB3T	30
6ch	AI-P1N-D6	10	2-P3-A1Z	30	31-P-A6	40	2-P3-A2Z	30	5X-P4-DB3B	40
7ch	AI-P1N-D7	10	2-P4-A1X	40	31-P-A7	40	2-P4-A2X	40	5X-P4-DB3T	40
8ch	AI-P1N-D8	10	2-P4-A1Y	40	31-P-A8	40	2-P4-A2Y	40	5X-PR-DB3B	40
9ch	AI-P1N-D9	10	2-P4-A1Z	40	31-P-A9	40	2-P4-A2Z	40	5X-P1-DC3T	30
10ch	AI-P1N-D10	10	2-PR-A1X	40	31-P-A10	40	2-PR-A2X	40	5X-P2-DC3B	30
11ch	AI-P3N-D11	20	2-PR-A1Y	40	31-P-A11	40	2-PR-A2Y	40	5X-P2-DC3T	30
12ch	AI-P3N-D12	20	2-PR-A1Z	40	31-P-A12	40	2-PR-A2Z	40	5X-P3-DC3B	30
13ch	AI-P3N-D13	20	3-P1-D1XT	10×1	31-P-A13	40	1-PL1	40	5X-P3-DC3T	30
14ch	AI-P3N-D14	20	3-P1-D1XB	10×1	31-P-A14	40	1-PL2	40	5X-P4-DC3B	40
15ch	AI-P4N-D15	30	3-P1-D1YT	10×1	31-P-A15	40	7-P1-DC3aNE	30	5X-P4-DC3T	40
16ch	AI-P4N-D16	30	3-P1-D1YB	10×1	31-P-A16	40	7-P1-DC3aSE	30	5X-PR-DC3B	40
17ch			3-P2-D1XT	10×3	31-P-A17	40	7-P1-DC3aSW	30	5Y-P1-DB3T	30
18ch			3-P2-D1XB	10×3	31-P-A18	40	7-P1-DC3aNW	30	5Y-P2-DB3B	30
19ch			3-P2-D1YT	10×3	31-P-A19	40	7-P2-DC3aNE	30	5Y-P2-DB3T	30
20ch			3-P2-D1YB	10×3	31-P-A20	40	7-P2-DC3aSE	30	5Y-P3-DB3B	30
21ch	2-P1-A1X	20	3-P3-D1XT	10×3	31-P-A21	40	7-P2-DC3aSW	30	5Y-P3-DB3T	30
22ch	2-P1-A1Y	20	3-P3-D1XB	10×3	31-P-A22	40	7-P2-DC3aNW	30	5Y-P4-DB3B	40
23ch	2-P1-A1Z	20	3-P3-D1YT	10×3	31-P-A23	40	7-P3-DC3aNE	30	5Y-P4-DB3T	40
24ch	2-P1-A2X	30	3-P3-D1YB	10×3	31-P-A24	40	7-P3-DC3aSE	30	5Y-PR-DB3B	40
25ch	2-P1-A2Y	30	3-P4-D1XT	10×3	31-P-A25	40	7-P3-DC3aSW	30	5Y-P1-DC3T	30
26ch	2-P1-A2Z	30	3-P4-D1XB	10×3	31-P-A26	40	7-P3-DC3aNW	30	5Y-P2-DC3B	30
27ch	2-R1-A1X	30	3-P4-D1YT	10×3	31-P-A27	40	7-P4-DC3aNE	40	5Y-P2-DC3T	30
28ch	2-R1-A1Y	30	3-P4-D1YB	10×3	31-P-A28	40	7-P4-DC3aSE	40	5Y-P3-DC3B	30
29ch	2-R1-A1Z	30	32-P1-D1Z	30	31-P-A29	40	7-P4-DC3aSW	40	5Y-P3-DC3T	30
30ch	2-R1-A2X	40	32-P1-D2Z	30	31-P-A30	40	7-P4-DC3aNW	40	5Y-P4-DC3B	40
31ch	2-R1-A2Y	40	32-P2-D1Z	30	31-P-A31	40	8-P1-DC3aY	30	5Y-P4-DC3T	40
32ch	2-R1-A2Z	40	32-P2-D2Z	30	32-P-S1	40	8-P2-DC3aY	30	5Y-PR-DC3B	40
33ch			32-P3-D1Z	30	32-P-S2	40	8-P3-DC3aY	30	5Y-P1-DC3aT	30
34ch			32-P3-D2Z	40	32-P-S3	40	8-P4-DC3aY	40	5Y-P2-DC3aB	30
35ch			32-P4-D1Z	40	32-P-S4	40	22-P-S1	30	5Y-P2-DC3aT	30
36ch			32-P4-D2Z	40	32-P-S5	40	22-P-S2	30	5Y-P3-DC3aB	30
37ch			4-P1-D2XT	30	32-P-S6	40	22-P-S3	30	5Y-P3-DC3aT	30
38ch			4-P1-D2XB	30	32-P-S7	40	22-P-S4	30	5Y-P4-DC3aB	40
39ch			4-P1-D2YT	30	32-P-S8	40	23-P-S1	30	5Y-P4-DC3aT	40
40ch			4-P1-D2YB	30	32-P-S9	40	23-P-S2	30	5Y-PR-DC3aB	40
41ch			4-P1-D3XT	30	32-P-S10	40	24-P-S1	30	6-P1-DB3N	30
42ch			4-P1-D3XB	30	32-P-S11	40	24-P-S2	30	6-P1-DB3E	30
43ch			4-P1-D3YT	30	32-P-S12	40			6-P1-DB3S	30
44ch			4-P1-D3YB	30	32-P-S13	40			6-P1-DB3W	30
45ch			4-P2-D2XT	30	32-P-S14	40	AI-P1S-D1	10	6-P1-DC3N	30
46ch			4-P2-D2XB	30	32-P-S15	40	AI-P1S-D2	10	6-P1-DC3E	30
47ch			4-P2-D2YT	30	32-P-S16	40	AI-P1S-D3	10	6-P1-DC3S	30
48ch			4-P2-D2YB	30	32-P-S17	40	AI-P1S-D4	10	6-P1-DC3W	30
49ch			4-P2-D3XT	30	32-P-S18	40	AI-P1S-D5	10		
50ch			4-P2-D3XB	30	32-P-S19	40	AI-P1S-D6	10		
51ch			4-P2-D3YT	30	32-P-S20	40	AI-P1S-D7	10	11-P0-D1Y	30
52ch			4-P2-D3YB	30	32-P-S21	40	AI-P1S-D8	10	11-P0-D2X	10
53ch			4-P3-D2XT	40	32-P-S22	40	AI-P1S-D9	10	11-P0-D2Y	10
54ch			4-P3-D2XB	40	32-P-S23	40	AI-P1S-D10	10	11Z-P0-D1Z	10
55ch			4-P3-D2YT	40	32-P-S24	40	AI-R1S-D1	30	11Z-P0-D2Z	10
56ch			4-P3-D2YB	40	32-P-S25	40	AI-R1S-D2	30	11-R0-D1Y	30
57ch			4-P3-D3XT	40	32-P-S26	40	AI-R1S-D3	30	11-R0-D2X	10
58ch			4-P3-D3XB	40	32-P-S27	40	AI-R1S-D4	30	11-R0-D2Y	10
59ch			4-P3-D3YT	40			AI-R1S-D5	30	11Z-R0-D1Z	30
60ch			4-P3-D3YB	40			AI-R1S-D6	30	11Z-R0-D2Z	30
61ch			4-P4-D2XT	40			AI-R1S-D7	30		
62ch			4-P4-D2XB	40			AI-R1S-D8	30		
63ch			4-P4-D2YT	40			AI-R1S-D9	30		
64ch			4-P4-D2YB	40			AI-R1S-D10	30		

チャンネル	JB13		JB14		JB15	EDX	
	マルチアンプ		マルチアンプ		マルチアンプ	専用アンプ	
	名称	長さ	名称	長さ	名称	名称	長さ
1ch	31-R-A1	40	2-R2-A2X	30	Target X	A4-P1-D1	30
2ch	31-R-A2	40	2-R2-A2Y	30	Target Y	A4-P1-D2	30
3ch	31-R-A3	40	2-R2-A2Z	30	Target Z	A4-P1-D3	30
4ch	31-R-A4	40	2-R3-A2X	30	Target Roll	A4-P1-D4	30
5ch	31-R-A5	40	2-R3-A2Y	30	Target Pitch	A4-P1-D5	30
6ch	31-R-A6	40	2-R3-A2Z	30	Target Yaw	A4-P1-D6	30
7ch	31-R-A7	40	2-R4-A2X	40	Accref X	A4-P1-D7	30
8ch	31-R-A8	40	2-R4-A2Y	40	Accref Y	A4-P1-D8	30
9ch	31-R-A9	40	2-R4-A2Z	40	Accref Z	A4-P1-D9	30
10ch	31-R-A10	40	2-RR-A2X	40	Accref Roll	A4-P1-D10	30
11ch	31-R-A11	40	2-RR-A2Y	40	Accref Pitch	A4-P1-D11	30
12ch	31-R-A12	40	2-RR-A2Z	40	Accref Yaw	A4-P1-D12	30
13ch	31-R-A13	40	9X-R0-DB1T	30	Acc fbk X	A4-P1-D13	30
14ch	31-R-A14	40	9X-R0-DB1B	30	Acc fbk Y	A4-P1-D14	30
15ch	31-R-A15	40	9X-R0-DC1T	30	Acc fbk Z	A2-P1S-D1	[illegible]
16ch	31-R-A16	40	9X-R0-DC1B	30	Acc fbk Roll	A2-P1S-D2	[illegible]
17ch	31-R-A17	40	9Y-R0-DB1T	30	Acc fbk Pitch	A2-P1S-D3	[illegible]
18ch	31-R-A18	40	9Y-R0-DB1B	30	Acc fbk Yaw	A2-P1S-D4	[illegible]
19ch	31-R-A19	40	9Y-R0-DC1T	30	Vel fbk X	A2-R1S-D1	[illegible]
20ch	31-R-A20	40	9Y-R0-DC1B	30	Vel fbk Y	A2-R1S-D2	[illegible]
21ch	31-R-A21	40	9Y-R0-DC1aT	30	Vel fbk Z	A2-R1S-D3	[illegible]
22ch	31-R-A22	40	9Y-R0-DC1aB	30	Vel fbk Roll	A2-R1S-D4	[illegible]
23ch	31-R-A23	40	10-R1-DC1aNE	30	Vel fbk Pitch		
24ch	31-R-A24	40	10-R1-DC1aSE	30	Vel fbk Yaw		
25ch	31-R-A25	40	10-R1-DC1aSW	30	Dis fbk X		
26ch	31-R-A26	40	10-R1-DC1aNW	30	Dis fbk Y		
27ch	31-R-A27	40			Dis fbk Z		
28ch	31-R-A28	40	ACC-X		Dis fbk Roll		
29ch	31-R-A29	40	ACC-Y		Dis fbk Pitch		
30ch	31-R-A30	40	ACC-Z		Dis fbk Yaw		
31ch	31-R-A31	40	PLUS		Force fbk X		
32ch	31-R-A32	40	ATURYOKU		Force fbk Y		
33ch	31-R-A33	40			Force fbk Z		
34ch	31-R-A34	40			Force fbk Roll		
35ch	31-R-A35	40			Force fbk Pitch		
36ch	31-R-A36	40			Force fbk Yaw		
37ch	31-R-A37	40			Dis fbk X1		
38ch	31-R-A38	40			Dis fbk X5		
39ch	31-R-A39	40			Dis fbk Y1		
40ch	32-R-S1	40			Dis fbk Y5		
41ch	32-R-S2	40			Dis fbk Z1		
42ch	32-R-S3	40			Dis fbk Z4		
43ch	32-R-S4	40			Dis fbk Z8		
44ch	32-R-S5	40			Dis fbk Z11		
45ch	32-R-S6	40			A Acc fbk X1		
46ch	32-R-S7	40			A Acc fbk X2		
47ch	32-R-S8	40			A Acc fbk X3		
48ch	32-R-S9	40			A Acc fbk X4		
49ch	32-R-S10	40			A Acc fbk X5		
50ch	32-R-S11	40			A Acc fbk Y1		
51ch	32-R-S12	40			A Acc fbk Y2		
52ch	32-R-S13	40			A Acc fbk Y3		
53ch	32-R-S14	40			A Acc fbk Y4		
54ch	32-R-S15	40			A Acc fbk Y5		
55ch	32-R-S16	40			A Acc fbk Z1		
56ch	32-R-S17	40			A Acc fbk Z2		
57ch	32-R-S18	40			A Acc fbk Z3		
58ch	32-R-S19	40			A Acc fbk Z4		
59ch	32-R-S20	40			A Acc fbk Z5		
60ch	32-R-S21	40				共通10m	30
61ch	32-R-S22	40				共通20m	29
62ch	32-R-S23	40				共通30m	339
63ch	32-R-S24	40				共通40m	263
64ch	33-R-D1	40				レーザ用	82

計測センサの記号		
1	壁ワイヤ	荷重
2	層加速度	加速度
3	層間水平変位(レーザ)	変位
32	層間鉛直変位(CDP)	
4	層間水平変位(ワイヤ)	
5X	梁端変形－長辺(CDP)	
5Y	梁端変形－短辺(ワイヤ)	
6	柱脚変形(ワイヤ)	
7	壁脚部変形(ワイヤ)	
8	壁端滑り(CDP)	
9X	梁端変形－長辺(ワイヤ)	
9Y	梁端変形－短辺(ワイヤ)	
10	壁脚部変形(ワイヤ)	
11	基礎滑り(CDP)	
11Z	基礎浮上り(CDP)	
12	梁主筋歪－短辺	歪ゲージ
13	梁補強筋歪－短辺	
14	梁主筋歪－長辺	
15	梁補強筋歪－長辺	
16	柱主筋歪	
17	柱補強筋歪	
18	壁縦筋歪	
19	壁横筋歪	
20	壁付帯柱主筋歪	
21	壁付帯柱補強筋歪	
22	壁脚部鉄筋	
23	壁柱主筋	
24	壁補強筋	
25	RC柱梁接合部	
31	設備計測(歪加速度)	加速度
32	設備計測(歪ゲージ)	歪ゲージ
33	設備計測(変位)	変位
A1	壁変形	変位
A2	壁せん断変形	
A3	柱接合部(インダクタンス)	
A4	層間鉛直変位(ワイヤ)	

計測センサチャンネルリスト一覧-ch表示

青字：PT試験体用センサー
赤字：RC試験体用センサー

チャンネル		JB01			JB02			JB03			JB04	
		マルチアンプ			マルチアンプ			マルチアンプ			マルチアンプ	
		名称	長さ		名称	長さ		名称	長さ		名称	長さ
1ch	1	12-R-S1	30	65	15-R-S1	30	129	16-R-S41	30	193	18-R-S1	30
2ch	2	12-R-S2	30	66	15-R-S2	30	130	16-R-S42	30	194	18-R-S2	30
3ch	3	12-R-S3	30	67	15-R-S3	30	131	16-R-S43	30	195	18-R-S3	30
4ch	4	12-R-S4	30	68	15-R-S4	30	132	16-R-S44	30	196	18-R-S4	30
5ch	5	12-R-S5	30	69	15-R-S5	40	133	16-R-S45	30	197	18-R-S5	30
6ch	6	12-R-S6	30	70	15-R-S6	40	134	16-R-S46	30	198	18-R-S6	30
7ch	7	12-R-S7	30	71	15-R-S7	40	135	16-R-S47	30	199	19-R-S1	30
8ch	8	12-R-S8	30	72	15-R-S8	40	136	16-R-S48	30	200	19-R-S2	30
9ch	9	12-R-S9	30	73	25-R-S1	40	137	16-R-S49	30	201	19-R-S3	30
10ch	10	12-R-S10	30	74	25-R-S2	40	138	16-R-S50	30	202	19-R-S4	30
11ch	11	12-R-S11	30	75	25-R-S3	40	139	16-R-S51	30	203	19-R-S5	30
12ch	12	12-R-S12	30	76	25-R-S4	40	140	16-R-S52	30	204	19-R-S6	30
13ch	13	12-R-S13	30	77	25-R-S5	40	141	16-R-S53	30	205	20-R-S1	30
14ch	14	12-R-S14	30	78	25-R-S6	40	142	16-R-S54	30	206	20-R-S2	30
15ch	15	12-R-S15	30	79	25-R-S7	40	143	16-R-S55	30	207	20-R-S3	30
16ch	16	12-R-S16	30	80	25-R-S8	40	144	16-R-S56	30	208	20-R-S4	30
17ch	17	12-R-S17	30	81	16-R-S1	30	145	16-R-S57	40	209	20-R-S5	40
18ch	18	12-R-S18	30	82	16-R-S2	30	146	16-R-S58	40	210	20-R-S6	40
19ch	19	12-R-S19	30	83	16-R-S3	30	147	16-R-S59	40	211	20-R-S7	40
20ch	20	12-R-S20	30	84	16-R-S4	30	148	16-R-S60	40	212	20-R-S8	40
21ch	21	12-R-S21	30	85	16-R-S5	30	149	16-R-S61	40	213	20-R-S9	40
22ch	22	12-R-S22	30	86	16-R-S6	30	150	16-R-S62	40	214	20-R-S10	40
23ch	23	12-R-S23	30	87	16-R-S7	30	151	16-R-S63	40	215	20-R-S11	40
24ch	24	12-R-S24	30	88	16-R-S8	30	152	16-R-S64	40	216	20-R-S12	40
25ch	25	13-R-S1	30	89	16-R-S9	30	153	16-R-S65	40	217	21-R-S1	40
26ch	26	13-R-S2	30	90	16-R-S10	30	154	16-R-S66	40	218	21-R-S2	40
27ch	27	13-R-S3	30	91	16-R-S11	30	155	16-R-S67	40	219	21-R-S3	40
28ch	28	13-R-S4	30	92	16-R-S12	30	156	16-R-S68	40	220	21-R-S4	40
29ch	29	13-R-S5	30	93	16-R-S13	30	157	16-R-S69	40	221		
30ch	30	13-R-S6	30	94	16-R-S14	30	158	16-R-S70	40	222		
31ch	31	14-R-S1	30	95	16-R-S15	30	159	16-R-S71	40	223	A1-R1N-D1	20
32ch	32	14-R-S2	30	96	16-R-S16	30	160	16-R-S72	40	224	A1-R1N-D2	20
33ch	33	14-R-S3	30	97	16-R-S17	30	161	17-R-S1	30	225	A1-R1N-D3	20
34ch	34	14-R-S4	30	98	16-R-S18	30	162	17-R-S2	30	226	A1-R1N-D4	20
35ch	35	14-R-S5	30	99	16-R-S19	30	163	17-R-S3	30	227	A1-R1N-D5	20
36ch	36	14-R-S6	30	100	16-R-S20	30	164	17-R-S4	30	228	A1-R1N-D6	20
37ch	37	14-R-S7	30	101	16-R-S21	30	165	17-R-S5	30	229	A1-R1N-D7	20
38ch	38	14-R-S8	30	102	16-R-S22	30	166	17-R-S6	30	230	A1-R1N-D8	20
39ch	39	14-R-S9	30	103	16-R-S23	30	167	17-R-S7	30	231	A1-R1N-D9	20
40ch	40	14-R-S10	30	104	16-R-S24	30	168	17-R-S8	30	232	A1-R1N-D10	20
41ch	41	14-R-S11	30	105	16-R-S25	30	169	17-R-S9	30	233	A1-R3N-D11	20
42ch	42	14-R-S12	30	106	16-R-S26	30	170	17-R-S10	30	234	A1-R3N-D12	20
43ch	43	14-R-S13	30	107	16-R-S27	30	171	17-R-S11	30	235	A1-R3N-D13	20
44ch	44	14-R-S14	30	108	16-R-S28	30	172	17-R-S12	30	236	A1-R3N-D14	20
45ch	45	14-R-S15	30	109	16-R-S29	30	173	17-R-S13	30	237	A1-R4N-D15	30
46ch	46	14-R-S16	30	110	16-R-S30	30	174	17-R-S14	30	238	A1-R4N-D16	30
47ch	47	14-R-S17	40	111	16-R-S31	30	175	17-R-S15	30	239		
48ch	48	14-R-S18	40	112	16-R-S32	30	176	17-R-S16	30	240		
49ch	49	14-R-S19	40	113	16-R-S33	30	177	17-R-S17	30	241		
50ch	50	14-R-S20	40	114	16-R-S34	30	178	17-R-S18	30	242		
51ch	51	14-R-S21	40	115	16-R-S35	30	179	17-R-S19	30	243	A3-R1-D1	20
52ch	52	14-R-S22	40	116	16-R-S36	30	180	17-R-S20	30	244	A3-R1-D2	20
53ch	53	14-R-S23	40	117	16-R-S37	30	181	17-R-S21	30	245	A3-R2-D3	30
54ch	54	14-R-S24	40	118	16-R-S38	30	182	17-R-S22	30	246	A3-R2-D4	30
55ch	55	14-R-S25	40	119	16-R-S39	30	183	17-R-S23	30	247	A3-R3-D5	30
56ch	56	14-R-S26	40	120	16-R-S40	30	184	17-R-S24	30	248	A3-R3-D6	30
57ch	57	14-R-S27	40	121			185	17-R-S25	40	249	A3-R3-D7	30
58ch	58	14-R-S28	40	122			186	17-R-S26	40	250	A3-R3-D8	30
59ch	59	14-R-S29	40	123			187	17-R-S27	40	251	A3-R4-D9	40
60ch	60	14-R-S30	40	124			188	17-R-S28	40	252	A3-R4-D10	40
61ch	61	14-R-S31	40	125			189	17-R-S29	40	253		
62ch	62	14-R-S32	40	126			190	17-R-S30	40	254		
63ch	63			127	8-R1-DA1aY	20	191	17-R-S31	40	255		
64ch	64			128	8-R1-DC1aY	20	192	17-R-S32	40	256		

チャンネル		JB05			JB06			JB07			JB10	
		マルチアンプ			マルチアンプ			マルチアンプ			マルチアンプ	
		名称	長さ		名称	長さ		名称	長さ		名称	長さ
1ch	257	2-R2-A1X	30	321	A1-P1N-D1	10	385	2-P2-A1X	30	577	31-P-A1	40
2ch	258	2-R2-A1Y	30	322	A1-P1N-D2	10	386	2-P2-A1Y	30	578	31-P-A2	40
3ch	259	2-R2-A1Z	30	323	A1-P1N-D3	10	387	2-P2-A1Z	30	579	31-P-A3	40
4ch	260	2-R3-A1X	30	324	A1-P1N-D4	10	388	2-P3-A1X	30	580	31-P-A4	40
5ch	261	2-R3-A1Y	30	325	A1-P1N-D5	10	389	2-P3-A1Y	30	581	31-P-A5	40
6ch	262	2-R3-A1Z	30	326	A1-P1N-D6	10	390	2-P3-A1Z	30	582	31-P-A6	40
7ch	263	2-R4-A1X	40	327	A1-P1N-D7	10	391	2-P4-A1X	40	583	31-P-A7	40
8ch	264	2-R4-A1Y	40	328	A1-P1N-D8	10	392	2-P4-A1Y	40	584	31-P-A8	40
9ch	265	2-R4-A1Z	40	329	A1-P1N-D9	10	393	2-P4-A1Z	40	585	31-P-A9	40
10ch	266	2-RR-A1X	40	330	A1-P1N-D10	10	394	2-PR-A1X	40	586	31-P-A10	40
11ch	267	2-RR-A1Y	40	331	A1-P3N-D11	20	395	2-PR-A1Y	40	587	31-P-A11	40
12ch	268	2-RR-A1Z	40	332	A1-P3N-D12	20	396	2-PR-A1Z	40	588	31-P-A12	40
13ch	269	3-R1-D1XT	10+1	333	A1-P3N-D13	20	397	3-P1-D1XT	10+1	589	31-P-A13	40
14ch	270	3-R1-D1XB	10+1	334	A1-P3N-D14	20	398	3-P1-D1XB	10+1	590	31-P-A14	40
15ch	271	3-R1-D1YT	10+1	335	A1-P4N-D15	30	399	3-P1-D1YT	10+1	591	31-P-A15	40
16ch	272	3-R1-D1YB	10+1	336	A1-P4N-D16	30	400	3-P1-D1YB	10+1	592	31-P-A16	40
17ch	273	3-R2-D1XT	10+5	337			401	3-P2-D1XT	10+5	593	31-P-A17	40
18ch	274	3-R2-D1XB	10+5	338			402	3-P2-D1XB	10+5	594	31-P-A18	40
19ch	275	3-R2-D1YT	10+5	339			403	3-P2-D1YT	10+5	595	31-P-A19	40
20ch	276	3-R2-D1YB	10+5	340			404	3-P2-D1YB	10+5	596	31-P-A20	40
21ch	277	3-R3-D1XT	10+5	341	2-P1-A1X	20	405	3-P3-D1XT	10+5	597	31-P-A21	40
22ch	278	3-R3-D1XB	10+5	342	2-P1-A1Y	20	406	3-P3-D1XB	10+5	598	31-P-A22	40
23ch	279	3-R3-D1YT	10+5	343	2-P1-A1Z	20	407	3-P3-D1YT	10+5	599	31-P-A23	40
24ch	280	3-R3-D1YB	10+5	344	2-P1-A2X	30	408	3-P3-D1YB	10+5	600	31-P-A24	40
25ch	281	3-R4-D1XT	10+5	345	2-P1-A2Y	30	409	3-P4-D1XT	10+5	601	31-P-A25	40
26ch	282	3-R4-D1XB	10+5	346	2-P1-A2Z	30	410	3-P4-D1XB	10+5	602	31-P-A26	40
27ch	283	3-R4-D1YT	10+5	347	2-R1-A1X	30	411	3-P4-D1YT	10+5	603	31-P-A27	40
28ch	284	3-R4-D1YB	10+5	348	2-R1-A1Y	30	412	3-P4-D1YB	10+5	604	31-P-A28	40
29ch	285	3Z-R1-D1Z	30	349	2-R1-A1Z	30	413	3Z-P1-D1Z	30	605	31-P-A29	40
30ch	286	3Z-R1-D2Z	30	350	2-R1-A2X	40	414	3Z-P1-D2Z	30	606	31-P-A30	40
31ch	287	3Z-R2-D1Z	30	351	2-R1-A2Y	40	415	3Z-P2-D1Z	30	607	31-P-A31	40
32ch	288	3Z-R2-D2Z	30	352	2-R1-A2Z	40	416	3Z-P2-D2Z	30	608	32-P-S1	40
33ch	289	3Z-R3-D1Z	30	353			417	3Z-P3-D1Z	30	609	32-P-S2	40
34ch	290	3Z-R3-D2Z	40	354			418	3Z-P3-D2Z	40	610	32-P-S3	40
35ch	291	3Z-R4-D1Z	40	355			419	3Z-P4-D1Z	40	611	32-P-S4	40
36ch	292	3Z-R4-D2Z	40	356			420	3Z-P4-D2Z	40	612	32-P-S5	40
37ch	293	4-R1-D2XT	30	357			421	4-P1-D2XT	30	613	32-P-S6	40
38ch	294	4-R1-D2XB	30	358			422	4-P1-D2XB	30	614	32-P-S7	40
39ch	295	4-R1-D2YT	30	359			423	4-P1-D2YT	30	615	32-P-S8	40
40ch	296	4-R1-D2YB	30	360			424	4-P1-D2YB	30	616	32-P-S9	40
41ch	297	4-R1-D3XT	30	361			425	4-P1-D3XT	30	617	32-P-S10	40
42ch	298	4-R1-D3XB	30	362			426	4-P1-D3XB	30	618	32-P-S11	40
43ch	299	4-R1-D3YT	30	363			427	4-P1-D3YT	30	619	32-P-S12	40
44ch	300	4-R1-D3YB	30	364			428	4-P1-D3YB	30	620	32-P-S13	40
45ch	301	4-R2-D2XT	30	365			429	4-P2-D2XT	30	621	32-P-S14	40
46ch	302	4-R2-D2XB	30	366			430	4-P2-D2XB	30	622	32-P-S15	40
47ch	303	4-R2-D2YT	30	367			431	4-P2-D2YT	30	623	32-P-S16	40
48ch	304	4-R2-D2YB	30	368			432	4-P2-D2YB	30	624	32-P-S17	40
49ch	305	4-R2-D3XT	30	369			433	4-P2-D3XT	30	625	32-P-S18	40
50ch	306	4-R2-D3XB	30	370			434	4-P2-D3XB	30	626	32-P-S19	40
51ch	307	4-R2-D3YT	30	371			435	4-P2-D3YT	30	627	32-P-S20	40
52ch	308	4-R2-D3YB	30	372			436	4-P2-D3YB	30	628	32-P-S21	40
53ch	309	4-R3-D2XT	40	373			437	4-P3-D2XT	40	629	32-P-S22	40
54ch	310	4-R3-D2XB	40	374			438	4-P3-D2XB	40	630	32-P-S23	40
55ch	311	4-R3-D2YT	40	375			439	4-P3-D2YT	40	631	32-P-S24	40
56ch	312	4-R3-D2YB	40	376			440	4-P3-D2YB	40	632	32-P-S25	40
57ch	313	4-R3-D3XT	40	377			441	4-P3-D3XT	40	633	32-P-S26	40
58ch	314	4-R3-D3XB	40	378			442	4-P3-D3XB	40	634	32-P-S27	40
59ch	315	4-R3-D3YT	40	379			443	4-P3-D3YT	40	635		
60ch	316	4-R3-D3YB	40	380			444	4-P3-D3YB	40	636		
61ch	317	4-R4-D2XT	40	381			445	4-P4-D2XT	40	637		
62ch	318	4-R4-D2XB	40	382			446	4-P4-D2XB	40	638		
63ch	319	4-R4-D2YT	40	383			447	4-P4-D2YT	40	639		
64ch	320	4-R4-D2YB	40	384			448	4-P4-D2YB	40	640		

チャンネル		JB11			JB12			JB13			JB14			JB15
		マルチアンプ			マルチアンプ			マルチアンプ			マルチアンプ			マルチアンプ
		名称	長さ		名称	長さ		名称	長さ		名称	長さ		名称
1ch	641	2-P2-A2X	30	705	5X-P1-DB3T	30	769	31-R-A1	40	833	2-R2-A2X	30	897	Target X
2ch	642	2-P2-A2Y	30	706	5X-P2-DB3B	30	770	31-R-A2	40	834	2-R2-A2Y	30	898	Target Y
3ch	643	2-P2-A2Z	30	707	5X-P2-DB3T	30	771	31-R-A3	40	835	2-R2-A2Z	30	899	Target Z
4ch	644	2-P3-A2X	30	708	5X-P3-DB3B	30	772	31-R-A4	40	836	2-R3-A2X	30	900	Target Roll
5ch	645	2-P3-A2Y	30	709	5X-P3-DB3T	30	773	31-R-A5	40	837	2-R3-A2Y	30	901	Target Pitch
6ch	646	2-P3-A2Z	30	710	5X-P4-DB3B	40	774	31-R-A6	40	838	2-R3-A2Z	30	902	Target Yaw
7ch	647	2-P4-A2X	40	711	5X-P4-DB3T	40	775	31-R-A7	40	839	2-R4-A2X	40	903	Acc ref X
8ch	648	2-P4-A2Y	40	712	5X-PR-DB3B	40	776	31-R-A8	40	840	2-R4-A2Y	40	904	Acc ref Y
9ch	649	2-P4-A2Z	40	713	5X-P1-DC3T	30	777	31-R-A9	40	841	2-R4-A2Z	40	905	Acc ref Z
10ch	650	2-PR-A2X	40	714	5X-P2-DC3B	30	778	31-R-A10	40	842	2-RR-A2X	40	906	Acc ref Roll
11ch	651	2-PR-A2Y	40	715	5X-P2-DC3T	30	779	31-R-A11	40	843	2-RR-A2Y	40	907	Acc ref Pitch
12ch	652	2-PR-A2Z	40	716	5X-P3-DC3B	30	780	31-R-A12	40	844	2-RR-A2Z	40	908	Acc ref Yaw
13ch	653	1-PL1	40	717	5X-P3-DC3T	30	781	31-R-A13	40	845	9X-R0-DB1T	30	909	Acc fbk X
14ch	654	1-PL2	40	718	5X-P4-DC3B	40	782	31-R-A14	40	846	9X-R0-DB1B	30	910	Acc fbk Y
15ch	655	7-P1-DC3aNE	30	719	5X-P4-DC3T	40	783	31-R-A15	40	847	9X-R0-DC1T	30	911	Acc fbk Z
16ch	656	7-P1-DC3aSE	30	720	5X-PR-DC3B	40	784	31-R-A16	40	848	9X-R0-DC1B	30	912	Acc fbk Roll
17ch	657	7-P1-DC3aSW	30	721	5Y-P1-DB3T	30	785	31-R-A17	40	849	9Y-R0-DB1T	30	913	Acc fbk Pitch
18ch	658	7-P1-DC3aNW	30	722	5Y-P2-DB3B	30	786	31-R-A18	40	850	9Y-R0-DB1B	30	914	Acc fbk Yaw
19ch	659	7-P2-DC3aNE	30	723	5Y-P2-DB3T	30	787	31-R-A19	40	851	9Y-R0-DC1T	30	915	Vel fbk X
20ch	660	7-P2-DC3aSE	30	724	5Y-P3-DB3B	30	788	31-R-A20	40	852	9Y-R0-DC1B	30	916	Vel fbk Y
21ch	661	7-P2-DC3aSW	30	725	5Y-P3-DB3T	30	789	31-R-A21	40	853	9Y-R0-DC1aT	30	917	Vel fbk Z
22ch	662	7-P2-DC3aNW	30	726	5Y-P4-DB3B	40	790	31-R-A22	40	854	9Y-R0-DC1aB	30	918	Vel fbk Roll
23ch	663	7-P3-DC3aNE	30	727	5Y-P4-DB3T	40	791	31-R-A23	40	855	10-R1-DC3aNE	30	919	Vel fbk Pitch
24ch	664	7-P3-DC3aSE	30	728	5Y-PR-DB3B	40	792	31-R-A24	40	856	10-R1-DC3aSE	30	920	Vel fbk Yaw
25ch	665	7-P3-DC3aSW	30	729	5Y-P1-DC3T	30	793	31-R-A25	40	857	10-R1-DC3aSW	30	921	Dis fbk X
26ch	666	7-P3-DC3aNW	30	730	5Y-P2-DC3B	30	794	31-R-A26	40	858	10-R1-DC3aNW	30	922	Dis fbk Y
27ch	667	7-P4-DC3aNE	40	731	5Y-P2-DC3T	30	795	31-R-A27	40	859			923	Dis fbk Z
28ch	668	7-P4-DC3aSE	40	732	5Y-P3-DC3B	30	796	31-R-A28	40	860	ACC-X		924	Dis fbk Roll
29ch	669	7-P4-DC3aSW	40	733	5Y-P3-DC3T	30	797	31-R-A29	40	861	ACC-Y		925	Dis fbk Pitch
30ch	670	7-P4-DC3aNW	40	734	5Y-P4-DC3B	40	798	31-R-A30	40	862	ACC-Z		926	Dis fbk Yaw
31ch	671	8-P1-DC3aY	30	735	5Y-P4-DC3T	40	799	31-R-A31	40	863	PLUS		927	Force fbk X
32ch	672	8-P2-DC3aY	30	736	5Y-PR-DC3B	40	800	31-R-A32	40	864	ATURYOKU		928	Force fbk Y
33ch	673	8-P3-DC3aY	30	737	5Y-P1-DC3aT	30	801	31-R-A33	40				929	Force fbk Z
34ch	674	8-P4-DC3aY	40	738	5Y-P2-DC3aB	30	802	31-R-A34	40				930	Force fbk Roll
35ch	675	22-P-S1	30	739	5Y-P2-DC3aT	30	803	31-R-A35	40				931	Force fbk Pitch
36ch	676	22-P-S2	30	740	5Y-P3-DC3aB	30	804	31-R-A36	40				932	Force fbk Yaw
37ch	677	22-P-S3	30	741	5Y-P3-DC3aT	30	805	31-R-A37	40				933	Dis fbk X1
38ch	678	22-P-S4	30	742	5Y-P4-DC3aB	40	806	31-R-A38	40		EDX		934	Dis fbk X5
39ch	679	23-P-S1	30	743	5Y-P4-DC3aT	40	807	31-R-A39	40		専用アンプ		935	Dis fbk Y1
40ch	680	23-P-S2	30	744	5Y-PR-DC3aB	40	808	32-R-S1	40		名称	長さ	936	Dis fbk Y5
41ch	681	24-P-S1	30	745	6-P1-DB3N	30	809	32-R-S2	40	1	A4-P1-D1	30	937	Dis fbk Z1
42ch	682	24-P-S2	30	746	6-P1-DB3E	30	810	32-R-S3	40	2	A4-P1-D2	30	938	Dis fbk Z4
43ch	683			747	6-P1-DB3S	30	811	32-R-S4	40	3	A4-P1-D3	30	939	Dis fbk Z8
44ch	684			748	6-P1-DB3W	30	812	32-R-S5	40	4	A4-P1-D4	30	940	Dis fbk Z11
45ch	685	A1-P1S-D1	10	749	6-P1-DC3N	30	813	32-R-S6	40	5	A4-P1-D5	30	941	A. Acc fbk X1
46ch	686	A1-P1S-D2	10	750	6-P1-DC3E	30	814	32-R-S7	40	6	A4-P1-D6	30	942	A. Acc fbk X2
47ch	687	A1-P1S-D3	10	751	6-P1-DC3S	30	815	32-R-S8	40	7	A4-P1-D7	30	943	A. Acc fbk X3
48ch	688	A1-P1S-D4	10	752	6-P1-DC3W	30	816	32-R-S9	40	8	A4-P1-D8	30	944	A. Acc fbk X4
49ch	689	A1-P1S-D5	10	753			817	32-R-S10	40	9	A4-P1-D9	30	945	A. Acc fbk X5
50ch	690	A1-P1S-D6	10	754			818	32-R-S11	40	10	A4-P1-D10	30	946	A. Acc fbk Y1
51ch	691	A1-P1S-D7	10	755	11-P0-D1Y	30	819	32-R-S12	40	11	A4-P1-D11	30	947	A. Acc fbk Y2
52ch	692	A1-P1S-D8	10	756	11-P0-D2X	10	820	32-R-S13	40	12	A4-P1-D12	30	948	A. Acc fbk Y3
53ch	693	A1-P1S-D9	10	757	11-P0-D2Y	10	821	32-R-S14	40	13	A4-P1-D13	30	949	A. Acc fbk Y4
54ch	694	A1-P1S-D10	10	758	11Z-P0-D1Z	10	822	32-R-S15	40	14	A4-P1-D14	30	950	A. Acc fbk Y5
55ch	695	A1-R1S-D1	30	759	11Z-P0-D2Z	10	823	32-R-S16	40	15	A2-P1S-D1	10→40	951	A. Acc fbk Z1
56ch	696	A1-R1S-D2	30	760	11-R0-D1Y	30	824	32-R-S17	40	16	A2-P1S-D2	10→40	952	A. Acc fbk Z2
57ch	697	A1-R1S-D3	30	761	11-R0-D2X	10	825	32-R-S18	40	17	A2-P1S-D3	10→40	953	A. Acc fbk Z3
58ch	698	A1-R1S-D4	30	762	11-R0-D2Y	10	826	32-R-S19	40	18	A2-P1S-D4	10→40	954	A. Acc fbk Z4
59ch	699	A1-R1S-D5	30	763	11Z-R0-D1Z	30	827	32-R-S20	40	19	A2-R1S-D1	20→40	955	A. Acc fbk Z5
60ch	700	A1-R1S-D6	30	764	11Z-R0-D2Z	30	828	32-R-S21	40	20	A2-R1S-D2	20→40	956	
61ch	701	A1-R1S-D7	30	765			829	32-R-S22	40	21	A2-R1S-D3	20→40	957	
62ch	702	A1-R1S-D8	30	766			830	32-R-S23	40	22	A2-R1S-D4	20→40	958	
63ch	703	A1-R1S-D9	30	767			831	32-R-S24	40				959	
64ch	704	A1-R1S-D10	30	768			832	33-R-D1	40				960	

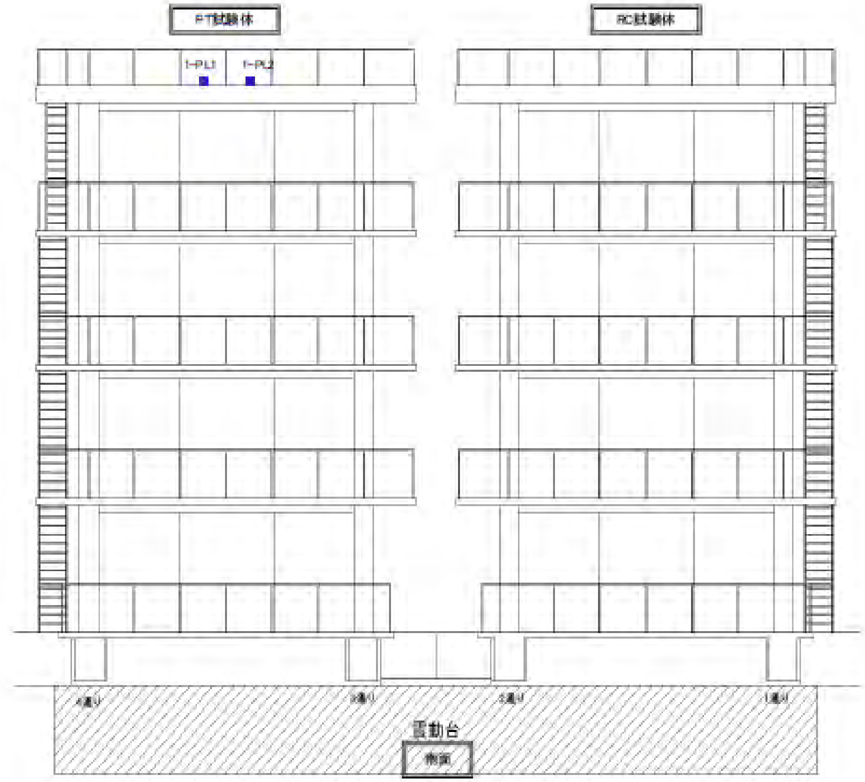

センサ名称	センサタグ	計測機器	合計点数
■:壁ワイヤ	1−PL*	センターホールロードセル	2台＝2ch(PC2ch)

・PT試験体取付ロードセルからの計測

1 壁ワイヤ 設置位置図

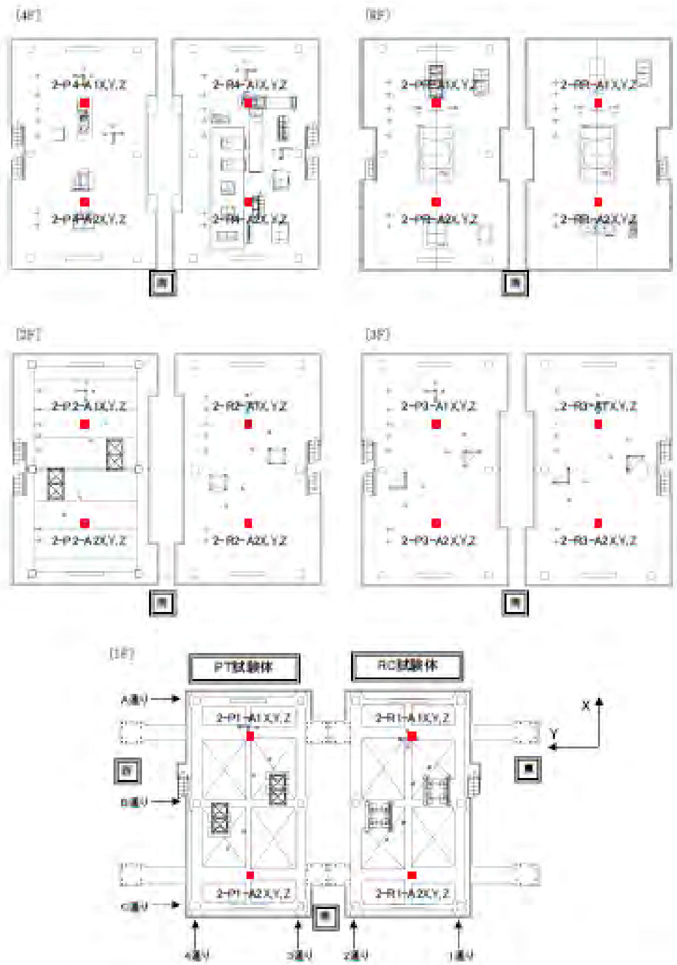

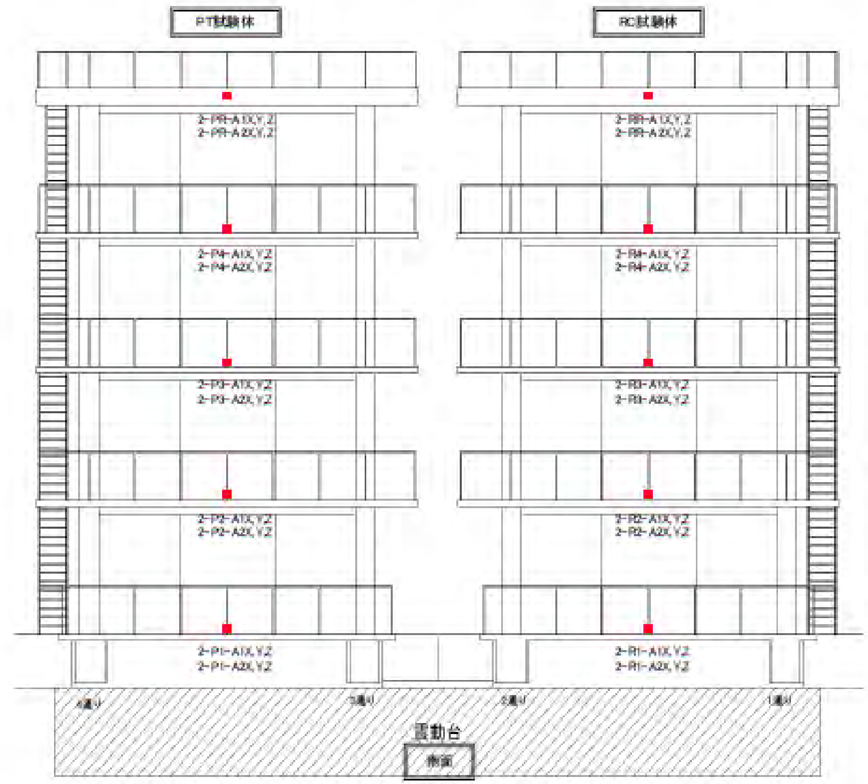

センサ名称	センサタグ	計測機器	合計点数
■ 2層加速度計3方向	2-P*-A#X,Y,Z	TA-25E-10-1(トキメック)	20台×3方向＝60ch(PC30ch,RC30ch)

・各部屋柱位置から中心点に設置

2層加速度計 設置位置図

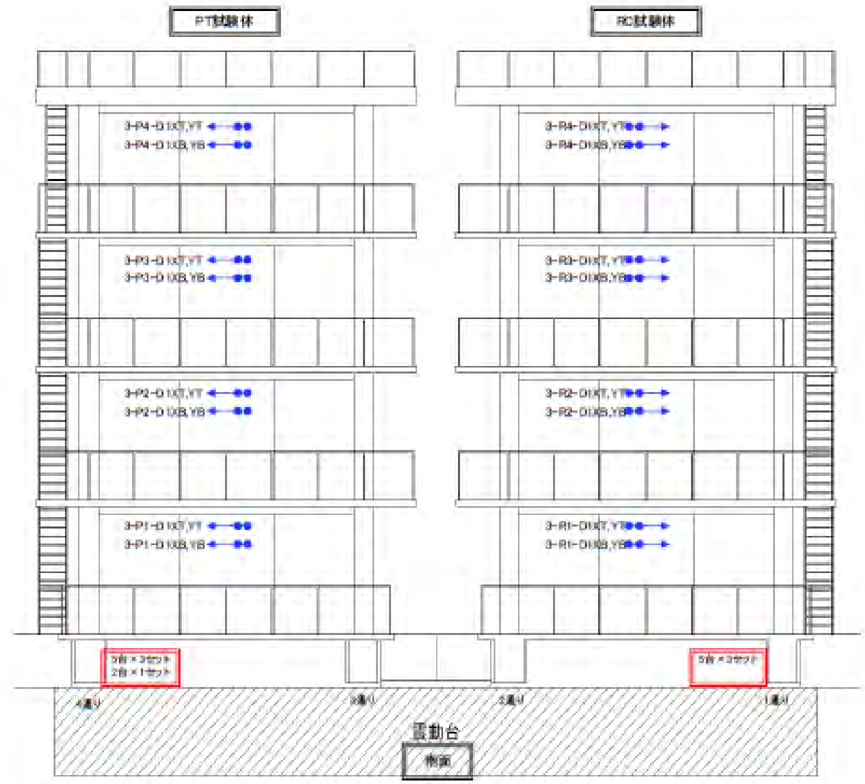

センサ名称	センサタグ	計測機器	合計点数
● 3層間変位(レーザー変位形)	3-P*-D*X,Y T,B	LK-500(KEYENCE)	32台=32ch(PC16ch,RC16ch)

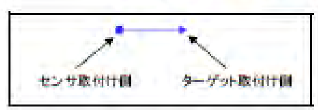

- ・□ ･･･レーザー変位形用アンプ
- ・RC試験体3-R1-D1XBのみPC試験体側のアンプへ接続
- ・LK-500のセンサとターゲット間は約500mmに設定
- ・3-P1-D1YT,B, 3-P2-D1YT,B, 3-P3-D1YT,B, 3-P4-D1YT,Bは位相反転

3 層間変位(レーザー変位形) 設置位置図

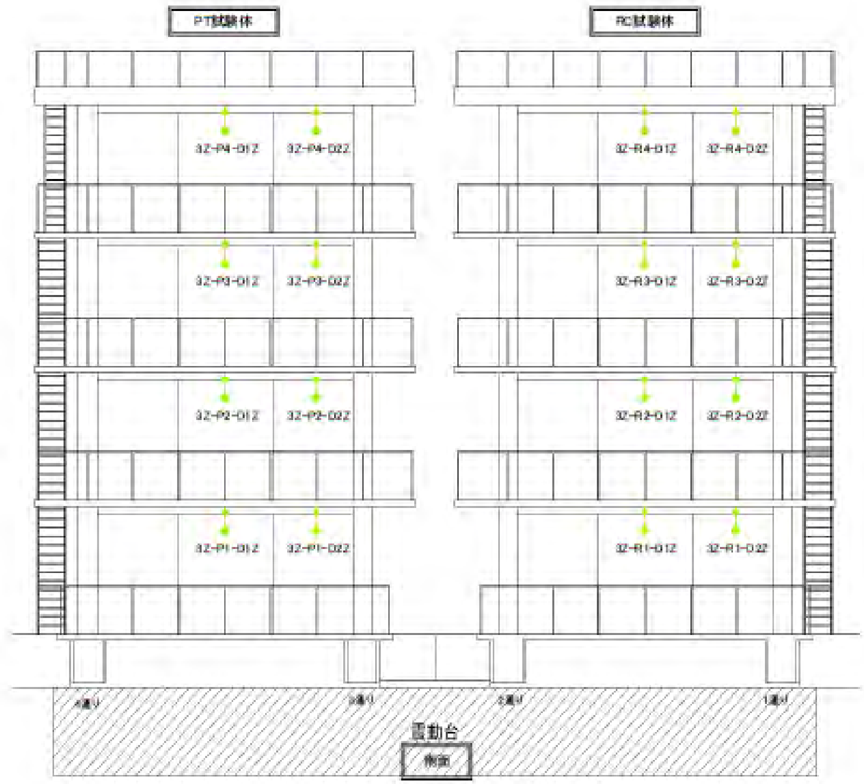

センサ名称	センサタグ	計測機器	合計点数
● :3Z層間鉛直変位(CDP変位形)	3Z-P*-D*Z	DTH-A-100(共和電業)	16台＝16ch(PC8ch, RC8ch)

・DTH-A-100センサは位相反転

3Z層間鉛直変位 設置位置図

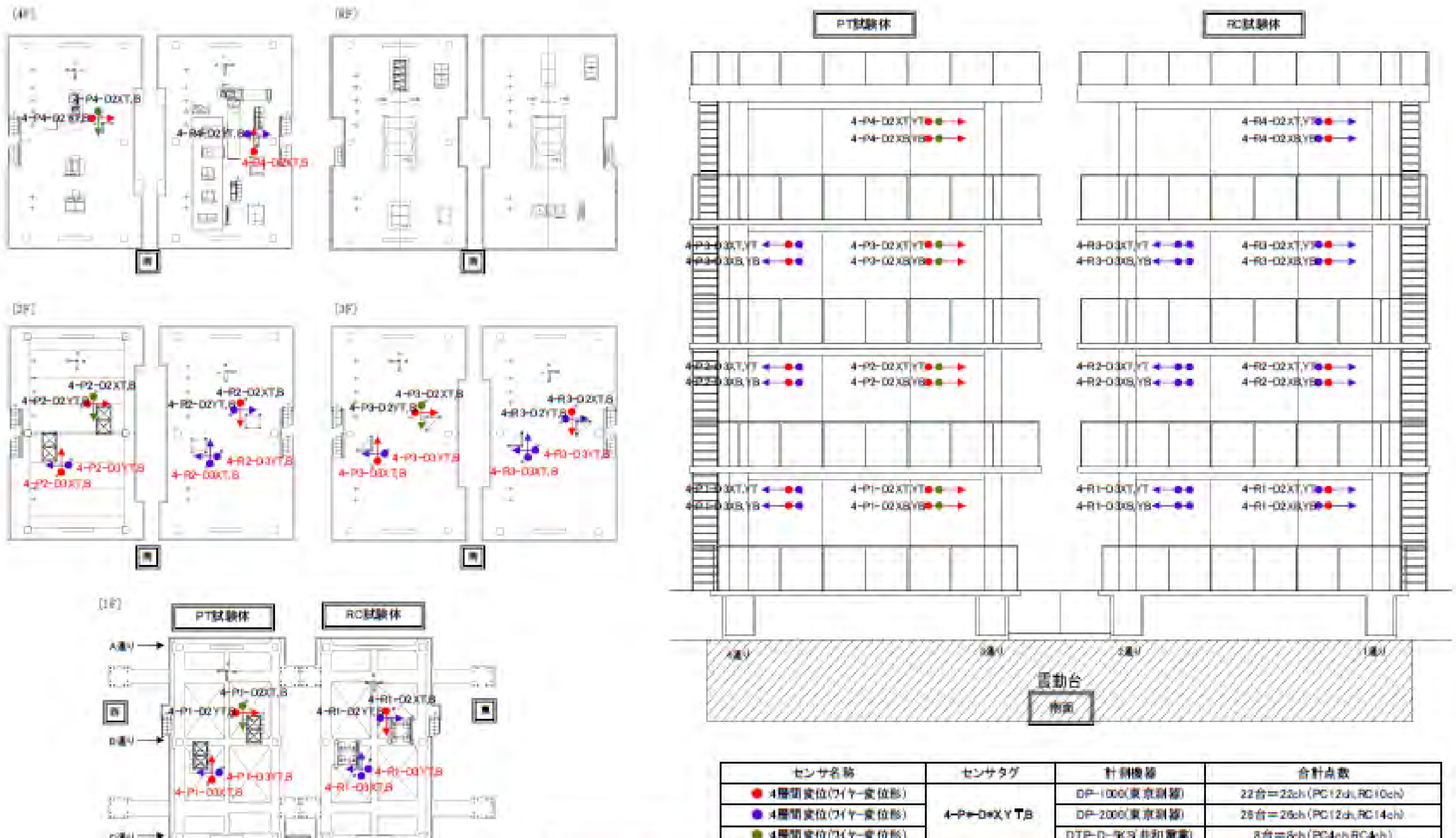

センサ名称	センサタグ	計測機器	合計点数
● 4層間変位(ワイヤー変位形)	4-P※-D※X,Y T,B	DP-1000(東京測器)	22台=22ch(PC12ch,RC10ch)
● 4層間変位(ワイヤー変位形)		DP-2000(東京測器)	26台=26ch(PC12ch,RC14ch)
● 4層間変位(ワイヤー変位形)		DTP-D-5KS(共和電業)	8台=8ch(PC4ch,RC4ch)

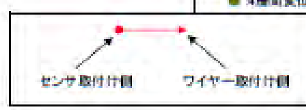

・4-P1-D3XT,B,D3YT,B、4-P2-D3XT,B,D3YT,B、4-P3-D3XT,B,D3YT,Bは位相反転

・4-R1-D3XT,B,D3YT,B、4-R2-D3XT,B,D3YT,B、4-R3-D3XT,B,D3YT,B、4-R4-D2XT,Bは位相反転

4 層間変位(ワイヤー変位形) 設置位置図

センサ名称	センサタグ	計測機器	合計点数
5XPT梁端変形(CDP変位形)	5X-P*-D**T,B	DTH-A-100(共和電業)	16台＝16ch(PC16ch)
5YPT梁端変形(ワイヤー変位形)	5Y-P*-D**T,B	DP-500(東京測器)	24台＝24ch(PC24ch)
9XRC梁端変形(ワイヤー変位形)	9X-P*-D**T,B	DP-500(東京測器)	4台＝4ch(RC4ch)
9YRC梁端変形(ワイヤー変位形)	9Y-P*-D**T,B	DTP-D-2KS(共和電業)	6台＝6ch(RC6ch)

・DTH-A-100センサは位相反転

5XPT梁端変形　5YPT梁端変形　9XRC梁端変形　9YRC梁端変形 設置位置図

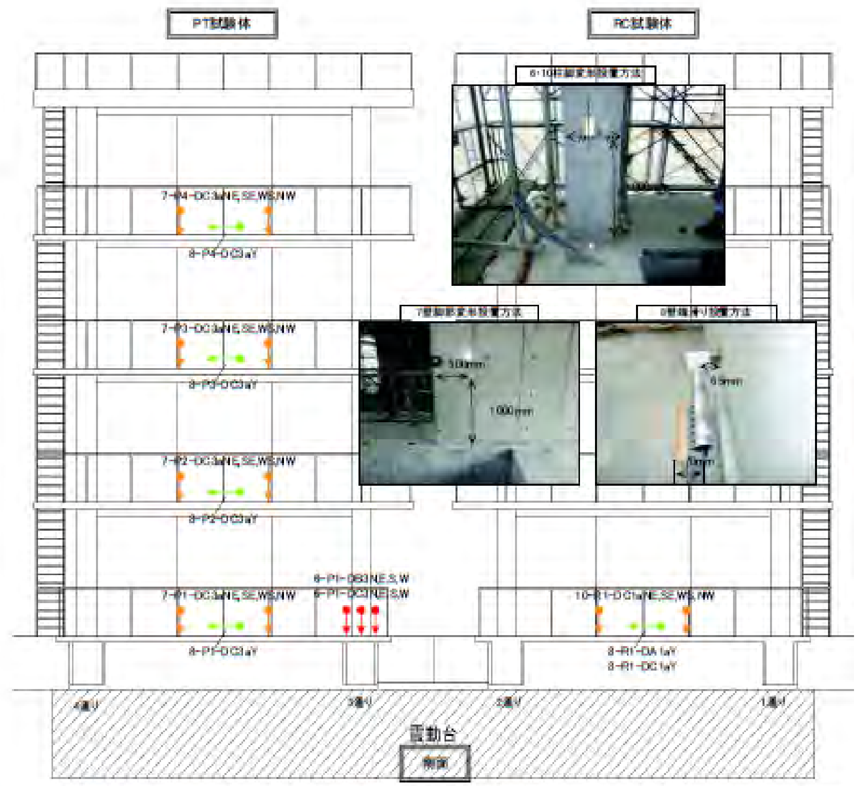

センサ名称	センサタグ	計測機器	合計点数
● 6PT柱脚変形(ワイヤー変位形)	6-P1-D***	DP-500(東京測器)	8台=8ch(PC8ch)
● 7PT壁脚部変形(ワイヤー変位形)	7-P*-DC3a**	DTP-D-300(共和電業)	16台=16ch(PC16ch)
● 8壁端滑り(CDP変位形)	8-**-DC*aY	DTH-A-100(共和電業)	5台=5ch(PC4ch,RC1ch)
● 8壁端滑り(CDP変位形)	8-R1-DA1aY	CDP-50(東京測器)	1台=1ch(RC1ch)
● 10RC壁脚部変形(ワイヤー変位形)	10-R1-DC1a**	DTP-D-300(共和電業)	4台=4ch(RC4ch)

・DTH-A-100センサは位相反転

6PT柱脚変形 7PT壁脚部変形 8PT壁端滑り 10RC壁脚部変形 設置位置図

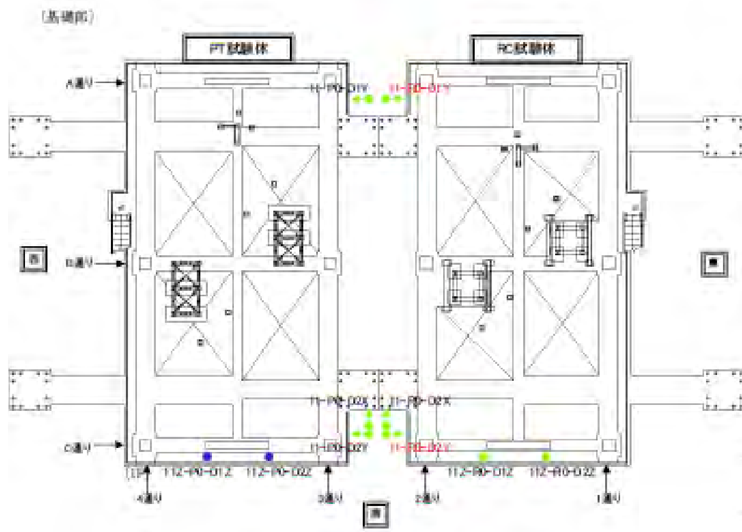

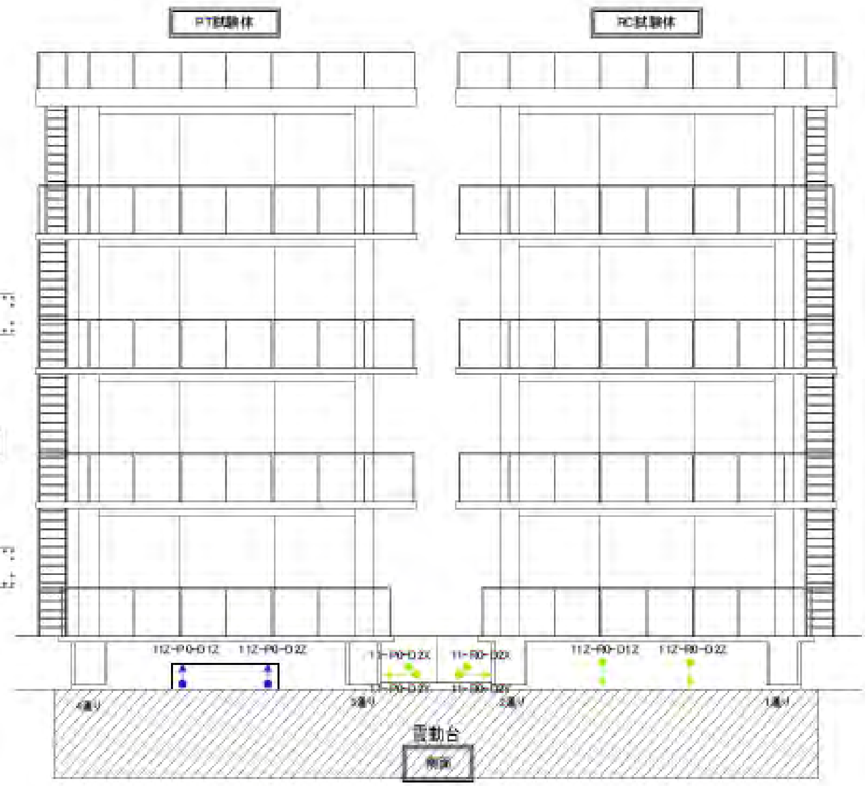

センサ名称	センサタグ	計測機器	合計点数
11基礎滑り(CDP変位形)	11-P0-D*X,Y	DTH-A-100(共和電業)	6台＝6ch（PC3ch,RC3ch）
11Z基礎浮き上がり(CDP変位形)	11Z-R0-D*Z	DTH-A-100(共和電業)	2台＝2ch（RC2ch）
11Z基礎浮き上がり(CDP変位形)	11Z-P0-D*Z	CDP-25(東京測器)	2台＝2ch（PC2ch）

・DTH-A-100センサは位相反転

・11-R0-D1Y，11-R0-D2Yは位相反転

11基礎滑り　11Z基礎浮き上がり 設置位置図

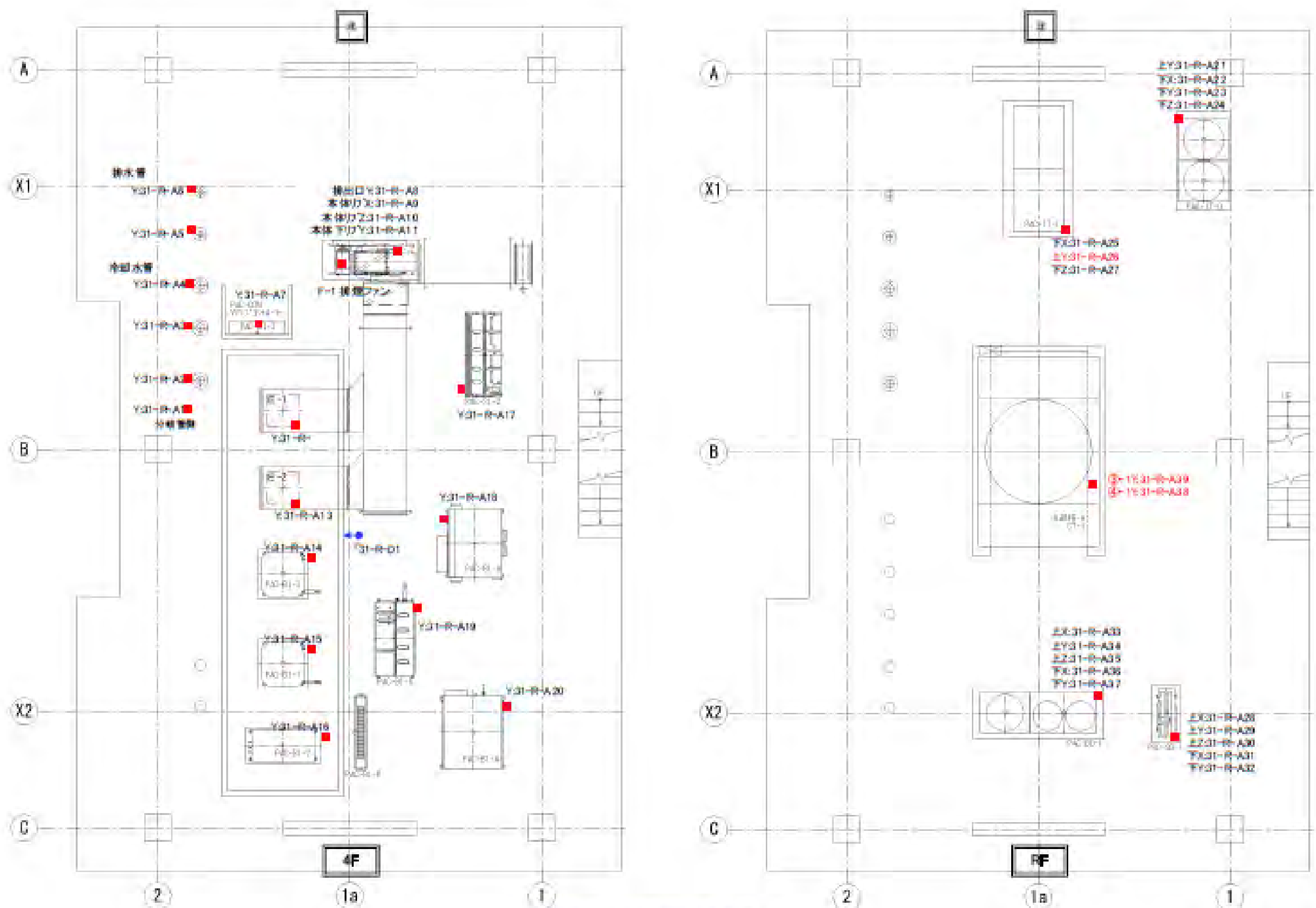

RC試験体ー設備機器設置位置

詳細は添付写真に記載

PT試験体-設備機器設置位置

詳細は添付写真に記載

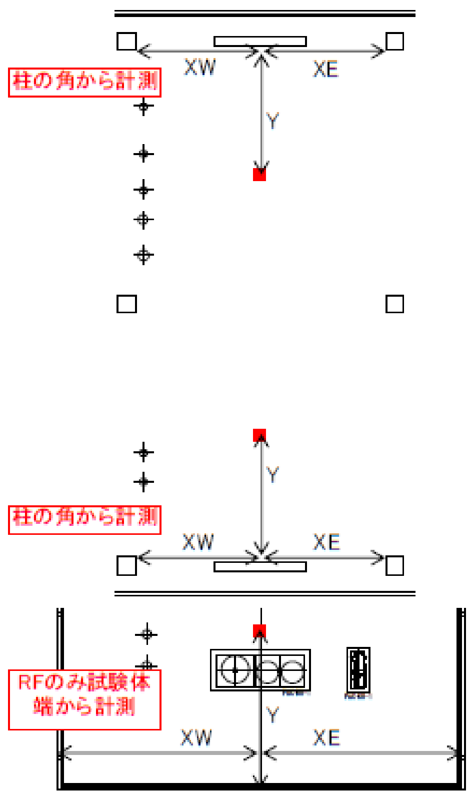

計測位置

センサータグ	寸法計測点 XW	XE	Y	センサータグ	寸法計測点 XW	XE	Y
2-P1-A1X	3375	3375	1850	2-R1-A1X	3180	3220	2075
2-P1-A1Y				2-R1-A1Y			
2-P1-A1Z				2-R1-A1Z			
2-P2-A1X	3374	3375	3480	2-R2-A1X	3351	3350	4381
2-P2-A1Y				2-R2-A1Y			
2-P2-A1Z				2-R2-A1Z			
2-P3-A1X	3376	3374	3483	2-R3-A1X	3350	3352	4383
2-P3-A1Y				2-R3-A1Y			
2-P3-A1Z				2-R3-A1Z			
2-P4-A1X	3375	3375	3050	2-R4-A1X	3348	3351	3410
2-P4-A1Y				2-R4-A1Y			
2-P4-A1Z				2-R4-A1Z			
2-PR-A1X	5025（端より）	5025（端より）	3505（端より）	2-RR-A1X	5010（端より）	5010（端より）	4300（端より）
2-PR-A1Y				2-RR-A1Y			
2-PR-A1Z				2-RR-A1Z			
2-P1-A2X	3375	3375	1780	2-R1-A2X	3180	3220	1725
2-P1-A2Y				2-R1-A2Y			
2-P1-A2Z				2-R1-A2Z			
2-P2-A2X	3373	3376	4378	2-R2-A2X	3347	3352	4376
2-P2-A2Y				2-R2-A2Y			
2-P2-A2Z				2-R2-A2Z			
2-P3-A2X	3376	3375	7382	2-R3-A2X	3350	3351	4380
2-P3-A2Y				2-R3-A2Y			
2-P3-A2Z				2-R3-A2Z			
2-P4-A2X	3375	3375	3050	2-R4-A2X	3353	3347	3500
2-P4-A2Y				2-R4-A2Y			
2-P4-A2Z				2-R4-A2Z			
2-PR-A2X	5025（端より）	5025（端より）	3505（端より）	2-RR-A2X	5010（端より）	5010（端より）	4303（端より）
2-PR-A2Y				2-RR-A2Y			
2-PR-A2Z				2-RR-A2Z			

２ 層加速度計ー寸法計測

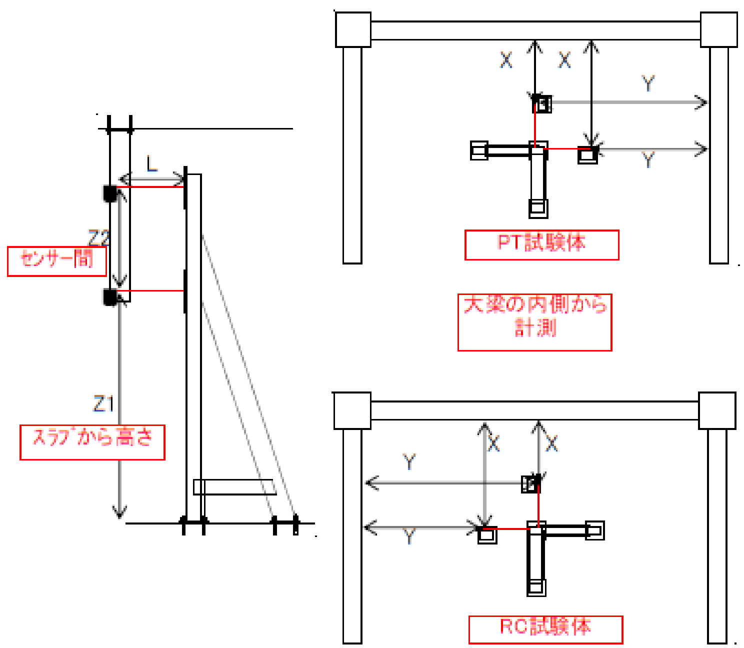

計測位置

センサータグ	寸法計測点				
	L	Z1	Z2	X	Y
3-P1-D1XT	501		750	1020	3494
3-P1-D1XB	502	1640		1020	3494
3-P1-D1YT	502		750	1025	2905
3-P1-D1YB	501	1800		1025	2905
3-P2-D1XT	499		750	1040	3490
3-P2-D1XB	501	1650		1040	3490
3-P2-D1YT	501		750	1770	2910
3-P2-D1YB	500	1795		1770	2910
3-P3-D1XT	499		750	1105	3470
3-P3-D1XB	501	1635		1100	3470
3-P3-D1YT	500		750	1800	2840
3-P3-D1YB	500	1775		1800	2840
3-P4-D1XT	501		745	1105	3470
3-P4-D1XB	500	1645		1105	3470
3-P4-D1YT	500		755	1800	2840
3-P4-D1YB	501	1785		1800	2840
3-R1-D1XT	500		755	1920	3420
3-R1-D1XB	499	1610		1920	3420
3-R1-D1YT	500		750	2590	4000
3-R1-D1YB	500	1758		2590	4000
3-R2-D1XT	499		743	3490	1900
3-R2-D1XB	500	1635		3490	1906
3-R2-D1YT	503		747	2900	2630
3-R2-D1YB	502	1768		2900	2620
3-R3-D1XT	500		745	3490	1907
3-R3-D1XB	501	1615		3490	1910
3-R3-D1YT	502		747	2900	2640
3-R3-D1YB	503	1765		2900	2640
3-R4-D1XT	501		745	3500	680
3-R4-D1XB	502	1570		3500	680
3-R4-D1YT	499		746	2890	1420
3-R4-D1YB	499	1729		2890	1420

3 層間変位(レーザー変位形)-寸法計測

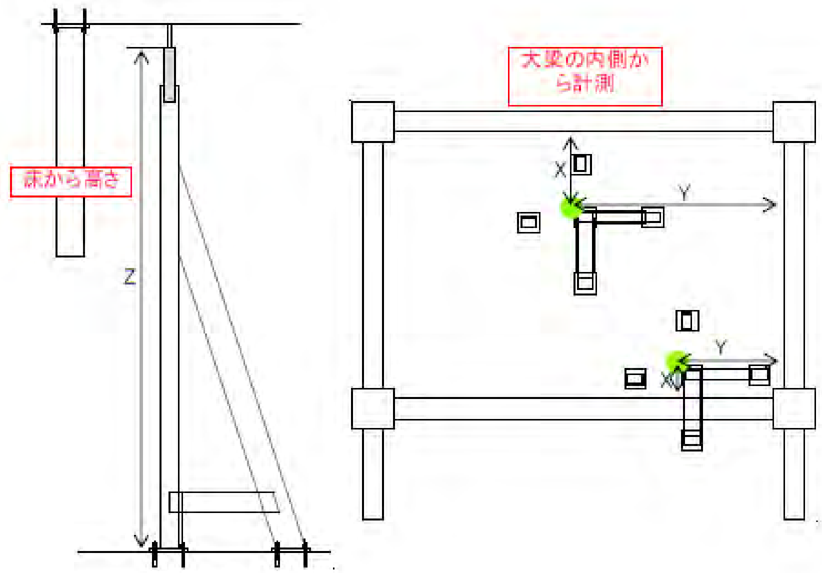

センサータグ	寸法計測点		
	Z	X	Y
3Z-P1-D1Z	2770	1740	3510
3Z-P1-D2Z	2780	1910	2050
3Z-P2-D1Z	2780	1710	3620
3Z-P2-D2Z	2780	1940	2030
3Z-P3-D1Z	2750	1780	3490
3Z-P3-D2Z	2760	1100	1370
3Z-P4-D1Z	2770	1780	3490
3Z-P4-D2Z	2790	1095	1410
3Z-R1-D1Z	2760	2530	3310
3Z-R1-D2Z	2750	1080	1660
3Z-R2-D1Z	2778	2505	3310
3Z-R2-D2Z	2778	1070	1650
3Z-R3-D1Z	2760	2530	3310
3Z-R3-D2Z	2760	745	1382
3Z-R4-D1Z	2800	2271	3310
3Z-R4-D2Z	2780	230	920

計測位置

3Z 層間鉛直変位ー寸法計測

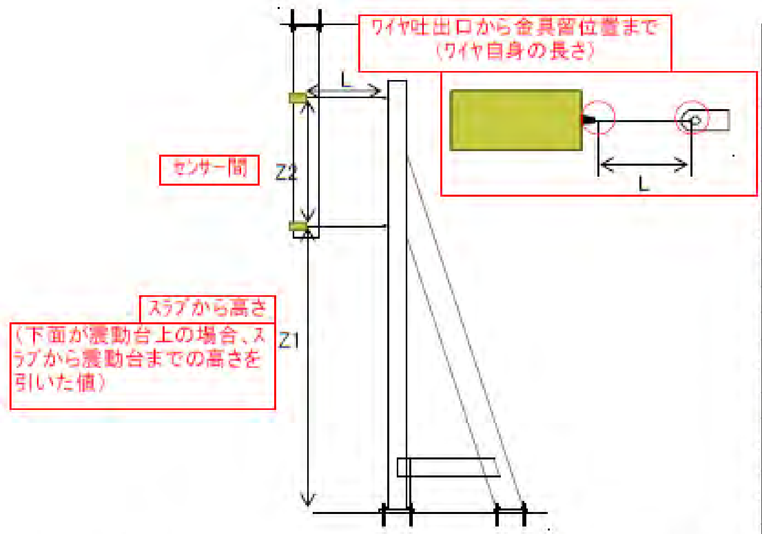

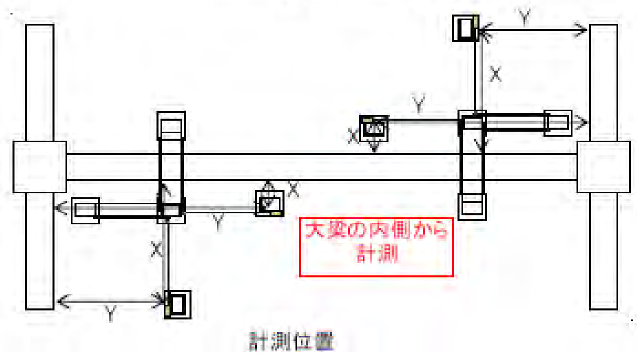

センサータグ	寸法計測点				
	L	Z1	Z2	X	Y
4-P1-D2XT	970		750	2885	1920
4-P1-D2XB	950	1770		2885	1920
4-P1-D2YT	1030		750	1850	3100
4-P1-D2YB	1050	1773		1850	3100
4-P1-D3XT	985		750	2965	1950
4-P1-D3XB	985	1750		2965	1950
4-P1-D3YT	995		750	1970	3055
4-P1-D3YB	995	1750		1970	3055
4-P2-D2XT	943		750	2870	1940
4-P2-D2XB	943	1762		2870	1940
4-P2-D2YT	1040		750	1830	3040
4-P2-D2YB	1030	1750		1830	3040
4-P2-D3XT	985		750	2930	1950
4-P2-D3XB	990	1745		2930	1950
4-P2-D3YT	1035		750	1850	3000
4-P2-D3YB	1015	1450		1850	3000
4-P3-D2XT	990		745	2220	4130
4-P3-D2XB	1040	1730		2220	4130
4-P3-D2YT	975		750	1120	2570
4-P3-D2YB	1065	1750		1120	2570
4-P3-D3XT	976		750	1120	2240
4-P3-D3XB	1073	1745		1120	2240
4-P3-D3YT	965		750	1135	2570
4-P3-D3YB	1013	1755		1135	2570
4-P4-D2XT	328		750	1700	1420
4-P4-D2XB	316	1745		1700	1420
4-P4-D2YT	407		750	1300	1940
4-P4-D2YB	398	1760		1300	1940

4-1 層間変位（ワイヤー変位形）PT棟-寸法計測

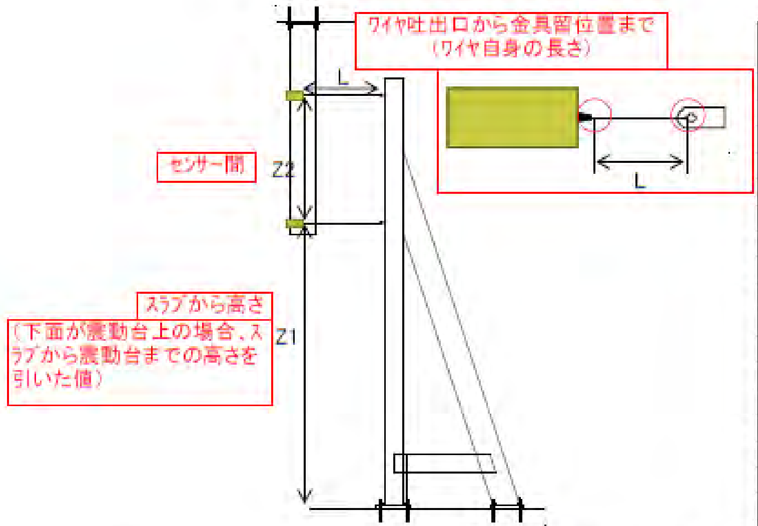

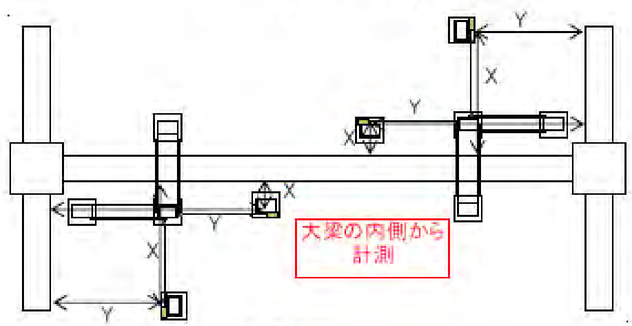

計測位置

センサータグ	寸法計測点				
	L	Z1	Z2	X	Y
4-R1-D2XT	980		745	2320	1900
4-R1-D2XB	980	1670		2320	1900
4-R1-D2YT	1035		750	1270	3000
4-R1-D2YB	1035	1670		1270	3000
4-R1-D3XT	1000		755	2320	2000
4-R1-D3XB	1000	1650		2320	2000
4-R1-D3YT	1040		750	1300	3050
4-R1-D3YB	1040	1650		1300	3050
4-R2-D2XT	1010		755	2400	1920
4-R2-D2XB	1010	1680		2400	1920
4-R2-D2YT	1025		750	1240	3000
4-R2-D2YB	1025	1680		1240	3000
4-R2-D3XT	990		755	2350	1900
4-R2-D3XB	995	1680		2350	1900
4-R2-D3YT	1045		755	1260	3050
4-R2-D3YB	1050	1680		1260	3050
4-R3-D2XT	1025		750	1875	1420
4-R3-D2XB	1065	1680		1875	1420
4-R3-D2YT	968		754	780	2570
4-R3-D2YB	980	1660		780	1565
4-R3-D3XT	1050		760	1860	1400
4-R3-D3XB	1050	1670		1860	1400
4-R3-D3YT	1050		755	760	2500
4-R3-D3YB	1050	1670		760	2500
4-R4-D2XT	673		740	290	1020
4-R4-D2XB	550	1695		280	1030
4-R4-D2YT	397		754	220	1540
4-R4-D2YB	405	1690		200	1550

4-2 層間変位（ワイヤー変位形）RC棟ー寸法計測

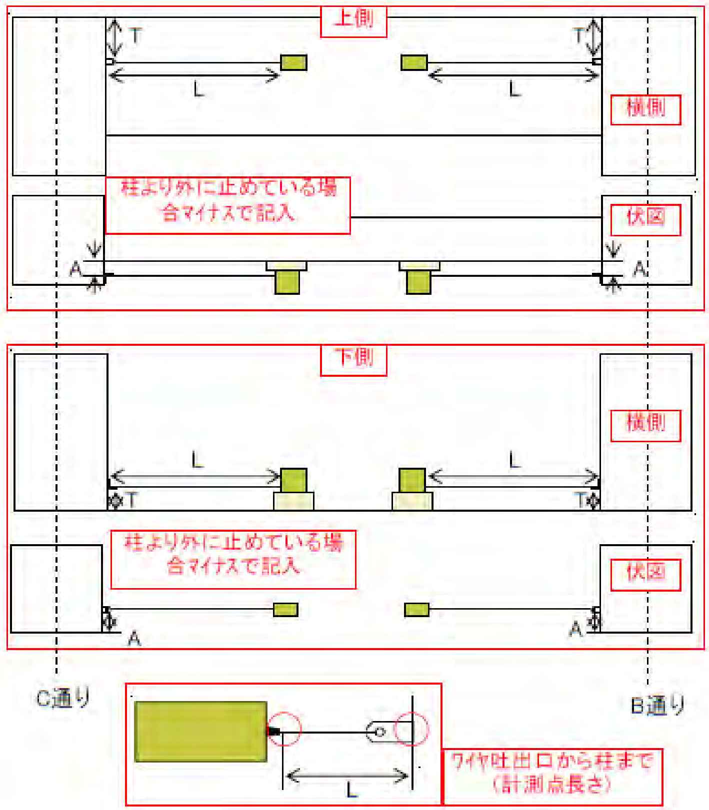

計測位置

センサータグ	寸法計測点		
	L	T	A
5X-P1-DB3T	1002	330	135
5X-P2-DB3B	750	60	10
5X-P2-DB3T	1002	331	136
5X-P3-DB3B	1010	140	-60
5X-P3-DB3T	1000	331	135
5X-P4-DB3B	1010	135	-55
5X-P4-DB3T	1001	330	-136
5X-PR-DB3B	1007	140	-50
5X-P1-DC3T	1015	325	-130
5X-P2-DC3B	1005	140	-50
5X-P2-DC3T	1006	325	135
5X-P3-DC3B	1010	130	-55
5X-P3-DC3T	1015	320	135
5X-P4-DC3B	1005	140	-50
5X-P4-DC3T	1006	325	135
5X-PR-DC3B	1015	115	-60
9X-R2-DB1T	940	70	40
9X-R3-DB1B	1005	65	35
9X-R2-DC1T	995	65	35
9X-R3-DC1B	1005	70	35

5XPT梁端変形　9XRC梁端変形ー寸法計測

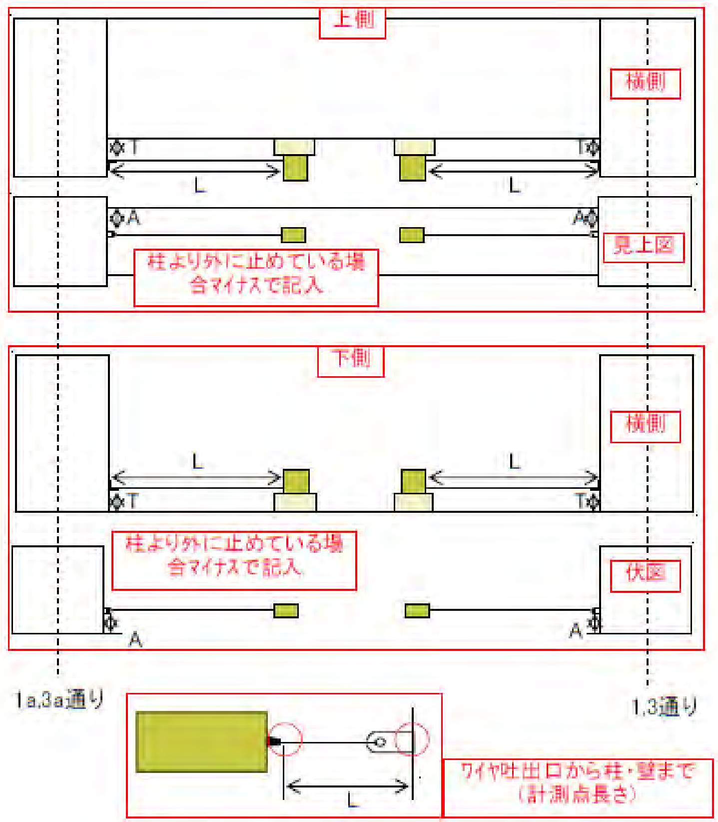

計測位置

センサータグ	寸法計測点		
	L	T	A
5Y-P1-DB3T	735	120	-75
5Y-P2-DB3B	750	60	10
5Y-P2-DB3T	740	130	-65
5Y-P3-DB3B	750	65	10
5Y-P3-DB3T	750	130	-60
5Y-P4-DB3B	750	65	10
5Y-P4-DB3T	740	130	65
5Y-PR-DB3B	750	65	10
5Y-P1-DC3T	745	45	30
5Y-P2-DC3B	760	60	110
5Y-P2-DC3T	750	45	25
5Y-P3-DC3B	750	60	100
5Y-P3-DC3T	745	45	100
5Y-P4-DC3B	703	65	100
5Y-P4-DC3T	698	45	25
5Y-PR-DC3B	760	65	35
5Y-P1-DC3aT	750	45	30
5Y-P2-DC3aB	765	70	35
5Y-P2-DC3aT	760	45	25
5Y-P3-DC3aB	750	65	30
5Y-P3-DC3aT	750	45	30
5Y-P4-DC3aB	696	70	100
5Y-P4-DC3aT	695	45	25
5Y-PR-DC3aB	760	65	30
9Y-R2-DB1T	850	65	40
9Y-R3-DB1B	750	65	30
9Y-R2-DC1T	755	40	25
9Y-R3-DC1B	750	70	135
9Y-R2-DC1aT	765	40	35
9Y-R3-DC1aB	745	65	135

5YPT梁端変形　9YRC梁端変形−寸法計測

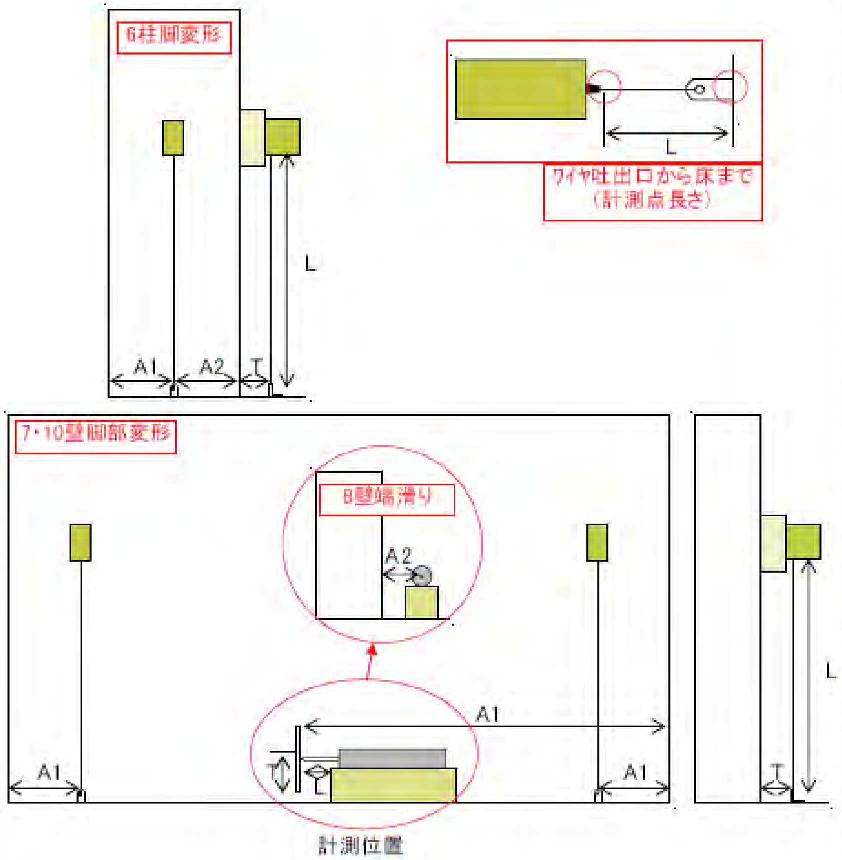

センサータグ	寸法計測点			
	L	T	A1	A2
6-P1-DB3N	1000	70	240	210
6-P1-DB3E	1000	70	230	220
6-P1-DB3S	990	65	220	230
6-P1-DB3W	990	70	240	210
6-P1-DC3N	1000	70	230	230
6-P1-DC3E	990	65	230	230
6-P1-DC3S	990	65	240	220
6-P1-DC3W	990	70	250	200
7-P1-DC3aNE	1000	65	505	
7-P1-DC3aSE	1000	145	505	
7-P1-DC3aSW	996	145	515	
7-P1-DC3aNW	990	65	515	
7-P2-DC3aNE	1000	65	510	
7-P2-DC3aSE	998	60	510	
7-P2-DC3aSW	1000	65	500	
7-P2-DC3aNW	998	65	500	
7-P3-DC3aNE	1000	60	510	
7-P3-DC3aSE	1005	60	495	
7-P3-DC3aSW	995	65	505	
7-P3-DC3aNW	1000	65	505	
7-P4-DC3aNE	1000	60	500	
7-P4-DC3aSE	1000	60	510	
7-P4-DC3aSW	1000	65	505	
7-P4-DC3aNW	1000	65	495	
10-R1-DC1aNE	990	60	510	
10-R1-DC1aSE	1050	145	500	
10-R1-DC1aSW	995	145	505	
10-R1-DC1aNW	1000	60	500	
8-P1-DC3aY	180	135	1260	65
8-P2-DC3aY	70	135	1250	65
8-P3-DC3aY	50	140	1255	65
8-P4-DC3aY	50	140	1250	65
8-R1-DA1aY	70	140	1250	65
8-R1-DC1aY	70	140	1250	65

6PT柱脚変形　7PT壁脚部変形　8PT壁端滑り　10RC壁脚部変形-寸法計測

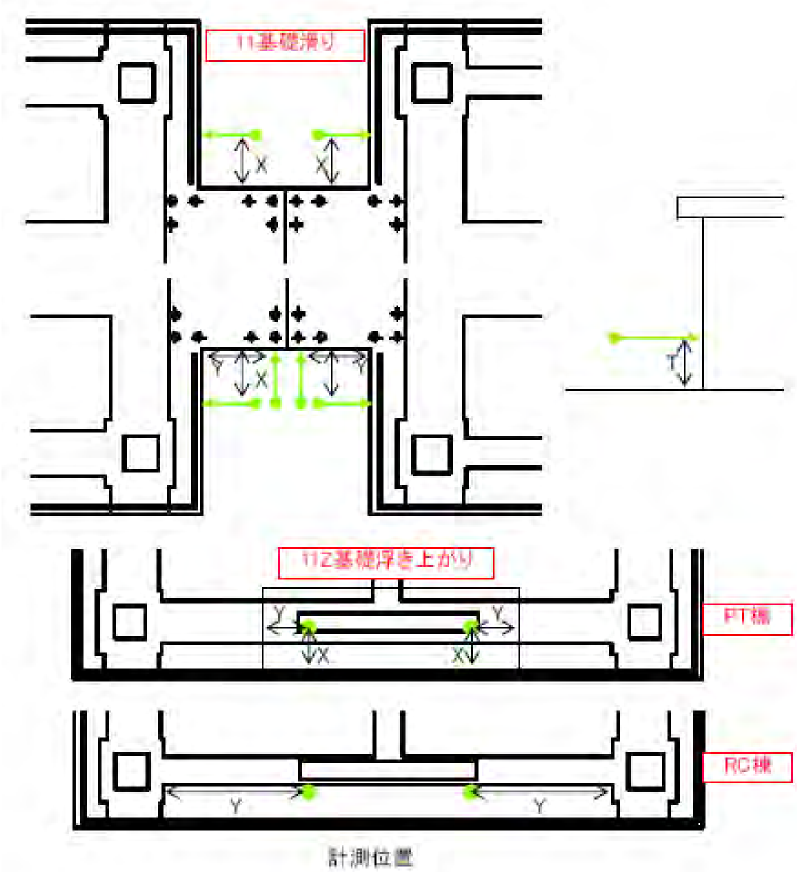

センサータグ	寸法計測点		
	X	Y	T
11-P0-D1Y	850		230
11-P0-D2X		1090	230
11-P0-D2Y	850		230
11-R0-D1Y	850		230
11-R0-D2X		1090	230
11-R0-D2Y	850		230
11Z-P0-D1Z	255	38	
11Z-P0-D2Z	270	32	
11Z-R0-D1Z		1970	
11Z-R0-D2Z		1365	

11基礎滑り　11Z基礎浮き上がり-寸法計測

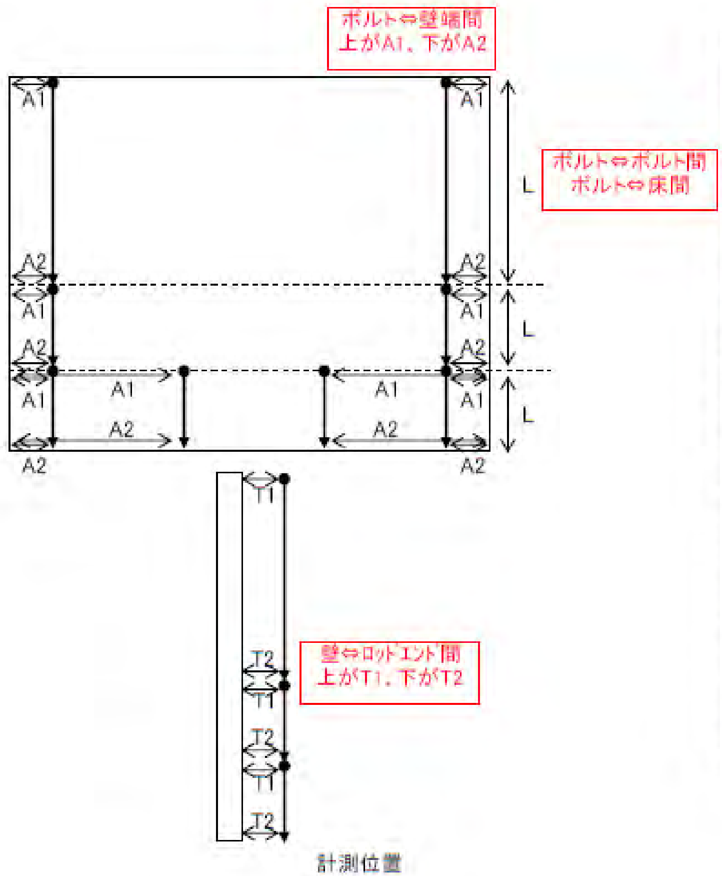

センサータグ	寸法計測点				
	L	T1	T2	A1	A2
A1-P1N-D1	20		85		150
A1-P1N-D2	20		85		140
A1-P1N-D3	20		90		85
A1-P1N-D4	20		85		1050
A1-P1N-D5	20		85		1050
A1-P1N-D6	20		85		65
A1-P1N-D7	490	35	35	110	105
A1-P1N-D8	500	40	40	105	105
A1-P1N-D9	1860	75	75	110	110
A1-P1N-D10	1870	70	70	140	120
A1-P2N-D11	2815	75	75	125	125
A1-P2N-D12	2820	70	70	125	125
A1-P3N-D13	2800	80	80	130	130
A1-P3N-D14	2800	70	70	130	130
A1-P4N-D15	2820	130	130	130	130
A1-P4N-D16	2820	130	130	130	130
A1-P1S-D1	20		90		150
A1-P1S-D2	20		85		120
A1-P1S-D3	20		90		85
A1-P1S-D4	20		90		1010
A1-P1S-D5	20		85		1040
A1-P1S-D6	20		85		90
A1-P1S-D7	500	40	40	110	110
A1-P1S-D8	500	45	40	100	100
A1-P1S-D9	1870	75	75	115	110
A1-P1S-D10	1870	75	75	110	110

A1-1 PT棟壁変形計測

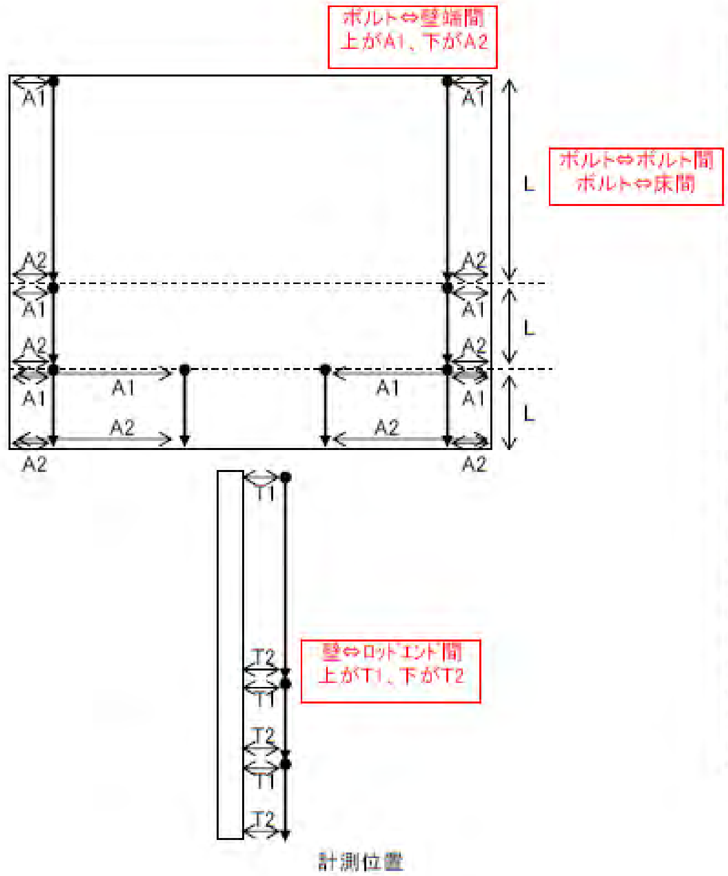

センサータグ	寸法計測点				
	L	T1	T2	A1	A2
A1-R1N-D1	245		76		135
A1-R1N-D2	245		73		130
A1-R1N-D3	545	104	100	104	96
A1-R1N-D4	542	100	102	1020	1020
A1-R1N-D5	545	102	100	1030	1020
A1-R1N-D6	550	104	104	100	105
A1-R1N-D7	483	37	40	98	102.5
A1-R1N-D8	497	42	40	104	100
A1-R1N-D9	1850	69	67	124	98
A1-R1N-D10	1845	69	70	130	104
A1-R2N-D11	2815	70	72	128	120
A1-R2N-D12	2820	73	67	127	128
A1-R3N-D13	2805	75	70	130	125
A1-R3N-D14	2815	78	72	135	135
A1-R4N-D15	2855	70	67	130	125
A1-R4N-D16	2855	68	65	130	130
A1-R1S-D1	252		90		135
A1-R1S-D2	250		93		110
A1-R1S-D3	554	105	105	99	98
A1-R1S-D4	560	98	100	1027	1015
A1-R1S-D5	550	105	107	1024	1019
A1-R1S-D6	550	106	105	100	102
A1-R1S-D7	510	43	40	98	96
A1-R1S-D8	505	41	40	100	100
A1-R1S-D9	2830	64	70	134	98
A1-R1S-D10	2850	64	70	128	100

A1−2 RC棟壁変形計測

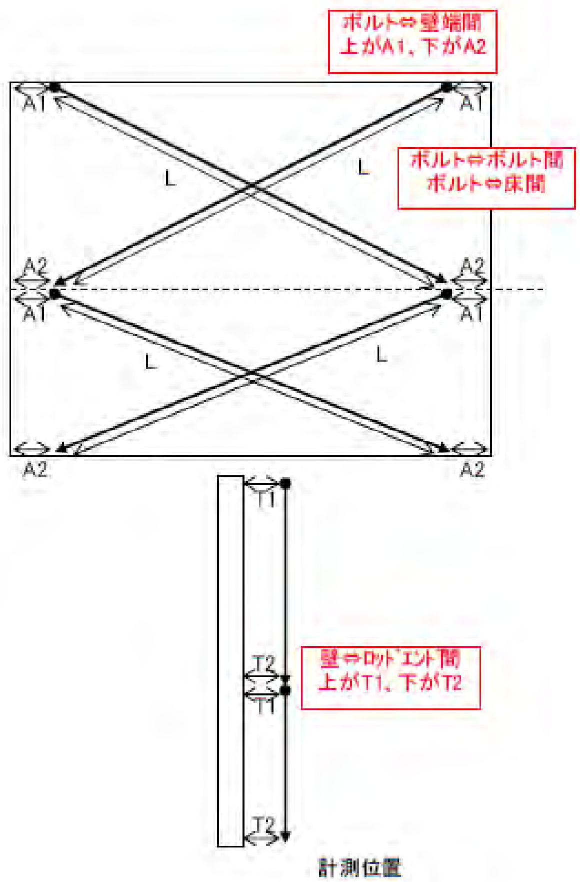

センサータグ	寸法計測点				
	L	T1	T2	A1	A2
A2-PIS-D1	2530	85	120	100	70
A2-PIS-D2	2470	40	70	100	130
A2-PIS-D3	2970	110	90	80	100
A2-PIS-D4	2930	70	40	130	100
A2-RIS-D1	2528	80	115	103	65
A2-RIS-D2	2475	78	68	95	130
A2-RIS-D3	2975	120	78	75	95
A2-RIS-D4	2920	77	33	110	103

A2 壁せん断変形

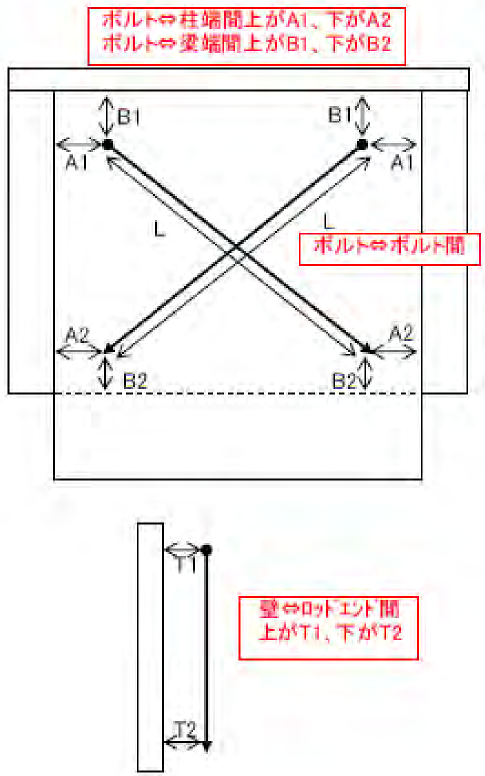

計測位置

センサータグ	寸法計測点						
	L	T1	T2	A1	A2	B1	B2
A3-R1-D1	475	67	65	82	85	52	88
A3-R1-D2	470	32	29	85	83	48	90
A3-R2-D3	470	63	65	85	94	56	75
A3-R2-D4	475	27	31	85	84	55	84
A3-R3-D5	475	65	65	89	95	55	68
A3-R3-D6	470	30	30	90	91	48	80
A3-R3-D7	480	75	65	85	86	50	74
A3-R3-D8	485	30	30	85	80	52	70
A3-R4-D9	480	65	65	90	84	55	70
A3-R4-D10	465	28	30	100	92	50	76

A3柱接合部

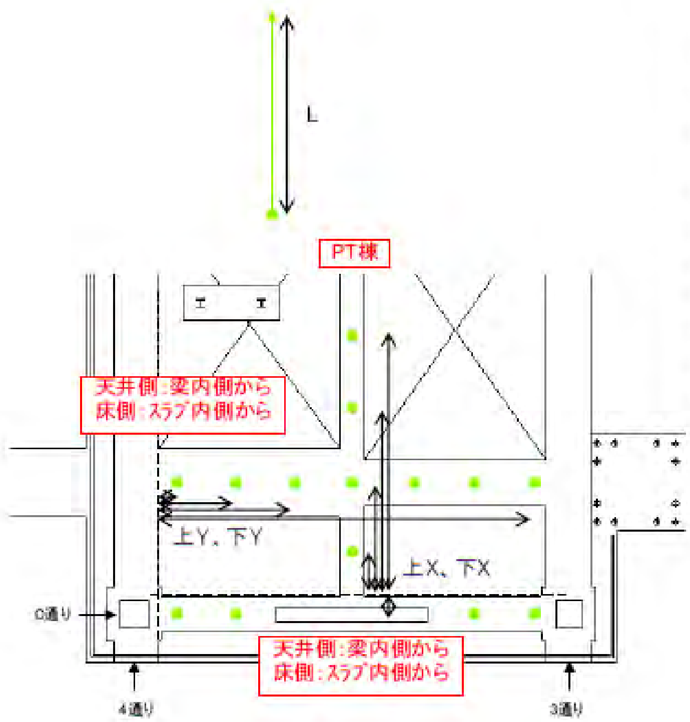

計測位置

センサータグ	寸法計測点				
	L	上X	下X	上Y	下Y
A4-P1-D1	2700	4530	1250	3440	3170
A4-P1-D2	2700	3280	3100	3440	3170
A4-P1-D3	2700	2030	1850	440	170
A4-P1-D4	2700	2030	1850	1440	1170
A4-P1-D5	2700	2030	1850	2440	2170
A4-P1-D6	2700	2030	1850	3440	3170
A4-P1-D7	2700	2030	1850	4440	4170
A4-P1-D8	2700	2030	1850	5440	5170
A4-P1-D9	2700	2030	1850	6440	6170
A4-P1-D10	2700	795	600	3440	3170
A4-P1-D11	2700	-160	-350	460	200
A4-P1-D12	2700	-160	-350	1460	1200
A4-P1-D13	2700	-160	-350	5420	5150
A4-P1-D14	2700	-160	-350	6420	6150

A4層間鉛直変位（ワイヤ）

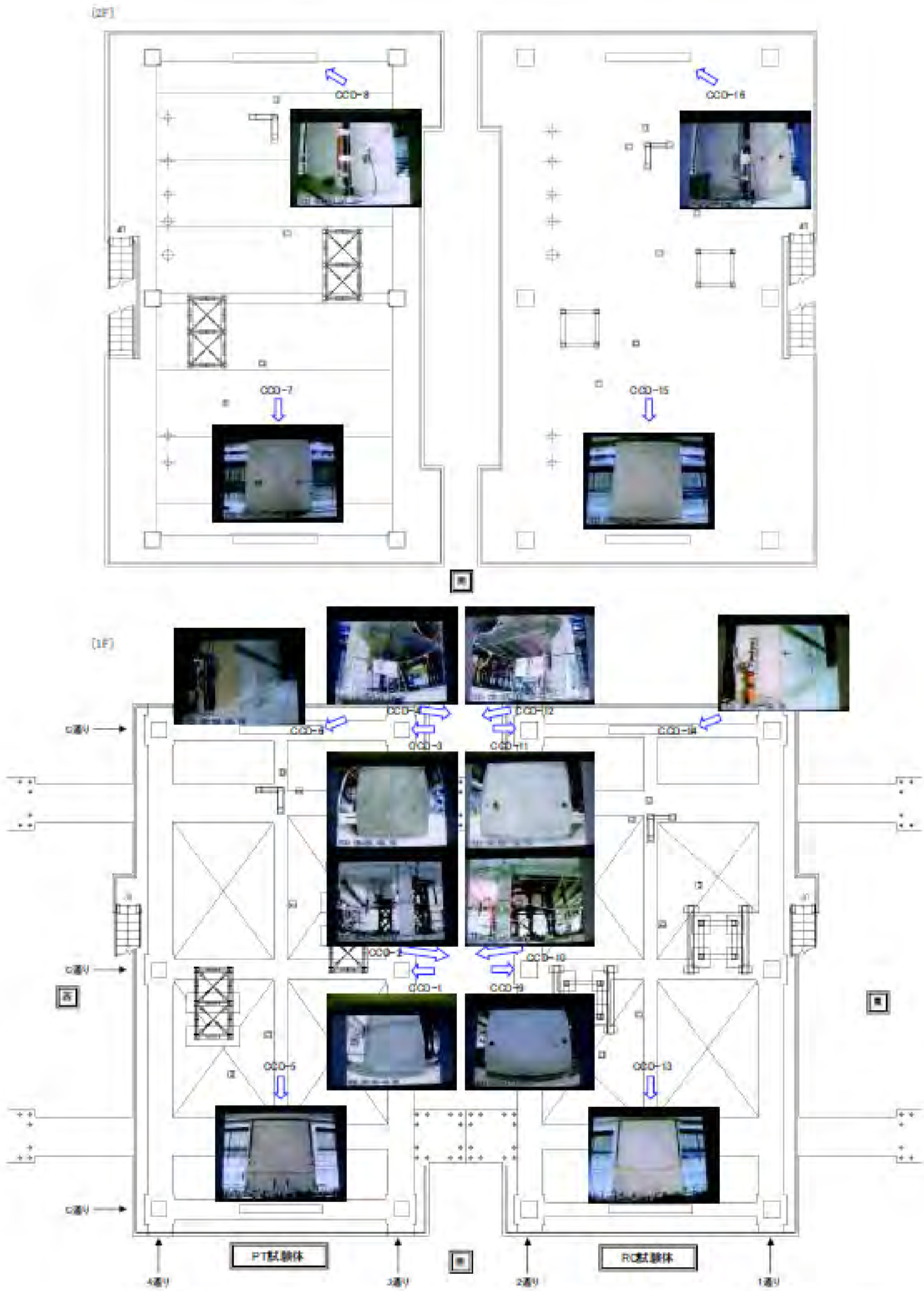

名称	タグ	機器	合計点数
⇨ CCDカメラ	CCD-*	CCDカメラ	16台

CCDカメラ設置位置

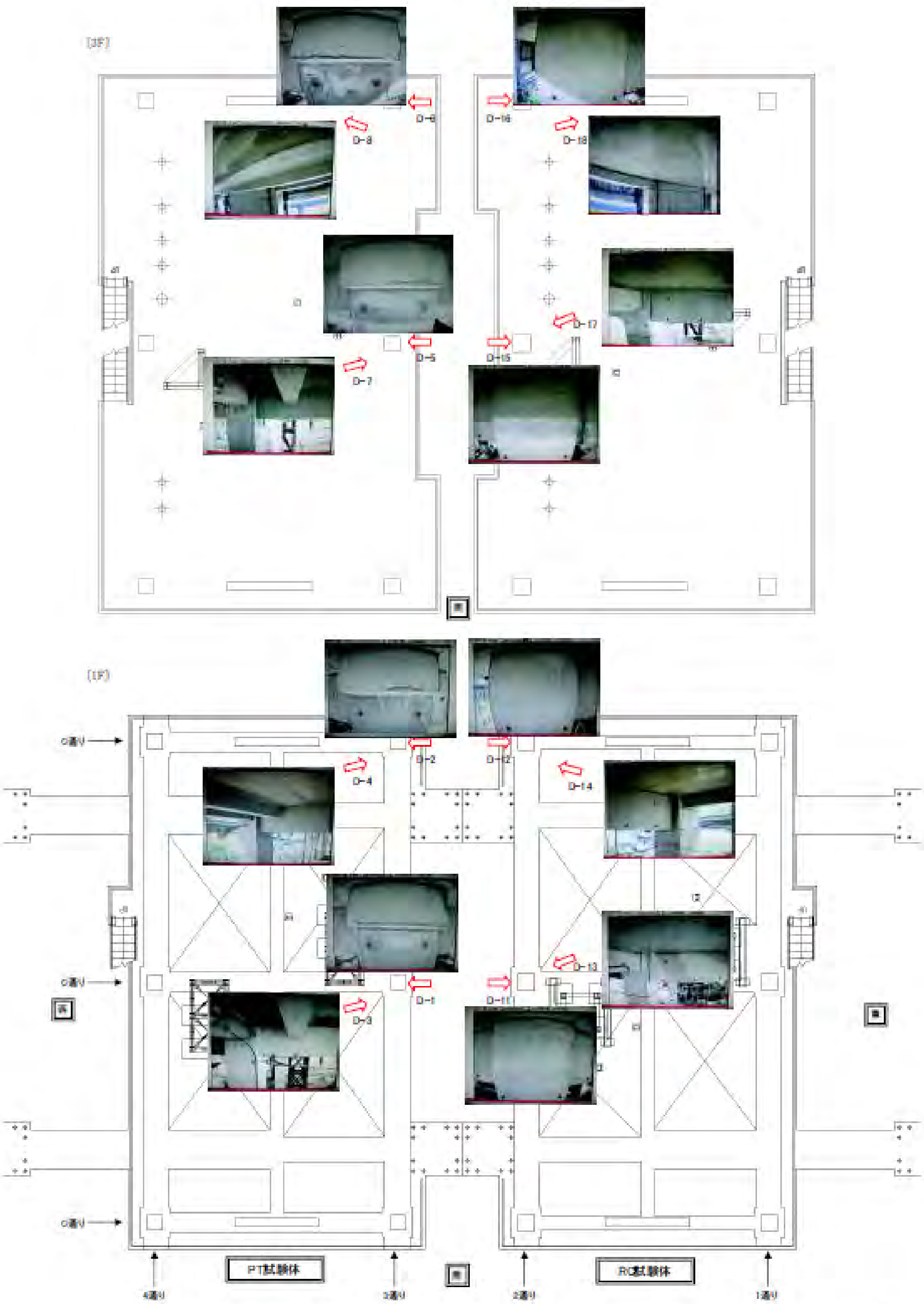

名称	タグ	機器	合計点数
デジタルカメラ	D-*	デジタルカメラ	20台

デジタルカメラ 設置位置1

[4F]

名称	タグ	機器	合計点数
⇨ デジタルカメラ	D-●	デジタルカメラ	20台

<u>デジタルカメラ 設置位置2 設備機器</u>

ブリッジボックス接続表1

黒字：1ゲージ法
赤字：2ゲージ法

RC棟 1F BB01

BB番号	歪ゲージ	部材	センサ	JB番号	ケーブル
BB01-01	16-1 16-2	C1	16-R-S1	JB02-17	30m
BB01-02	16-3 16-4	C1	16-R-S2	JB02-18	30m
BB01-03	16-5 16-6	C1	16-R-S3	JB02-19	30m
BB01-04	16-7 16-8	C1	16-R-S4	JB02-20	30m
BB01-05	16-9 16-10	B1	16-R-S5	JB02-21	30m
BB01-06	16-11 16-12	B1	16-R-S6	JB02-22	30m
BB01-07	16-13 16-14	B1	16-R-S7	JB02-23	30m
BB01-08	16-15 16-16	B1	16-R-S8	JB02-24	30m
BB01-09					
BB01-10					

RC棟 1F BB04

BB番号	歪ゲージ	部材	センサ	JB番号	ケーブル
BB04-01	17-1	C1	17-R-S1	JB03-33	30m
BB04-02	17-2	C1	17-R-S2	JB03-34	30m
BB04-03	17-3	B1	17-R-S3	JB03-35	30m
BB04-04	17-4	B1	17-R-S4	JB03-36	30m
BB04-05	17-5	C1	17-R-S5	JB03-37	30m
BB04-06	17-6	C1	17-R-S6	JB03-38	30m
BB04-07	17-7	B1	17-R-S7	JB03-39	30m
BB04-08	17-8	B1	17-R-S8	JB03-40	30m
BB04-09					
BB04-10					

RC棟 2F BB07

BB番号	歪ゲージ	部材	センサ	JB番号	ケーブル
BB07-01	12-1 12-2	C1	12-R-S1	JB01-01	30m
BB07-02	12-3 12-4	C1	12-R-S2	JB01-02	30m
BB07-03	12-5 12-6	C1	12-R-S3	JB01-03	30m
BB07-04	12-7 12-8	C1	12-R-S4	JB01-04	30m
BB07-05	12-9 12-10	C1a	12-R-S5	JB01-05	30m
BB07-06	12-11 12-12	C1a	12-R-S6	JB01-06	30m
BB07-07	12-13 12-14	C1a	12-R-S7	JB01-07	30m
BB07-08	12-15 12-16	C1a	12-R-S8	JB01-08	30m
BB07-09					
BB07-10					

RC棟 2F BB10

BB番号	歪ゲージ	部材	センサ	JB番号	ケーブル
BB10-01	16-49 16-50	C1	16-R-S25	JB02-41	30m
BB10-02	16-51 16-52	C1	16-R-S26	JB02-42	30m
BB10-03	16-53 16-54	C1	16-R-S27	JB02-43	30m
BB10-04	16-55 16-56	C1	16-R-S28	JB02-44	30m
BB10-05	16-57 16-58	B1	16-R-S29	JB02-45	30m
BB10-06	16-59 16-60	B1	16-R-S30	JB02-46	30m
BB10-07	16-61 16-62	B1	16-R-S31	JB02-47	30m
BB10-08	16-63 16-64	B1	16-R-S32	JB02-48	30m
BB10-09					
BB10-10					

RC棟 2F BB13

BB番号	歪ゲージ	部材	センサ	JB番号	ケーブル
BB13-01	18-4	C1a	18-R-S4	JB04-04	30m
BB13-02	18-5	C1a	18-R-S5	JB04-05	30m
BB13-03	18-6	C1a	18-R-S6	JB04-06	30m
BB13-04	19-4	C1a	19-R-S4	JB04-10	30m
BB13-05	19-5	C1a	19-R-S5	JB04-11	30m
BB13-06	19-6	C1a	19-R-S6	JB04-12	30m
BB13-07	21-3	C1a	21-R-S3	JB04-27	30m
BB13-08	21-4	C1a	21-R-S4	JB04-28	30m
BB13-09					
BB13-10					

RC棟 1F BB02

BB番号	歪ゲージ	部材	センサ	JB番号	ケーブル
BB02-01	16-17 16-18	C1	16-R-S9	JB02-25	30m
BB02-02	16-19 16-20	C1	16-R-S10	JB02-26	30m
BB02-03	16-21 16-22	C1	16-R-S11	JB02-27	30m
BB02-04	16-23 16-24	C1	16-R-S12	JB02-28	30m
BB02-05	16-25 16-26	B1	16-R-S13	JB02-29	30m
BB02-06	16-27 16-28	B1	16-R-S14	JB02-30	30m
BB02-07	16-29 16-30	B1	16-R-S15	JB02-31	30m
BB02-08	16-31 16-32	B1	16-R-S16	JB02-32	30m
BB02-09					
BB02-10					

RC棟 1F BB05

BB番号	歪ゲージ	部材	センサ	JB番号	ケーブル
BB05-01	18-1	C1a	18-R-S1	JB04-01	30m
BB05-02	18-2	C1a	18-R-S2	JB04-02	30m
BB05-03	18-3	C1a	18-R-S3	JB04-03	30m
BB05-04	19-1	C1a	19-R-S1	JB04-07	30m
BB05-05	19-2	C1a	19-R-S2	JB04-08	30m
BB05-06	19-3	C1a	19-R-S3	JB04-09	30m
BB05-07	21-1	C1a	21-R-S1	JB04-25	30m
BB05-08	21-2	C1a	21-R-S2	JB04-26	30m
BB05-09					
BB05-10					

RC棟 2F BB08

BB番号	歪ゲージ	部材	センサ	JB番号	ケーブル
BB08-01	12-17 12-18	B1	12-R-S9	JB01-09	30m
BB08-02	12-19 12-20	B1	12-R-S10	JB01-10	30m
BB08-03	12-21 12-22	B1	12-R-S11	JB01-11	30m
BB08-04	12-23 12-24	B1	12-R-S12	JB01-12	30m
BB08-05					
BB08-06	13-1	C1	13-R-S1	JB01-25	30m
BB08-07	13-2	C1a	13-R-S2	JB01-26	30m
BB08-08	13-3	B1	13-R-S3	JB01-27	30m
BB08-09	15-1	C1	15-R-S1	JB02-01	30m
BB08-10	15-2	B1	15-R-S2	JB02-02	30m

RC棟 2F BB11

BB番号	歪ゲージ	部材	センサ	JB番号	ケーブル
BB11-01	16-65 16-66	C1	16-R-S33	JB02-49	30m
BB11-02	16-67 16-68	C1	16-R-S34	JB02-50	30m
BB11-03	16-69 16-70	C1	16-R-S35	JB02-51	30m
BB11-04	16-71 16-72	C1	16-R-S36	JB02-52	30m
BB11-05	16-73 16-74	B1	16-R-S37	JB02-53	30m
BB11-06	16-75 16-76	B1	16-R-S38	JB02-54	30m
BB11-07	16-77 16-78	B1	16-R-S39	JB02-55	30m
BB11-08	16-79 16-80	B1	16-R-S40	JB02-56	30m
BB11-09					
BB11-10					

RC棟 2F BB14

BB番号	歪ゲージ	部材	センサ	JB番号	ケーブル
BB14-01	20-13 20-14	C1a	20-R-S7	JB04-19	30m
BB14-02	20-15 20-16	C1a	20-R-S8	JB04-20	30m
BB14-03	20-17 20-18	C1a	20-R-S9	JB04-21	30m
BB14-04	20-19 20-20	C1a	20-R-S10	JB04-22	30m
BB14-05	20-21 20-22	C1a	20-R-S11	JB04-23	30m
BB14-06	20-23 20-24	C1a	20-R-S12	JB04-24	30m
BB14-07					
BB14-08					
BB14-09					
BB14-10					

RC棟 1F BB03

BB番号	歪ゲージ	部材	センサ	JB番号	ケーブル
BB03-01	16-33 16-34	C1	16-R-S17	JB02-33	30m
BB03-02	16-35 16-36	C1	16-R-S18	JB02-34	30m
BB03-03	16-37 16-38	C1	16-R-S19	JB02-35	30m
BB03-04	16-39 16-40	C1	16-R-S20	JB02-36	30m
BB03-05	16-41 16-42	B1	16-R-S21	JB02-37	30m
BB03-06	16-43 16-44	B1	16-R-S22	JB02-38	30m
BB03-07	16-45 16-46	B1	16-R-S23	JB02-39	30m
BB03-08	16-47 16-48	B1	16-R-S24	JB02-40	30m
BB03-09					
BB03-10					

RC棟 1F BB06

BB番号	歪ゲージ	部材	センサ	JB番号	ケーブル
BB06-01	20-1 20-2	C1a	20-R-S1	JB04-13	30m
BB06-02	20-3 20-4	C1a	20-R-S2	JB04-14	30m
BB06-03	20-5 20-6	C1a	20-R-S3	JB04-15	30m
BB06-04	20-7 20-8	C1a	20-R-S4	JB04-16	30m
BB06-05	20-9 20-10	C1a	20-R-S5	JB04-17	30m
BB06-06	20-11 20-12	C1a	20-R-S6	JB04-18	30m
BB06-07					
BB06-08					
BB06-09					
BB06-10					

RC棟 2F BB09

BB番号	歪ゲージ	部材	センサ	JB番号	ケーブル
BB09-01	14-1 14-2	C1	14-R-S1	JB01-31	30m
BB09-02	14-3 14-4	C1	14-R-S2	JB01-32	30m
BB09-03	14-5 14-6	C1	14-R-S3	JB01-33	30m
BB09-04	14-7 14-8	C1	14-R-S4	JB01-34	30m
BB09-05	14-9 14-10	B1	14-R-S5	JB01-35	30m
BB09-06	14-11 14-12	B1	14-R-S6	JB01-36	30m
BB09-07	14-13 14-14	B1	14-R-S7	JB01-37	30m
BB09-08	14-15 14-16	B1	14-R-S8	JB01-38	30m
BB09-09					
BB09-10					

RC棟 2F BB12

BB番号	歪ゲージ	部材	センサ	JB番号	ケーブル
BB12-01	17-9	C1	17-R-S9	JB03-41	30m
BB12-02	17-10	C1	17-R-S10	JB03-42	30m
BB12-03	17-11	B1	17-R-S11	JB03-43	30m
BB12-04	17-12	B1	17-R-S12	JB03-44	30m
BB12-05	17-13	C1	17-R-S13	JB03-45	30m
BB12-06	17-14	C1	17-R-S14	JB03-46	30m
BB12-07	17-15	B1	17-R-S15	JB03-47	30m
BB12-08	17-16	B1	17-R-S16	JB03-48	30m
BB12-09					
BB12-10					

ブリッジボックス接続表2

黒字：1ゲージ法
赤字：2ゲージ法

RC棟 3F / BB15

BB番号	歪ｹﾞｰｼﾞ	部材	ｾﾝｻｸﾞ	JB番号	ｹｰﾌﾞﾙ
BB15-01	12-25 12-26	C1	12-R-S13	JB01-13	30m
BB15-02	12-27 12-28	C1	12-R-S14	JB01-14	30m
BB15-03	12-29 12-30	C1	12-R-S15	JB01-15	30m
BB15-04	12-31 12-32	C1	12-R-S16	JB01-16	30m
BB15-05	12-33 12-34	C1a	12-R-S17	JB01-17	30m
BB15-06	12-35 12-36	C1a	12-R-S18	JB01-18	30m
BB15-07	12-37 12-38	C1a	12-R-S19	JB01-19	30m
BB15-08	12-39 12-40	C1a	12-R-S20	JB01-20	30m
BB15-09					
BB15-10					

RC棟 3F / BB18

BB番号	歪ｹﾞｰｼﾞ	部材	ｾﾝｻｸﾞ	JB番号	ｹｰﾌﾞﾙ
BB18-01	16-81 16-82	C1	16-R-S41	JB03-01	30m
BB18-02	16-83 16-84	C1	16-R-S42	JB03-02	30m
BB18-03	16-85 16-86	C1	16-R-S43	JB03-03	30m
BB18-04	16-87 16-88	C1	16-R-S44	JB03-04	30m
BB18-05	16-89 16-90	B1	16-R-S45	JB03-05	30m
BB18-06	16-91 16-92	B1	16-R-S46	JB03-06	30m
BB18-07	16-93 16-94	B1	16-R-S47	JB03-07	30m
BB18-08	16-95 16-96	B1	16-R-S48	JB03-08	30m
BB18-09					
BB18-10					

RC棟 4F / BB21

BB番号	歪ｹﾞｰｼﾞ	部材	ｾﾝｻｸﾞ	JB番号	ｹｰﾌﾞﾙ
BB21-01	14-33 14-34	C1	14-R-S17	JB01-47	40m
BB21-02	14-35 14-36	C1	14-R-S18	JB01-48	40m
BB21-03	14-37 14-38	C1	14-R-S19	JB01-49	40m
BB21-04	14-39 14-40	C1	14-R-S20	JB01-50	40m
BB21-05	14-41 14-42	B1	14-R-S21	JB01-51	40m
BB21-06	14-43 14-44	B1	14-R-S22	JB01-52	40m
BB21-07	14-45 14-46	B1	14-R-S23	JB01-53	40m
BB21-08	14-47 14-48	B1	14-R-S24	JB01-54	40m
BB21-09					
BB21-10					

RC棟 4F / BB24

BB番号	歪ｹﾞｰｼﾞ	部材	ｾﾝｻｸﾞ	JB番号	ｹｰﾌﾞﾙ
BB24-01	17-25	C1	17-R-S25	JB03-57	40m
BB24-02	17-26	C1	17-R-S26	JB03-58	40m
BB24-03	17-27	B1	17-R-S27	JB03-59	40m
BB24-04	17-28	B1	17-R-S28	JB03-60	40m
BB24-05	17-29	C1	17-R-S29	JB03-61	40m
BB24-06	17-30	C1	17-R-S30	JB03-62	40m
BB24-07	17-31	B1	17-R-S31	JB03-63	40m
BB24-08	17-32	B1	17-R-S32	JB03-64	40m
BB24-09					
BB24-10					

RC棟 RF / BB27

BB番号	歪ｹﾞｰｼﾞ	部材	ｾﾝｻｸﾞ	JB番号	ｹｰﾌﾞﾙ
BB27-01	15-11	C1	15-R-S7	JB02-07	40m
BB27-02	15-12	B1	15-R-S8	JB02-08	40m
BB27-03	15-13	C1	25-R-S5	JB02-13	40m
BB27-04	15-14	C1	25-R-S6	JB02-14	40m
BB27-05	15-15	B1	25-R-S7	JB02-15	40m
BB27-06	15-16	B1	25-R-S8	JB02-16	40m
BB27-07					
BB27-08					
BB27-09					
BB27-10					

RC棟 3F / BB16

BB番号	歪ｹﾞｰｼﾞ	部材	ｾﾝｻｸﾞ	JB番号	ｹｰﾌﾞﾙ
BB16-01	12-41 12-42	B1	12-R-S21	JB01-21	30m
BB16-02	12-43 12-44	B1	12-R-S22	JB01-22	30m
BB16-03	12-45 12-46	B1	12-R-S23	JB01-23	30m
BB16-04	12-47 12-48	B1	12-R-S24	JB01-24	30m
BB16-05					
BB16-06	13-4	C1	13-R-S4	JB01-28	30m
BB16-07	13-5	C1a	13-R-S5	JB01-29	30m
BB16-08	13-6	B1	13-R-S6	JB01-30	30m
BB16-09	15-3	C1	15-R-S3	JB02-03	30m
BB16-10	15-4	B1	15-R-S4	JB02-04	30m

RC棟 3F / BB19

BB番号	歪ｹﾞｰｼﾞ	部材	ｾﾝｻｸﾞ	JB番号	ｹｰﾌﾞﾙ
BB19-01	16-97 16-98	C1	16-R-S49	JB03-09	30m
BB19-02	16-99 16-100	C1	16-R-S50	JB03-10	30m
BB19-03	16-101 16-102	C1	16-R-S51	JB03-11	30m
BB19-04	16-103 16-104	C1	16-R-S52	JB03-12	30m
BB19-05	16-105 16-106	B1	16-R-S53	JB03-13	30m
BB19-06	16-107 16-108	B1	16-R-S54	JB03-14	30m
BB19-07	16-109 16-110	B1	16-R-S55	JB03-15	30m
BB19-08	16-111 16-112	B1	16-R-S56	JB03-16	30m
BB19-09					
BB19-10					

RC棟 4F / BB22

BB番号	歪ｹﾞｰｼﾞ	部材	ｾﾝｻｸﾞ	JB番号	ｹｰﾌﾞﾙ
BB22-01	16-113 16-114	C1	16-R-S57	JB03-17	40m
BB22-02	16-115 16-116	C1	16-R-S58	JB03-18	40m
BB22-03	16-117 16-118	C1	16-R-S59	JB03-19	40m
BB22-04	16-119 16-120	C1	16-R-S60	JB03-20	40m
BB22-05	16-121 16-122	B1	16-R-S61	JB03-21	40m
BB22-06	16-123 16-124	B1	16-R-S62	JB03-22	40m
BB22-07	16-125 16-126	B1	16-R-S63	JB03-23	40m
BB22-08	16-127 16-128	B1	16-R-S64	JB03-24	40m
BB22-09					
BB22-10					

RC棟 4F / BB25

BB番号	歪ｹﾞｰｼﾞ	部材	ｾﾝｻｸﾞ	JB番号	ｹｰﾌﾞﾙ
BB25-01	15-5	C1	15-R-S5	JB02-05	40m
BB25-02	15-6	B1	15-R-S6	JB02-06	40m
BB25-03	15-7	C1	25-R-S1	JB02-09	40m
BB25-04	15-8	C1	25-R-S2	JB02-10	40m
BB25-05	15-9	B1	25-R-S3	JB02-11	40m
BB25-06	15-10	B1	25-R-S4	JB02-12	40m
BB25-07					
BB25-08					
BB25-09					
BB25-10					

RC棟 3F / BB17

BB番号	歪ｹﾞｰｼﾞ	部材	ｾﾝｻｸﾞ	JB番号	ｹｰﾌﾞﾙ
BB17-01	14-17 14-18	C1	14-R-S9	JB01-39	30m
BB17-02	14-19 14-20	C1	14-R-S10	JB01-40	30m
BB17-03	14-21 14-22	C1	14-R-S11	JB01-41	30m
BB17-04	14-23 14-24	C1	14-R-S12	JB01-42	30m
BB17-05	14-25 14-26	B1	14-R-S13	JB01-43	30m
BB17-06	14-27 14-28	B1	14-R-S14	JB01-44	30m
BB17-07	14-29 14-30	B1	14-R-S15	JB01-45	30m
BB17-08	14-31 14-32	B1	14-R-S16	JB01-46	30m
BB17-09					
BB17-10					

RC棟 3F / BB20

BB番号	歪ｹﾞｰｼﾞ	部材	ｾﾝｻｸﾞ	JB番号	ｹｰﾌﾞﾙ
BB20-01	17-17	C1	17-R-S17	JB03-49	30m
BB20-02	17-18	C1	17-R-S18	JB03-50	30m
BB20-03	17-19	B1	17-R-S19	JB03-51	30m
BB20-04	17-20	B1	17-R-S20	JB03-52	30m
BB20-05	17-21	C1	17-R-S21	JB03-53	30m
BB20-06	17-22	C1	17-R-S22	JB03-54	30m
BB20-07	17-23	B1	17-R-S23	JB03-55	30m
BB20-08	17-24	B1	17-R-S24	JB03-56	30m
BB20-09					
BB20-10					

RC棟 4F / BB23

BB番号	歪ｹﾞｰｼﾞ	部材	ｾﾝｻｸﾞ	JB番号	ｹｰﾌﾞﾙ
BB23-01	16-129 16-130	C1	16-R-S65	JB03-25	40m
BB23-02	16-131 16-132	C1	16-R-S66	JB03-26	40m
BB23-03	16-133 16-134	C1	16-R-S67	JB03-27	40m
BB23-04	16-135 16-136	C1	16-R-S68	JB03-28	40m
BB23-05	16-137 16-138	B1	16-R-S69	JB03-29	40m
BB23-06	16-139 16-140	B1	16-R-S70	JB03-30	40m
BB23-07	16-141 16-142	B1	16-R-S71	JB03-31	40m
BB23-08	16-143 16-144	B1	16-R-S72	JB03-32	40m
BB23-09					
BB23-10					

RC棟 RF / BB26

BB番号	歪ｹﾞｰｼﾞ	部材	ｾﾝｻｸﾞ	JB番号	ｹｰﾌﾞﾙ
BB26-01	14-49 14-50	C1	14-R-S25	JB01-55	40m
BB26-02	14-51 14-52	C1	14-R-S26	JB01-56	40m
BB26-03	14-53 14-54	C1	14-R-S27	JB01-57	40m
BB26-04	14-55 14-56	C1	14-R-S28	JB01-58	40m
BB26-05	14-57 14-58	B1	14-R-S29	JB01-59	40m
BB26-06	14-59 14-60	B1	14-R-S30	JB01-60	40m
BB26-07	14-61 14-62	B1	14-R-S31	JB01-61	40m
BB26-08	14-63 14-64	B1	14-R-S32	JB01-62	40m
BB26-09					
BB26-10					

PT棟1F / BB28

BB番号	歪ｹﾞｰｼﾞ	部材	ｾﾝｻｸﾞ	JB番号	ｹｰﾌﾞﾙ
BB28-01	22-1	C3a	22-P-S1	JB11-35	30m
BB28-02	22-2	C3a	22-P-S2	JB11-36	30m
BB28-03	22-3	C3a	22-P-S3	JB11-37	30m
BB28-04	22-4	C3a	22-P-S4	JB11-38	30m
BB28-05	23-1 23-2	C3a	23-P-S1	JB11-39	30m
BB28-06	23-3 23-4	C3a	23-P-S2	JB11-40	30m
BB28-07	24-1	C3a	24-P-S1	JB11-41	30m
BB28-08	24-2	C3a	24-P-S2	JB11-42	30m
BB28-09					
BB28-10					

ブリッジボックス接続表3

黒字：1ゲージ法
赤字：2ゲージ法

	BB番号	[illegible]	[illegible]	[illegible]	JB番号	ケーブル
PT棟 RF	BB29-01	①-1.1	①-1	32-P-S1	JB10-32	40m
	BB29-02	①-1.2	①-1	32-P-S2	JB10-33	40m
	BB29-03	①-1.3	①-1	32-P-S3	JB10-34	40m
	BB29-04	①-2.1	①-2	32-P-S4	JB10-35	40m
	BB29-05	①-2.2	①-2	32-P-S5	JB10-36	40m
BB29	BB29-06	①-2.3	①-2	32-P-S6	JB10-37	40m
	BB29-07					
	BB29-08					
	BB29-09					
	BB29-10					

	BB番号	[illegible]	[illegible]	[illegible]	JB番号	ケーブル
PT棟 RF	BB32-01	④-1.1	④-1	32-P-S22	JB10-53	40m
	BB32-02	④-1.2	④-1	32-P-S23	JB10-54	40m
	BB32-03	④-1.3	④-1	32-P-S24	JB10-55	40m
	BB32-04	⑤-1.1	⑤-1	32-P-S25	JB10-56	40m
	BB32-05	⑤-1.2	⑤-1	32-P-S26	JB10-57	40m
BB32	BB32-06	⑤-1.3	⑤-1	32-P-S27	JB10-58	40m
	BB32-07					
	BB32-08					
	BB32-09					
	BB32-10					

	BB番号	[illegible]	[illegible]	[illegible]	JB番号	ケーブル
RC棟 RF	BB35-01	③-1.1	③-1	32-R-S13	JB13-52	40m
	BB35-02	③-1.2	③-1	32-R-S14	JB13-53	40m
	BB35-03	③-1.3	③-1	32-R-S15	JB13-54	40m
	BB35-04	③-3.1	③-3	32-R-S16	JB13-55	40m
	BB35-05	③-3.2	③-3	32-R-S17	JB13-56	40m
BB35	BB35-06	③-3.3	③-3	32-R-S18	JB13-57	40m
	BB35-07					
	BB35-08					
	BB35-09					
	BB35-10					

	BB番号	[illegible]	[illegible]	[illegible]	JB番号	ケーブル
PT棟 RF	BB30-01	②-1.1	②-1	32-P-S7	JB10-38	40m
	BB30-02	②-1.2	②-1	32-P-S8	JB10-39	40m
	BB30-03	②-1.3	②-1	32-P-S9	JB10-40	40m
	BB30-04	②-2.1	②-2	32-P-S10	JB10-41	40m
	BB30-05	②-2.2	②-2	32-P-S11	JB10-42	40m
BB30	BB30-06	②-2.3	②-2	32-P-S12	JB10-43	40m
	BB30-07					
	BB30-08					
	BB30-09					
	BB30-10					

	BB番号	[illegible]	[illegible]	[illegible]	JB番号	ケーブル
RC棟 RF	BB33-01	①-1.1	①-1	32-R-S1	JB13-40	40m
	BB33-02	①-1.2	①-1	32-R-S2	JB13-41	40m
	BB33-03	①-1.3	①-1	32-R-S3	JB13-42	40m
	BB33-04	①-2.1	①-2	32-R-S4	JB13-43	40m
	BB33-05	①-2.2	①-2	32-R-S5	JB13-44	40m
BB33	BB33-06	①-2.3	①-2	32-R-S6	JB13-45	40m
	BB33-07					
	BB33-08					
	BB33-09					
	BB33-10					

	BB番号	[illegible]	[illegible]	[illegible]	JB番号	ケーブル
RC棟 RF	BB36-01	④-1.1	④-1	32-R-S19	JB13-58	40m
	BB36-02	④-1.2	④-1	32-R-S20	JB13-59	40m
	BB36-03	④-1.3	④-1	32-R-S21	JB13-60	40m
	BB36-04	⑤-1.1	⑤-1	32-R-S22	JB13-61	40m
	BB36-05	⑤-1.2	⑤-1	32-R-S23	JB13-62	40m
BB36	BB36-06	⑤-1.3	⑤-1	32-R-S24	JB13-63	40m
	BB36-07					
	BB36-08					
	BB36-09					
	BB36-10					

	BB番号	[illegible]	[illegible]	[illegible]	JB番号	ケーブル
PT棟 RF	BB31-01	③-1.1	③-1	32-P-S13	JB10-44	40m
	BB31-02	③-1.2	③-1	32-P-S14	JB10-45	40m
	BB31-03	③-1.3	③-1	32-P-S15	JB10-46	40m
	BB31-04	③-2.1	③-2	32-P-S16	JB10-47	40m
	BB31-05	③-2.2	③-2	32-P-S17	JB10-48	40m
BB31	BB31-06	③-2.3	③-2	32-P-S18	JB10-49	40m
	BB31-07	③-3.1	③-3	32-P-S19	JB10-50	40m
	BB31-08	③-3.2	③-3	32-P-S20	JB10-51	40m
	BB31-09	③-3.3	③-3	32-P-S21	JB10-52	40m
	BB31-10					

	BB番号	[illegible]	[illegible]	[illegible]	JB番号	ケーブル
RC棟 RF	BB34-01	②-1.1	②-1	32-R-S7	JB13-46	40m
	BB34-02	②-1.2	②-1	32-R-S8	JB13-47	40m
	BB34-03	②-1.3	②-1	32-R-S9	JB13-48	40m
	BB34-04	②-2.1	②-2	32-R-S10	JB13-49	40m
	BB34-05	②-2.2	②-2	32-R-S11	JB13-50	40m
BB34	BB34-06	②-2.3	②-2	32-R-S12	JB13-51	40m
	BB34-07					
	BB34-08					
	BB34-09					
	BB34-10					

RC試験体　鉄筋歪ｹﾞｰｼﾞﾌﾟﾛｯﾄ図　1F柱、2F梁①

C通　1F柱C1　　B通　1F柱C2

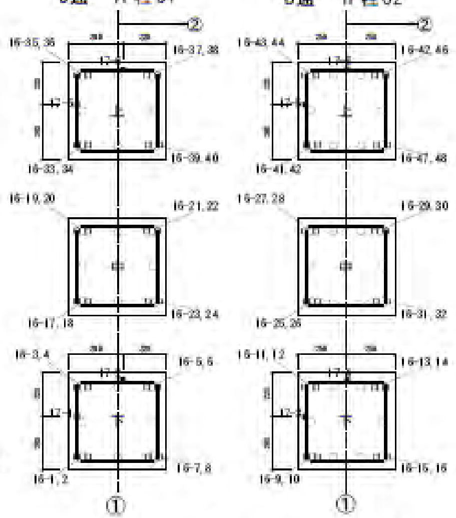

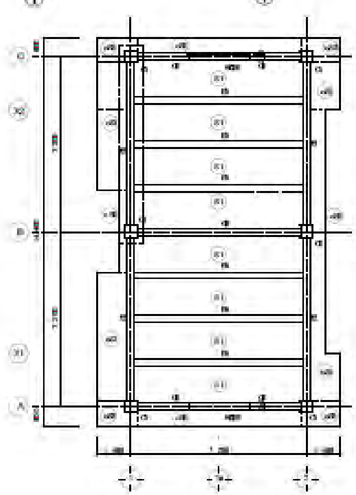

2F梁G1　C通端

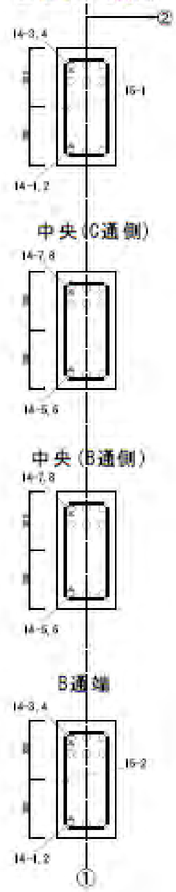

ゲージNo	凡例	呼称(対象部位)	ゲージNo	凡例	呼称(対象部位)
12	○	梁主筋歪(短辺方向)	17	■	柱補強筋歪
13	●	梁補強筋歪(短辺方向)	18	◇	壁縦筋歪
14	△	梁主筋歪(長辺方向)	19	◆	壁横筋歪
15	▲	梁補強筋歪(長辺方向)	20	☆	壁付帯柱主筋歪
16	□	柱主筋歪	21	★	壁付帯柱補強筋歪

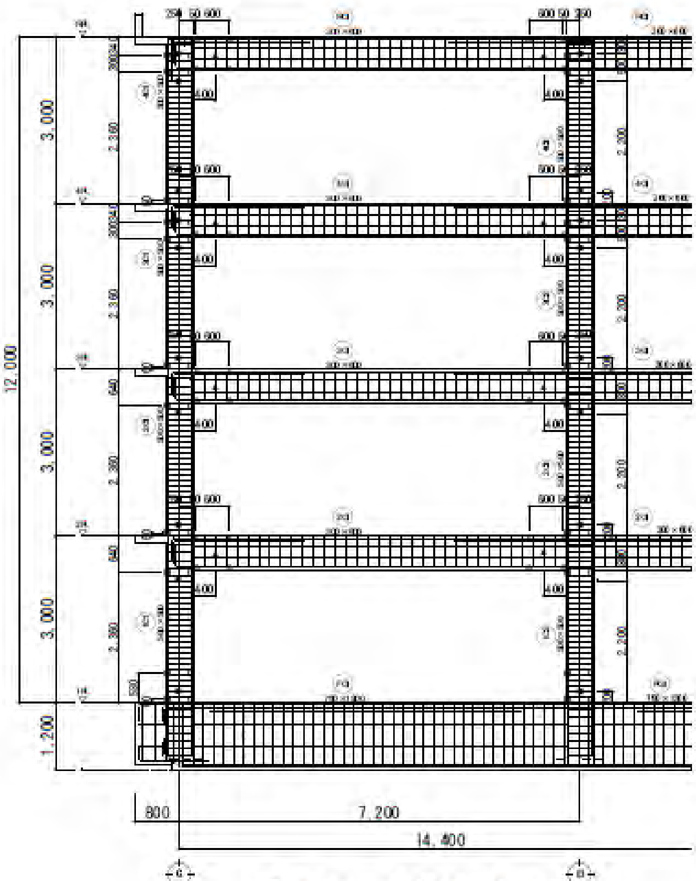

①通り　架構配筋図

RC試験体　鉄筋歪ゲージプロット図　1F柱、2F梁②

ゲージNo	凡例	呼称(対象部位)	ゲージNo	凡例	呼称(対象部位)
12	○	梁主筋歪(短辺方向)	17	■	柱補強筋歪
13	●	梁補強筋歪(短辺方向)	18	◇	壁縦筋歪
14	△	梁主筋歪(長辺方向)	19	◆	壁横筋歪
15	▲	梁補強筋歪(長辺方向)	20	☆	壁付帯柱主筋歪
16	□	柱主筋歪	21	★	壁付帯柱補強筋歪

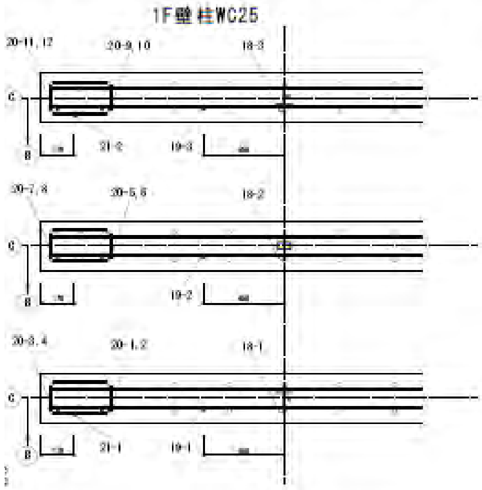

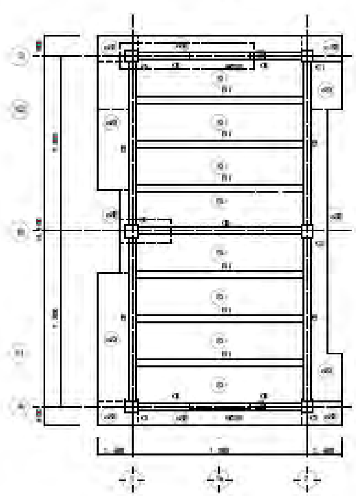

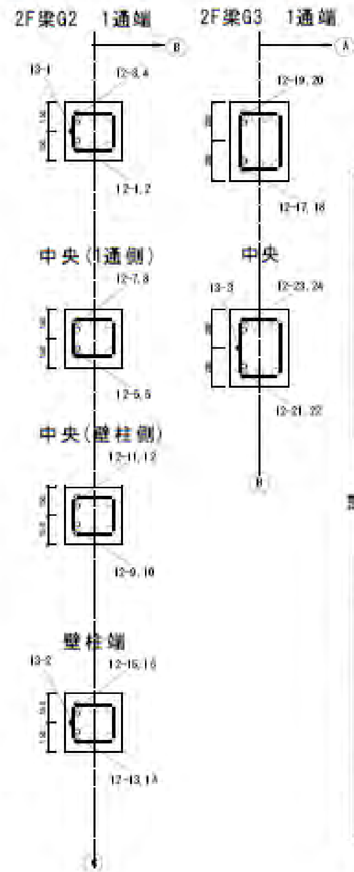

62

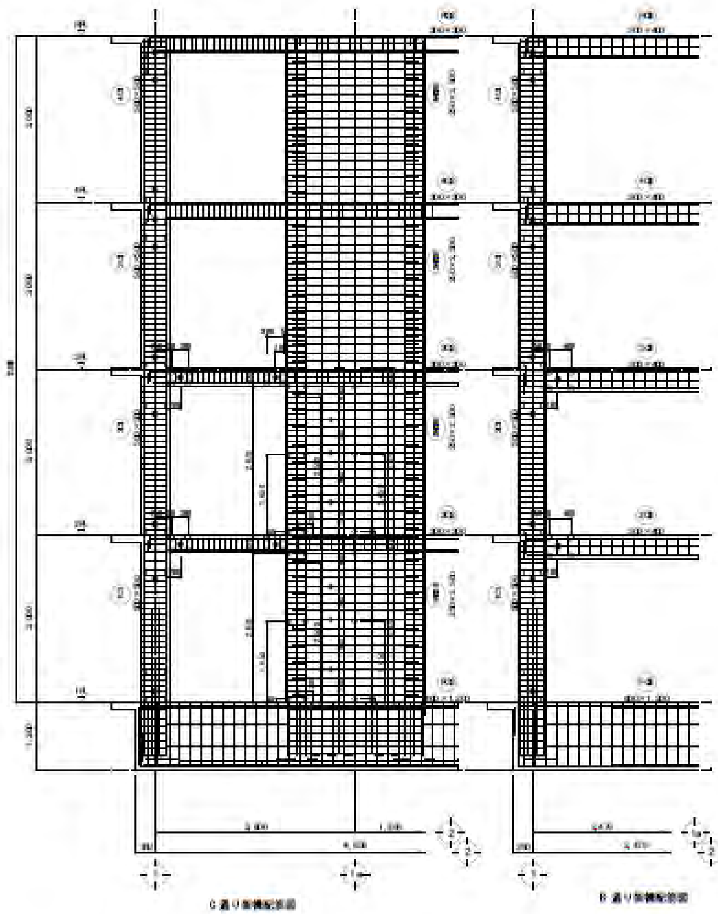

RC試験体　鉄筋歪ゲージプロット図　3F柱、4F梁

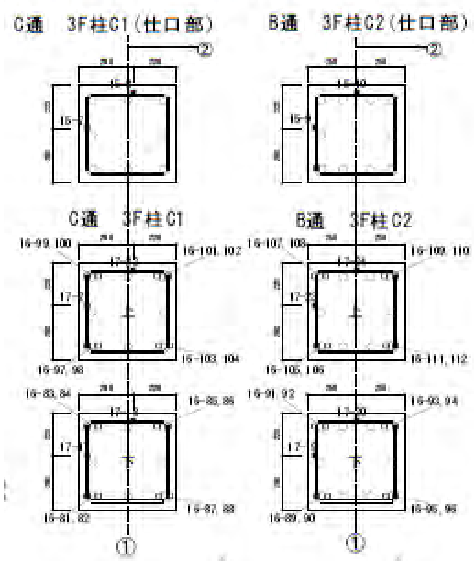

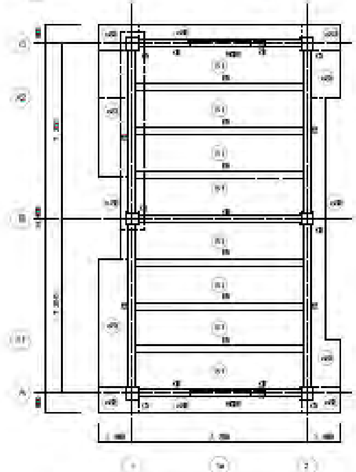

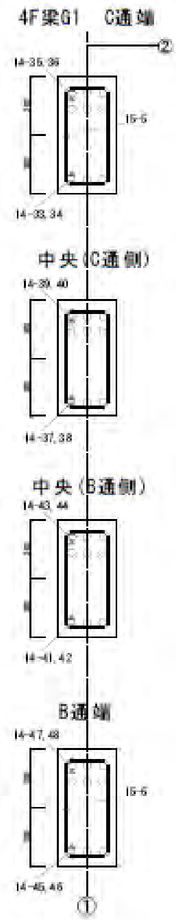

ゲージNo.	凡例	呼称(対象部位)	ゲージNo.	凡例	呼称(対象部位)
12	○	梁主筋歪(短辺方向)	17	■	柱補強筋歪
13	●	梁補強筋歪(短辺方向)	18	◇	壁縦筋歪
14	△	梁主筋歪(長辺方向)	19	◆	壁横筋歪
16	▲	梁補強筋歪(長辺方向)	20	☆	壁付帯柱主筋歪
16	□	柱主筋歪	21	★	壁付帯柱補強筋歪

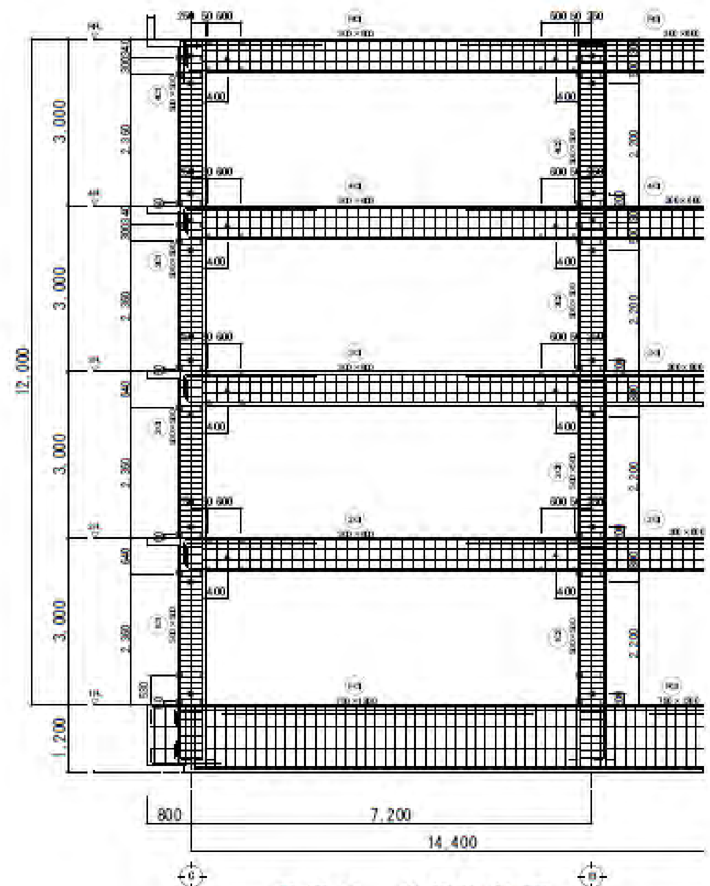

①通り　架構配筋図

RC試験体　鉄筋歪ｹﾞｰｼﾞﾌﾟﾛｯﾄ図　4F柱、RF梁

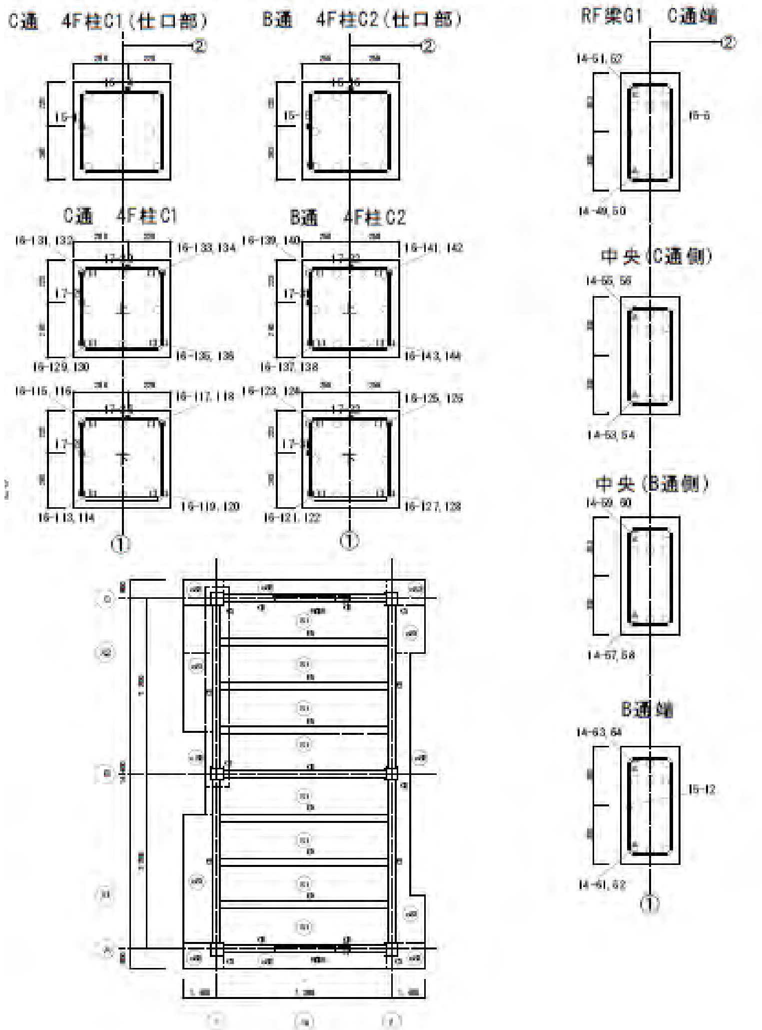

ゲージNo.	凡例	呼称（対象部位）	ゲージNo.	凡例	呼称（対象部位）
12	○	梁主筋歪（短辺方向）	17	■	柱補強筋歪
13	●	梁補強筋歪（短辺方向）	18	◇	壁縦筋歪
14	△	梁主筋歪（長辺方向）	19	◆	壁横筋歪
15	▲	梁補強筋歪（長辺方向）	20	☆	壁付帯柱主筋歪
16	□	柱主筋歪	21	★	壁付帯柱補強筋歪

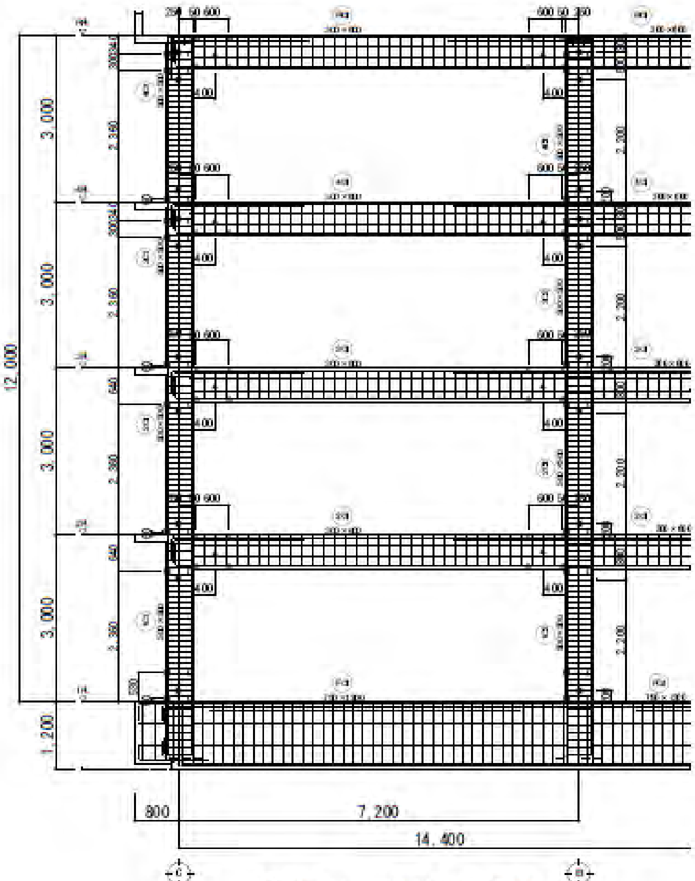

①通り　架構配筋図

PT試験体　鉄筋歪ゲージプロット図　1F壁

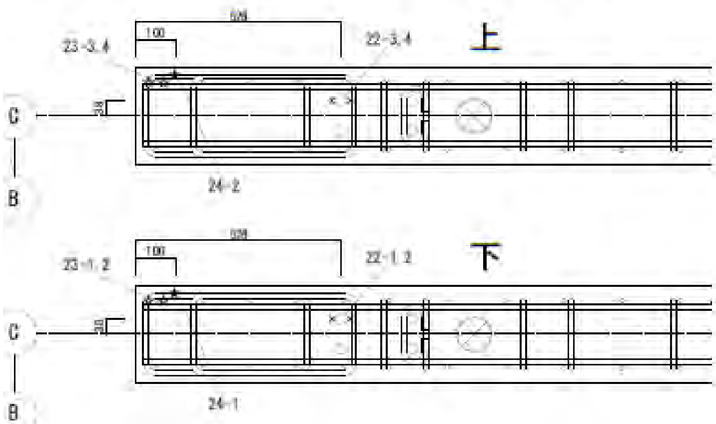

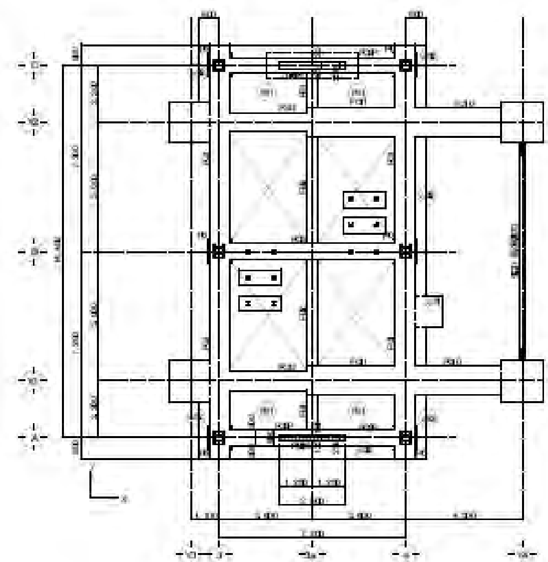

ゲージNo.	凡例	呼称（対象部位）
22	×	PC壁縦補強筋（塑性ゲージ使用）
23	☆	PC壁付帯柱主筋
24	★	PC壁付帯柱補強筋

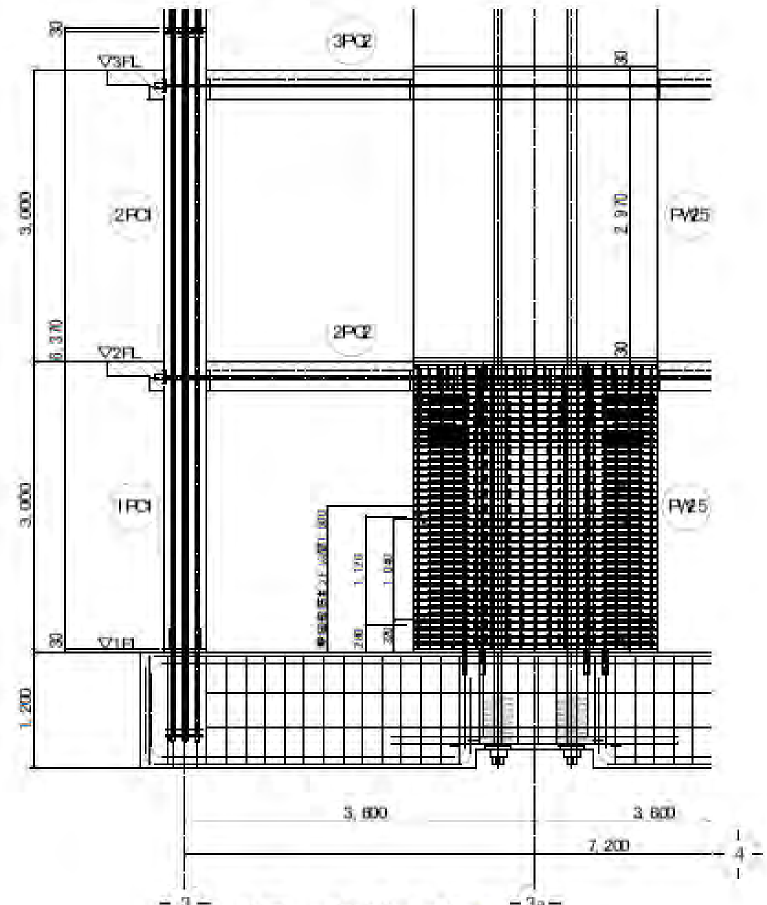

C通　架構配筋図

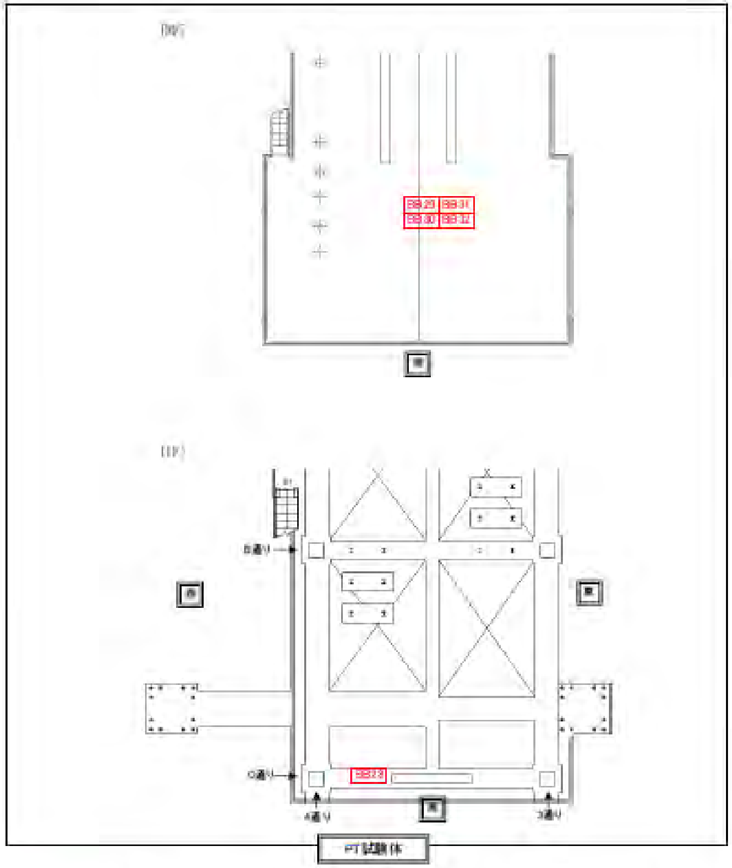

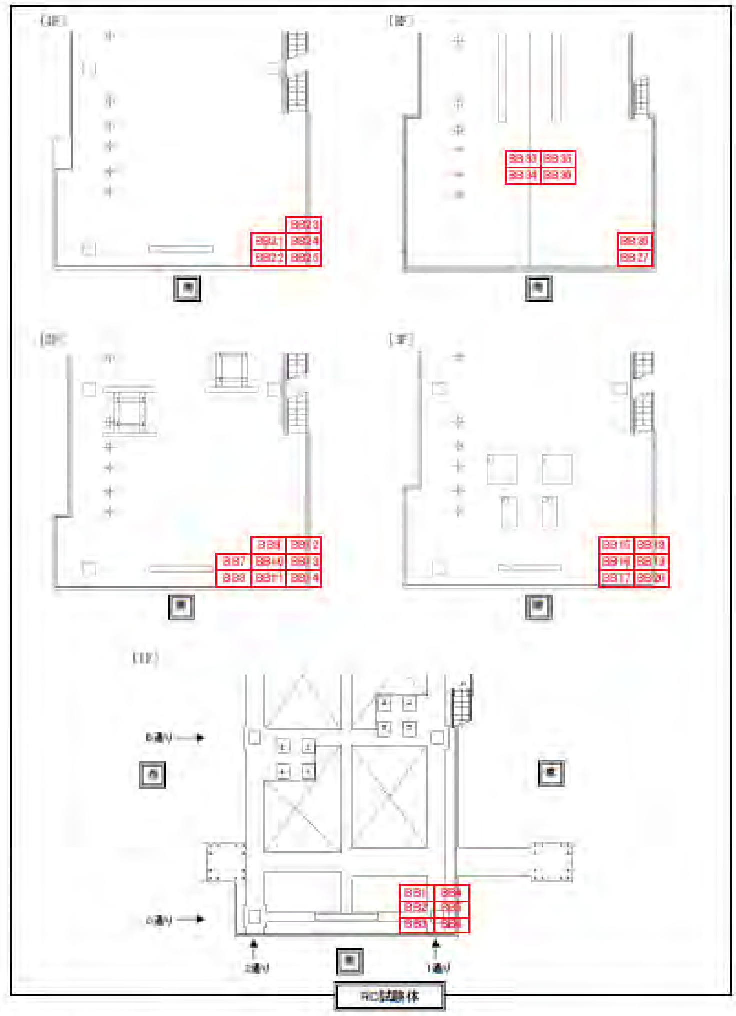

名称	機器	合計点数
BB ブリッジボックス	DBB-120A(共和電業)	36台＝PT5台＋RC31台

ブリッジボックス設置位置図

ケーブル準備表1

JB1

名称	センサータグ	長さ	ケーブル番号	接続先	試験体	種類
1-1	12-R-S1	30m	NIED-MC6-30mm-101	JB01-01	RC2F	30m4本
	12-R-S2	30m	NIED-MC6-30mm-102	JB01-02		
	12-R-S3	30m	NIED-MC6-30mm-103	JB01-03		
	12-R-S4	30m	NIED-MC6-30mm-104	JB01-04		
1-2	12-R-S5	30m	NIED-MC6-30mm-105	JB01-05	RC2F	30m4本
	12-R-S6	30m	NIED-MC6-30mm-106	JB01-06		
	12-R-S7	30m	NIED-MC6-30mm-107	JB01-07		
	12-R-S8	30m	NIED-MC6-30mm-108	JB01-08		
1-3	12-R-S9	30m	NIED-MC6-30mm-109	JB01-09	RC2F	30m4本
	12-R-S10	30m	NIED-MC6-30mm-110	JB01-10		
	12-R-S11	30m	NIED-MC6-30mm-111	JB01-11		
	12-R-S12	30m	NIED-MC6-30mm-112	JB01-12		
1-4	12-R-S13	30m	NIED-MC6-30mm-113	JB01-13	RC2F	30m4本
	12-R-S14	30m	NIED-MC6-30mm-114	JB01-14		
	12-R-S15	30m	NIED-MC6-30mm-115	JB01-15		
	12-R-S16	30m	NIED-MC6-30mm-116	JB01-16		
1-5	12-R-S17	30m	NIED-MC6-30mm-117	JB01-17	RC2F	30m4本
	12-R-S18	30m	NIED-MC6-30mm-118	JB01-18		
	12-R-S19	30m	NIED-MC6-30mm-119	JB01-19		
	12-R-S20	30m	NIED-MC6-30mm-120	JB01-20		
1-6	12-R-S21	30m	NIED-MC6-30mm-121	JB01-21	RC2F	30m4本
	12-R-S22	30m	NIED-MC6-30mm-122	JB01-22		
	12-R-S23	30m	NIED-MC6-30mm-123	JB01-23		
	12-R-S24	30m	NIED-MC6-30mm-124	JB01-24		
1-7	13-R-S1	30m	NIED-MC6-30mm-125	JB01-25	RC2F	30m3本
	13-R-S2	30m	NIED-MC6-30mm-126	JB01-26		
	13-R-S3	30m	NIED-MC6-30mm-127	JB01-27		
1-8	13-R-S4	30m	NIED-MC6-30mm-128	JB01-28	RC2F	30m3本
	13-R-S5	30m	NIED-MC6-30mm-129	JB01-29		
	13-R-S6	30m	NIED-MC6-30mm-130	JB01-30		
1-9	14-R-S1	30m	NIED-MC6-30mm-131	JB01-31	RC2F	30m4本
	14-R-S2	30m	NIED-MC6-30mm-132	JB01-32		
	14-R-S3	30m	NIED-MC6-30mm-133	JB01-33		
	14-R-S4	30m	NIED-MC6-30mm-134	JB01-34		
1-10	14-R-S5	30m	NIED-MC6-30mm-135	JB01-35	RC2F	30m4本
	14-R-S6	30m	NIED-MC6-30mm-136	JB01-36		
	14-R-S7	30m	NIED-MC6-30mm-137	JB01-37		
	14-R-S8	30m	NIED-MC6-30mm-138	JB01-38		
1-11	14-R-S9	30m	NIED-MC6-30mm-139	JB01-39	RC2F	30m4本
	14-R-S10	30m	NIED-MC6-30mm-140	JB01-40		
	14-R-S11	30m	NIED-MC6-30mm-141	JB01-41		
	14-R-S12	30m	NIED-MC6-30mm-142	JB01-42		
1-12	14-R-S13	30m	NIED-MC6-30mm-143	JB01-43	RC2F	30m4本
	14-R-S14	30m	NIED-MC6-30mm-144	JB01-44		
	14-R-S15	30m	NIED-MC6-30mm-145	JB01-45		
	14-R-S16	30m	NIED-MC6-30mm-146	JB01-46		
1-13	14-R-S17	40m	NIED-2008-40mm-001	JB01-47	RC4F	40m4本
	14-R-S18	40m	NIED-2008-40mm-002	JB01-48		
	14-R-S19	40m	NIED-2008-40mm-003	JB01-49		
	14-R-S20	40m	NIED-2008-40mm-004	JB01-50		
1-14	14-R-S21	40m	NIED-2008-40mm-005	JB01-51	RC4F	40m4本
	14-R-S22	40m	NIED-2008-40mm-006	JB01-52		
	14-R-S23	40m	NIED-2008-40mm-007	JB01-53		
	14-R-S24	40m	NIED-2008-40mm-008	JB01-54		
1-15	14-R-S25	40m	NIED-2008-40mm-009	JB01-55	RCRF	40m4本
	14-R-S26	40m	NIED-2008-40mm-010	JB01-56		
	14-R-S27	40m	NIED-2008-40mm-011	JB01-57		
	14-R-S28	40m	NIED-2008-40mm-012	JB01-58		
1-16	14-R-S29	40m	NIED-2008-40mm-013	JB01-59	RCRF	40m4本
	14-R-S30	40m	NIED-2008-40mm-014	JB01-60		
	14-R-S31	40m	NIED-2008-40mm-015	JB01-61		
	14-R-S32	40m	NIED-2008-40mm-016	JB01-62		

JB02

名称	センサータグ	長さ	ケーブル番号	接続先	試験体	種類
2-1	15-R-S1	30m	NIED-MC8-30mm-147	JB02-01	RC2F	30m2本
	15-R-S2	30m	NIED-MC8-30mm-148	JB02-02		
2-2	15-R-S3	30m	NIED-MC8-30mm-149	JB02-03	RC3F	30m2本
	15-R-S4	30m	NIED-MC8-30mm-150	JB02-04		
2-3	15-R-S5	40m	NIED-2008-40mm-017	JB02-05	RC4F	40m2本
	15-R-S6	40m	NIED-2008-40mm-018	JB02-06		
2-4	15-R-S7	40m	NIED-2008-40mm-019	JB02-07	RCRF	40m2本
	15-R-S8	40m	NIED-2008-40mm-020	JB02-08		
2-5	25-R-S1	40m	NIED-2008-40mm-021	JB02-09	RC4F	40m4本
	25-R-S2	40m	NIED-2008-40mm-022	JB02-10		
	25-R-S3	40m	NIED-2008-40mm-023	JB02-11		
	25-R-S4	40m	NIED-2008-40mm-024	JB02-12		
2-6	25-R-S5	40m	NIED-2008-40mm-025	JB02-13	RCRF	40m4本
	25-R-S6	40m	NIED-2008-40mm-026	JB02-14		
	25-R-S7	40m	NIED-2008-40mm-027	JB02-15		
	25-R-S8	40m	NIED-2008-40mm-028	JB02-16		
2-7	16-R-S1	30m	NIED-MC8-30mm-151	JB02-17	RC1F	30m4本
	16-R-S2	30m	NIED-MC8-30mm-152	JB02-18		
	16-R-S3	30m	NIED-MC8-30mm-153	JB02-19		
	16-R-S4	30m	NIED-MC8-30mm-154	JB02-20		
2-8	16-R-S5	30m	NIED-MC8-30mm-155	JB02-21	RC1F	30m4本
	16-R-S6	30m	NIED-MC8-30mm-156	JB02-22		
	16-R-S7	30m	NIED-MC8-30mm-157	JB02-23		
	16-R-S8	30m	NIED-MC8-30mm-158	JB02-24		
2-9	16-R-S9	30m	NIED-MC8-30mm-159	JB02-25	RC1F	30m4本
	16-R-S10	30m	NIED-MC8-30mm-160	JB02-26		
	16-R-S11	30m	NIED-MC8-30mm-161	JB02-27		
	16-R-S12	30m	NIED-MC8-30mm-162	JB02-28		
2-10	16-R-S13	30m	NIED-MC8-30mm-163	JB02-29	RC1F	30m4本
	16-R-S14	30m	NIED-MC8-30mm-164	JB02-30		
	16-R-S15	30m	NIED-MC8-30mm-165	JB02-31		
	16-R-S16	30m	NIED-MC8-30mm-166	JB02-32		
2-11	16-R-S17	30m	NIED-MC8-30mm-167	JB02-33	RC1F	30m4本
	16-R-S18	30m	NIED-MC8-30mm-168	JB02-34		
	16-R-S19	30m	NIED-MC8-30mm-169	JB02-35		
	16-R-S20	30m	NIED-MC8-30mm-170	JB02-36		
2-12	16-R-S21	30m	NIED-MC8-30mm-171	JB02-37	RC1F	30m4本
	16-R-S22	30m	NIED-MC8-30mm-172	JB02-38		
	16-R-S23	30m	NIED-MC8-30mm-173	JB02-39		
	16-R-S24	30m	NIED-MC8-30mm-174	JB02-40		
2-13	16-R-S25	30m	NIED-MC8-30mm-175	JB02-41	RC2F	30m4本
	16-R-S26	30m	NIED-MC8-30mm-176	JB02-42		
	16-R-S27	30m	NIED-MC8-30mm-177	JB02-43		
	16-R-S28	30m	NIED-MC8-30mm-178	JB02-44		
2-14	16-R-S29	30m	NIED-MC8-30mm-179	JB02-45	RC2F	30m4本
	16-R-S30	30m	NIED-MC8-30mm-180	JB02-46		
	16-R-S31	30m	NIED-MC8-30mm-181	JB02-47		
	16-R-S32	30m	NIED-MC8-30mm-182	JB02-48		
2-15	16-R-S33	30m	NIED-MC8-30mm-183	JB02-49	RC2F	30m4本
	16-R-S34	30m	NIED-MC8-30mm-184	JB02-50		
	16-R-S35	30m	NIED-MC8-30mm-185	JB02-51		
	16-R-S36	30m	NIED-MC8-30mm-186	JB02-52		
2-16	16-R-S37	30m	NIED-MC8-30mm-187	JB02-53	RC2F	30m4本
	16-R-S38	30m	NIED-MC8-30mm-188	JB02-54		
	16-R-S39	30m	NIED-MC8-30mm-189	JB02-55		
	16-R-S40	30m	NIED-MC8-30mm-190	JB02-56		
2-17	8-R1-DA1aY	20m		JB02-63	RC1F	20m1本
2-18	8-R1-DC1aY	20m		JB02-64	RC1F	20m1本

JB03

名称	センサータグ	長さ	ケーブル番号	接続先	試験体	種類
3-1	16-R-S41	30m	NIED-MC8-30mm-191	JB03-01	RC3F	30m4本
	16-R-S42	30m	NIED-MC8-30mm-192	JB03-02		
	16-R-S43	30m	NIED-MC8-30mm-193	JB03-03		
	16-R-S44	30m	NIED-MC8-30mm-194	JB03-04		
3-2	16-R-S45	30m	NIED-MC8-30mm-195	JB03-05	RC3F	30m4本
	16-R-S46	30m	NIED-MC8-30mm-196	JB03-06		
	16-R-S47	30m	NIED-MC8-30mm-197	JB03-07		
	16-R-S48	30m	NIED-MC8-30mm-198	JB03-08		
3-3	16-R-S49	30m	NIED-MC8-30mm-199	JB03-09	RC3F	30m4本
	16-R-S50	30m	NIED-MC8-30mm-200	JB03-10		
	16-R-S51	30m	NIED-MC8-30mm-201	JB03-11		
	16-R-S52	30m	NIED-MC8-30mm-202	JB03-12		
3-4	16-R-S53	30m	NIED-MC8-30mm-203	JB03-13	RC3F	30m4本
	16-R-S54	30m	NIED-MC8-30mm-204	JB03-14		
	16-R-S55	30m	NIED-MC8-30mm-205	JB03-15		
	16-R-S56	30m	NIED-MC8-30mm-206	JB03-16		
3-5	16-R-S57	40m	NIED-2008-40mm-029	JB03-17	RC4F	40m4本
	16-R-S58	40m	NIED-2008-40mm-030	JB03-18		
	16-R-S59	40m	NIED-2008-40mm-031	JB03-19		
	16-R-S60	40m	NIED-2008-40mm-032	JB03-20		
3-6	16-R-S61	40m	NIED-2008-40mm-033	JB03-21	RC4F	40m4本
	16-R-S62	40m	NIED-2008-40mm-034	JB03-22		
	16-R-S63	40m	NIED-2008-40mm-035	JB03-23		
	16-R-S64	40m	NIED-2008-40mm-036	JB03-24		
3-7	16-R-S65	40m	NIED-2008-40mm-037	JB03-25	RC4F	40m4本
	16-R-S66	40m	NIED-2008-40mm-038	JB03-26		
	16-R-S67	40m	NIED-2008-40mm-039	JB03-27		
	16-R-S68	40m	NIED-2008-40mm-040	JB03-28		
3-8	16-R-S69	40m	NIED-2008-40mm-041	JB03-29	RC4F	40m4本
	16-R-S70	40m	NIED-2008-40mm-042	JB03-30		
	16-R-S71	40m	NIED-2008-40mm-043	JB03-31		
	16-R-S72	40m	NIED-2008-40mm-044	JB03-32		
3-9	17-R-S1	30m	NIED-MC8-30mm-207	JB03-33	RC1F	30m4本
	17-R-S2	30m	NIED-MC8-30mm-208	JB03-34		
	17-R-S3	30m	NIED-MC8-30mm-209	JB03-35		
	17-R-S4	30m	NIED-MC8-30mm-210	JB03-36		
3-10	17-R-S5	30m	NIED-MC8-30mm-211	JB03-37	RC1F	30m4本
	17-R-S6	30m	NIED-MC8-30mm-212	JB03-38		
	17-R-S7	30m	NIED-MC8-30mm-213	JB03-39		
	17-R-S8	30m	NIED-MC8-30mm-214	JB03-40		
3-11	17-R-S9	30m	NIED-MC8-30mm-215	JB03-41	RC2F	30m4本
	17-R-S10	30m	NIED-MC8-30mm-216	JB03-42		
	17-R-S11	30m	NIED-MC8-30mm-217	JB03-43		
	17-R-S12	30m	NIED-MC8-30mm-218	JB03-44		
3-12	17-R-S13	30m	NIED-MC8-30mm-219	JB03-45	RC2F	30m4本
	17-R-S14	30m	NIED-MC8-30mm-220	JB03-46		
	17-R-S15	30m	H19/9-6芯-オスメス-001	JB03-47		
	17-R-S16	30m	H19/9-6芯-オスメス-002	JB03-48		
3-13	17-R-S17	30m	H19/9-6芯-オスメス-003	JB03-49	RC2F	30m4本
	17-R-S18	30m	H19/9-6芯-オスメス-004	JB03-50		
	17-R-S19	30m	H19/9-6芯-オスメス-005	JB03-51		
	17-R-S20	30m	H19/9-6芯-オスメス-006	JB03-52		
3-14	17-R-S21	30m	H19/9-6芯-オスメス-007	JB03-53	RC2F	30m4本
	17-R-S22	30m	H19/9-6芯-オスメス-008	JB03-54		
	17-R-S23	30m	H19/9-6芯-オスメス-009	JB03-55		
	17-R-S24	30m	H19/9-6芯-オスメス-010	JB03-56		
3-15	17-R-S25	40m	NIED-2008-40mm-045	JB03-57	RC4F	40m4本
	17-R-S26	40m	NIED-2008-40mm-046	JB03-58		
	17-R-S27	40m	NIED-2008-40mm-047	JB03-59		
	17-R-S28	40m	NIED-2008-40mm-048	JB03-60		
3-16	17-R-S29	40m	NIED-2008-40mm-049	JB03-61	RC4F	40m4本
	17-R-S30	40m	NIED-2008-40mm-050	JB03-62		
	17-R-S31	40m	NIED-2008-40mm-051	JB03-63		
	17-R-S32	40m	NIED-2008-40mm-052	JB03-64		

ケーブル準備表2

JB04

名称	センサータグ	長さ	ケーブル番号	接続先	試験体	種類
4-1	18-R-S1	30m	H19/9-6芯-オスメス-011	JB04-01	RC1F	30m3本
	18-R-S2	30m	H19/9-6芯-オスメス-012	JB04-02		
	18-R-S3	30m	H19/9-6芯-オスメス-013	JB04-03		
4-2	18-R-S4	30m	H19/9-6芯-オスメス-014	JB04-04	RC2F	30m3本
	18-R-S5	30m	H19/9-6芯-オスメス-015	JB04-05		
	18-R-S6	30m	H19/9-6芯-オスメス-016	JB04-06		
4-3	19-R-S1	30m	H19/9-6芯-オスメス-017	JB04-07	RC1F	30m3本
	19-R-S2	30m	H19/9-6芯-オスメス-018	JB04-08		
	19-R-S3	30m	H19/9-6芯-オスメス-019	JB04-09		
4-4	19-R-S4	30m	H19/9-6芯-オスメス-020	JB04-10	RC2F	30m3本
	19-R-S5	30m	H19/9-6芯-オスメス-021	JB04-11		
	19-R-S6	30m	H19/9-6芯-オスメス-022	JB04-12		
4-5	20-R-S1	30m	H19/9-6芯-オスメス-023	JB04-13	RC1F	30m3本
	20-R-S2	30m	H19/9-6芯-オスメス-024	JB04-14		
	20-R-S3	30m	H19/9-6芯-オスメス-025	JB04-15		
4-6	20-R-S4	30m	H19/9-6芯-オスメス-026	JB04-16	RC1F	30m3本
	20-R-S5	30m	H19/9-6芯-オスメス-027	JB04-17		
	20-R-S6	30m	H19/9-6芯-オスメス-028	JB04-18		
4-7	20-R-S7	30m	H19/9-6芯-オスメス-029	JB04-19	RC2F	30m3本
	20-R-S8	30m	H19/9-6芯-オスメス-030	JB04-20		
	20-R-S9	30m	H19/9-6芯-オスメス-031	JB04-21		
4-8	20-R-S10	30m	H19/9-6芯-オスメス-032	JB04-22	RC2F	30m3本
	20-R-S11	30m	H19/9-6芯-オスメス-033	JB04-23		
	20-R-S12	30m	H19/9-6芯-オスメス-034	JB04-24		
4-9	21-R-S1	30m	H19/9-6芯-オスメス-035	JB04-25	RC1F	30m2本
	21-R-S2	30m	H19/9-6芯-オスメス-036	JB04-26		
4-10	21-R-S3	30m	H19/9-6芯-オスメス-037	JB04-27	RC2F	30m2本
	21-R-S4	30m	H19/9-6芯-オスメス-038	JB04-28		
4-A1	A1-R1N-D1	20m	NIED-MC6-20m-001	JB04-31	RC1F	20m6本
	A1-R1N-D2	20m	NIED-MC6-20m-002	JB04-32		
	A1-R1N-D3	20m	NIED-MC6-20m-003	JB04-33		
	A1-R1N-D4	20m	NIED-MC6-20m-004	JB04-34		
	A1-R1N-D5	20m	NIED-MC6-20m-005	JB04-35		
	A1-R1N-D6	20m	NIED-MC6-20m-006	JB04-36		
4-A2	A1-R1N-D7	20m	NIED-MC6-20m-007	JB04-37	RC1F	20m4本
	A1-R1N-D8	20m	NIED-MC6-20m-008	JB04-38		
	A1-R1N-D9	20m	NIED-MC6-20m-009	JB04-39		
	A1-R1N-D10	20m	NIED-MC6-20m-010	JB04-40		
4-A3	A1-R2N-D11	20m	NIED-MC6-20m-011	JB04-41	RC2F	20m2本
	A1-R2N-D12	20m	NIED-MC6-20m-012	JB04-42		
4-A4	A1-R3N-D13	20m	NIED-MC6-20m-013	JB04-43	RC3F	20m2本
	A1-R3N-D14	20m	NIED-MC6-20m-014	JB04-44		
4-A5	A1-R4N-D15	30m	H19/9-6芯-オスメス-049	JB04-45	RC4F	30m2本
	A1-R4N-D16	30m	H19/9-6芯-オスメス-050	JB04-46		
4-A6	A3-R1-D1	20m	NIED-MC6-20m-019	JB04-51	RC1F	20m2本
	A3-R1-D2	20m	NIED-MC6-20m-020	JB04-52		
4-A7	A3-R2-D3	30m	H19/9-6芯-オスメス-077	JB04-53	RC2F	30m2本
	A3-R2-D4	30m	H19/9-6芯-オスメス-078	JB04-54		
4-A8	A3-R3-D5	30m	H21-NIED-MC6-30mm-087	JB04-55	RC3F	30m2本
	A3-R3-D6	30m	H21-NIED-MC6-30mm-088	JB04-56		
4-A9	A3-R3-D7	30m	H21-NIED-MC6-30mm-089	JB04-57	RC3F	30m2本
	A3-R3-D8	30m	H21-NIED-MC6-30mm-090	JB04-58		
4-A10	A3-R4-D9	40m	H21-NIED-MC6-40mm-075	JB04-59	RC4F	40m2本
	A3-R4-D10	40m	H21-NIED-MC6-40mm-076	JB04-60		

JB05

名称	センサータグ	長さ	ケーブル番号	接続先	試験体	種類
5-1	2-R2-A1X	30m	H19/9-6芯-オスメス-039	JB05-01	RC2F	30m3本
	2-R2-A1Y	30m	H19/9-6芯-オスメス-040	JB05-02		
	2-R2-A1Z	30m	H19/9-6芯-オスメス-041	JB05-03		
5-2	2-R3-A1X	30m	H19/9-6芯-オスメス-042	JB05-04	RC3F	30m3本
	2-R3-A1Y	30m	H19/9-6芯-オスメス-043	JB05-05		
	2-R3-A1Z	30m	H19/9-6芯-オスメス-044	JB05-06		
5-3	2-R4-A1X	40m	NIED-2008-40mm-053	JB05-07	RC4F	40m3本
	2-R4-A1Y	40m	NIED-2008-40mm-054	JB05-08		
	2-R4-A1Z	40m	NIED-2008-40mm-055	JB05-09		
5-4	2-RR-A1X	40m	NIED-2008-40mm-056	JB05-10	RCRF	40m3本
	2-RR-A1Y	40m	NIED-2008-40mm-057	JB05-11		
	2-RR-A1Z	40m	NIED-2008-40mm-058	JB05-12		
5-5	3-R1-D1XT	レ1本	アンプ側 85	JB05-13	RC1F	レーザ
	3-R1-D1XB	レ3本	アンプ側 89－507－508	JB05-14		
	3-R1-D1YT	レ1本	アンプ側 88	JB05-15	アンプ－JB接続の為	
	3-R1-D1YB	レ1本	アンプ側 87	JB05-16		
	3-R1-D1XB	30m		JB05-14		30m1本
5-6	3-R2-D1XT	レ2本	アンプ側 83－84	JB05-17	RC2F	レーザ
	3-R2-D1XB	レ2本	アンプ側 80－72	JB05-18		
	3-R2-D1YT	レ2本	アンプ側 79－78	JB05-19		
	3-R2-D1YB	レ2本	アンプ側 23－509	JB05-20		
5-7	3-R3-D1XT	レ3本	アンプ側 22－31－21	JB05-21	RC3F	レーザ
	3-R3-D1XB	レ3本	アンプ側 35－36－39	JB05-22		
	3-R3-D1YT	レ3本	アンプ側 33－32－40	JB05-23		
	3-R3-D1YB	レ3本	アンプ側 11－12－10	JB05-24		
5-8	3-R4-D1XT	レ3本	アンプ側 9－6－5	JB05-25	RC4F	レーザ
	3-R4-D1XB	レ3本	アンプ側 4－2－1	JB05-26		
	3-R4-D1YT	レ3本	アンプ側 90－61－13	JB05-27		
	3-R4-D1YB	レ3本	アンプ側 45－42－51	JB05-28		
5-9	32-R1-D1Z	30m	H19/9-6芯-オスメス-045	JB05-29	RC1F	30m1本
5-10	32-R2-D1Z	30m	H19/9-6芯-オスメス-047	JB05-31	RC2F	30m1本
5-11	32-R3-D1Z	40m	H21-NIED-MC6-40mm-038	JB05-33	RC3F	40m1本
5-12	32-R4-D1Z	40m	NIED-2008-40mm-059	JB05-35	RC4F	40m1本
5-13	32-R1-D2Z	30m	H19/9-6芯-オスメス-046	JB05-30	RC1F	30m5本
	4-R1-D2XT	30m	H19/9-6芯-オスメス-051	JB05-37		
	4-R1-D2XB	30m	H19/9-6芯-オスメス-052	JB05-38		
	4-R1-D2YT	30m	H19/9-6芯-オスメス-053	JB05-39		
	4-R1-D2YB	30m	H19/9-6芯-オスメス-054	JB05-40		
5-14	4-R1-D3XT	30m	H19/9-6芯-オスメス-055	JB05-41	RC1F	30m4本
	4-R1-D3XB	30m	H19/9-6芯-オスメス-056	JB05-42		
	4-R1-D3YT	30m	H19/9-6芯-オスメス-057	JB05-43		
	4-R1-D3YB	30m	H19/9-6芯-オスメス-058	JB05-44		
5-15	32-R2-D2Z	30m	H19/9-6芯-オスメス-048	JB05-32	RC2F	30m5本
	4-R2-D2XT	30m	H19/9-6芯-オスメス-059	JB05-45		
	4-R2-D2XB	30m	H19/9-6芯-オスメス-060	JB05-46		
	4-R2-D2YT	30m	H19/9-6芯-オスメス-061	JB05-47		
	4-R2-D2YB	30m	H19/9-6芯-オスメス-062	JB05-48		
5-16	4-R2-D3XT	30m	H19/9-6芯-オスメス-063	JB05-49	RC2F	30m4本
	4-R2-D3XB	30m	H19/9-6芯-オスメス-064	JB05-50		
	4-R2-D3YT	30m	H19/9-6芯-オスメス-065	JB05-51		
	4-R2-D3YB	30m	H19/9-6芯-オスメス-066	JB05-52		
5-17	32-R3-D2Z	40m	H21-NIED-MC6-40mm-039	JB05-34	RC3F	40m5本
	4-R3-D2XT	40m	NIED-2008-40mm-061	JB05-53		
	4-R3-D2XB	40m	NIED-2008-40mm-062	JB05-54		
	4-R3-D2YT	40m	NIED-2008-40mm-063	JB05-55		
	4-R3-D2YB	40m	NIED-2008-40mm-064	JB05-56		
5-18	4-R3-D3XT	40m	NIED-2008-40mm-065	JB05-57	RC3F	40m4本
	4-R3-D3XB	40m	NIED-2008-40mm-066	JB05-58		
	4-R3-D3YT	40m	NIED-2008-40mm-067	JB05-59		
	4-R3-D3YB	40m	NIED-2008-40mm-068	JB05-60		
5-19	32-R4-D2Z	40m	NIED-2008-40mm-060	JB05-36	RC4F	40m5本
	4-R4-D2XT	40m	NIED-2008-40mm-069	JB05-61		
	4-R4-D2XB	40m	NIED-2008-40mm-070	JB05-62		
	4-R4-D2YT	40m	NIED-2008-40mm-071	JB05-63		
	4-R4-D2YB	40m	NIED-2008-40mm-072	JB05-64		

JB06

名称	センサータグ	長さ	ケーブル番号	接続先	試験体	種類
6-A1	A1-P1N-D1	10m		JB06-01	PT1F	10m2本
	A1-P1N-D2	10m		JB06-02		
6-A2	A1-P1N-D3	10m	NIED-MC6-10mm-001	JB06-03	PT1F	10m4本
	A1-P1N-D4	10m	NIED-MC6-10mm-002	JB06-04		
	A1-P1N-D5	10m	NIED-MC6-10mm-003	JB06-05		
	A1-P1N-D6	10m	NIED-MC6-10mm-004	JB06-06		
6-A3	A1-P1N-D7	10m	NIED-MC6-10mm-005	JB06-07	PT1F	10m4本
	A1-P1N-D8	10m	NIED-MC6-10mm-006	JB06-08		
	A1-P1N-D9	10m	NIED-MC6-10mm-007	JB06-09		
	A1-P1N-D10	10m	NIED-MC6-10mm-008	JB06-10		
6-A4	A1-P2N-D11	20m	NIED-MC6-20mm-021	JB06-11	PT2F	20m2本
	A1-P2N-D12	20m	NIED-MC6-20mm-022	JB06-12		
6-A5	A1-P3N-D13	20m	NIED-MC6-20mm-023	JB06-13	PT3F	20m2本
	A1-P3N-D14	20m	NIED-MC6-20mm-024	JB06-14		
6-A6	A1-P4N-D15	30m	H21-NIED-MC6-30mm-091	JB06-15	PT4F	30m2本
	A1-P4N-D16	30m	H21-NIED-MC6-30mm-092	JB06-16		
6-1	2-P1-A1X	20m		JB06-21	PT1F	20m3本
	2-P1-A1Y	20m		JB06-22		
	2-P1-A1Z	20m		JB06-23		
6-2	2-P1-A2X	30m		JB06-24	PT1F	30m3本
	2-P1-A2Y	30m		JB06-25		
	2-P1-A2Z	30m		JB06-26		
6-3	2-R1-A1X	30m		JB06-27	RC1F	30m3本
	2-R1-A1Y	30m		JB06-28		
	2-R1-A1Z	30m		JB06-29		
6-4	2-R1-A2X	40m		JB06-30	RC1F	40m3本
	2-R1-A2Y	40m		JB06-31		
	2-R1-A2Z	40m		JB06-32		

ケーブル準備表3

JB07						
名称	センサータグ	長さ	ケーブル番号	接続先	試験体	種類
7-1	2-P2-A1X	30m	H19/9-6芯-オスメス-067	JB07-01	PT2F	30m3本
	2-P2-A1Y	30m	H19/9-6芯-オスメス-068	JB07-02		
	2-P2-A1Z	30m	H19/9-6芯-オスメス-069	JB07-03		
7-2	2-P3-A1X	30m	H19/9-6芯-オスメス-070	JB07-04	PT3F	30m3本
	2-P3-A1Y	30m	H19/9-6芯-オスメス-071	JB07-05		
	2-P3-A1Z	30m	H19/9-6芯-オスメス-072	JB07-06		
7-3	2-P4-A1X	40m	NIED-2008-40mm-073	JB07-07	PT4F	40m3本
	2-P4-A1Y	40m	NIED-2008-40mm-074	JB07-08		
	2-P4-A1Z	40m	NIED-2008-40mm-075	JB07-09		
7-4	2-PR-A1X	40m	NIED-2008-40mm-076	JB07-10	PTRF	40m3本
	2-PR-A1Y	40m	NIED-2008-40mm-077	JB07-11		
	2-PR-A1Z	40m	NIED-2008-40mm-078	JB07-12		
7-5	3-P1-D1XT	L1本	アンプ側 69	JB07-13	PT1F	レーザ
	3-P1-D1XB	L1本	アンプ側 68	JB07-14		
	3-P1-D1YT	L1本	アンプ側 65	JB07-15		
	3-P1-D1YB	L1本	アンプ側 501	JB07-16		
7-6	3-P2-D1XT	L2本	アンプ側 60 − 70	JB07-17	PT2F	レーザ
	3-P2-D1XB	L2本	アンプ側 55 − 54	JB07-18		
	3-P2-D1YT	L2本	アンプ側 17 − 15	JB07-19		
	3-P2-D1YB	L2本	アンプ側 19 − 18	JB07-20		
7-7	3-P3-D1XT	L3本	アンプ側 8 − 59 − 63	JB07-21	PT3F	レーザ
	3-P3-D1XB	L3本	アンプ側 28 − 25 − 24	JB07-22		
	3-P3-D1YT	L3本	アンプ側 502 − 503 − 504	JB07-23		
	3-P3-D1YB	L3本	アンプ側 27 − 29 − 30	JB07-24		
7-8	3-P4-D1XT	L3本	アンプ側 73 − 78 − 74	JB07-25	PT4F	レーザ
	3-P4-D1XB	L3本	アンプ側 44 − 41 − 77	JB07-26		
	3-P4-D1YT	L3本	アンプ側 34 − 505 − 506	JB07-27		
	3-P4-D1YB	L3本	アンプ側 49 − 50 − 48	JB07-28		
7-9	32-P1-D1Z	30m	H19/9-6芯-オスメス-073	JB07-29	PT1F	30m1本
7-10	32-P2-D1Z	30m	H19/9-6芯-オスメス-075	JB07-31	PT2F	30m1本
7-11	32-P3-D1Z	40m	H21-NIED-MO6-40mm-040	JB07-33	PT3F	40m1本
7-12	32-P4-D1Z	40m	NIED-2008-40mm-079	JB07-35	PT4F	40m1本
7-13	32-P1-D2Z	30m	H19/9-6芯-オスメス-074	JB07-30	PT1F	30m5本
	4-P1-D2XT	30m	H19/9-6芯-オスメス-079	JB07-37		
	4-P1-D2XB	30m	H19/9-6芯-オスメス-080	JB07-38		
	4-P1-D2YT	30m	H19/9-6芯-オスメス-081	JB07-39		
	4-P1-D2YB	30m	H19/9-6芯-オスメス-082	JB07-40		
7-14	4-P1-D3XT	30m	H19/9-6芯-オスメス-083	JB07-41	PT1F	30m4本
	4-P1-D3XB	30m	H19/9-6芯-オスメス-084	JB07-42		
	4-P1-D3YT	30m	H19/9-6芯-オスメス-085	JB07-43		
	4-P1-D3YB	30m	H19/9-6芯-オスメス-086	JB07-44		
7-15	32-P2-D2Z	30m	H19/9-6芯-オスメス-076	JB07-32	PT2F	30m5本
	4-P2-D2XT	30m	H19/9-6芯-オスメス-087	JB07-45		
	4-P2-D2XB	30m	H19/9-6芯-オスメス-088	JB07-46		
	4-P2-D2YT	30m	H19/9-6芯-オスメス-089	JB07-47		
	4-P2-D2YB	30m	H19/9-6芯-オスメス-090	JB07-48		
7-16	4-P2-D3XT	30m	H19/9-6芯-オスメス-091	JB07-49	PT2F	30m4本
	4-P2-D3XB	30m	H19/9-6芯-オスメス-092	JB07-50		
	4-P2-D3YT	30m	H19/9-6芯-オスメス-093	JB07-51		
	4-P2-D3YB	30m	H19/9-6芯-オスメス-094	JB07-52		
7-17	32-P3-D2Z	40m	H21-NIED-MO6-40mm-041	JB07-34	PT3F	40m5本
	4-P3-D2XT	40m	NIED-2008-40mm-081	JB07-53		
	4-P3-D2XB	40m	NIED-2008-40mm-083	JB07-54		
	4-P3-D2YT	40m	NIED-2008-40mm-084	JB07-55		
	4-P3-D2YB	40m	NIED-2008-40mm-085	JB07-56		
7-18	4-P3-D3XT	40m	NIED-2008-40mm-086	JB07-57	PT3F	40m4本
	4-P3-D3XB	40m	NIED-2008-40mm-087	JB07-58		
	4-P3-D3YT	40m	NIED-2008-40mm-088	JB07-59		
	4-P3-D3YB	40m	NIED-2008-40mm-089	JB07-60		
7-19	32-P4-D2Z	40m	NIED-2008-40mm-080	JB07-36	PT4F	40m5本
	4-P4-D2XT	40m	NIED-2008-40mm-090	JB07-61		
	4-P4-D2XB	40m	NIED-2008-40mm-091	JB07-62		
	4-P4-D2YT	40m	NIED-2008-40mm-092	JB07-63		
	4-P4-D2YB	40m	NIED-2008-40mm-093	JB07-64		

JB10						
名称	センサータグ	長さ	ケーブル番号	接続先	試験体	種類
10-1	31-P-A1	40m	NIED-2008-40mm-095	JB10-01	PT4F	40m4本
	31-P-A2	40m	NIED-2008-40mm-096	JB10-02		
	31-P-A3	40m	NIED-2008-40mm-097	JB10-03		
	31-P-A4	40m	NIED-2008-40mm-098	JB10-04		
10-2	31-P-A5	40m	NIED-2008-40mm-099	JB10-05	PT4F	40m5本
	31-P-A6	40m	NIED-2008-40mm-100	JB10-06		
	31-P-A7	40m	NIED-2008-40mm-101	JB10-07		
	31-P-A8	40m	NIED-2008-40mm-102	JB10-08		
	31-P-A9	40m	NIED-2008-40mm-103	JB10-09		
10-3	31-P-A10	40m	NIED-2008-40mm-104	JB10-10	PT4F	40m5本
	31-P-A11	40m	NIED-2008-40mm-105	JB10-11		
	31-P-A12	40m	NIED-2008-40mm-106	JB10-12		
	31-P-A13	40m	NIED-2008-40mm-107	JB10-13		
	31-P-A14	40m	NIED-2008-40mm-108	JB10-14		
10-4	31-P-A15	40m	NIED-2008-40mm-109	JB07-15	PTRF	40m3本
	31-P-A16	40m	NIED-2008-40mm-110	JB07-16		
	31-P-A17	40m	NIED-2008-40mm-111	JB07-17		
10-5	31-P-A18	40m	NIED-2008-40mm-112	JB10-18	PTRF	40m4本
	31-P-A19	40m	NIED-2008-40mm-113	JB10-19		
	31-P-A20	40m	NIED-2008-40mm-114	JB10-20		
	31-P-A21	40m	NIED-2008-40mm-115	JB10-21		
10-6	31-P-A22	40m	NIED-2008-40mm-116	JB10-22	PTRF	40m3本
	31-P-A23	40m	NIED-2008-40mm-117	JB10-23		
	31-P-A24	40m	NIED-2008-40mm-118	JB10-24		
10-7	31-P-A25	40m	NIED-2008-40mm-119	JB10-25	PTRF	40m3本
	31-P-A26	40m	NIED-2008-40mm-120	JB10-26		
	31-P-A27	40m	NIED-2008-40mm-121	JB10-27		
10-8	31-P-A28	40m	NIED-2008-40mm-122	JB10-28	PTRF	40m2本
	31-P-A29	40m	NIED-2008-40mm-123	JB10-29		
10-9	31-P-A30	40m	NIED-2008-40mm-124	JB10-30	PTRF	40m2本
	31-P-A31	40m	NIED-2008-40mm-125	JB10-31		
10-10	32-P-S1	40m	NIED-2008-40mm-126	JB10-32	PTRF	40m3本
	32-P-S2	40m	NIED-2008-40mm-127	JB10-33		
	32-P-S3	40m	NIED-2008-40mm-128	JB10-34		
10-11	32-P-S4	40m	NIED-2008-40mm-129	JB10-35	PTRF	40m3本
	32-P-S5	40m	NIED-2008-40mm-130	JB10-36		
	32-P-S6	40m	NIED-2008-40mm-131	JB10-37		
10-12	32-P-S7	40m	NIED-2008-40mm-132	JB10-38	PTRF	40m3本
	32-P-S8	40m	NIED-2008-40mm-133	JB10-39		
	32-P-S9	40m	NIED-2008-40mm-134	JB10-40		
10-13	32-P-S10	40m	NIED-2008-40mm-135	JB10-41	PTRF	40m3本
	32-P-S11	40m	NIED-2008-40mm-136	JB10-42		
	32-P-S12	40m	NIED-2008-40mm-137	JB10-43		
10-14	32-P-S13	40m	NIED-2008-40mm-138	JB10-44	PTRF	40m3本
	32-P-S14	40m	NIED-2008-40mm-167	JB10-45		
	32-P-S15	40m	NIED-2008-40mm-168	JB10-46		
10-15	32-P-S16	40m	NIED-2008-40mm-169	JB10-47	PTRF	40m3本
	32-P-S17	40m	NIED-2008-40mm-170	JB10-48		
	32-P-S18	40m	NIED-2008-40mm-171	JB10-49		
10-16	32-P-S19	40m	NIED-2008-40mm-172	JB10-50	PTRF	40m3本
	32-P-S20	40m	NIED-2008-40mm-173	JB10-51		
	32-P-S21	40m	NIED-2008-40mm-174	JB10-52		
10-17	32-P-S22	40m	NIED-2008-40mm-175	JB10-53	PTRF	40m3本
	32-P-S23	40m	NIED-2008-40mm-176	JB10-54		
	32-P-S24	40m	NIED-2008-40mm-177	JB10-55		
10-18	32-P-S25	40m	NIED-2008-40mm-178	JB10-56	PTRF	40m3本
	32-P-S26	40m	NIED-2008-40mm-179	JB10-57		
	32-P-S27	40m	NIED-2008-40mm-180	JB10-58		

JB11						
名称	センサータグ	長さ	ケーブル番号	接続先	試験体	種類
11-1	2-P2-A2X	30m	H19/9-6芯-オスメス-095	JB11-01	PT2F	30m3本
	2-P2-A2Y	30m	H19/9-6芯-オスメス-096	JB11-02		
	2-P2-A2Z	30m	H19/9-6芯-オスメス-097	JB11-03		
11-2	2-P3-A2X	30m	H19/9-6芯-オスメス-098	JB11-04	PT3F	30m3本
	2-P3-A2Y	30m	H19/9-6芯-オスメス-099	JB11-05		
	2-P3-A2Z	30m	H19/9-6芯-オスメス-100	JB11-06		
11-3	2-P4-A2X	40m	NIED-2008-40mm-139	JB11-07	PT4F	40m3本
	2-P4-A2Y	40m	NIED-2008-40mm-140	JB11-08		
	2-P4-A2Z	40m	NIED-2008-40mm-141	JB11-09		
11-4	2-PR-A2X	40m	NIED-2008-40mm-142	JB11-10	PTRF	40m3本
	2-PR-A2Y	40m	NIED-2008-40mm-143	JB11-11		
	2-PR-A2Z	40m	NIED-2008-40mm-144	JB11-12		
11-5	1-PL1	40m	NIED-2008-40mm-145	JB11-13	PTRF	40m2本
	1-PL2	40m	NIED-2008-40mm-146	JB11-14		
11-6	7-P1-DC3aNE	30m	H21-NIED-MC6-30mm-001	JB11-15	PT1F	30m5本
	7-P1-DC3aSE	30m	H21-NIED-MC6-30mm-002	JB11-16		
	7-P1-DC3aSW	30m	H21-NIED-MC6-30mm-003	JB11-17		
	7-P1-DC3aNW	30m	H21-NIED-MC6-30mm-004	JB11-18		
	8-P1-DC3aY	30m	H21-NIED-MC6-30mm-013	JB11-31		
11-7	7-P2-DC3aNE	30m	H21-NIED-MC6-30mm-005	JB11-19	PT2F	30m5本
	7-P2-DC3aSE	30m	H21-NIED-MC6-30mm-006	JB11-20		
	7-P2-DC3aSW	30m	H21-NIED-MC6-30mm-007	JB11-21		
	7-P2-DC3aNW	30m	H21-NIED-MC6-30mm-008	JB11-22		
	8-P2-DC3aY	30m	H21-NIED-MC6-30mm-014	JB11-32		
11-8	7-P3-DC3aNE	30m	H21-NIED-MC6-30mm-009	JB11-23	PT3F	30m5本
	7-P3-DC3aSE	30m	H21-NIED-MC6-30mm-010	JB11-24		
	7-P3-DC3aSW	30m	H21-NIED-MC6-30mm-011	JB11-25		
	7-P3-DC3aNW	30m	H21-NIED-MC6-30mm-012	JB11-26		
	8-P3-DC3aY	30m	H21-NIED-MC6-30mm-015	JB11-33		
11-9	7-P4-DC3aNE	40m	NIED-2008-40mm-147	JB11-27	PT4F	40m5本
	7-P4-DC3aSE	40m	NIED-2008-40mm-148	JB11-28		
	7-P4-DC3aSW	40m	NIED-2008-40mm-149	JB11-29		
	7-P4-DC3aNW	40m	NIED-2008-40mm-150	JB11-30		
	8-P4-DC3aY	40m	NIED-2008-40mm-151	JB11-34		
11-10	22-P-S1	30m	H21-NIED-MC6-30mm-016	JB11-35	PT1F	30m4本
	22-P-S2	30m	H21-NIED-MC6-30mm-017	JB11-36		
	22-P-S3	30m	H21-NIED-MC6-30mm-018	JB11-37		
	22-P-S4	30m	H21-NIED-MC6-30mm-019	JB11-38		
11-11	23-P-S1	30m	H21-NIED-MC6-30mm-020	JB11-39	PT1F	30m4本
	23-P-S2	30m	H21-NIED-MC6-30mm-021	JB11-40		
	24-P-S1	30m	H21-NIED-MC6-30mm-022	JB11-41		
	24-P-S2	30m	H21-NIED-MC6-30mm-023	JB11-42		
11-A1	A1-P1S-D1	10m		JB11-45	PT1F	10m2本
	A1-P1S-D2	10m		JB11-46		
11-A2	A1-P1S-D3	10m	NIED-MO6-10mm-013	JB11-47	PT1F	10m4本
	A1-P1S-D4	10m	NIED-MO6-10mm-014	JB11-48		
	A1-P1S-D5	10m	NIED-MO6-10mm-015	JB11-49		
	A1-P1S-D6	10m	NIED-MO6-10mm-016	JB11-50		
11-A3	A1-P1S-D7	10m	NIED-MO6-10mm-017	JB11-51	PT1F	10m4本
	A1-P1S-D8	10m	NIED-MO6-10mm-018	JB11-52		
	A1-P1S-D9	10m	NIED-MO6-10mm-019	JB11-53		
	A1-P1S-D10	10m	NIED-MO6-10mm-020	JB11-54		
11-A4	A1-R1S-D1	30m	H21-NIED-MC6-30mm-093	JB11-55	RC1F	30m6本
	A1-R1S-D2	30m	H21-NIED-MC6-30mm-094	JB11-56		
	A1-R1S-D3	30m	H21-NIED-MC6-30mm-095	JB11-57		
	A1-R1S-D4	30m	H21-NIED-MC6-30mm-096	JB11-58		
	A1-R1S-D5	30m	H21-NIED-MC6-30mm-097	JB11-59		
	A1-R1S-D6	30m	H21-NIED-MC6-30mm-098	JB11-60		
11-A5	A1-R1S-D7	30m	H21-NIED-MC6-30mm-099	JB11-61	RC1F	30m4本
	A1-R1S-D8	30m	H21-NIED-MC6-30mm-100	JB11-62		
	A1-R1S-D9	30m	NIED-MO6-30mm-001	JB11-63		
	A1-R1S-D10	30m	NIED-MO6-30mm-002	JB11-64		

ケーブル準備表4

JB12

名称	センサータグ	長さ	ケーブル番号	接続先	試験体	種類
12-1	5X-P1-DB3T	30m	H21-NIED-MC6-30mm-024	JB12-01	PT1F	30m2本
	5Y-P1-DB3T	30m	H21-NIED-MC6-30mm-034	JB12-17		
12-2	5X-P1-DC3T	30m	H21-NIED-MC6-30mm-029	JB12-09	PT1F	30m3本
	5Y-P1-DC3T	30m	H21-NIED-MC6-30mm-039	JB12-25		
	5Y-P1-DC3aT	30m	H21-NIED-MC6-30mm-044	JB12-33		
12-3	5X-P2-DB3B	30m	H21-NIED-MC6-30mm-025	JB12-02	PT2F	30m2本
	5Y-P2-DB3B	30m	H21-NIED-MC6-30mm-035	JB12-18		
12-4	5X-P2-DC3B	30m	H21-NIED-MC6-30mm-030	JB12-10	PT2F	30m3本
	5Y-P2-DC3B	30m	H21-NIED-MC6-30mm-040	JB12-26		
	5Y-P2-DC3aB	30m	H21-NIED-MC6-30mm-045	JB12-34		
12-5	5X-P2-DB3T	30m	H21-NIED-MC6-30mm-026	JB12-03	PT2F	30m2本
	5Y-P2-DB3T	30m	H21-NIED-MC6-30mm-036	JB12-19		
12-6	5X-P2-DC3T	30m	H21-NIED-MC6-30mm-031	JB12-11	PT2F	30m3本
	5Y-P2-DC3T	30m	H21-NIED-MC6-30mm-041	JB12-27		
	5Y-P2-DC3aT	30m	H21-NIED-MC6-30mm-046	JB12-35		
12-7	5X-P3-DB3B	30m	H21-NIED-MC6-30mm-027	JB12-04	PT3F	30m2本
	5Y-P3-DB3B	30m	H21-NIED-MC6-30mm-037	JB12-20		
12-8	5X-P3-DC3B	30m	H21-NIED-MC6-30mm-032	JB12-12	PT3F	30m3本
	5Y-P3-DC3B	30m	H21-NIED-MC6-30mm-042	JB12-28		
	5Y-P3-DC3aB	30m	H21-NIED-MC6-30mm-047	JB12-36		
12-9	5X-P3-DB3T	30m	H21-NIED-MC6-30mm-028	JB12-05	PT3F	30m2本
	5Y-P3-DB3T	30m	H21-NIED-MC6-30mm-038	JB12-21		
12-10	5X-P3-DC3T	30m	H21-NIED-MC6-30mm-033	JB12-13	PT3F	30m3本
	5Y-P3-DC3T	30m	H21-NIED-MC6-30mm-043	JB12-29		
	5Y-P3-DC3aT	30m	H21-NIED-MC6-30mm-048	JB12-37		
12-11	5X-P4-DB3B	40m	NIED-2008-40mm-152	JB12-06	PT4F	40m2本
	5Y-P4-DB3B	40m	NIED-2008-40mm-158	JB12-22		
12-12	5X-P4-DC3B	40m	NIED-2008-40mm-155	JB12-14	PT4F	40m3本
	5Y-P4-DC3B	40m	NIED-2008-40mm-161	JB12-30		
	5Y-P4-DC3aB	40m	NIED-2008-40mm-164	JB12-38		
12-13	5X-P4-DB3T	40m	NIED-2008-40mm-153	JB12-07	PT4F	40m2本
	5Y-P4-DB3T	40m	NIED-2008-40mm-159	JB12-23		
12-14	5X-P4-DC3T	40m	NIED-2008-40mm-156	JB12-15	PT4F	40m3本
	5Y-P4-DC3T	40m	NIED-2008-40mm-162	JB12-31		
	5Y-P4-DC3aT	40m	NIED-2008-40mm-165	JB12-39		
12-15	5X-PR-DB3B	40m	NIED-2008-40mm-154	JB12-08	PTRF	40m2本
	5Y-PR-DB3B	40m	NIED-2008-40mm-160	JB12-24		
12-16	5X-PR-DC3B	40m	NIED-2008-40mm-157	JB12-16	PTRF	40m3本
	5Y-PR-DC3B	40m	NIED-2008-40mm-163	JB12-32		
	5Y-PR-DC3aB	40m	NIED-2008-40mm-166	JB12-40		
12-17	6-P1-DB3N	30m	H21-NIED-MC6-30mm-049	JB12-41	PT1F	30m4本
	6-P1-DB3E	30m	H21-NIED-MC6-30mm-050	JB12-42		
	6-P1-DB3S	30m	H21-NIED-MC6-30mm-051	JB12-43		
	6-P1-DB3W	30m	H21-NIED-MC6-30mm-052	JB12-44		
12-18	6-P1-DC3N	30m	H21-NIED-MC6-30mm-053	JB12-45	PT1F	30m4本
	6-P1-DC3E	30m	H21-NIED-MC6-30mm-054	JB12-46		
	6-P1-DC3S	30m	H21-NIED-MC6-30mm-055	JB12-47		
	6-P1-DC3W	30m	H21-NIED-MC6-30mm-056	JB12-48		
12-19	11-P0-D1Y	30m	H21-NIED-MC6-30mm-057	JB12-51	基礎	30m2本
	11-R0-D1Y	30m	H21-NIED-MC6-30mm-058	JB12-56		
12-20	11-P0-D2X	30m	H21-NIED-MC6-30mm-059	JB12-52	基礎	30m4本
	11-P0-D2Y	30m	H21-NIED-MC6-30mm-060	JB12-53		
	11-R0-D2X	30m	H21-NIED-MC6-30mm-061	JB12-57		
	11-R0-D2Y	30m	H21-NIED-MC6-30mm-062	JB12-58		
12-21	11Z-P0-D1Z	30m	H21-NIED-MC6-30mm-063	JB12-54	PT基礎	30m2本
	11Z-P0-D2Z	30m	H21-NIED-MC6-30mm-064	JB12-55		
12-22	11Z-R0-D1Z	30m	H21-NIED-MC6-30mm-065	JB12-59	RC基礎	30m2本
	11Z-R0-D2Z	30m	H21-NIED-MC6-30mm-066	JB12-60		

JB13

名称	センサータグ	長さ	ケーブル番号	接続先	試験体	種類
13-1	31-R-A1	40m	H21-NIED-MC6-40mm-001	JB13-01	RC4F	40m4本
	31-R-A2	40m	H21-NIED-MC6-40mm-002	JB13-02		
	31-R-A3	40m	H21-NIED-MC6-40mm-003	JB13-03		
	31-R-A4	40m	H21-NIED-MC6-40mm-004	JB13-04		
13-2	31-R-A5	40m	H21-NIED-MC6-40mm-005	JB13-05	RC4F	40m3本
	31-R-A6	40m	H21-NIED-MC6-40mm-006	JB13-06		
	31-R-A7	40m	H21-NIED-MC6-40mm-007	JB13-07		
13-3	31-R-A8	40m	H21-NIED-MC6-40mm-008	JB13-08	RC4F	40m4本
	31-R-A9	40m	H21-NIED-MC6-40mm-009	JB13-09		
	31-R-A10	40m	H21-NIED-MC6-40mm-010	JB13-10		
	31-R-A11	40m	H21-NIED-MC6-40mm-011	JB13-11		
13-4	31-R-A12	40m	H21-NIED-MC6-40mm-012	JB13-12	RC4F	40m3本
	31-R-A13	40m	H21-NIED-MC6-40mm-013	JB13-13		
	31-R-D1	40m	H21-NIED-MC6-40mm-074	JB13-64		
13-5	31-R-A14	40m	H21-NIED-MC6-40mm-014	JB13-14	RC4F	40m3本
	31-R-A15	40m	H21-NIED-MC6-40mm-015	JB13-15		
	31-R-A16	40m	H21-NIED-MC6-40mm-016	JB13-16		
13-6	31-R-A17	40m	H21-NIED-MC6-40mm-017	JB13-17	RC4F	40m4本
	31-R-A18	40m	H21-NIED-MC6-40mm-018	JB13-18		
	31-R-A19	40m	H21-NIED-MC6-40mm-019	JB13-19		
	31-R-A20	40m	H21-NIED-MC6-40mm-020	JB13-20		
13-7	31-R-A21	40m	H21-NIED-MC6-40mm-021	JB13-21	RCRF	40m4本
	31-R-A22	40m	H21-NIED-MC6-40mm-022	JB13-22		
	31-R-A23	40m	H21-NIED-MC6-40mm-023	JB13-23		
	31-R-A24	40m	H21-NIED-MC6-40mm-024	JB13-24		
13-8	31-R-A25	40m	H21-NIED-MC6-40mm-025	JB13-25	RCRF	40m3本
	31-R-A26	40m	H21-NIED-MC6-40mm-026	JB13-26		
	31-R-A27	40m	H21-NIED-MC6-40mm-027	JB13-27		
13-9	31-R-A28	40m	H21-NIED-MC6-40mm-028	JB13-28	RCRF	40m5本
	31-R-A29	40m	H21-NIED-MC6-40mm-029	JB13-29		
	31-R-A30	40m	H21-NIED-MC6-40mm-030	JB13-30		
	31-R-A31	40m	H21-NIED-MC6-40mm-031	JB13-31		
	31-R-A32	40m	H21-NIED-MC6-40mm-042	JB13-32		
13-10	31-R-A33	40m	H21-NIED-MC6-40mm-043	JB13-33	RCRF	40m5本
	31-R-A34	40m	H21-NIED-MC6-40mm-044	JB13-34		
	31-R-A35	40m	H21-NIED-MC6-40mm-045	JB13-35		
	31-R-A36	40m	H21-NIED-MC6-40mm-046	JB13-36		
	31-R-A37	40m	H21-NIED-MC6-40mm-047	JB13-37		
13-11	31-R-A38	40m	H21-NIED-MC6-40mm-048	JB13-38	RCRF	40m2本
	31-R-A39	40m	H21-NIED-MC6-40mm-049	JB13-39		
13-12	32-R-S1	40m	H21-NIED-MC6-40mm-050	JB13-40	RCRF	40m3本
	32-R-S2	40m	H21-NIED-MC6-40mm-051	JB13-41		
	32-R-S3	40m	H21-NIED-MC6-40mm-052	JB13-42		
13-13	32-R-S4	40m	H21-NIED-MC6-40mm-053	JB13-43	RCRF	40m3本
	32-R-S5	40m	H21-NIED-MC6-40mm-054	JB13-44		
	32-R-S6	40m	H21-NIED-MC6-40mm-055	JB13-45		
13-14	32-R-S7	40m	H21-NIED-MC6-40mm-056	JB13-46	RCRF	40m3本
	32-R-S8	40m	H21-NIED-MC6-40mm-057	JB13-47		
	32-R-S9	40m	H21-NIED-MC6-40mm-058	JB13-48		
13-15	32-R-S10	40m	H21-NIED-MC6-40mm-059	JB13-49	RCRF	40m3本
	32-R-S11	40m	H21-NIED-MC6-40mm-060	JB13-50		
	32-R-S12	40m	H21-NIED-MC6-40mm-061	JB13-51		
13-16	32-R-S13	40m	H21-NIED-MC6-40mm-062	JB13-52	RCRF	40m3本
	32-R-S14	40m	H21-NIED-MC6-40mm-063	JB13-53		
	32-R-S15	40m	H21-NIED-MC6-40mm-064	JB13-54		
13-17	32-R-S16	40m	H21-NIED-MC6-40mm-065	JB13-55	RCRF	40m3本
	32-R-S17	40m	H21-NIED-MC6-40mm-066	JB13-56		
	32-R-S18	40m	H21-NIED-MC6-40mm-067	JB13-57		
13-18	32-R-S19	40m	H21-NIED-MC6-40mm-068	JB13-58	RCRF	40m3本
	32-R-S20	40m	H21-NIED-MC6-40mm-069	JB13-59		
	32-R-S21	40m	H21-NIED-MC6-40mm-070	JB13-60		
13-19	32-R-S22	40m	H21-NIED-MC6-40mm-071	JB13-61	RCRF	40m3本
	32-R-S23	40m	H21-NIED-MC6-40mm-072	JB13-62		
	32-R-S24	40m	H21-NIED-MC6-40mm-073	JB13-63		

JB14

名称	センサータグ	長さ	ケーブル番号	接続先	試験体	種類
14-1	2-R2-A2X	30m	H21-NIED-MC6-30mm-067	JB14-01	RC2F	30m3本
	2-R2-A2Y	30m	H21-NIED-MC6-30mm-068	JB14-02		
	2-R2-A2Z	30m	H21-NIED-MC6-30mm-069	JB14-03		
14-2	2-R3-A2X	30m	H21-NIED-MC6-30mm-070	JB14-04	RC3F	30m3本
	2-R3-A2Y	30m	H21-NIED-MC6-30mm-071	JB14-05		
	2-R3-A2Z	30m	H21-NIED-MC6-30mm-072	JB14-06		
14-3	2-R4-A2X	40m	H21-NIED-MC6-40mm-032	JB14-07	RC4F	40m3本
	2-R4-A2Y	40m	H21-NIED-MC6-40mm-033	JB14-08		
	2-R4-A2Z	40m	H21-NIED-MC6-40mm-034	JB14-09		
14-4	2-RR-A2X	40m	H21-NIED-MC6-40mm-035	JB14-10	RCRF	40m3本
	2-RR-A2Y	40m	H21-NIED-MC6-40mm-036	JB14-11		
	2-RR-A2Z	40m	H21-NIED-MC6-40mm-037	JB14-12		
14-5	9X-R2-DB1T	30m	H21-NIED-MC6-30mm-073	JB14-13	RC2F	30m2本
	9Y-R2-DB1T	30m	H21-NIED-MC6-30mm-077	JB14-17		
14-6	9X-R2-DC1T	30m	H21-NIED-MC6-30mm-075	JB14-15	RC2F	30m3本
	9Y-R2-DC1T	30m	H21-NIED-MC6-30mm-079	JB14-19		
	9Y-R2-DC1aT	30m	H21-NIED-MC6-30mm-081	JB14-21		
14-7	9X-R3-DB1B	30m	H21-NIED-MC6-30mm-074	JB14-14	RC3F	30m2本
	9Y-R3-DB1B	30m	H21-NIED-MC6-30mm-078	JB14-18		
14-8	9X-R3-DC1B	30m	H21-NIED-MC6-30mm-076	JB14-16	RC3F	30m3本
	9Y-R3-DC1B	30m	H21-NIED-MC6-30mm-080	JB14-20		
	9Y-R3-DC1aB	30m	H21-NIED-MC6-30mm-082	JB14-22		
14-9	10-R1-DC1aNE	30m	H21-NIED-MC6-30mm-083	JB14-23	RC1F	30m4本
	10-R1-DC1aSE	30m	H21-NIED-MC6-30mm-084	JB14-24		
	10-R1-DC1aSW	30m	H21-NIED-MC6-30mm-085	JB14-25		
	10-R1-DC1aNW	30m	H21-NIED-MC6-30mm-086	JB14-26		

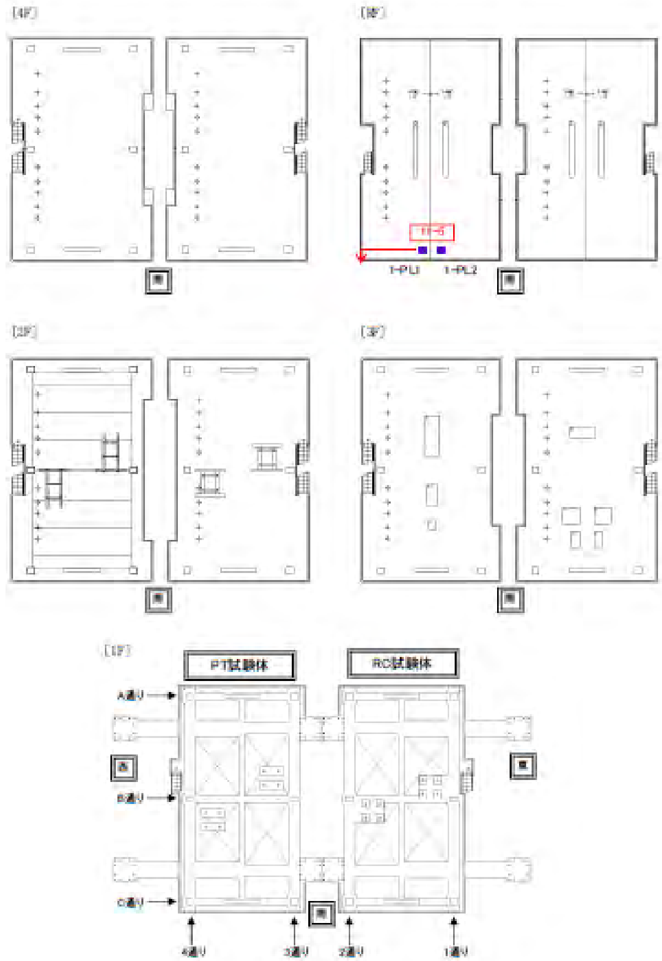

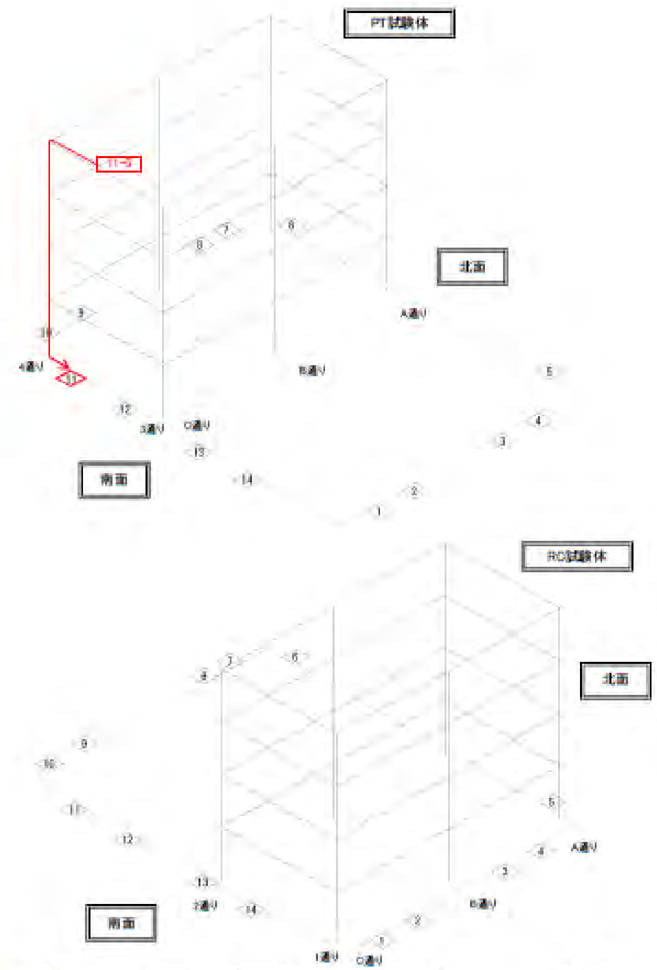

センサ名称	センサタグ	計測機器	合計点数
1壁ワイヤ	1-PL*	センターホールロードセル	2台＝2ch(PC2ch)

1 壁ワイヤ 配線ルート

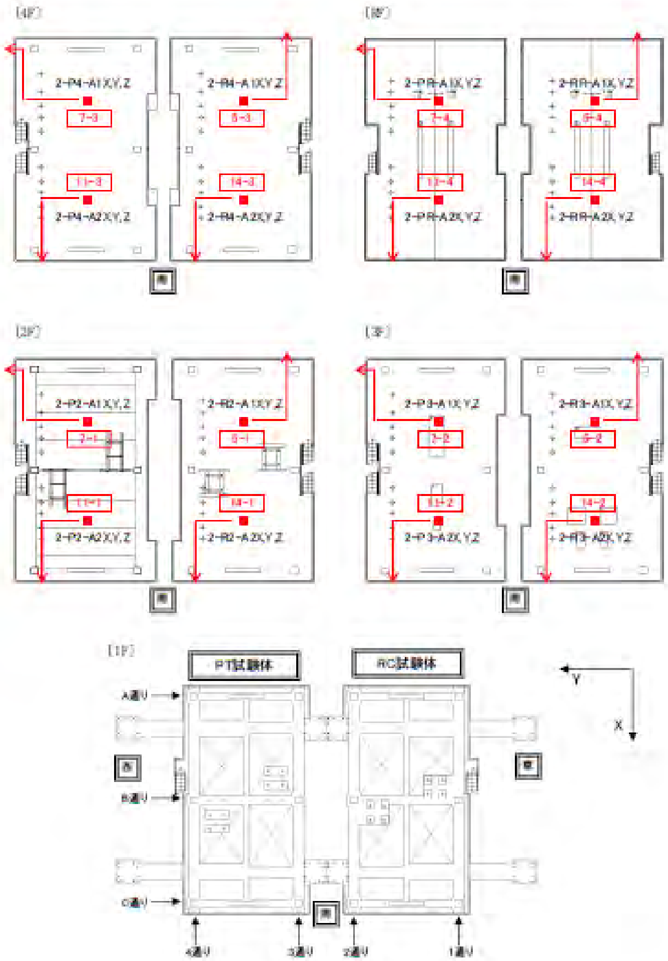

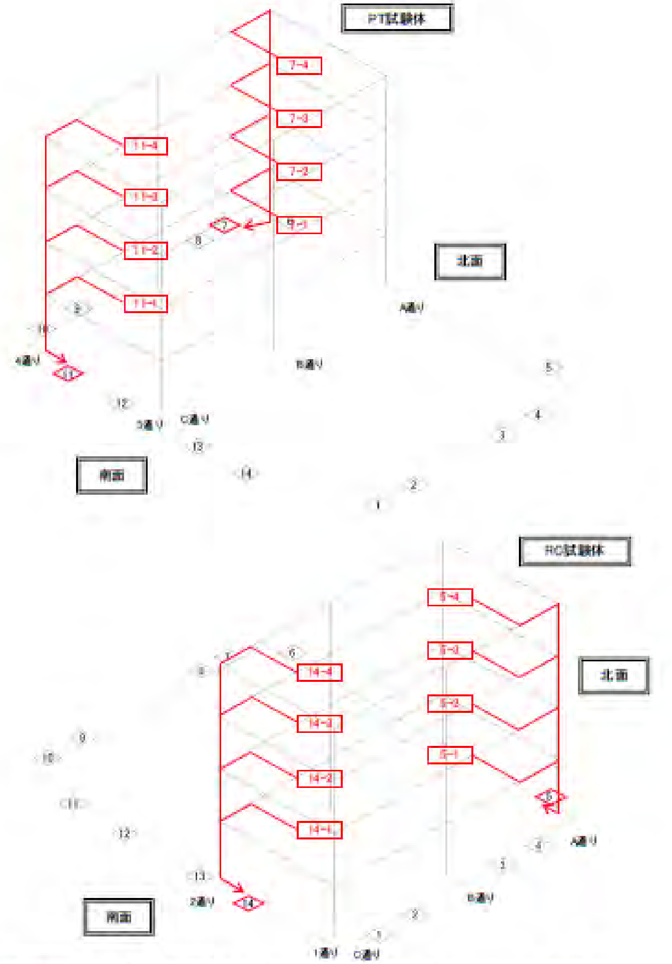

センサ名称	センサタグ	計測機器	合計点数
■ 2層加速度計3方向	2-P*-A*X,Y,Z	TA-25E-10-1(トキメック)	16台 ×3方向＝48ch(PC24ch,RC24ch)

2 層加速度計　配線ルート

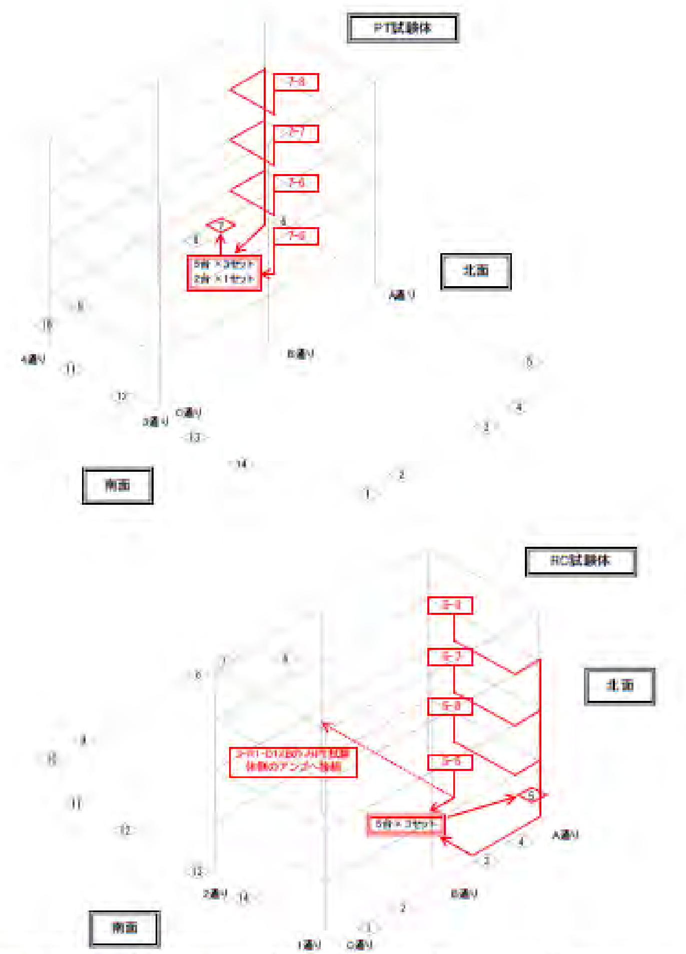

センサ名称	センサタグ	計測機器	合計点数
● 3層間変位(レーザー変位形)	3-P*-D*X,Y,T,B	LK-500(KEYENCE)	32台＝32ch（PC16ch,RC16ch）

···レーザー変位形用アンプ

3 層間変位（レーザー変位形） 配線ルート

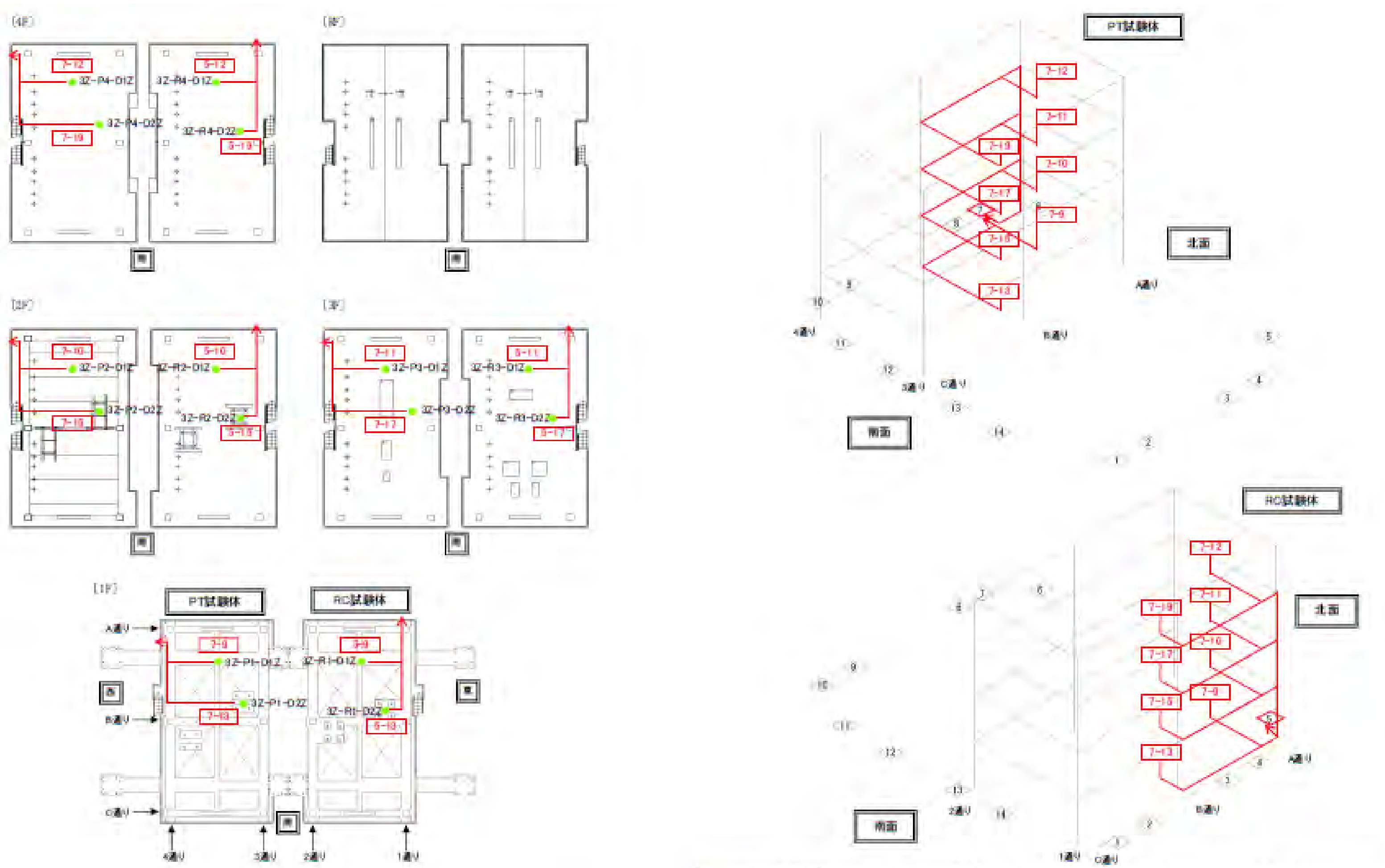

センサ名称	センサタグ	計測機器	合計点数
● 3Z 層間鉛直変位(CDP変位形)	3Z-P*-D*Z	DTH-A-100(共和電業)	16台 = 16ch (PC8ch,RC8ch)

3Z 層間鉛直変位　配線ルート

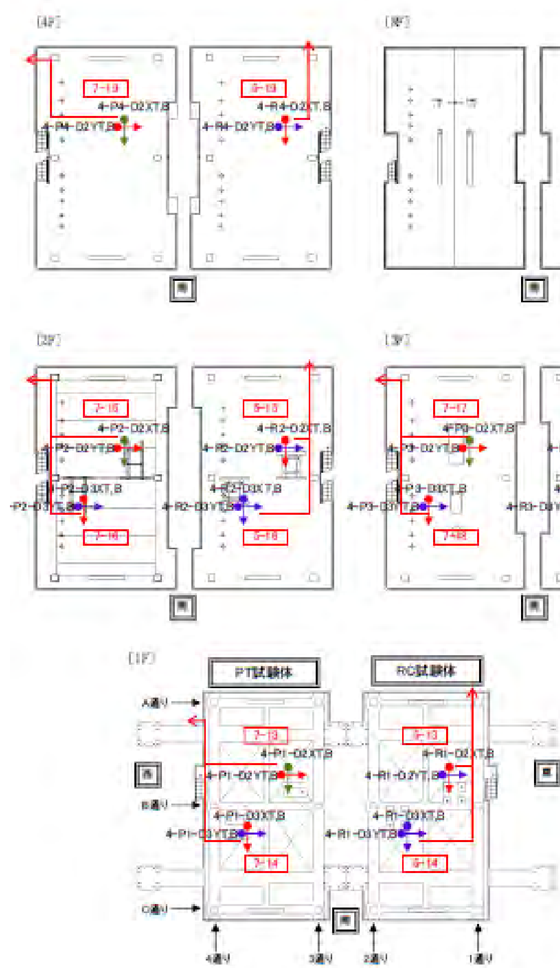

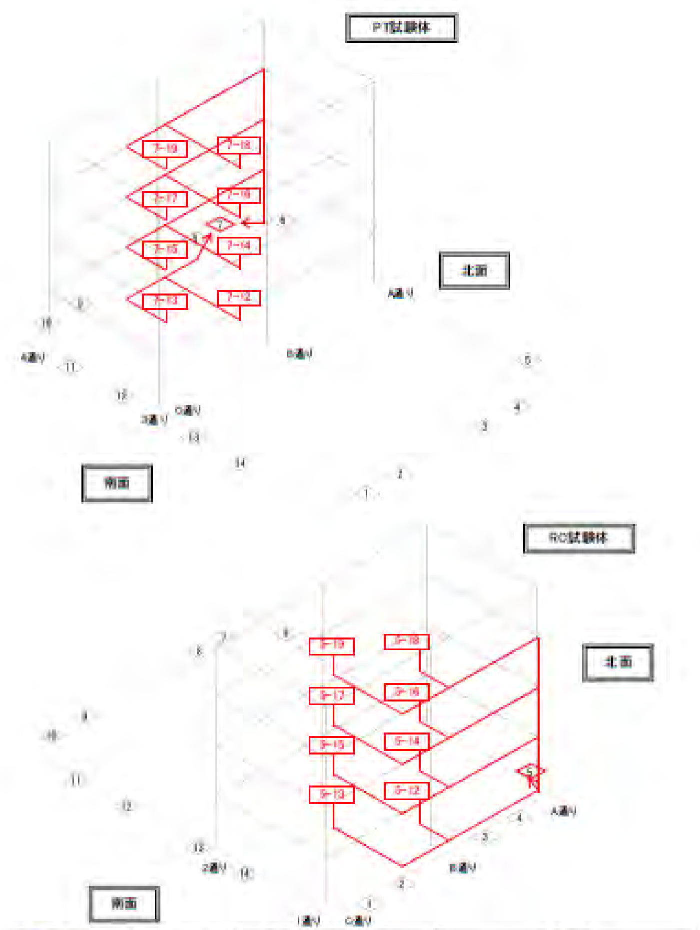

センサ名称	センサタグ	計測機器	合計点数
●:4層間変位(ワイヤー変位形)	4-P*-D*X,Y T,B	DP-1000(東京測器)	22台＝22ch(PC12ch,RC10ch)
●:4層間変位(ワイヤー変位形)		DP-2000(東京測器)	26台＝26ch(PC12ch,RC14ch)
●:4層間変位(ワイヤー変位形)		DTP-D-5KS(共和電業)	8台＝8ch(PC4ch,RC4ch)

4 層間変位（ワイヤー変位形） 配線ルート

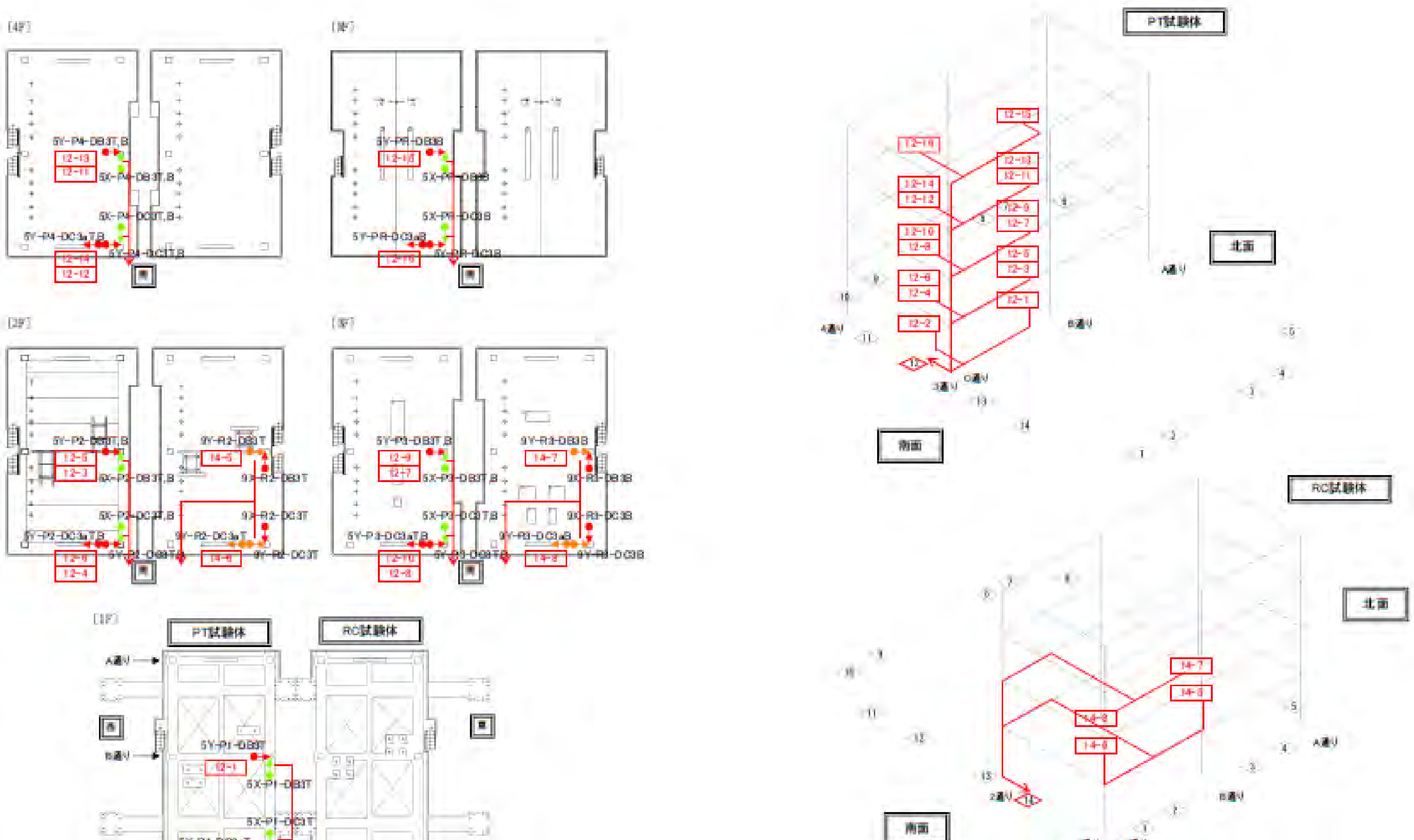

センサ名称	センサタグ	計測機器	合計点数
5XPT梁端変形(CDP変位形)	5X-P*-D**T,B	DTH-A-100(共和電業)	16台＝16ch(PC16ch)
5YPT梁端変形(ワイヤー変位形)	5Y-P*-D**T,B	DP-500(東京測器)	24台＝24ch(PC24ch)
9XRC梁端変形(ワイヤー変位形)	9X-P*-D**T,B	DP-500(東京測器)	4台＝4ch(RC4ch)
9YRC梁端変形(ワイヤー変位形)	9Y-P*-D**T,B	DTP-D-2KS(共和電業)	8台＝8ch(RC8ch)

5XPT梁端変形　5YPT梁端変形　9XRC梁端変形　9YRC梁端変形　配線ルート

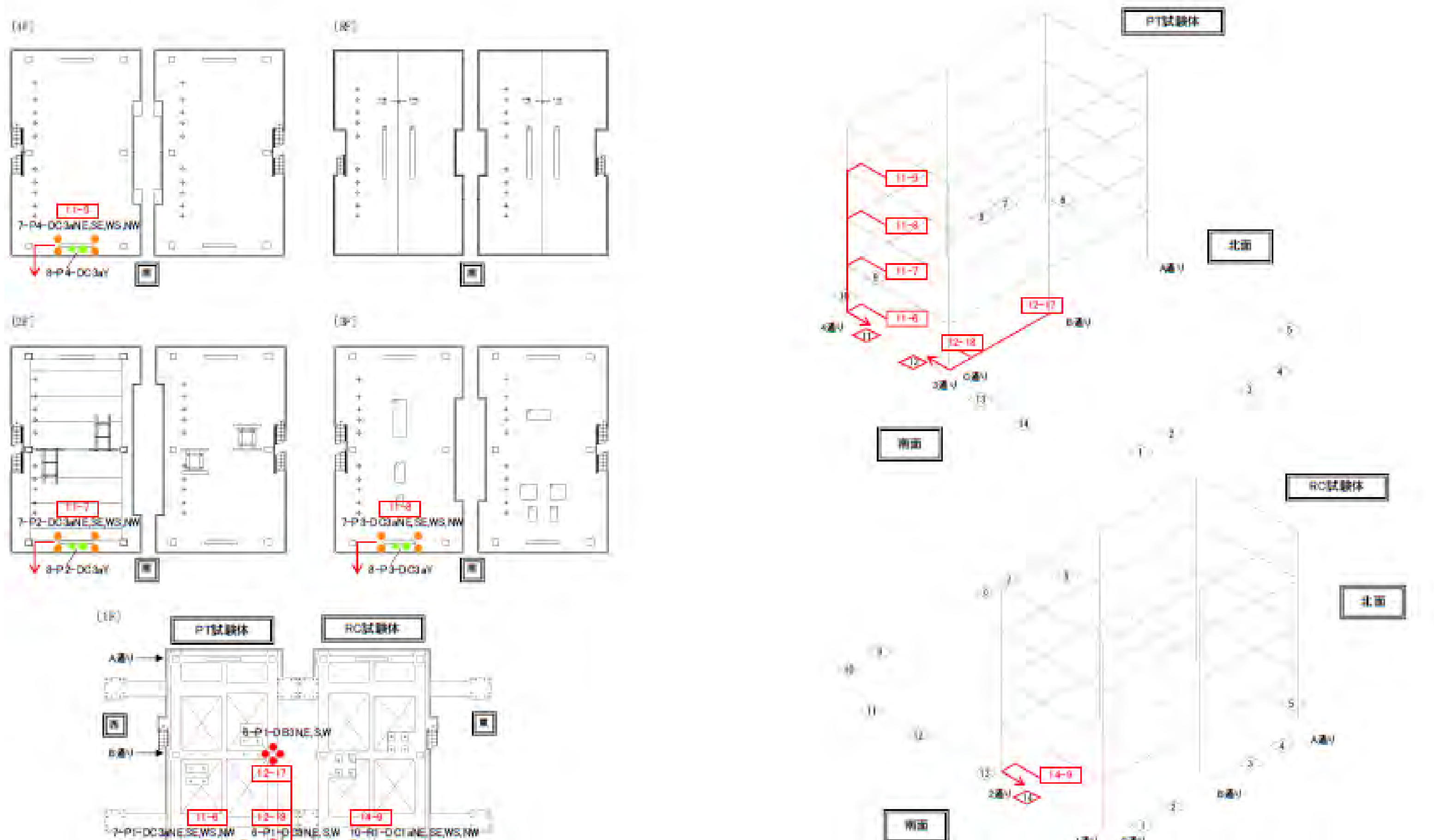

センサ名称	センサタグ	計測機器	合計点数
● 6PT柱脚変形(ワイヤー変位形)	6-P1-D***	DP-500(東京測器)	8台=8ch(PC8ch)
● 7PT壁脚部変形(ワイヤー変位形)	7-P*-DC3a**	DTP-D-300(共和電業)	16台=16ch(PC16ch)
● 8PT壁端滑り(CDP変位形)	8-P*-DC3aY	DTH-A-100(共和電業)	4台=4ch(PC4ch)
● 10RC壁脚部変形(ワイヤー変位形)	10-R1-DC1a**	DTP-D-300(共和電業)	4台=4ch(RC4ch)

6PT柱脚変形　7PT壁脚部変形　8PT壁端滑り　10RC壁脚部変形　配線ルート

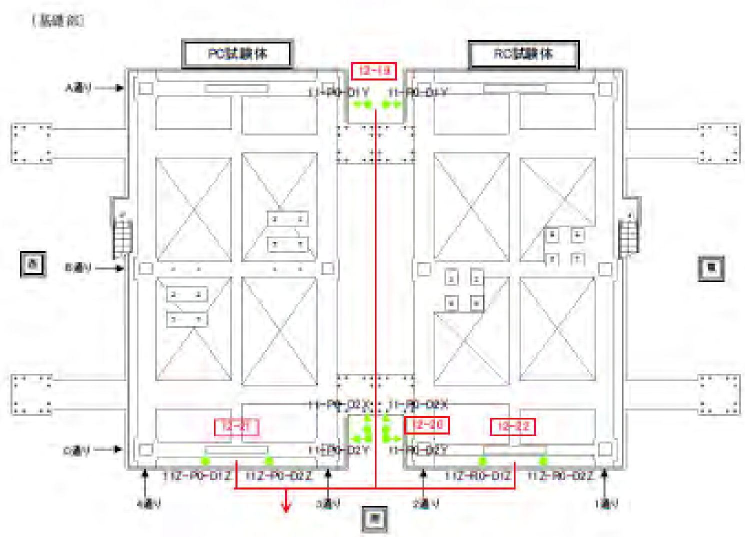

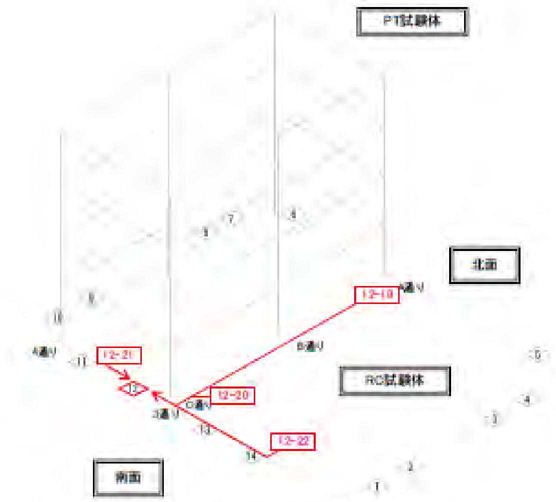

センサ名称	センサタグ	計測機器	合計点数
11基礎滑り(CDP変位形)	11-P0-D*X,Y	DTH-A-100(共和電業)	6台＝6ch(PC3ch,RC3ch)
11Z基礎浮き上がり(CDP変位形)	11Z-P0-D*Z	DTH-A-100(共和電業)	4台＝4ch(PC2ch,RC2ch)

11基礎滑り　11Z基礎浮き上がり　配線ルート

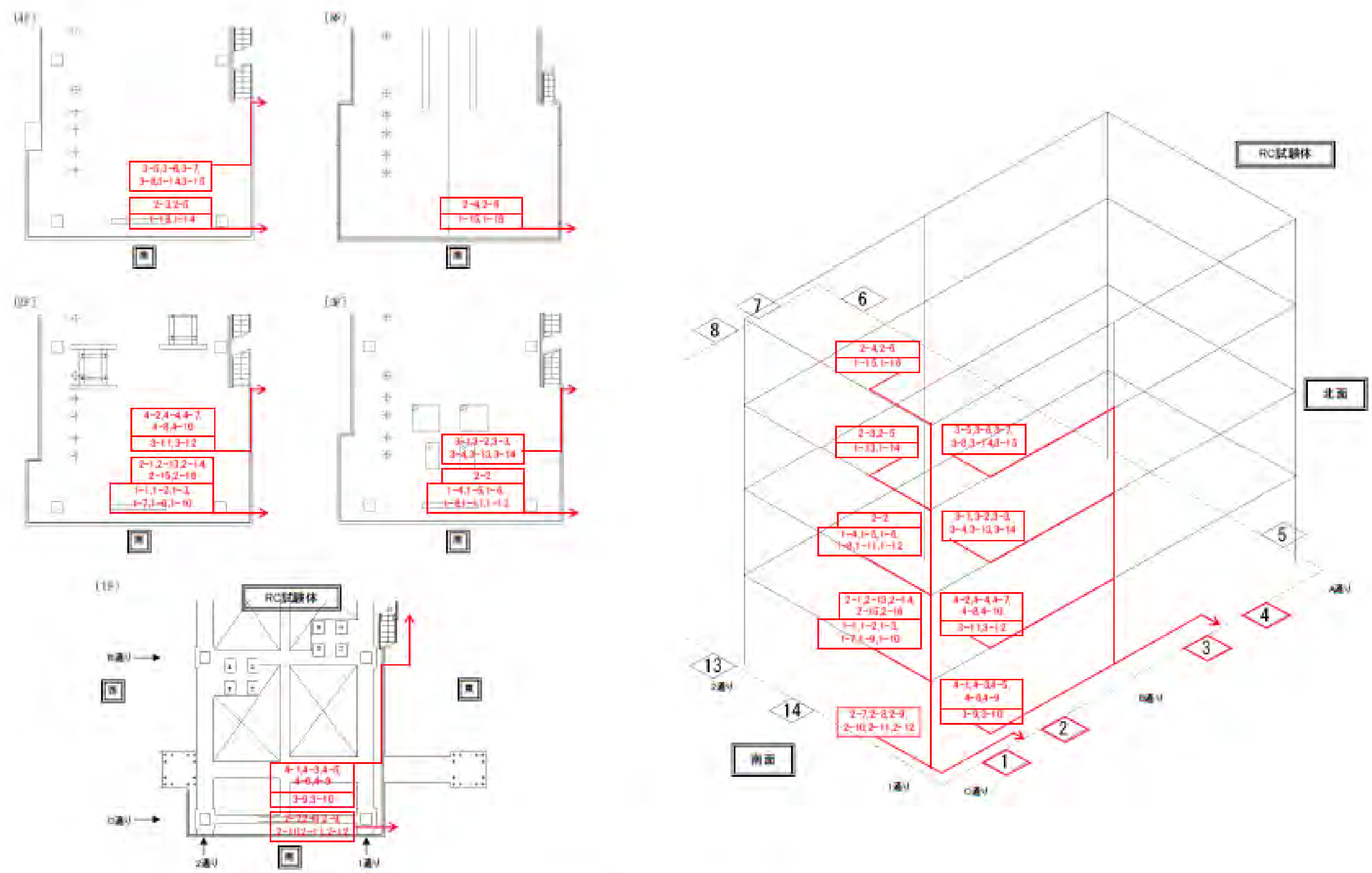

RC試験体歪ゲージ 配線ルート

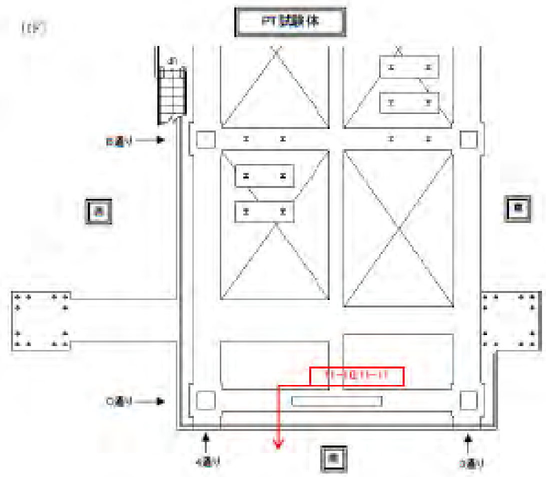

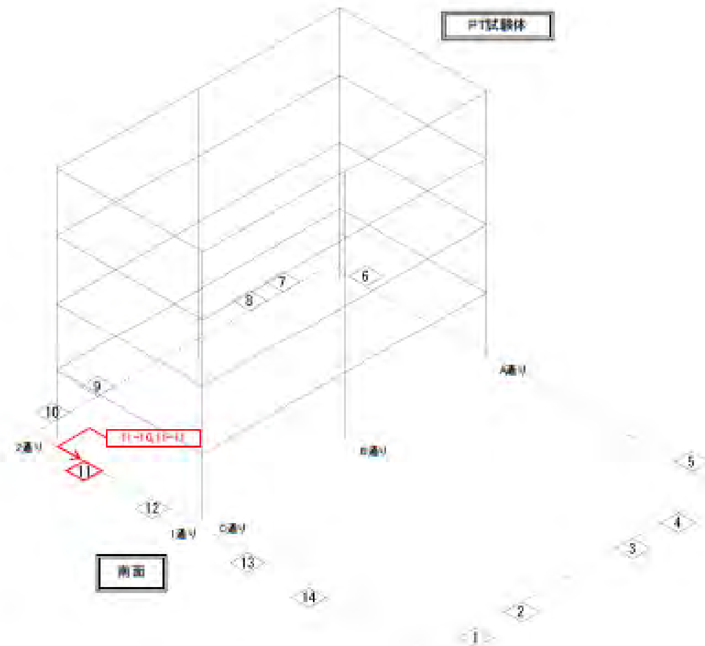

PT試験体歪ゲージ　配線ルート

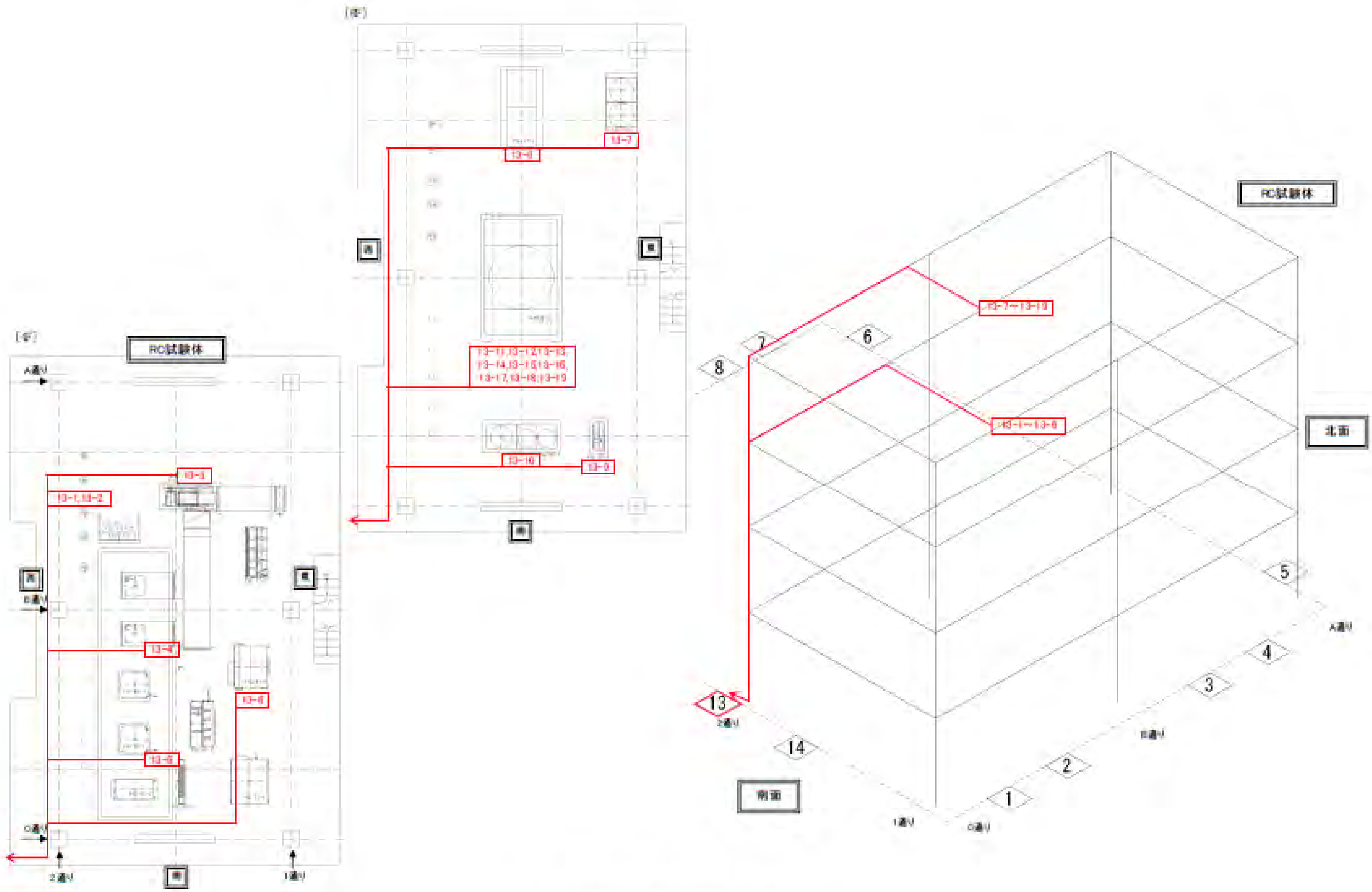

RC試験体設備機器　配線ルート

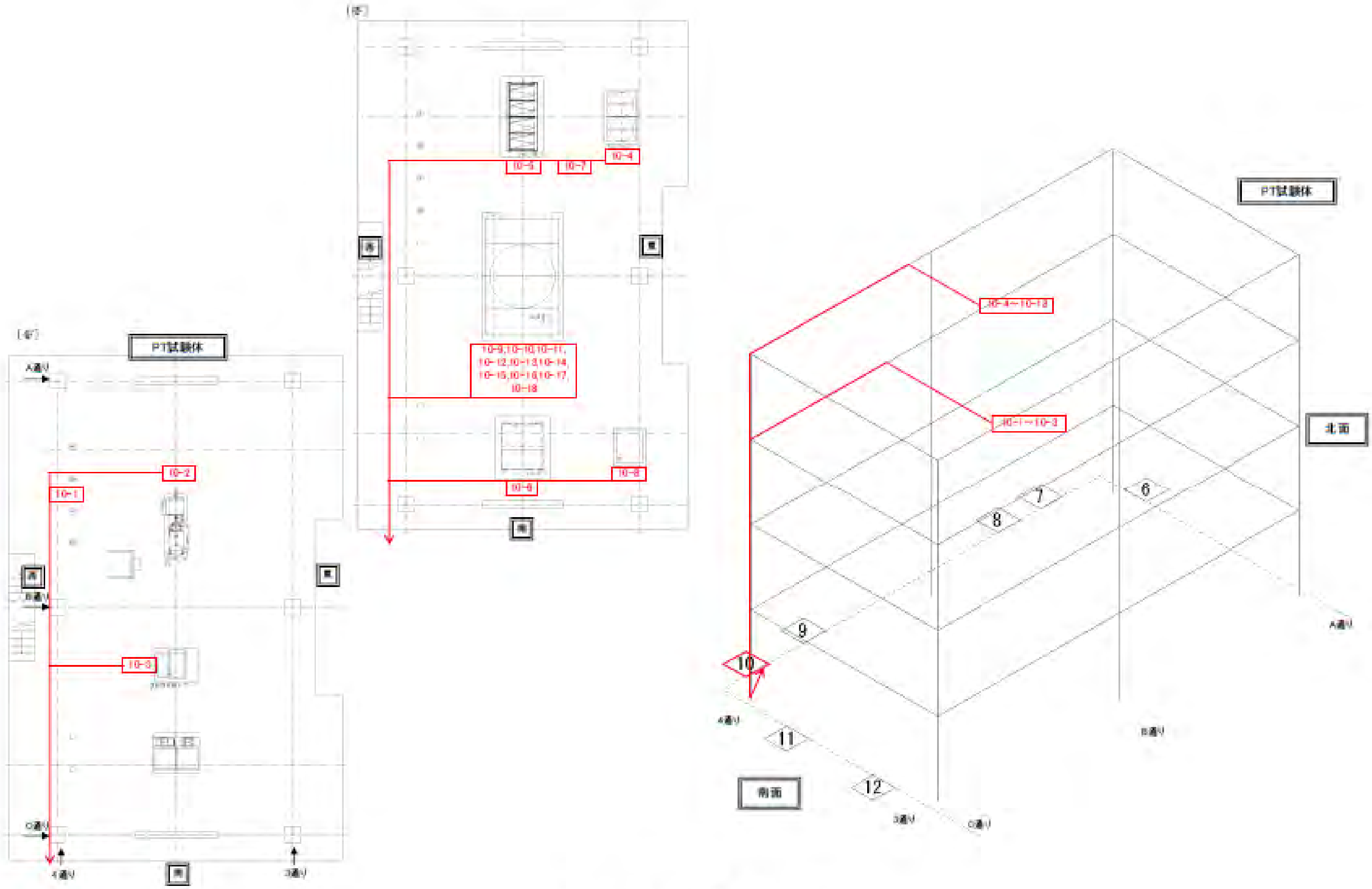

PT試験体設備機器　配線ルート

Appendix E

E.1 PSEUDO ACCELERATION SPECTRA OF THE GROUND MOTIONS

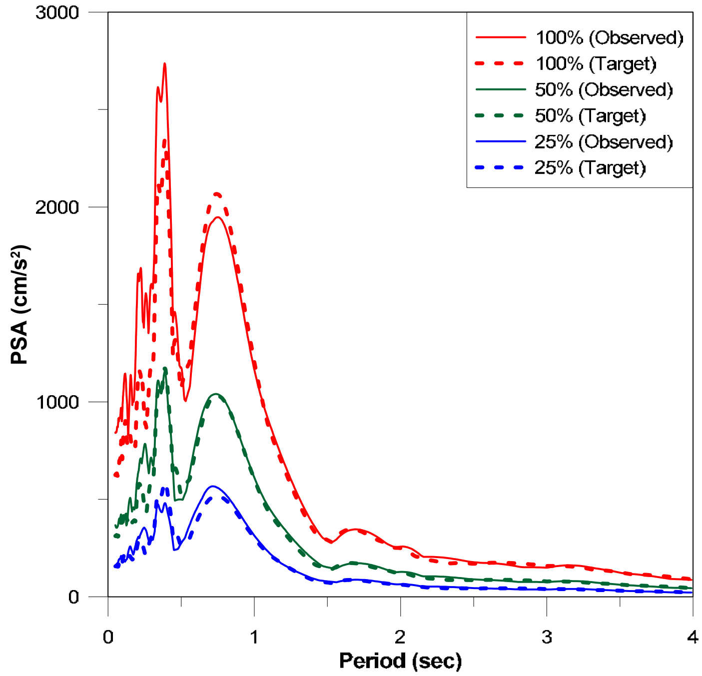

Figure E.1 Acceleration spectra for JMA-Kobe ground motion (*x*-direction).

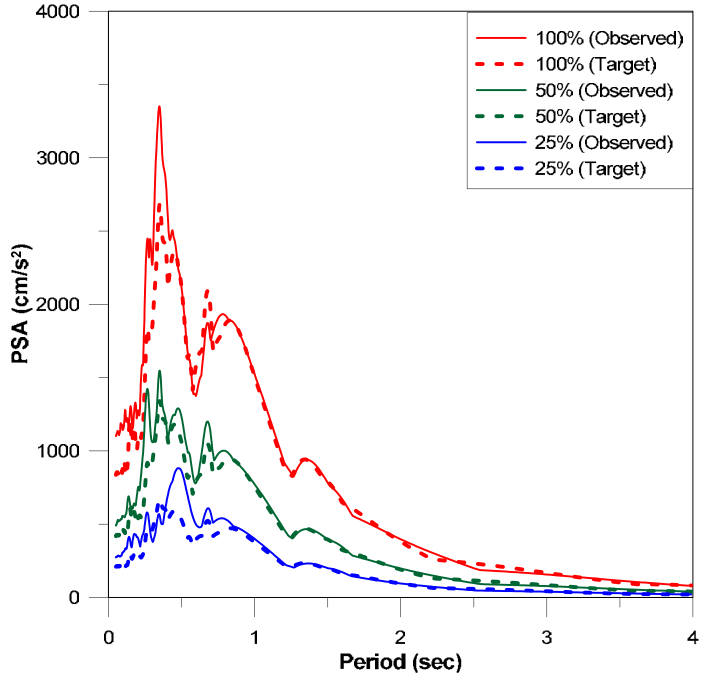

E.2 Acceleration spectra for JMA-Kobe ground motion (*y*-direction).

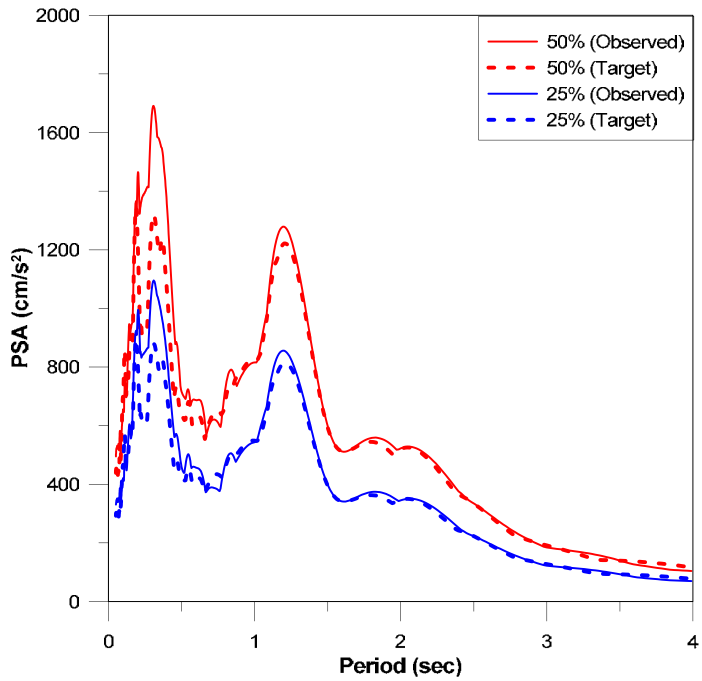

E.3 Acceleration spectra for Takatori ground motion (*x*-direction).

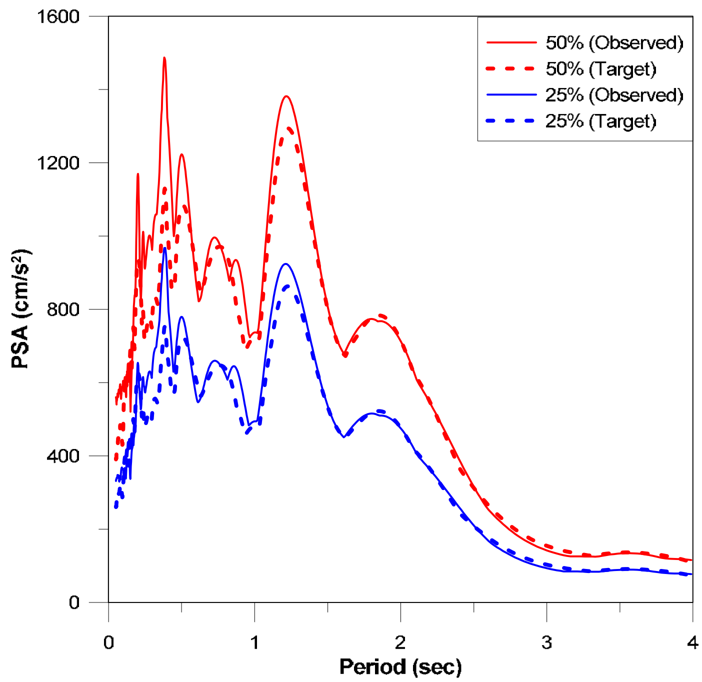

Figure E.4 Acceleration spectra for Takatori ground motion (*y*-direction).

E.2 PSEUDO VELOCITY SPECTRA OF THE GROUND MOTIONS

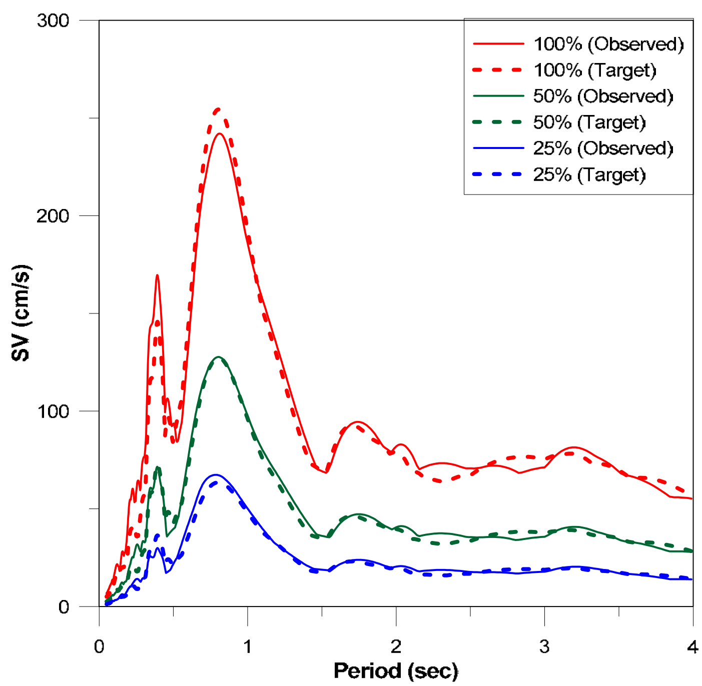

Figure E.5 Pseudo velocity spectra for JMA-Kobe ground motion (*x*-direction).

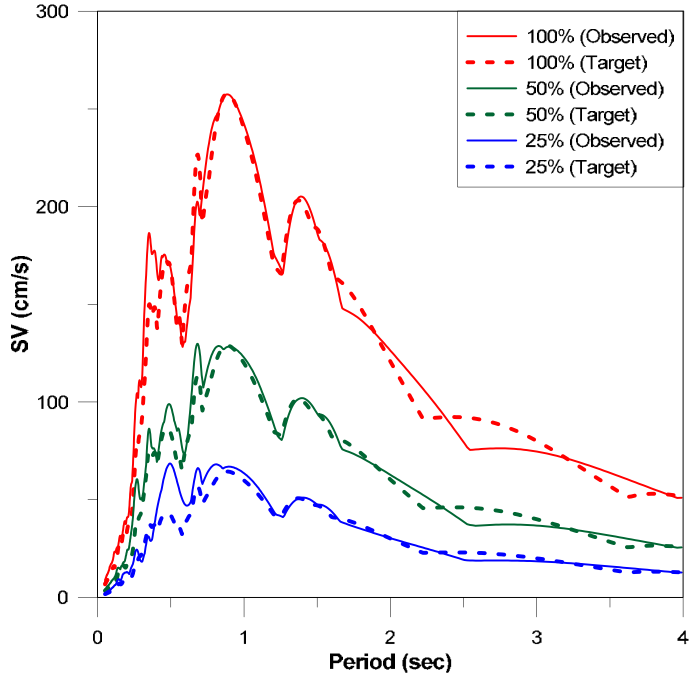

Figure E.6 Pseudo velocity spectra for JMA-Kobe ground motion (*y*-direction)

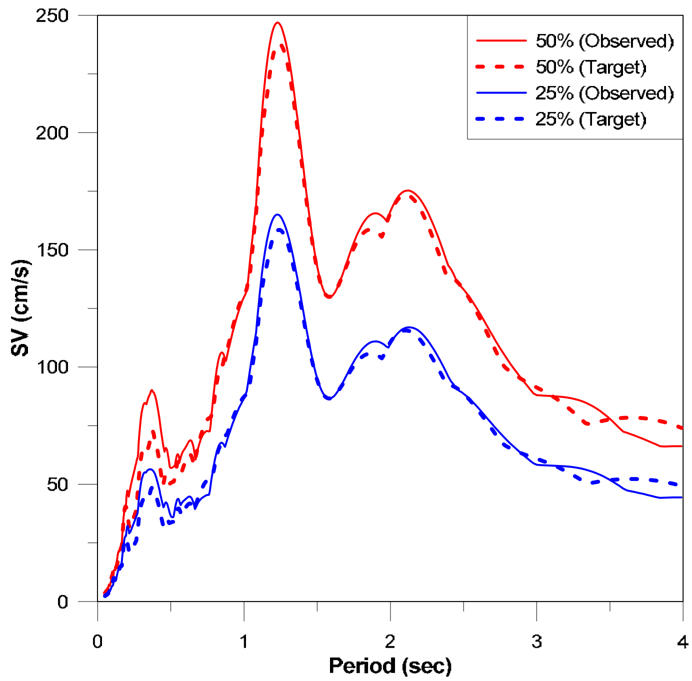

Figure E.7 Pseudo velocity spectra for Takatori ground motion (*x*-direction)

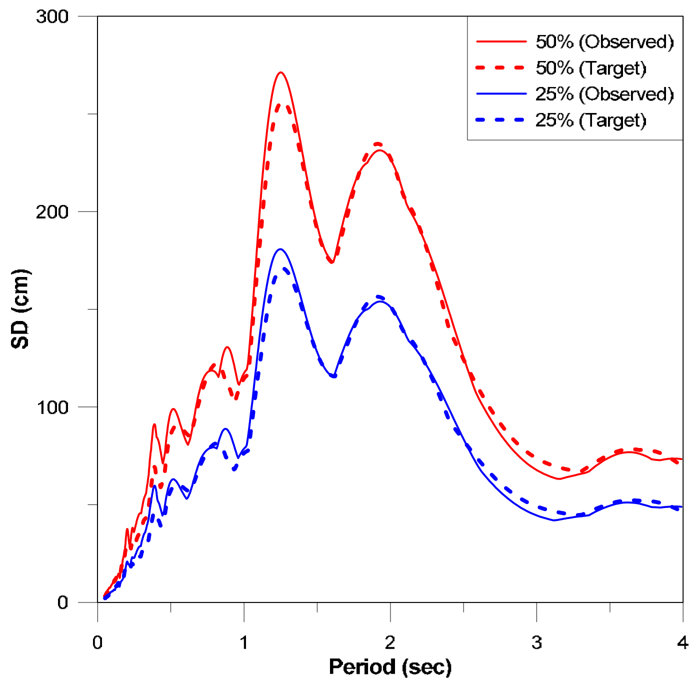

Figure E.8 Pseudo velocity spectra for Takatori ground motion (*y*-direction)

E.3 DISPLACEMENT SPECTRA OF THE GROUND MOTIONS

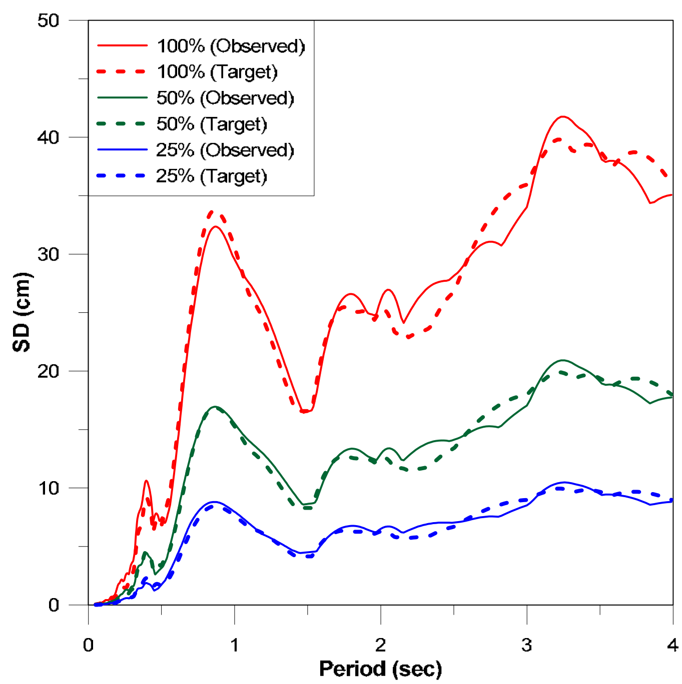

Figure E.9 Displacement spectra for the Kobe ground motion (*x*-direction).

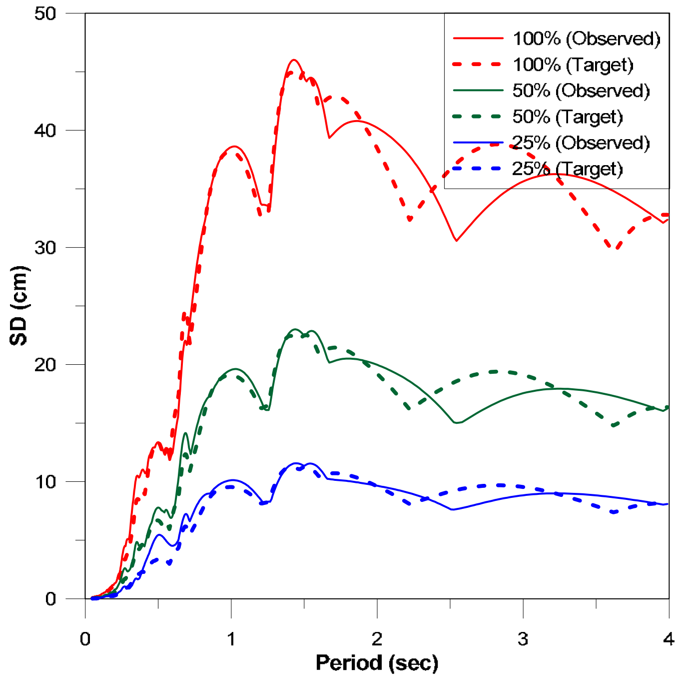

Figure E.10 Displacement spectra for the Kobe ground motion (*y*-direction)

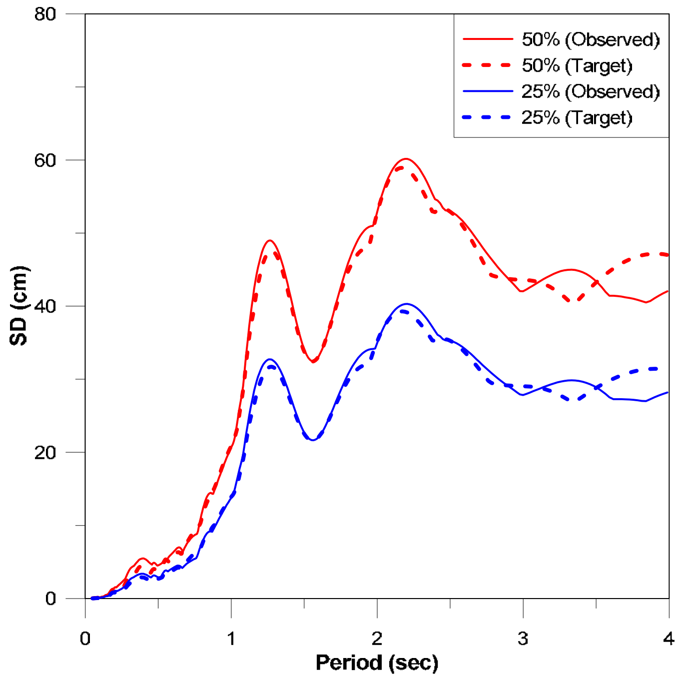

Figure E.11 Displacement spectra for the Takatori ground motion *(x*-direction)

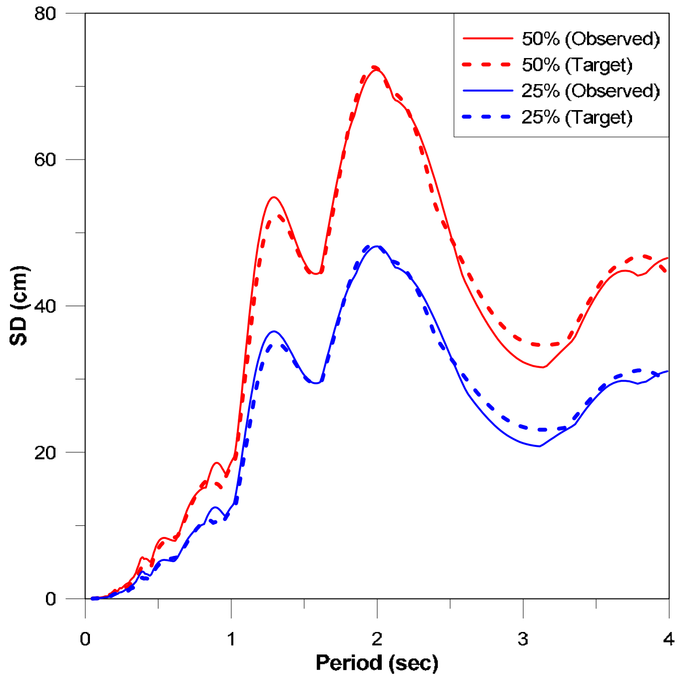

Figure E.12 Displacement spectra for the Takatori ground motion (*y*-direction)

PEER REPORTS

PEER reports are available individually or by yearly subscription. PEER reports can be ordered at http://peer.berkeley.edu/publications/peer_reports.html or by contacting the Pacific Earthquake Engineering Research Center, 325 Davis Hall mail code 1792, Berkeley, CA 94720. Tel.: (510) 642-3437; Fax: (510) 665-1655; Email: peer_editor@berkeley.edu

PEER 2011/03 *New Ground Motion Selection Procedures and Selected Motions for the PEER Transportation Research Program.* Jack W. Baker, Ting Lin, Shrey K. Shahi, and Nirmal Jayaram. March 2011.

PEER 2011/02 *A Bayesian Network Methodology for Infrastructure Seismic Risk Assessment and Decision Support.* Michelle T. Bensi, Armen Der Kiureghian, and Daniel Straub. March 2011.

PEER 2011/01 *Demand Fragility Surfaces for Bridges in Liquefied and Laterally Spreading Ground.* Scott J. Brandenberg, Jian Zhang, Pirooz Kashighandi, Yili Huo, and Minxing Zhao. March 2011.

PEER 2010/05 *Guidelines for Performance-Based Seismic Design of Tall Buildings.* Developed by the Tall Buildings Initiative. November 2010.

PEER 2010/04 *Application Guide for the Design of Flexible and Rigid Bus Connections between Substation Equipment Subjected to Earthquakes.* Jean-Bernard Dastous and Armen Der Kiureghian. September 2010.

PEER 2010/03 *Shear Wave Velocity as a Statistical Function of Standard Penetration Test Resistance and Vertical Effective Stress at Caltrans Bridge Sites.* Scott J. Brandenberg, Naresh Bellana, and Thomas Shantz. June 2010.

PEER 2010/02 *Stochastic Modeling and Simulation of Ground Motions for Performance-Based Earthquake Engineering.* Sanaz Rezaeian and Armen Der Kiureghian. June 2010.

PEER 2010/01 *Structural Response and Cost Characterization of Bridge Construction Using Seismic Performance Enhancement Strategies.* Ady Aviram, Božidar Stojadinović, Gustavo J. Parra-Montesinos, and Kevin R. Mackie. March 2010.

PEER 2009/03 *The Integration of Experimental and Simulation Data in the Study of Reinforced Concrete Bridge Systems Including Soil-Foundation-Structure Interaction.* Matthew Dryden and Gregory L. Fenves. November 2009.

PEER 2009/02 *Improving Earthquake Mitigation through Innovations and Applications in Seismic Science, Engineering, Communication, and Response. Proceedings of a U.S.-Iran Seismic Workshop.* October 2009.

PEER 2009/01 *Evaluation of Ground Motion Selection and Modification Methods: Predicting Median Interstory Drift Response of Buildings.* Curt B. Haselton, Ed. June 2009.

PEER 2008/10 *Technical Manual for Strata.* Albert R. Kottke and Ellen M. Rathje. February 2009.

PEER 2008/09 *NGA Model for Average Horizontal Component of Peak Ground Motion and Response Spectra.* Brian S.-J. Chiou and Robert R. Youngs. November 2008.

PEER 2008/08 *Toward Earthquake-Resistant Design of Concentrically Braced Steel Structures.* Patxi Uriz and Stephen A. Mahin. November 2008.

PEER 2008/07 *Using OpenSees for Performance-Based Evaluation of Bridges on Liquefiable Soils.* Stephen L. Kramer, Pedro Arduino, and HyungSuk Shin. November 2008.

PEER 2008/06 *Shaking Table Tests and Numerical Investigation of Self-Centering Reinforced Concrete Bridge Columns.* Hyung IL Jeong, Junichi Sakai, and Stephen A. Mahin. September 2008.

PEER 2008/05 *Performance-Based Earthquake Engineering Design Evaluation Procedure for Bridge Foundations Undergoing Liquefaction-Induced Lateral Ground Displacement.* Christian A. Ledezma and Jonathan D. Bray. August 2008.

PEER 2008/04 *Benchmarking of Nonlinear Geotechnical Ground Response Analysis Procedures.* Jonathan P. Stewart, Annie On-Lei Kwok, Yousseff M. A. Hashash, Neven Matasovic, Robert Pyke, Zhiliang Wang, and Zhaohui Yang. August 2008.

PEER 2008/03 *Guidelines for Nonlinear Analysis of Bridge Structures in California.* Ady Aviram, Kevin R. Mackie, and Božidar Stojadinović. August 2008.

PEER 2008/02 *Treatment of Uncertainties in Seismic-Risk Analysis of Transportation Systems.* Evangelos Stergiou and Anne S. Kiremidjian. July 2008.

PEER 2008/01 *Seismic Performance Objectives for Tall Buildings.* William T. Holmes, Charles Kircher, William Petak, and Nabih Youssef. August 2008.

PEER 2007/12 *An Assessment to Benchmark the Seismic Performance of a Code-Conforming Reinforced Concrete Moment-Frame Building.* Curt Haselton, Christine A. Goulet, Judith Mitrani-Reiser, James L. Beck, Gregory G. Deierlein, Keith A. Porter, Jonathan P. Stewart, and Ertugrul Taciroglu. August 2008.

PEER 2007/11 *Bar Buckling in Reinforced Concrete Bridge Columns.* Wayne A. Brown, Dawn E. Lehman, and John F. Stanton. February 2008.

PEER 2007/10 *Computational Modeling of Progressive Collapse in Reinforced Concrete Frame Structures.* Mohamed M. Talaat and Khalid M. Mosalam. May 2008.

PEER 2007/09 *Integrated Probabilistic Performance-Based Evaluation of Benchmark Reinforced Concrete Bridges.* Kevin R. Mackie, John-Michael Wong, and Božidar Stojadinović. January 2008.

PEER 2007/08 *Assessing Seismic Collapse Safety of Modern Reinforced Concrete Moment-Frame Buildings.* Curt B. Haselton and Gregory G. Deierlein. February 2008.

PEER 2007/07 *Performance Modeling Strategies for Modern Reinforced Concrete Bridge Columns.* Michael P. Berry and Marc O. Eberhard. April 2008.

PEER 2007/06 *Development of Improved Procedures for Seismic Design of Buried and Partially Buried Structures.* Linda Al Atik and Nicholas Sitar. June 2007.

PEER 2007/05 *Uncertainty and Correlation in Seismic Risk Assessment of Transportation Systems.* Renee G. Lee and Anne S. Kiremidjian. July 2007.

PEER 2007/04 *Numerical Models for Analysis and Performance-Based Design of Shallow Foundations Subjected to Seismic Loading.* Sivapalan Gajan, Tara C. Hutchinson, Bruce L. Kutter, Prishati Raychowdhury, José A. Ugalde, and Jonathan P. Stewart. May 2008.

PEER 2007/03 *Beam-Column Element Model Calibrated for Predicting Flexural Response Leading to Global Collapse of RC Frame Buildings.* Curt B. Haselton, Abbie B. Liel, Sarah Taylor Lange, and Gregory G. Deierlein. May 2008.

PEER 2007/02 *Campbell-Bozorgnia NGA Ground Motion Relations for the Geometric Mean Horizontal Component of Peak and Spectral Ground Motion Parameters.* Kenneth W. Campbell and Yousef Bozorgnia. May 2007.

PEER 2007/01 *Boore-Atkinson NGA Ground Motion Relations for the Geometric Mean Horizontal Component of Peak and Spectral Ground Motion Parameters.* David M. Boore and Gail M. Atkinson. May. May 2007.

PEER 2006/12 *Societal Implications of Performance-Based Earthquake Engineering.* Peter J. May. May 2007.

PEER 2006/11 *Probabilistic Seismic Demand Analysis Using Advanced Ground Motion Intensity Measures, Attenuation Relationships, and Near-Fault Effects.* Polsak Tothong and C. Allin Cornell. March 2007.

PEER 2006/10 *Application of the PEER PBEE Methodology to the I-880 Viaduct.* Sashi Kunnath. February 2007.

PEER 2006/09 *Quantifying Economic Losses from Travel Forgone Following a Large Metropolitan Earthquake.* James Moore, Sungbin Cho, Yue Yue Fan, and Stuart Werner. November 2006.

PEER 2006/08 *Vector-Valued Ground Motion Intensity Measures for Probabilistic Seismic Demand Analysis*. Jack W. Baker and C. Allin Cornell. October 2006.

PEER 2006/07 *Analytical Modeling of Reinforced Concrete Walls for Predicting Flexural and Coupled–Shear-Flexural Responses.* Kutay Orakcal, Leonardo M. Massone, and John W. Wallace. October 2006.

PEER 2006/06 *Nonlinear Analysis of a Soil-Drilled Pier System under Static and Dynamic Axial Loading.* Gang Wang and Nicholas Sitar. November 2006.

PEER 2006/05 *Advanced Seismic Assessment Guidelines.* Paolo Bazzurro, C. Allin Cornell, Charles Menun, Maziar Motahari, and Nicolas Luco. September 2006.

PEER 2006/04 *Probabilistic Seismic Evaluation of Reinforced Concrete Structural Components and Systems.* Tae Hyung Lee and Khalid M. Mosalam. August 2006.

PEER 2006/03 *Performance of Lifelines Subjected to Lateral Spreading.* Scott A. Ashford and Teerawut Juirnarongrit. July 2006.

PEER 2006/02 *Pacific Earthquake Engineering Research Center Highway Demonstration Project.* Anne Kiremidjian, James Moore, Yue Yue Fan, Nesrin Basoz, Ozgur Yazali, and Meredith Williams. April 2006.

PEER 2006/01 *Bracing Berkeley. A Guide to Seismic Safety on the UC Berkeley Campus.* Mary C. Comerio, Stephen Tobriner, and Ariane Fehrenkamp. January 2006.

PEER 2005/16 *Seismic Response and Reliability of Electrical Substation Equipment and Systems.* Junho Song, Armen Der Kiureghian, and Jerome L. Sackman. April 2006.

PEER 2005/15 *CPT-Based Probabilistic Assessment of Seismic Soil Liquefaction Initiation.* R. E. S. Moss, R. B. Seed, R. E. Kayen, J. P. Stewart, and A. Der Kiureghian. April 2006.

PEER 2005/14 *Workshop on Modeling of Nonlinear Cyclic Load-Deformation Behavior of Shallow Foundations.* Bruce L. Kutter, Geoffrey Martin, Tara Hutchinson, Chad Harden, Sivapalan Gajan, and Justin Phalen. March 2006.

PEER 2005/13 *Stochastic Characterization and Decision Bases under Time-Dependent Aftershock Risk in Performance-Based Earthquake Engineering.* Gee Liek Yeo and C. Allin Cornell. July 2005.

PEER 2005/12 *PEER Testbed Study on a Laboratory Building: Exercising Seismic Performance Assessment.* Mary C. Comerio, editor. November 2005.

PEER 2005/11 *Van Nuys Hotel Building Testbed Report: Exercising Seismic Performance Assessment.* Helmut Krawinkler, editor. October 2005.

PEER 2005/10 *First NEES/E-Defense Workshop on Collapse Simulation of Reinforced Concrete Building Structures.* September 2005.

PEER 2005/09 *Test Applications of Advanced Seismic Assessment Guidelines.* Joe Maffei, Karl Telleen, Danya Mohr, William Holmes, and Yuki Nakayama. August 2006.

PEER 2005/08 *Damage Accumulation in Lightly Confined Reinforced Concrete Bridge Columns.* R. Tyler Ranf, Jared M. Nelson, Zach Price, Marc O. Eberhard, and John F. Stanton. April 2006.

PEER 2005/07 *Experimental and Analytical Studies on the Seismic Response of Freestanding and Anchored Laboratory Equipment.* Dimitrios Konstantinidis and Nicos Makris. January 2005.

PEER 2005/06 *Global Collapse of Frame Structures under Seismic Excitations*. Luis F. Ibarra and Helmut Krawinkler. September 2005.

PEER 2005//05 *Performance Characterization of Bench- and Shelf-Mounted Equipment.* Samit Ray Chaudhuri and Tara C. Hutchinson. May 2006.

PEER 2005/04 *Numerical Modeling of the Nonlinear Cyclic Response of Shallow Foundations.* Chad Harden, Tara Hutchinson, Geoffrey R. Martin, and Bruce L. Kutter. August 2005.

PEER 2005/03 *A Taxonomy of Building Components for Performance-Based Earthquake Engineering.* Keith A. Porter. September 2005.

PEER 2005/02 *Fragility Basis for California Highway Overpass Bridge Seismic Decision Making*. Kevin R. Mackie and Božidar Stojadinović. June 2005.

PEER 2005/01 *Empirical Characterization of Site Conditions on Strong Ground Motion.* Jonathan P. Stewart, Yoojoong Choi, and Robert W. Graves. June 2005.

PEER 2004/09 *Electrical Substation Equipment Interaction: Experimental Rigid Conductor Studies.* Christopher Stearns and André Filiatrault. February 2005.

PEER 2004/08 *Seismic Qualification and Fragility Testing of Line Break 550-kV Disconnect Switches.* Shakhzod M. Takhirov, Gregory L. Fenves, and Eric Fujisaki. January 2005.

PEER 2004/07 *Ground Motions for Earthquake Simulator Qualification of Electrical Substation Equipment.* Shakhzod M. Takhirov, Gregory L. Fenves, Eric Fujisaki, and Don Clyde. January 2005.

PEER 2004/06 *Performance-Based Regulation and Regulatory Regimes.* Peter J. May and Chris Koski. September 2004.

PEER 2004/05 *Performance-Based Seismic Design Concepts and Implementation: Proceedings of an International Workshop.* Peter Fajfar and Helmut Krawinkler, editors. September 2004.

PEER 2004/04 *Seismic Performance of an Instrumented Tilt-up Wall Building.* James C. Anderson and Vitelmo V. Bertero. July 2004.

PEER 2004/03 *Evaluation and Application of Concrete Tilt-up Assessment Methodologies.* Timothy Graf and James O. Malley. October 2004.

PEER 2004/02 *Analytical Investigations of New Methods for Reducing Residual Displacements of Reinforced Concrete Bridge Columns.* Junichi Sakai and Stephen A. Mahin. August 2004.

PEER 2004/01 *Seismic Performance of Masonry Buildings and Design Implications.* Kerri Anne Taeko Tokoro, James C. Anderson, and Vitelmo V. Bertero. February 2004.

PEER 2003/18 *Performance Models for Flexural Damage in Reinforced Concrete Columns.* Michael Berry and Marc Eberhard. August 2003.

PEER 2003/17 *Predicting Earthquake Damage in Older Reinforced Concrete Beam-Column Joints.* Catherine Pagni and Laura Lowes. October 2004.

PEER 2003/16 *Seismic Demands for Performance-Based Design of Bridges.* Kevin Mackie and Božidar Stojadinović. August 2003.

PEER 2003/15 *Seismic Demands for Nondeteriorating Frame Structures and Their Dependence on Ground Motions.* Ricardo Antonio Medina and Helmut Krawinkler. May 2004.

PEER 2003/14 *Finite Element Reliability and Sensitivity Methods for Performance-Based Earthquake Engineering.* Terje Haukaas and Armen Der Kiureghian. April 2004.

PEER 2003/13 *Effects of Connection Hysteretic Degradation on the Seismic Behavior of Steel Moment-Resisting Frames.* Janise E. Rodgers and Stephen A. Mahin. March 2004.

PEER 2003/12 *Implementation Manual for the Seismic Protection of Laboratory Contents: Format and Case Studies.* William T. Holmes and Mary C. Comerio. October 2003.

PEER 2003/11 *Fifth U.S.-Japan Workshop on Performance-Based Earthquake Engineering Methodology for Reinforced Concrete Building Structures.* February 2004.

PEER 2003/10 *A Beam-Column Joint Model for Simulating the Earthquake Response of Reinforced Concrete Frames*. Laura N. Lowes, Nilanjan Mitra, and Arash Altoontash. February 2004.

PEER 2003/09 *Sequencing Repairs after an Earthquake: An Economic Approach.* Marco Casari and Simon J. Wilkie. April 2004.

PEER 2003/08 *A Technical Framework for Probability-Based Demand and Capacity Factor Design (DCFD) Seismic Formats*. Fatemeh Jalayer and C. Allin Cornell. November 2003.

PEER 2003/07 *Uncertainty Specification and Propagation for Loss Estimation Using FOSM Methods.* Jack W. Baker and C. Allin Cornell. September 2003.

PEER 2003/06 *Performance of Circular Reinforced Concrete Bridge Columns under Bidirectional Earthquake Loading*. Mahmoud M. Hachem, Stephen A. Mahin, and Jack P. Moehle. February 2003.

PEER 2003/05 *Response Assessment for Building-Specific Loss Estimation.* Eduardo Miranda and Shahram Taghavi. September 2003.

PEER 2003/04 *Experimental Assessment of Columns with Short Lap Splices Subjected to Cyclic Loads*. Murat Melek, John W. Wallace, and Joel Conte. April 2003.

PEER 2003/03 *Probabilistic Response Assessment for Building-Specific Loss Estimation.* Eduardo Miranda and Hesameddin Aslani. September 2003.

PEER 2003/02 *Software Framework for Collaborative Development of Nonlinear Dynamic Analysis Program*. Jun Peng and Kincho H. Law. September 2003.

PEER 2003/01 *Shake Table Tests and Analytical Studies on the Gravity Load Collapse of Reinforced Concrete Frames.* Kenneth John Elwood and Jack P. Moehle. November 2003.

PEER 2002/24 *Performance of Beam to Column Bridge Joints Subjected to a Large Velocity Pulse.* Natalie Gibson, André Filiatrault, and Scott A. Ashford. April 2002.

PEER 2002/23 *Effects of Large Velocity Pulses on Reinforced Concrete Bridge Columns.* Greg L. Orozco and Scott A. Ashford. April 2002.

PEER 2002/22 *Characterization of Large Velocity Pulses for Laboratory Testing.* Kenneth E. Cox and Scott A. Ashford. April 2002.

PEER 2002/21 *Fourth U.S.-Japan Workshop on Performance-Based Earthquake Engineering Methodology for Reinforced Concrete Building Structures*. December 2002.

PEER 2002/20 *Barriers to Adoption and Implementation of PBEE Innovations.* Peter J. May. August 2002.

PEER 2002/19 *Economic-Engineered Integrated Models for Earthquakes: Socioeconomic Impacts.* Peter Gordon, James E. Moore II, and Harry W. Richardson. July 2002.

PEER 2002/18 *Assessment of Reinforced Concrete Building Exterior Joints with Substandard Details.* Chris P. Pantelides, Jon Hansen, Justin Nadauld, and Lawrence D. Reaveley. May 2002.

PEER 2002/17 *Structural Characterization and Seismic Response Analysis of a Highway Overcrossing Equipped with Elastomeric Bearings and Fluid Dampers: A Case Study.* Nicos Makris and Jian Zhang. November 2002.

PEER 2002/16 *Estimation of Uncertainty in Geotechnical Properties for Performance-Based Earthquake Engineering.* Allen L. Jones, Steven L. Kramer, and Pedro Arduino. December 2002.

PEER 2002/15 *Seismic Behavior of Bridge Columns Subjected to Various Loading Patterns.* Asadollah Esmaeily-Gh. and Yan Xiao. December 2002.

PEER 2002/14 *Inelastic Seismic Response of Extended Pile Shaft Supported Bridge Structures.* T.C. Hutchinson, R.W. Boulanger, Y.H. Chai, and I.M. Idriss. December 2002.

PEER 2002/13 *Probabilistic Models and Fragility Estimates for Bridge Components and Systems.* Paolo Gardoni, Armen Der Kiureghian, and Khalid M. Mosalam. June 2002.

PEER 2002/12 *Effects of Fault Dip and Slip Rake on Near-Source Ground Motions: Why Chi-Chi Was a Relatively Mild M7.6 Earthquake.* Brad T. Aagaard, John F. Hall, and Thomas H. Heaton. December 2002.

PEER 2002/11 *Analytical and Experimental Study of Fiber-Reinforced Strip Isolators*. James M. Kelly and Shakhzod M. Takhirov. September 2002.

PEER 2002/10 *Centrifuge Modeling of Settlement and Lateral Spreading with Comparisons to Numerical Analyses***.** Sivapalan Gajan and Bruce L. Kutter. January 2003.

PEER 2002/09 *Documentation and Analysis of Field Case Histories of Seismic Compression during the 1994 Northridge, California, Earthquake.* Jonathan P. Stewart, Patrick M. Smith, Daniel H. Whang, and Jonathan D. Bray. October 2002.

PEER 2002/08 *Component Testing, Stability Analysis and Characterization of Buckling-Restrained Unbonded Braces™.* Cameron Black, Nicos Makris, and Ian Aiken. September 2002.

PEER 2002/07 *Seismic Performance of Pile-Wharf Connections.* Charles W. Roeder, Robert Graff, Jennifer Soderstrom, and Jun Han Yoo. December 2001.

PEER 2002/06 *The Use of Benefit-Cost Analysis for Evaluation of Performance-Based Earthquake Engineering Decisions*. Richard O. Zerbe and Anthony Falit-Baiamonte. September 2001.

PEER 2002/05 *Guidelines, Specifications, and Seismic Performance Characterization of Nonstructural Building Components and Equipment*. André Filiatrault, Constantin Christopoulos, and Christopher Stearns. September 2001.

PEER 2002/04 *Consortium of Organizations for Strong-Motion Observation Systems and the Pacific Earthquake Engineering Research Center Lifelines Program: Invited Workshop on Archiving and Web Dissemination of Geotechnical Data, 4–5 October 2001*. September 2002.

PEER 2002/03 *Investigation of Sensitivity of Building Loss Estimates to Major Uncertain Variables for the Van Nuys Testbed.* Keith A. Porter, James L. Beck, and Rustem V. Shaikhutdinov. August 2002.

PEER 2002/02 *The Third U.S.-Japan Workshop on Performance-Based Earthquake Engineering Methodology for Reinforced Concrete Building Structures*. July 2002.

PEER 2002/01 *Nonstructural Loss Estimation: The UC Berkeley Case Study.* Mary C. Comerio and John C. Stallmeyer. December 2001.

PEER 2001/16 *Statistics of SDF-System Estimate of Roof Displacement for Pushover Analysis of Buildings.* Anil K. Chopra, Rakesh K. Goel, and Chatpan Chintanapakdee. December 2001.

PEER 2001/15 *Damage to Bridges during the 2001 Nisqually Earthquake.* R. Tyler Ranf, Marc O. Eberhard, and Michael P. Berry. November 2001.

PEER 2001/14 *Rocking Response of Equipment Anchored to a Base Foundation.* Nicos Makris and Cameron J. Black. September 2001.

PEER 2001/13 *Modeling Soil Liquefaction Hazards for Performance-Based Earthquake Engineering.* Steven L. Kramer and Ahmed-W. Elgamal. February 2001.

PEER 2001/12 *Development of Geotechnical Capabilities in OpenSees.* Boris Jeremić. September 2001.

PEER 2001/11 *Analytical and Experimental Study of Fiber-Reinforced Elastomeric Isolators.* James M. Kelly and Shakhzod M. Takhirov. September 2001.

PEER 2001/10 *Amplification Factors for Spectral Acceleration in Active Regions.* Jonathan P. Stewart, Andrew H. Liu, Yoojoong Choi, and Mehmet B. Baturay. December 2001.

PEER 2001/09 *Ground Motion Evaluation Procedures for Performance-Based Design.* Jonathan P. Stewart, Shyh-Jeng Chiou, Jonathan D. Bray, Robert W. Graves, Paul G. Somerville, and Norman A. Abrahamson. September 2001.

PEER 2001/08 *Experimental and Computational Evaluation of Reinforced Concrete Bridge Beam-Column Connections for Seismic Performance.* Clay J. Naito, Jack P. Moehle, and Khalid M. Mosalam. November 2001.

PEER 2001/07 *The Rocking Spectrum and the Shortcomings of Design Guidelines.* Nicos Makris and Dimitrios Konstantinidis. August 2001.

PEER 2001/06 *Development of an Electrical Substation Equipment Performance Database for Evaluation of Equipment Fragilities*. Thalia Agnanos. April 1999.

PEER 2001/05 *Stiffness Analysis of Fiber-Reinforced Elastomeric Isolators.* Hsiang-Chuan Tsai and James M. Kelly. May 2001.

PEER 2001/04 *Organizational and Societal Considerations for Performance-Based Earthquake Engineering.* Peter J. May. April 2001.

PEER 2001/03 *A Modal Pushover Analysis Procedure to Estimate Seismic Demands for Buildings: Theory and Preliminary Evaluation.* Anil K. Chopra and Rakesh K. Goel. January 2001.

PEER 2001/02 *Seismic Response Analysis of Highway Overcrossings Including Soil-Structure Interaction.* Jian Zhang and Nicos Makris. March 2001.

PEER 2001/01 *Experimental Study of Large Seismic Steel Beam-to-Column Connections.* Egor P. Popov and Shakhzod M. Takhirov. November 2000.

PEER 2000/10 *The Second U.S.-Japan Workshop on Performance-Based Earthquake Engineering Methodology for Reinforced Concrete Building Structures.* March 2000.

PEER 2000/09 *Structural Engineering Reconnaissance of the August 17, 1999 Earthquake: Kocaeli (Izmit), Turkey.* Halil Sezen, Kenneth J. Elwood, Andrew S. Whittaker, Khalid Mosalam, John J. Wallace, and John F. Stanton. December 2000.

PEER 2000/08 *Behavior of Reinforced Concrete Bridge Columns Having Varying Aspect Ratios and Varying Lengths of Confinement.* Anthony J. Calderone, Dawn E. Lehman, and Jack P. Moehle. January 2001.

PEER 2000/07 *Cover-Plate and Flange-Plate Reinforced Steel Moment-Resisting Connections.* Taejin Kim, Andrew S. Whittaker, Amir S. Gilani, Vitelmo V. Bertero, and Shakhzod M. Takhirov. September 2000.

PEER 2000/06 *Seismic Evaluation and Analysis of 230-kV Disconnect Switches.* Amir S. J. Gilani, Andrew S. Whittaker, Gregory L. Fenves, Chun-Hao Chen, Henry Ho, and Eric Fujisaki. July 2000.

PEER 2000/05 *Performance-Based Evaluation of Exterior Reinforced Concrete Building Joints for Seismic Excitation.* Chandra Clyde, Chris P. Pantelides, and Lawrence D. Reaveley. July 2000.

PEER 2000/04 *An Evaluation of Seismic Energy Demand: An Attenuation Approach.* Chung-Che Chou and Chia-Ming Uang. July 1999.

PEER 2000/03 *Framing Earthquake Retrofitting Decisions: The Case of Hillside Homes in Los Angeles*. Detlof von Winterfeldt, Nels Roselund, and Alicia Kitsuse. March 2000.

PEER 2000/02 *U.S.-Japan Workshop on the Effects of Near-Field Earthquake Shaking.* Andrew Whittaker, ed. July 2000.

PEER 2000/01 *Further Studies on Seismic Interaction in Interconnected Electrical Substation Equipment.* Armen Der Kiureghian, Kee-Jeung Hong, and Jerome L. Sackman. November 1999.

PEER 1999/14 *Seismic Evaluation and Retrofit of 230-kV Porcelain Transformer Bushings*. Amir S. Gilani, Andrew S. Whittaker, Gregory L. Fenves, and Eric Fujisaki. December 1999.

PEER 1999/13 *Building Vulnerability Studies: Modeling and Evaluation of Tilt-up and Steel Reinforced Concrete Buildings.* John W. Wallace, Jonathan P. Stewart, and Andrew S. Whittaker, editors. December 1999.

PEER 1999/12 *Rehabilitation of Nonductile RC Frame Building Using Encasement Plates and Energy-Dissipating Devices.* Mehrdad Sasani, Vitelmo V. Bertero, James C. Anderson. December 1999.

PEER 1999/11 *Performance Evaluation Database for Concrete Bridge Components and Systems under Simulated Seismic Loads.* Yael D. Hose and Frieder Seible. November 1999.

PEER 1999/10 *U.S.-Japan Workshop on Performance-Based Earthquake Engineering Methodology for Reinforced Concrete Building Structures.* December 1999.

PEER 1999/09 *Performance Improvement of Long Period Building Structures Subjected to Severe Pulse-Type Ground Motions*. James C. Anderson, Vitelmo V. Bertero, and Raul Bertero. October 1999.

PEER 1999/08 *Envelopes for Seismic Response Vectors.* Charles Menun and Armen Der Kiureghian. July 1999.

PEER 1999/07 *Documentation of Strengths and Weaknesses of Current Computer Analysis Methods for Seismic Performance of Reinforced Concrete Members.* William F. Cofer. November 1999.

PEER 1999/06 *Rocking Response and Overturning of Anchored Equipment under Seismic Excitations.* Nicos Makris and Jian Zhang. November 1999.

PEER 1999/05 *Seismic Evaluation of 550 kV Porcelain Transformer Bushings.* Amir S. Gilani, Andrew S. Whittaker, Gregory L. Fenves, and Eric Fujisaki. October 1999.

PEER 1999/04 *Adoption and Enforcement of Earthquake Risk-Reduction Measures.* Peter J. May, Raymond J. Burby, T. Jens Feeley, and Robert Wood.

PEER 1999/03 *Task 3 Characterization of Site Response General Site Categories*. Adrian Rodriguez-Marek, Jonathan D. Bray, and Norman Abrahamson. February 1999.

PEER 1999/02 *Capacity-Demand-Diagram Methods for Estimating Seismic Deformation of Inelastic Structures: SDF Systems*. Anil K. Chopra and Rakesh Goel. April 1999.

PEER 1999/01 *Interaction in Interconnected Electrical Substation Equipment Subjected to Earthquake Ground Motions.* Armen Der Kiureghian, Jerome L. Sackman, and Kee-Jeung Hong. February 1999.

PEER 1998/08 *Behavior and Failure Analysis of a Multiple-Frame Highway Bridge in the 1994 Northridge Earthquake.* Gregory L. Fenves and Michael Ellery. December 1998.

PEER 1998/07 *Empirical Evaluation of Inertial Soil-Structure Interaction Effects.* Jonathan P. Stewart, Raymond B. Seed, and Gregory L. Fenves. November 1998.

PEER 1998/06 *Effect of Damping Mechanisms on the Response of Seismic Isolated Structures.* Nicos Makris and Shih-Po Chang. November 1998.

PEER 1998/05 *Rocking Response and Overturning of Equipment under Horizontal Pulse-Type Motions.* Nicos Makris and Yiannis Roussos. October 1998.

PEER 1998/04 *Pacific Earthquake Engineering Research Invitational Workshop Proceedings, May 14–15, 1998: Defining the Links between Planning, Policy Analysis, Economics and Earthquake Engineering.* Mary Comerio and Peter Gordon. September 1998.

PEER 1998/03 *Repair/Upgrade Procedures for Welded Beam to Column Connections.* James C. Anderson and Xiaojing Duan. May 1998.

PEER 1998/02 *Seismic Evaluation of 196 kV Porcelain Transformer Bushings.* Amir S. Gilani, Juan W. Chavez, Gregory L. Fenves, and Andrew S. Whittaker. May 1998.

PEER 1998/01 *Seismic Performance of Well-Confined Concrete Bridge Columns.* Dawn E. Lehman and Jack P. Moehle. December 2000.

ONLINE REPORTS

The following PEER reports are available by Internet only at http://peer.berkeley.edu/publications/peer_reports.html

PEER 2011/104 *Design and Instrumentation of the 2010 E-Defense Four-Story Reinforced Concrete and Post-Tensioned Concrete Buildings.* Takuya Nagae, Kenichi Tahara, Taizo Matsumori, Hitoshi Shiohara, Toshimi Kabeyasawa, Susumu Kono, Minehiro Nishiyama (Japanese Research Team) and John Wallace, Wassim Ghannoum, Jack Moehle, Richard Sause, Wesley Keller, Zeynep Tuna (U.S. Research Team). June 2011.

PEER 2011/103 *In-Situ Monitoring of the Force Output of Fluid Dampers: Experimental Investigation.* Dimitrios Konstantinidis, James M. Kelly, and Nicos Makris. April 2011.

PEER 2011/102 *Ground-motion prediction equations 1964 - 2010.* John Douglas. April 2011.

PEER 2011/101 *Report of the Eighth Planning Meeting of NEES/E-Defense Collaborative Research on Earthquake Engineering.* Convened by the Hyogo Earthquake Engineering Research Center (NIED), NEES Consortium, Inc. February 2011.

PEER 2010/111 *Modeling and Acceptance Criteria for Seismic Design and Analysis of Tall Buildings.* Task 7 Report for the Tall Buildings Initiative - Published jointly by the Applied Technology Council. October 2010.

PEER 2010/110 *Seismic Performance Assessment and Probabilistic Repair Cost Analysis of Precast Concrete Cladding Systems for Multistory Buildlings.* Jeffrey P. Hunt and Božidar Stojadinovic. November 2010.

PEER 2010/109 *Report of the Seventh Joint Planning Meeting of NEES/E-Defense Collaboration on Earthquake Engineering. Held at the E-Defense, Miki, and Shin-Kobe, Japan, September 18–19, 2009.* August 2010.

PEER 2010/108 *Probabilistic Tsunami Hazard in California.* Hong Kie Thio, Paul Somerville, and Jascha Polet, preparers. October 2010.

PEER 2010/107 *Performance and Reliability of Exposed Column Base Plate Connections for Steel Moment-Resisting Frames.* Ady Aviram, Božidar Stojadinovic, and Armen Der Kiureghian. August 2010.

PEER 2010/106 *Verification of Probabilistic Seismic Hazard Analysis Computer Programs.* Patricia Thomas, Ivan Wong, and Norman Abrahamson. May 2010.

PEER 2010/105 *Structural Engineering Reconnaissance of the April 6, 2009, Abruzzo, Italy, Earthquake, and Lessons Learned.* M. Selim Günay and Khalid M. Mosalam. April 2010.

PEER 2010/104 *Simulating the Inelastic Seismic Behavior of Steel Braced Frames, Including the Effects of Low-Cycle Fatigue.* Yuli Huang and Stephen A. Mahin. April 2010.

PEER 2010/103 *Post-Earthquake Traffic Capacity of Modern Bridges in California.* Vesna Terzic and Božidar Stojadinović. March 2010.

PEER 2010/102 *Analysis of Cumulative Absolute Velocity (CAV) and JMA Instrumental Seismic Intensity (I_{JMA}) Using the PEER–NGA Strong Motion Database.* Kenneth W. Campbell and Yousef Bozorgnia. February 2010.

PEER 2010/101 *Rocking Response of Bridges on Shallow Foundations.* Jose A. Ugalde, Bruce L. Kutter, and Boris Jeremic. April 2010.

PEER 2009/109 *Simulation and Performance-Based Earthquake Engineering Assessment of Self-Centering Post-Tensioned Concrete Bridge Systems.* Won K. Lee and Sarah L. Billington. December 2009.

PEER 2009/108 *PEER Lifelines Geotechnical Virtual Data Center.* J. Carl Stepp, Daniel J. Ponti, Loren L. Turner, Jennifer N. Swift, Sean Devlin, Yang Zhu, Jean Benoit, and John Bobbitt. September 2009.

PEER 2009/107 *Experimental and Computational Evaluation of Current and Innovative In-Span Hinge Details in Reinforced Concrete Box-Girder Bridges: Part 2: Post-Test Analysis and Design Recommendations.* Matias A. Hube and Khalid M. Mosalam. December 2009.

PEER 2009/106 *Shear Strength Models of Exterior Beam-Column Joints without Transverse Reinforcement.* Sangjoon Park and Khalid M. Mosalam. November 2009.

PEER 2009/105 *Reduced Uncertainty of Ground Motion Prediction Equations through Bayesian Variance Analysis.* Robb Eric S. Moss. November 2009.

PEER 2009/104 *Advanced Implementation of Hybrid Simulation.* Andreas H. Schellenberg, Stephen A. Mahin, Gregory L. Fenves. November 2009.

PEER 2009/103 *Performance Evaluation of Innovative Steel Braced Frames.* T. Y. Yang, Jack P. Moehle, and Božidar Stojadinovic. August 2009.

PEER 2009/102 *Reinvestigation of Liquefaction and Nonliquefaction Case Histories from the 1976 Tangshan Earthquake.* Robb Eric Moss, Robert E. Kayen, Liyuan Tong, Songyu Liu, Guojun Cai, and Jiaer Wu. August 2009.

PEER 2009/101 *Report of the First Joint Planning Meeting for the Second Phase of NEES/E-Defense Collaborative Research on Earthquake Engineering.* Stephen A. Mahin et al. July 2009.

PEER 2008/104 *Experimental and Analytical Study of the Seismic Performance of Retaining Structures.* Linda Al Atik and Nicholas Sitar. January 2009.

PEER 2008/103 *Experimental and Computational Evaluation of Current and Innovative In-Span Hinge Details in Reinforced Concrete Box-Girder Bridges. Part 1: Experimental Findings and Pre-Test Analysis.* Matias A. Hube and Khalid M. Mosalam. January 2009.

PEER 2008/102 *Modeling of Unreinforced Masonry Infill Walls Considering In-Plane and Out-of-Plane Interaction.* Stephen Kadysiewski and Khalid M. Mosalam. January 2009.

PEER 2008/101 *Seismic Performance Objectives for Tall Buildings.* William T. Holmes, Charles Kircher, William Petak, and Nabih Youssef. August 2008.

PEER 2007/101 *Generalized Hybrid Simulation Framework for Structural Systems Subjected to Seismic Loading.* Tarek Elkhoraibi and Khalid M. Mosalam. July 2007.

PEER 2007/100 *Seismic Evaluation of Reinforced Concrete Buildings Including Effects of Masonry Infill Walls.* Alidad Hashemi and Khalid M. Mosalam. July 2007.

The Pacific Earthquake Engineering Research Center (PEER) is a multi-institutional research and education center with headquarters at the University of California, Berkeley. Investigators from over 20 universities, several consulting companies, and researchers at various state and federal government agencies contribute to research programs focused on performance-based earthquake engineering.

These research programs aim to identify and reduce the risks from major earthquakes to life safety and to the economy by including research in a wide variety of disciplines including structural and geotechnical engineering, geology/seismology, lifelines, transportation, architecture, economics, risk management, and public policy.

PEER is supported by federal, state, local, and regional agencies, together with industry partners.

PEER reports can be ordered at http://peer.berkeley.edu/publications/peer_reports.html or by contacting

Pacific Earthquake Engineering Research Center
University of California, Berkeley
325 Davis Hall, mail code 1792
Berkeley, CA 94720-1792
Tel: 510-642-3437
Fax: 510-642-1655
Email: peer_editor@berkeley.edu

ISSN 1547-0587X